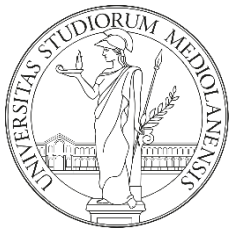

UNIVERSITÀ DEGLI STUDI DI MILANO

DEPARTMENT OF PHARMACEUTICAL SCIENCES

DOCTORAL SCHOOL IN PHARMACEUTICAL SCIENCES

PhD – Cycle the 33th

MICROALGAE PEPTIDES IN CARDIOVASCULAR DISEASE PREVENTION: STRUCTURE ELUCIDATION, BIOACTIVITY INVESTIGATION AND IN SILICO MOLECULAR MODELING ANALYSIS

Sector CHIM/10 – Food chemistry

Dr. Li Yuchen

R12098

Faculty advisor: Prof. Anna Arnoldi

PhD coordinator: Prof. Giancarlo Aldini

ACADEMIC YEAR

2020/2021

ACKNOWLEDGEMENT

Upon the completion of this thesis, I am deeply grateful to those who offered me encouragement and supports during my PhD period.

First of all, the profound gratitude should go to my supervisor, Professor Anna Arnoldi. She provided the precious opportunity and excellent research platform to me so that I can conduct my PhD project. In these years, her scientific supports and wise thinking inspired me a lot; her patience and care gave me a favorable working environment. The experiences in her laboratory will always be of great value to my future academic research.

Also, I would like to express my heartful thanks to Dr. Gilda Aiello and Dr. Carmen Lammi for their guidance throughout the years. Dr. Aiello Gilda introduced me to the field of biopeptide discovery and unreservedly imparted her knowledge and skills of analytical techniques to me. Plenty of fruitful discussions and troubleshooting finally resulted in s successful outcome, which would not have been possible without her support. Dr. Carmen Lammi directed me a lot on the biological techniques. She also helped me greatly to improve my manuscripts with her considerable experience and careful revision. Her idea and passion for research inspired me and let me feel science is beautiful.

Special thanks go to professor Giovanni Grazioso for his helpful instruction on my study of molecular modeling. He directed me to a new field and greatly enriched my knowledge. His specialized assistance and valuable suggestions are indispensable in my research and thesis.

I also want to express my deep thanks to technician Giovanna Boschin. She assisted me with experimental skills and technical issues, always shared useful scientific information to me. She is such a kind and considerate person that she never forgot my birthday in these years, which makes me, a foreign student feel really warm.

I am grateful to all the team members who made the daily lab work more enjoyable and forgettable. Many thanks go to the people in DISFARM who gave me help and

encouragement.

Especially, I would like express my sincere gratitude to China Scholarship Council for the financial support, which helped me to pursue my scientific career.

Finally, a very big and special thank goes to my family members for their spiritual company and support. Deep thanks and love go to my boyfriend, Wei Wei. Studying abroad with me together, he has been a faithful supporter to me both in life and work. Without all these people, I would not be where I am today.

INDEX

Aim of the thesis

Part I. State of the art

Part II. Scientific contribution

Scientific Publications & Communications

Aim of the thesis

Motivations and outlines of the PhD thesis

In recent years, food peptides are gaining much interest for their potential health benefits. In fact, short and medium size peptides released by food protein hydrolysis may be absorbed and modulate specific metabolic pathways by binding or inhibiting targeted receptors, with a final positive impact on metabolic diseases. This is very relevant, since the possibility of preventing or influencing the development of pathological conditions by dietary management rather than by drug use is in line with the current propensity of many persons for a healthier lifestyle. In addition, the toxic or adverse effects of bioactive peptides are generally very low or not-existing. Therefore, the discovery of bioactive peptides and the exploration of their mechanism of action open the possibilities of developing innovative functional foods and nutraceuticals.

Until now, the most common sources of bioactive peptides include eggs, meat, fish, soybean, wheat, milk, and its derivatives. However, more and more new food matrices are under investigation. In particular, microalgae have drawn the attention of different groups due to their easy growing and high protein contents. Despite this, in this area the studies on bioactive peptides are more focused on the bioactivity rather than on the analytical method applied to profile the peptide composition. Few studies have acquired amino acid sequence of the microalgal peptides, due to the technical challenge related to the isolation and identification of single peptides from complex food matrices.

Based on these considerations, the aim of my PhD thesis was focused on the evaluation of the potential of microalgae to generate bioactive peptides, the functional analysis and the discovery of promising microalgae peptides. To achieve these objectives, multidisciplinary approaches were employed, involving peptidomic techniques to profile the peptide sequences, biochemical tools to analyze the bioactivity, and emerging molecular modelling methods to predict potentially bioactive peptides as well as to explore their possible mechanism of action.

In my thesis, hypertension and diabetes were the targeted diseases, because they are among the major risk factors of cardiovascular disease (CVD) development. These two

diseases frequently occur together, reflecting substantial overlap in their aetiology and disease mechanisms. To prevent hypertension and diabetes, many potent peptides have been reported in literature, but only a few are from microalgae. In this case, efforts have been made here.

Briefly, the main objectives of my PhD study were:

- To characterize the preventing effects of spirulina protein hydrolysates towards hypertension and diabetes.
- To acquire peptide sequences from phycobiliprotein (PBP) hydrolysate and to understand their inhibition of dipeptidyl peptidase-IV (DPP-IV) activity expressed by Caco-2 cells.
- To screen multifunctional peptides from *Chlorella pyrenoidosa* by in silico structure-based approach.

The thesis includes three parts:

Part I introduces the state of the art of microalgae peptides. **Chapter I** discusses the value of microalgae protein as precursors of bioactive peptides and the discovered microalgae peptides with antihypertensive and antidiabetic effects. On the basis of numerous reports, it is highlighted that microalgae are promising sources to generate peptides with cardiovascular benefits. **Chapter II** states the classical strategies applying in the discovery of bioactive peptides, such as peptidomics, and also some newly emerging approaches like molecular modelling.

Part II presents my scientific contributions in the PhD period.

Chapter I is dedicated to investigate the potential of spirulina protein to produce antihypertensive and antidiabetic peptides by pursuing the therapeutic targets angiotensin converting enzyme (ACE) and DPP-IV, respectively. This work provides: i) a kinetic study of peptides released from protein in the enzymatic process; ii) the identification of peptide sequences in the spirulina protein hydrolysates; iii) an investigation of the bioactivity of spirulina protein hydrolysate by in vitro assays and in situ ones performed on intestinal cells.

Further study was focused on PBP, a group of pigment-protein complexes in spirulina. **Chapter II** presents the peptidomic analysis and antidiabetic evaluation of a PBP tryptic hydrolysate. By in vitro and cellular experiments, PBP peptides exert significant DPP-IV inhibiting effect. The kinetics study of peptides inhibition on DPP-IV expressed by Caco-2 cells reveals the possible metabolic process of peptides when working on the intestinal cells.

Chapter III presents a screening of peptides with both antihypertensive and antidiabetic activities from *Chlorella pyrenoidosa* (*C. pyrenoidosa*), which was performed by combining mass spectrometric techniques and structure-based prediction. Overall, this study achieved: i) an evaluation of the biological activities of *C. pyrenoidosa* protein hydrolysates towards the targets ACE and DPP-IV; ii) the mapping of released peptides by MS analysis; iii) a screening of multifunctional peptides by molecular docking and dynamic analysis; iv) an evaluation of the gastrointestinal (GI) stability of selected peptides by in vitro simulated digestion.

Finally, **Part III** presents the concluding remarks and the impact of this thesis on the field of microalgae bioactive peptides. In addition, the appendix contains my contributions to other two projects: i) the analysis of lupin proteins in lupin-enriched pasta and ii) the physicochemical and conformational evaluation of ultrasound-driven proteins extracted from soybean okara byproducts. By this additional work, I acquired more skills of proteome and physicochemical analysis.

Part I.

State of the art

CHAPTER 1

1. Introduction

1.1. Microalgae as a Promising Source of Proteins and Peptides

Microalgae are a group of simple organisms usually with dimensions between 3 and 20 μm that are prevalently autotrophic, i.e., capable of converting CO_2 and minerals to biomass by photosynthesis. The human consumption of microalgae dates back to very ancient times. Some edible microalgae species, such as *Nostoc commune, Arthrospira platensis* (spirulina), and *Aphanizomenon flos-aquae* have been used as food for thousands of years. Whereas in the 1960s and 1970s, the interest in microalgae had mainly the scope of providing protein supplements to meet the increasing demand of protein linked to the exponential growth of the world population, nowadays numerous studies have proven that these organisms are promising unconventional foods, since they exert a good nutritive value, being rich in nutrients, such as proteins, polyunsaturated fatty acids, polysaccharides, vitamins, pigments, and microelements. Due to commercial factors, market demand, specific preparations, and European food safety regulations, the most dominant species currently in the European market are spirulina and *Chlorella vulgaris*, whereas extracts of *Dunaliella salina*, *Haematococcus pluvialis*, or *Crypthecodinium cohnii* are commercialized for their high content of β-carotene, astaxanthin, or docosahexaenoic acid, respectively.

1.2. Microalgae Mass Cultivation and Protein Content

The mass cultivation of microalgae has been assessed for the production of sustainable biomass and high-value products, intended for human and animal consumption, and used by industries for chemical and biofuel production. The industrial culture of spirulina, a blue-green microalga, was started in the 1960s and 1970s and its large-scale production and commercialization have been already accomplished. As reported by

FAO the global production of spirulina in 2014 has achieved 86,000 tonnes. Classified based on the used carbon source, microalgae are generally cultured under three conditions: photoautotrophy, heterotrophy, and mixotrophy, matching open-ponds and closed photobioreactors (PBRs), the two mostly used culture systems.(Christien, Matthias, Maria, Lolke, Mauro, Claudia, et al., 2014) The selection and optimization of culture mode ensures the biomass productivity as protein source. In addition, high protein yield of microalgae could be achieved by optimizing the culture parameters. Environment factors, such as pH, temperature, light intensity, CO_2 concentration and nitrogen source, can easily affect the chemical composition of microalgae cells. Literatures suggests that the protein accumulation in microalgae generally prefers the suitable culture medium with sufficient nitrogen otherwise nitrogen starvation can lead the degradation of the protein to serve as the nitrogen source (Lupatini, Colla, Canan, & Colla, 2017; Soto-Sierra, Stoykova, & Nikolov, 2018). The addition of yeasts as source of nitrogen-supplements into culture medium is reported as a good and common practice for enhancing biomass and protein accumulation. This is the case of *Tetraselmis sp*. that utilizes organic nitrogen from yeast extract for both growth and protein accumulation (Kim, Mujtaba, & Lee, 2016). Nevertheless, the industrial goal of any cultivation process is to attain both high protein yield (g protein/g biomass) and biomass productivity (g biomass/L culture). In order to give an overview of protein levels in microalgae, **Table 1.1** collects the data of the three major nutrients in some microalgae species comparing them to some common foods. Although the microalgae protein content varies in the different species, it appears to be comparable or sometimes even superior than that of conventional foods. For example, spirulina, has a very high content of protein (46-71% on dry weight). (Lupatini, Colla, Canan, & Colla, 2017)

Table 1.1 General composition of different conventional food sources and microalgae (% of dry biomass)

Species	Protein	Carbohydrate	Lipid
Meat	43	1	34
Milk	26	38	28
Soybean	37	30	20
Wheat	13	71	1.5
Arthrospira maxima	60-71	13-16	6-7
Chlorella vulgaris	51-58	12-17	14-22
Dunaliella sp.	20-57	12.2-32	6-15
Haematococcus pluvialis	17-27	37-40	25
Nannochloropsis sp.	35	7.8	18
Nitzchia sp.	26	9.8	13
Phaeodactylum tricornutum	30	8.4	14
Scenedesmus obliquus	50-56	10-17	12-14
Arthrospira platensis	46-63	8-14	4-9

Interestingly, microalgae show a competitive amino acid pattern (**Table 1.2**) (Becker, 2007; Sui, Muys, Vermeir, D'Adamo, & Vlaeminck, 2019). In terms of the presence of indispensable amino acids (IAA), the content generally matches well that in conventional foods. Based on the IAA content and the digestibility of each amino acid, digestible IAA score (DIAAS), the newest protein quality measure recommended by FAO (FAO, 2011) in 2011, has been calculated as shown in **Table 1.2** This parameter depends on the lowest value of the digestible IAA reference ratio. For example, the DIAAS of *Chlorella sp.* is related to histidine, which has the lowest digestible reference ratio among all the IAA. Compared with high quality daily foods (i.e., egg and soybean), *Chlorella sp.* presents a higher DIAAS, while the other four microalgae species are inferior to different extents. One reason for this is the low content of one single amino acid, which limits the overall protein quality. This is the case, for example, of tryptophan in spirulina and *Scenedesmus obliquus*. Another reason lies in the rigid cell wall of most microalgae species, which is a key constraint factor to the bioavailability of nutrients. Encouragingly, with the help of suitable techniques in the downstream processing of microalgae, such as ball-milling and homogenization, the cell wall can be effectively disrupted, thus increasing the digestibility of microalgae nutrients as well as improving the protein quality (Neumann, Derwenskus, Gille, Louis, Schmid-Staiger, Briviba, et al., 2018).

Table 1.2 IAA profile and DIAAS of several microalgae species and conventional food source

Source	IAA content (mg/g protein) [a]									DIAAS (%)
	His	*Ile*	*Leu*	*Lys*	*SAA*	*AAA*	*Thr*	*Trp*	*Val*	
IAA reference pattern [b]	16	30	61	48	23	41	25	6.6	40	-
Egg (row)	24	66	88	53	55	100	50	17	72	74 (Leu)
Egg (cooked)	24	66	88	53	55	100	50	17	72	100 (Lys)
Soybean (cooked)	26	53	77	64	32	87	40	14	53	97 (SAA)
Chlorella sp.	20	38	88	84	36	84	48	21	55	111 (His)
Nannochloropsis sp.	21	48	78	61	20	104	55	16	65	23 (His)
Phaeodactylum tricornutum	17	49	56	56	23	107	54	16	59	75 (Leu)
Scenedesmus obliquus	21	36	73	56	21	80	51	3	60	40 (Trp)
Arthrospira platensis	22	67	98	48	34	106	62	3	71	34 (Trp)

[a] His, histidine; Ile, isoleucine; Leu, leucine; Lys, lysine; SAA, sulfur amino acids (methionine and cystine); AAA, aromatic amino acids (phenylalanine and tyrosine); Thr, threonine; Trp, tryptophan; Val, valine. [b] The IAA reference pattern is especially for the population group of older children, adolescents, and adults, as recommended by the FAO criterion.[15]

As microalgae display huge potential in nutritional and pharmacological applications, it is necessary to prove their safety by severe toxicity assessment. A report by the European Commission listed 23 microalgae genus or species used for food or feed consumption (Christien, et al., 2014). Among them spirulina, *Chlorella sp., Porphyridium cruentum*, *Crypthecodinium cohnii* have received the GRAS (generally recognized as safe) status by the US FDA (Food and Drug Administration). Others, such as *Chlamydomonas reinhardtii*, *H. pluvialis*, *Dunaliella sp*, *Navicula sp*., *Nitzschia dissipata*, *Phaeodactylum tricornutum* have been declared to have no toxic effects (Soto-Sierra, Stoykova, & Nikolov, 2018), which means that they do not produce toxins. However, there is the important issue of environment contaminants, such as pathogens, heavy metals, and pesticides (van der Spiegel, Noordam, & van der Fels-Klerx, 2013). In particular, heavy metals contamination is one of the prominent issues, affecting the microalgae cultivation, because as the bottom of the aquatic food chain, microalgae may easily accumulate heavy metals (e.g., mercury, cadmium, arsenic), which could induce severe side effects to human health (Barkia, Saari, & Manning, 2019; Gilroy, Kauffman, Hall, Huang, & Chu, 2000). According to World Health Organization (WHO), the level of heavy metals in algae biomass destined for human consumption should not exceed the following thresholds: Pb <0.1 ppm, Hg <0.001 ppm, Cd <0.01 ppm, As <0.05 ppm, meeting, therefore, the quality standards for conventional foods (Matos, 2017).

The fact that, microalgae proteins possess unique advantage in health benefits and bioactivity under strict supervision, supports the exploration of microalgae in nutritional development (Neumann, et al., 2018). Phycobiliproteins are a group of brilliantly colored and highly fluorescent protein-pigment components of the photosynthetic light-harvesting antenna complexes, generally existing in cyanobacteria, red algae and some cryptomonads (Neumann, et al., 2018). Commercially used as natural colorants in food and cosmetic industries as well as fluorescent markers in biomedical research and clinical diagnostics, phycobiliproteins have drawn much attention for their therapeutic value, since various biological properties have been reported in literature. Phycocyanin, the most significant member of the

phycobiliproteins family, has been mostly studied. The phycocyanin-oral treatment of numerous animal models has revealed a broad spectrum of bioactivities, including the anti-inflammatory, anti-cancer, antimicrobial, and antioxidant activities, with a protective function of multiple organs and tissues, such as heart, lung, liver, kidney, pancreas, eyes, and brain (Fernandez-Rojas, Hernandez-Juarez, & Pedraza-Chaverri, 2014; Gdara, Belgacem, Khemiri, Mannai, & Bitri, 2018). Currently, the active species are supposed to be some peptides released from phycocyanin hydrolysis and not the protein itself. In particular, 5 peptides, identified in a hydrolysate obtained by treating phycocyanin with pepsin in a simulated gastric fluid, have been proven to have significant antioxidant and metal-chelating activities and have shown cytotoxic effects on human cervical adenocarcinoma and epithelial colonic cancer cell lines (Minic, Stanic-Vucinic, Mihailovic, Krstic, Nikolic, & Cirkovic Velickovic, 2016). It is important however to underline that, although available literature is very promising, many studies are still necessary for a complete exploration of the bioactivities of peptides from phycocyanin or phycobiliproteins and other microalgae proteins.

1.3. Biological activities of microalgae-derived peptides

In this study, literature information was collected by means of ScienceDirect database using the keywords “microalgae bioactive peptides”. **Figure 1.1** indicates that a significant increase of the number of papers published annually has taken place in the period from 1995 to May 2019, with an increasing frequency in the last decade. The continuously rising research output suggests the enormous potential value of microalgae-derived bioactive peptides. On the basis of the numerous reports, microalgae bioactive peptides have shown promising effects that are useful in cardiovascular disease (CVD) prevention, i.e., the antioxidant, anti-inflammatory, anti-dyslipidemic, antidiabetic, and antihypertensive activities. In this dissertation, antidiabetic and antihypertensive properties are taken into consideration.

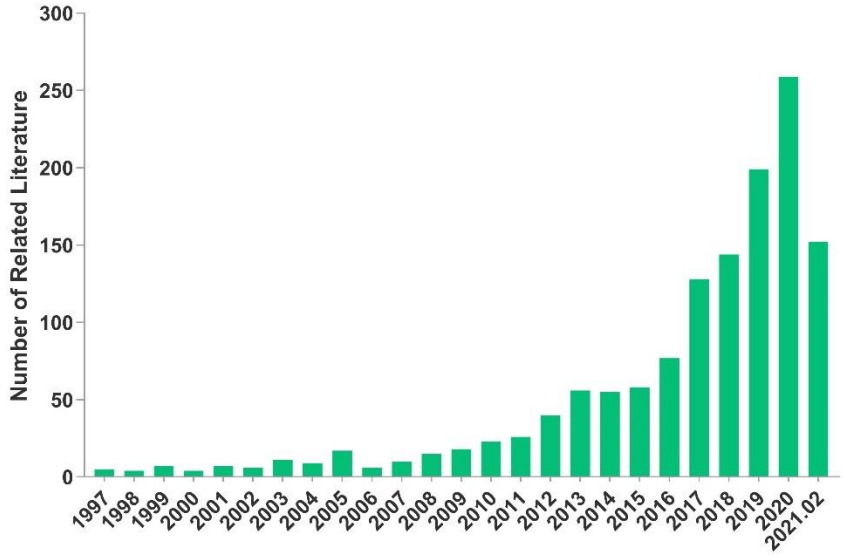

Figure 1.1 Number of papers about microalgae published from 1995 to February 2021.

1.3.1 Antidiabetic Activity

Diabetes is a chronic disease with the feature of high glucose levels in the circulatory system. Diabetes mellitus and its complications, such as cardiovascular disease, nephropathy, retinopathy, amputation, and nerve damage, are one of the major causes of mortality, accounting for 14.5% of global mortality among people aged 20−79 years (Santos Ade, Cecilio, Teston, de Arruda, Peternella, & Marcon, 2015).

Several bioactive peptides have been discovered with potential antidiabetic effects, and microalgae peptides have provided some encouraging results (**Table 1.3**). After *in vivo* gastrointestinal digestion, phycocyanin shows notable preventive effects on the development of diabetes through multiple mechanisms of action. In particular, it promotes the normalization of glucose and lipid metabolism in alloxan-induced diabetic mice by activating the insulin signaling pathway and glucokinase (GK) expression in the pancreas and liver (Ou, Lin, Pan, Yang, & Cheng, 2012a; Ou, Ren, Wang, & Yang, 2016). This kind of animal model features the destruction of pancreatic β cells, which is the main cause of type 1 diabetes. Other research has revealed that digested phycocyanin has therapeutic effects on mice with type 2 diabetes, manifesting as insulin resistance and decreases insulin sensitivity. The administration of phycocyanin

significantly ameliorated the glucolipid metabolism indices, improving peripheral target tissue responses to insulin regulation (Y. Ou, L. Lin, X. Yang, Q. Pan, & X. Cheng, 2013). In addition, the oral administration of phycocyanin protected mice with type 2 diabetes against diabetic nephropathy. This might occur via the antioxidant effects of phycocyanin on urinary and renal oxidative stress markers, favoring the normalization of NAD(P)H expression after treatment (Zheng, Inoguchi, Sasaki, Maeda, McCarty, Fujii, et al., 2013). The reduction of the activity of peptidyl-peptidase IV (DPPIV, EC 3.4.14.5), a new therapeutic target for type 2 diabetes, makes it possible to investigate the antidiabetic activities of the bioactive compounds *in vitro*. DPP-IV can degrade incretins, including glucagon-like peptide 1 (GLP-1) and glucose inhibitory polypeptide (GIP), resulting in loss of their ability to enhance insulin secretion (Koska, Sands, Burciu, & Reaven, 2015). Hence, the inhibition of DPP-IV feasibly improves insulin activity. It has been reported that protein hydrolysates from *Porphyridium purpureum* and *P. tricornutum* exhibit *in vitro* antidiabetic activity by inhibiting the effect of DPP-IV, with IC_{50} values of 2.28 and 2.68 mg/mL, respectively (Xu, Hong, Wu, & Yan, 2019). Six tripeptides from *C. vulgaris* have been identified by in silico gastrointestinal digestion as potential inhibitors of DPP-IV activities and then synthesized. Among them, two peptides (i.e., VPW and IPR) have shown the highest DPP-IV inhibitory activities both *in vitro* (IC_{50} values of 348.6 and 376.6 μM, respectively) and in mice serum (IC_{50} values of 2.5 and 2.7 mM, respectively). These are acceptable but not excellent data, when they are compared with the DPP-IV inhibitory activities exerted by peptides derived from different dietary proteins, such as IPI, WR, and IPIQY, which have IC_{50} values of 3.5, 37.8, and 35.2 μM, respectively (Nongonierma & FitzGerald, 2014). In addition, these two peptides have been confirmed to be resistant to gastrointestinal proteolysis and to enter the circulation in order to exert their activity. Interestingly, these peptides have Pro and Ala residues as the penultimate N-terminal residues and hydrophobic amino acids as the N-terminal amino acids. The structure−activity relationships of DPP-IV inhibitory peptides are based on numerous studies: a hydrophobic or aromatic amino acid at the N-terminus facilitates the binding of the peptides to DPP-IV, whereas a Pro or Ala residue at the

second N-terminal site contributes to DPP-IV inhibition. DPP-IV is in fact a post-proline-cleaving enzyme that especially removes Xaa−Pro and Xaa−Ala (Xaa being an amino acid residue) dipeptides from the N-termini of polypeptides (Q. Zhu, X. Chen, J. Wu, Y. Zhou, Y. Qian, M. Fang, et al., 2017).

Table 3. Anti-diabetic peptides derived from microalgae

Peptides	Protein Source	Hydrolytic enzyme	*In vitro/in vivo*	Mechanism of action and Potency	References
Digested phycocyanin	*Arthrospira platensis*	Gastrointestinal digestion	*In vivo* (mice with type 1 diabetes)	Activation of insulin signaling pathway and GK expression	(Ou, Lin, Pan, Yang, & Cheng, 2012; Ou, Ren, Wang, & Yang, 2016)
Digested phycocyanin	*Arthrospira platensis*	Gastrointestinal digestion	*In vivo* (mice with type 2 diabetes)	Improving the sensitivity of tissues to the insulin regulation	(Ou, Lin, Yang, Pan, & Cheng, 2013)
Digested phycocyanin	*Arthrospira platensis*	Gastrointestinal digestion	*In vivo* (mice with type 2 diabetes)	Alleviation of the diabetic nephropathy; decrease of the oxidant stress in urine and kidney	(Zheng, Inoguchi, Sasaki, Maeda, McCarty, Fujii, et al., 2013)
Protein hydrolysates	*Porphyridium purpureum*	Alcalase, Flavourzyme	*In vitro*	DPP-IV inhibition (IC_{50} 2.28 mg/mL)	(*Stack*, *Le Gouic*, A.*V.*, *P.R.*, *F.*, & *FitzGerald*, 2018)
Protein hydrolysates	*Phaeodactylum tricornutum*	Alcalase, Flavourzyme	*In vitro*	DPP-IV inhibition (IC_{50} 2.68 mg/mL)	(*Stack*, *Le Gouic*, A.*V.*, *P.R.*, *F.*, & *FitzGerald*, 2018)
VPW IPR	*Chlorella vulgaris*	Virtual digestion (pepsin, trypsin, chymotrypsin)	*In vitro* and in mouse serum	DPP-IV inhibition (IC_{50} of VPW 348.6 μM, IC_{50} of IPR 376.6 μM)	(Zhu, Chen, Wu, Zhou, Qian, Fang, et al., 2017)

1.3.2 Hypotensive Activity

Hypertension is another major risk factor in the development of CVD. Many serious diseases, such as chronic kidney failure, stroke, coronary events, and heart failure, are caused by persistent hypertension (FitzGerald, Murray, & Walsh, 2004). Angiotensin I converting enzyme (ACE, EC 3.4.15.1) is a main therapeutic target for the development of antihypertensive drugs, because the inhibition of ACE leads to a decrease in vasoconstrictor angiotensin II and an increase in vasodilator bradykinin, thus resulting in an antihypertensive effect (Lu, Ren, Xue, Sawano, Miyakawa, & Tanokura, 2010). Interacting with the ACE structure, food-derived peptides have been verified to exert huge potentials in fighting against hypertension and more and more active peptides are continuously discovered from various protein sources, including microalgae. **Table 1.4** lists ACE-inhibitory microalgae peptides. A recent review summarizes the major findings about microalgae peptides with antihypertensive activity (Ejike, Collins, Balasuriya, Swanson, Mason, & Udenigwe, 2017). Twelve sequences derived from *C. vulgaris*, *Chlorella sorokiniana*, spirulina, and *T. obliquus* are listed, among which peptide IAPG, derived from spirulina, gave the most potent ACE-inhibitory effect, with an IC_{50} value of 11.4 μM. Two more efficient ACE-inhibiting peptides, GPDRPKFLGPF and WYGPDRPKFL, have been identified in an Alcalase hydrolysate of *T. obliquus* proteins with IC_{50} values of 5.73 and 0.82 μM, respectively (Montone, Capriotti, Cavaliere, La Barbera, Piovesana, Zenezini Chiozzi, et al., 2018). In another study, after hot water extraction, the residues of *C. sorokiniana* were hydrolyzed by protease N, which was followed by gastrointestinal enzymatic hydrolysis. After fractionation, the most active fraction was identified to include three ACE-inhibitory dipeptides, VW, IW, and LW, with IC_{50} values of 0.58, 0.50, and 1.11 μM, respectively. Because dipeptides may derive from numerous different proteins, these hypotensive dipeptides have been also identified from other protein sources, such as ovalbumin and salmon (Lin, Chen, Yeh, Song, & Tsai, 2018). Interestingly, the oral administration of 10 mg/kg/day IQP, VEP, or a spirulina protein hydrolysate for 6 weeks to spontaneously hypertensive rats (SHRs) resulted in evident antihypertensive effects. IQP, VEP, and the

spirulina hydrolysate decreased rat blood pressure by affecting the expression of local kidney renin angiotensin system components via the downregulation of ACE, its enzymatic product angiotensin II (Ang-II), and angiotensin type 1 receptor (AT 1), while upregulating angiotensin-converting enzyme 2 (ACE2), Ang (1−7), Mas, and angiotensin type 2 receptor (AT 2), thus promoting a protective effect against CVD (Lin, Chen, Yeh, Song, & Tsai, 2018).

Two tripeptides, TTW and VHW, from *C. vulgaris* have been shown to be noncompetitive ACE inhibitors *in vitro*, with IC_{50} values of 0.61 and 0.91 μM, respectively, and to confer considerable blood pressure decreases when administered to SHRs at relatively low dosages (Xie, Chen, Wu, Zhang, Zhou, Zhang, et al., 2018). These two peptides were sorted out from 4334 peptides produced by virtual gastrointestinal digestion of *C. vulgaris* proteins. The screening criterion was based on the *in silico* prediction of ACE-inhibiting IC_{50} values as well as on what was known of the structure−activity relationship in the case of ACE inhibitors. In fact, it is known that peptides with an aromatic or cyclic amino acid (i.e., Trp, Tyr, and Pro) as their C-terminal amino acids are very likely to be highly active. In addition, two ACE-inhibitory peptides, IQP and VEP, derived from spirulina, were identified with IC_{50} values of 5.77 and 27.36 μM (Lu, Ren, Xue, Sawano, Miyakawa, & Tanokura, 2010). In detail, IQP seems to show an IC_{50} comparable to those observed for IPP and VPP, two well-characterized milk-derived peptides whose IC_{50} values are 5 and 9 μM, respectively (FitzGerald, Murray, & Walsh, 2004). In agreement with the structure−activity relationship, IQP might exert great potential for further *in vivo* study.

Table 1.4 ACE-inhibitor peptides derived from microalgae protein hydrolysis

Protein Source	Hydrolytic enzyme	Peptide sequence	IC_{50} (μM)	Reference
Tetradesmus obliquus	Alcalase	GPDRPKFLGPF	5.73	(Montone, Capriotti, Cavaliere, La Barbera, Piovesana, Zenezini Chiozzi, et al., 2018)
		WYGPDRPKFL	0.82	
Chlorella sorokiniana	Protease N, pepsin, pancreatin	WV	307.61	(Lin, Chen, Yeh, Song, & Tsai, 2018)
		VW	0.58	
		IW	0.50	
		LW	1.11	
Chlorella vulgaris	*In silico* digestion (pepsin, trypsin, chymotrypsin)	TTW	0.61	(Xie, Chen, Wu, Zhang, Zhou, Zhang, et al., 2018)
		VHW	0.91	
Arthrospira platensis	Alcalase	IQP	5.77	(Lu, Ren, Xue, Sawano, Miyakawa, & Tanokura, 2010; Lu, Sawano, Miyakawa, Xue, Cai, Egashira, et al., 2011)
		VEP	27.36	
Spirulina sp.	Pepsin, Trypsin, α-chymotrypsin	TMEPGKP	132	(Heo, Ko, Kim, Oh, Ryu, Qian, et al., 2017)
	Pepsin	IAPG	11.4	(Suetsuna & Chen, 2001)

1.3.3 Multifunctional Peptides from Microalgae

Some microalgae peptides exhibit more than one biological activity and may be classified as multifunctional peptides, a new definition indicating peptides that can favorably modulate more than one physiological process by affecting different targets.[64] The multifunctionality of some peptides is closely related to the multiple factors of some illnesses and the common factors at the bases of different diseases. The most typical example is the undecapeptide VECYGPNRPQF, derived from *C. vulgaris*, which shows multiple effects, including antihypertensive, antioxidant, anti-inflammatory, antiatherosclerotic, and anticancer activities. It fights against inflammation and oxidant stress in endothelial cells and inhibits the production of histamine, intracellular ROS, and adhesion molecules, thus showing potential benefits against atherosclerosis (Sheih, Fang, Wu, & Lin, 2010; Shih, 2010). In addition, because of the prevention of oxidation-induced cell damage and inflammation in macrophages, this peptide effectively suppresses cell proliferation (Sheih, Fang, Wu, & Lin, 2010). Similarly, two peptides from spirulina, LDAVNR and MMLDF, have been recognized as multifunctional peptides with antioxidant, anti-inflammatory, antiatherosclerotic, and antiallergenic activity (Vo & Kim, 2013). The spirulina heptapeptide TMEPGKP inhibits the activity of ACE and is therefore hypotensive as well as antioxidative; thus, it is capable of improving vascular dysfunction and also hindering the development of hypertension. In detail, in human endothelial cells, the angiotensin II induced production of nitric oxide and reactive oxygen species is inhibited, and the expression of iNOS and endothelin 1 (ET-1) is downregulated when the cells are incubated with the purified peptide (Heo, Ko, Kim, Oh, Ryu, Qian, et al., 2017a).

Microalgae protein hydrolysates also provide different health benefits. In particular, digested phycocyanin is very interesting, because it is antioxidant, anti-inflammatory, antihyperlipidemic, and hypocholesterolemic *in vivo*. However, because a hydrolysate has a very complex composition, it is impossible to attribute the observed effects to different specific peptides, which greatly limits the research of multifunctional peptides in microalgae. This is a pity, considering the advantages of multifunctional peptides compared with those of monofunctional peptides (Lammi, Aiello, Boschin, & Arnoldi, 2019).

CHAPTER 2

2. Peptidomics in the Characterization of Microalgae

It is nowadays widely acknowledged that MS proteomic and peptidomic technologies are the gold standard for peptide analysis. Peptidomics has become an important tool for the characterization of bioactive peptides from food sources. The peptidomic strategy normally includes protein extraction, the release of peptides by one or more enzymes (i.e., gastrointestinal enzymes, trypsin, pepsin, or microbial enzymes), the subsequent separation and identification of peptides, and biological activity measurement. This strategy allows the identification and quantification of bioactive peptides even in very complex mixtures, such as protein hydrolysates, using complementary and mutually compatible approaches ranging from protein extraction to peptide analysis. Some important aspects to consider in a driven bioactive peptide discovery from microalgae are reported below.

2.1 Microalgae Protein Extraction: Technological Aspects.

Protein extraction from microalgae is one of the main limiting steps for the production of bioactive peptides, either in small or large scales (Lupatini, Colla, Canan, & Colla, 2017). Marine algae cell walls, generally consisting of polysaccharides such as cellulose and xylan and sometimes including sulfated polysaccharides, phenol compounds, glycoproteins, and proteoglycans, are recalcitrant tissues that offer robustness and resilience to disruption (Doi & Kosugi, 2004; Fan, Bai, Zhu, Yang, & Zhang, 2014). Algal cell walls with a high cellulose contents (e.g., those of *C. vulgaris*) exhibit lower digestibility than those with thinner, easier to break cell walls (e.g., those of spirulina) (Soto-Sierra, Stoykova, & Nikolov, 2018).

Furthermore, the proteins trapped inside the cell walls and cell organelles cannot exhibit their full functional potential if not adequately extracted. For this reason, it is crucially important to select for the best the cell disruption method, depending on the cell wall structure, product location, size, and solubility. Several extraction methods have been proposed in the literature for the extraction of soluble proteins from microalgae. These methods can be classified into physical and chemical. Physical ones involve mechanical

shear, such as bead milling, high-pressure homogenization, ultrasonication, and microfluidization. Electric fields and thermal treatments (thermal shock or microwaves) are also considered methods of physical extraction (Soto-Sierra, Stoykova, & Nikolov, 2018). Chemical and biochemical methods include the use of solvents, ionic liquids, pH shifts, and enzymatic hydrolysis (Gunerken, D'Hondt, Eppink, Garcia-Gonzalez, Elst, & Wijffels, 2015; Phong, Show, Ling, Juan, Ng, & Chang, 2018).

2.2 Microalgae Peptide Preparations

Microalgae-derived peptides are routinely produced by the use of commercial proteases (i.e., papain, trypsin, pepsin, and α-chymotrypsin, the last of which is used for releasing antioxidant peptides from marine *C. ellipsoidea* (Ko, Kim, & Jeon, 2012).) or by single enzymes (i.e., pepsin) to liberate new antioxidative peptides, such as VECYGPNRPQF, from algae protein waste (Sheih, Wu, & Fang, 2009). Food-grade enzyme such as Alcalase and Flavourzyme have been selected to hydrolyze the red microalga *P. purpureum* and the diatom *P. tricornutum*, which are endowed with antidiabetic and antioxidant properties (Stack, Gouic, A.V., P.R., F., & FitzGerald, 2018).

2.3 The Challenge of Bioactive Peptide Discovery

Microalgae protein hydrolysates are very complex and generally contain hundreds of peptides of different lengths and relative abundances, making comprehensive detection a challenge. To overcome this problem, the common traditional approach is based on various purification steps (ultrafiltration, preparative HPLC, etc.), resulting in several purified fractions, whose maintained or altered activity must be monitored after each single purification stage. However, purification of the peptide fractions from hydrolysates is an expensive and complex process. The isolation of a single peptide becomes an excessively difficult task, especially when a relatively large amount is required. Nevertheless, the use of these methodologies is widespread in microalgae bioactive peptide discovery. The heptameric peptide TMEPGKP, endowed with ACE-inhibitory activity, has been separated from a spirulina gastrointestinal hydrolysate after multiple purification steps (i.e., fast liquid chromatography on a HiPrep DEAE FF ion-exchange column, followed by further purification by permeation reversed-phase high-performance liquid chromatography (RP-HPLC) on a PrimeSphere ODS C_{18} column) (Heo, et al., 2017a).

Likewise, IVVE (an ACE-activity inhibitor with an IC_{50} of 315.3 μM), AFL (IC_{50} of 63.8 μM), FAL (IC_{50} of 26.3 μM), AEL (IC_{50} of 57.1 μM), and VVPPA (IC_{50} of 79.5 μM) from *C. vulgaris* and IAE (IC_{50} of 34.7 μM), FAL, AEL, IAPG (IC_{50} of 11.4 μM), and VAF (IC_{50} of 35.8 μM) from spirulina have been obtained by ion-exchange chromatography and gel filtration. Gel filtration chromatography and two step RP-HPLC have been employed to purify peptide IQP from an Alcalase digest of spirulina. Ultrafiltration using a membrane with a 10 kDa molecular weight cutoff (MWCO) has been instead used for the purification of three peptide fractions with antioxidant, antimicrobial, and anti-inflammatory activities from microalgae biomass. A novel antioxidant peptide, PNN, has been purified by ultrafiltration, gel filtration chromatography, and RP-HPLC (Montalvo, Thomaz-Soccol, Vandenberghe, Carvalho, Faulds, Bertrand, et al., 2019). However, fractionation often does not lead to the desired results: the fractionated peptides may have lost or reduced activities because of the lack of synergism.

2.4 New Directions in the Discovery and Quantification of Bioactive Peptides by Mass Spectrometry

Hydrolysates often contain more than a hundred peptides, which makes difficult the isolation of specific entities. Because some peptides may have comparable physicochemical properties (mass, hydrophobicity, charge, solubility, etc.), their separation and purification may be very hard and problematic. Recently, with the improved accuracy (high resolution) of MS analyzers and the use of various bioinformatic tools, the identification of peptides has become less challenging, and numerous peptide sequences can be detected simultaneously (Capriotti, Cavaliere, Piovesana, Samperi, & Lagana, 2016; Dallas, Guerrero, Parker, Robinson, Gan, German, et al., 2015; Panchaud, Affolter, & Kussmann, 2012; Piovesana, Capriotti, Cavaliere, La Barbera, Montone, Zenezini Chiozzi, et al., 2018; Sanchez-Rivera, Martínez-Maqueda, Cruz-Huerta, Miralles, & Recio, 2014). The tendency to avoid long and expensive fractionations prior to MS characterization has led to the use of unfractionated hydrolysates, which are routinely characterized by LC-MS/MS, allowing the assessment of gross peptide composition. In detail, the most popular approach used for peptide sequence identification is called shotgun proteomics based on data-dependent acquisition (DDA). Peptide identification is realized by comparing

MS/MS spectra derived from peptide fragmentation with theoretical tandem mass spectra generated from in silico digestion of a protein database.

Although the DDA approach allows exploratory analysis, it suffers from one limitation: its sensitivity is strongly sample-dependent. Moreover, the biased intrinsic nature of the DDA approach may cause inconsistent run-to-run reproducibility in peptide identification, especially when complex samples, such as food hydrolysates, are analyzed. The selection of the ions to fragment is "dependent" upon some criteria previously set up in the analytical method and is usually sorted on the basis of the abundance. Nevertheless, the peptide abundances in hydrolysates cover huge orders of magnitude, which makes it difficult to conduct a proper investigation with only the shotgun approach. Most intense peptides deriving from very abundant proteins are usually very well-characterized, whereas missing values are often observed for peptides deriving from less abundant proteins. To overcome these limitations, a relatively new approach called data-independent acquisition (DIA) has been developed (Gillet, Navarro, Tate, Röst, Selevsek, Reiter, et al., 2012). DIA fragments every single peptide in a sample (Liu, Huttenhain, Surinova, Gillet, Mouritsen, Brunner, et al., 2013). In this mode, instead of selecting one specific ion for fragmentation, all peptide ions present into the mass analyzer are fragmented. The fragmentation is "independent" of any ion characteristics (such as the abundance). Because the entire precursor mass range is fragmented, no gaps in the data take place, and run-to-run reproducibility is extremely high. Therefore, the unbiased nature of data-independent acquisition makes it the best technique for discovery proteomics. This new methodology has been recently applied as a different method for shotgun proteomics to identify proteins of *C. vulgaris* in order to select the best extraction protocols (Gao, Lim, Lin, & Li, 2016). The ability to comprehensively identify peptides in very complex matrices over a large dynamic range and in an extremely reproducible mode opens up a world of application possibilities to bioactive peptide analysis by DIA. Because in addition to structure elucidation, the interest is to get information about the abundances of such bioactive peptides, MS quantitative approaches, including absolute or relative quantification of peptides by using labeled or label-free methodologies, are currently adopted. Although labeled methods provide the most accurate quantitative results, they demand complex experimental setup and expensive isotope labels. In contrast, label-free methodologies allow easy, reliable, versatile, and cost-effective quantification. Peak intensity or spectral counting are the most employed techniques for label-free quantification,

allowing precise and accurate evaluation of changes in abundance between samples (Bantscheff, Schirle, Sweetman, Rick, & Kuster, 2007; Gallego, Mora, & Toldrá, 2018). In addition to relative quantification, absolute quantification based on multiple reaction monitoring (MRM) using either label-based or label-free reagents is actually the most frequent strategy used to quantify the total levels of a given peptide in a sample within a wide linear range. In MRM experiments, multiple pre-established pairs of precursor and product ions, known as MRM transitions, are used concurrently with the retention times to detect and quantify peptides. Label-free targeted MRM has been widely adopted to quantify food-derived peptides. Absolute quantification using MRM has been also applied to bioactive ACE-inhibitory tripeptides extracted from rye malt sourdoughs, which show the highest concentrations in gluten sourdoughs fermented with *Lactobacillus reuteri* (Hu, Stromeck, Loponen, Lopes-Lutz, Schieber, & Gänzle, 2011), as well as during the bread-making process (Zhao, Hu, Schieber, & Gänzle, 2013). This approach has also been used to verify the absorption of the ACE-inhibitory dipeptide VY into the blood of SHR after administration and to detect the maximal absorption amount (Nakashima, Kudo, Iwaihara, Tanaka, Matsumoto, & Matsui, 2011). Despite its widespread use, to the best of our knowledge, no microalgae peptides have been quantified by a targeted approach so far. However, even if MRM is considered as the golden standard for peptide quantification, essentially because of its excellent reproducibility and quantitative accuracy for proteins and peptides spanning over 5 orders of magnitude (Picotti, Bodenmiller, Mueller, Domon, & Aebersold, 2009), it remains limited in the total number of targeted peptides. In addition, the development of a MRM assay requires prior knowledge of the peptide sequences to be quantified, a condition that rarely occurs in the field of food peptidomics. To overcome these limitations, the new MS data-independent acquisition coupled with peptide spectral library matching is able to provide label-free quantification in an MRM-like manner, showing higher quantification accuracy and precision (Huang, Yang, Luo, Guo, Wang, Yang, et al., 2015). In detail, targeted data extraction, at both the MS (precursor ion) and MS/MS (product ion) levels, coupled to matching against prerecorded spectral libraries, provides quantitative abilities similar to those of MRM analysis (Gillet, et al., 2012). A similar approach has been applied for quantifying proteins extracted from the green algae *C. vulgaris* using different methods (i.e., the direct lysis buffer method, TCA-acetone method, phenol method, and phenol/TCA-acetone method). This strategy has been also efficiently applied for the relative quantification of barley gluten in

selectively bred barley lines (Colgrave, Byrne, Blundell, Heidelberger, Lane, Tanner, et al., 2016). These findings highlight the clear benefit of data-independent analysis, which allows the use of non-tryptic peptide fragments identified in discovery experiments to examine the relative levels of C-hordeins, a family of trypsin-resistant gluten proteins, without the need for an alternative proteolytic strategy (Colgrave, et al., 2016). Because many hydrolysates are produced by the use of different food-grade enzymes (e.g., Alcalase, Protamex, and Flavourzyme), which are characterized by low cutting specificity, data-independent acquisition would be considerably beneficial in the analysis of biopeptides from microalgae. Definitively, by bridging the gap between discovery and targeted proteomics, this new method is very promising in food technology and nutrition, because of its ability to allow the identification and quantification of low-abundance peptides.

References

Bantscheff, M., Schirle, M., Sweetman, G., Rick, J., & Kuster, B. (2007). Quantitative mass spectrometry in proteomics: a critical review. *Anal Bioanal Chem, 389*(4), 1017-1031.

Barkia, I., Saari, N., & Manning, S. R. (2019). Microalgae for High-Value Products Towards Human Health and Nutrition. *Mar Drugs, 17*(5).

Becker, E. W. (2007). Micro-algae as a source of protein. *Biotechnol Adv, 25*(2), 207-210.

Capriotti, A. L., Cavaliere, C., Piovesana, S., Samperi, R., & Lagana, A. (2016). Recent trends in the analysis of bioactive peptides in milk and dairy products. *Anal Bioanal Chem, 408*(11), 2677-2685.

Christien, E., Matthias, P., Maria, B., Lolke, S., Mauro, V., Claudia, P., & Emilio, R. C. (2014). Microalgae-based products for the food and feed sector: an

outlook for Europe. In). EUR - Scientific and Technical Research Reports.

Colgrave, M. L., Byrne, K., Blundell, M., Heidelberger, S., Lane, C. S., Tanner, G. J., & Howitt, C. A. (2016). Comparing Multiple Reaction Monitoring and Sequential Window Acquisition of All Theoretical Mass Spectra for the Relative Quantification of Barley Gluten in Selectively Bred Barley Lines. *Analytical Chemistry, 88*(18), 9127-9135.

Dallas, D. C., Guerrero, A., Parker, E. A., Robinson, R. C., Gan, J., German, J. B., Barile, D., & Lebrilla, C. B. (2015). Current peptidomics: applications, purification, identification, quantification, and functional analysis. *Proteomics, 15*(5-6), 1026-1038.

Doi, R. H., & Kosugi, A. (2004). Cellulosomes: Plant-cell-wall-degrading enzyme complexes. *Nature Reviews Microbiology, 2*(7), 541-551.

Ejike, C. E. C. C., Collins, S. A., Balasuriya, N., Swanson, A. K., Mason, B., & Udenigwe, C. C. (2017). Prospects of microalgae proteins in producing peptide-based functional foods for promoting cardiovascular health. *Trends in Food Science & Technology, 59*, 30-36.

Fan, X. D., Bai, L., Zhu, L., Yang, L., & Zhang, X. W. (2014). Marine Algae-Derived Bioactive Peptides for Human Nutrition and Health. *J Agric Food Chem, 62*(38), 9211-9222.

FAO. (2011). Dietary protein quality evaluation in human nutrition. In). Report of an FAO Expert Consultation.

Fernandez-Rojas, B., Hernandez-Juarez, J., & Pedraza-Chaverri, J. (2014). Nutraceutical properties of phycocyanin. *Journal of Functional Foods, 11*, 375-392.

FitzGerald, R. J., Murray, B. A., & Walsh, D. J. (2004). Hypotensive Peptides from Milk Proteins. *The Journal of Nutrition, 134*(4), 980S-988S.

Gallego, M., Mora, L., & Toldrá, F. (2018). Perspectives in the Use of Peptidomics in Ham. *Proteomics, 18*(18), 1700422.

Gao, Y., Lim, T. K., Lin, Q., & Li, S. F. Y. (2016). Evaluation of sample extraction methods for proteomics analysis of green algae Chlorella vulgaris. *Electrophoresis, 37*(10), 1270-1276.

Gdara, N. B., Belgacem, A., Khemiri, I., Mannai, S., & Bitri, L. (2018). Protective effects of phycocyanin on ischemia/reperfusion liver injuries. *Biomed Pharmacother, 102*, 196-202.

Gillet, L. C., Navarro, P., Tate, S., Röst, H., Selevsek, N., Reiter, L., Bonner, R., & Aebersold, R. (2012). Targeted data extraction of the MS/MS spectra generated by data-independent acquisition: a new concept for consistent and accurate proteome analysis. *Molecular & cellular proteomics : MCP, 11*(6), O111.016717-O016111.016717.

Gilroy, D. J., Kauffman, K. W., Hall, R. A., Huang, X., & Chu, F. S. (2000). Assessing potential health risks from microcystin toxins in blue-green algae dietary supplements. *Environ Health Perspect, 108*(5), 435-439.

Gunerken, E., D'Hondt, E., Eppink, M. H., Garcia-Gonzalez, L., Elst, K., & Wijffels, R. H. (2015). Cell disruption for microalgae biorefineries. *Biotechnol Adv, 33*(2), 243-260.

Heo, S. Y., Ko, S. C., Kim, C. S., Oh, G. W., Ryu, B., Qian, Z. J., Kim, G., Park, W. S., Choi, I. W., Phan, T. T., Heo, S. J., Kang, D. H., Yi, M., & Jung, W. K. (2017a). A heptameric peptide purified from Spirulina sp. gastrointestinal hydrolysate inhibits angiotensin I-converting enzyme- and angiotensin II-induced vascular dysfunction in human endothelial cells. *Int J Mol Med, 39*(5), 1072-1082.

Heo, S. Y., Ko, S. C., Kim, C. S., Oh, G. W., Ryu, B., Qian, Z. J., Kim, G., Park, W. S., Choi, I. W., Phan, T. T., Heo, S. J., Kang, D. H., Yi, M., & Jung, W. K. (2017b). A heptameric peptide purified from Spirulina sp. gastrointestinal hydrolysate inhibits angiotensin I-converting enzyme- and angiotensin II-induced vascular dysfunction in human endothelial cells. *Int J Mol Med, 39*(5), 1072-1082.

Hu, Y., Stromeck, A., Loponen, J., Lopes-Lutz, D., Schieber, A., & Gänzle, M. G. (2011). LC-MS/MS Quantification of Bioactive Angiotensin I-Converting Enzyme Inhibitory Peptides in Rye Malt Sourdoughs. *J Agric Food Chem, 59*(22), 11983-11989.

Huang, Q., Yang, L., Luo, J., Guo, L., Wang, Z., Yang, X., Jin, W., Fang, Y., Ye, J., Shan, B., & Zhang, Y. (2015). SWATH enables precise label-free quantification on proteome scale. *Proteomics, 15*(7), 1215-1223.

Kim, G., Mujtaba, G., & Lee, K. (2016). Effects of nitrogen sources on cell growth and biochemical composition of marine chlorophyte Tetraselmis sp for lipid production. *Algae, 31*(3), 257-266.

Ko, S. C., Kim, D., & Jeon, Y. J. (2012). Protective effect of a novel antioxidative peptide purified from a marine Chlorella ellipsoidea protein against free radical-induced oxidative stress. *Food and Chemical Toxicology, 50*(7), 2294-2302.

Koska, J., Sands, M., Burciu, C., & Reaven, P. (2015). Cardiovascular effects of dipeptidyl peptidase-4 inhibitors in patients with type 2 diabetes. *Diab Vasc Dis Res, 12*(3), 154-163.

Lammi, C., Aiello, G., Boschin, G., & Arnoldi, A. (2019). Multifunctional peptides for the prevention of cardiovascular disease: A new concept in the area of bioactive food-derived peptides. *Journal of Functional Foods, 55*, 135-145.

Lin, Y. H., Chen, G. W., Yeh, C. H., Song, H., & Tsai, J. S. (2018). Purification and Identification of Angiotensin I-Converting Enzyme Inhibitory Peptides and the Antihypertensive Effect of Chlorella sorokiniana Protein Hydrolysates. *Nutrients, 10*(10).

Liu, Y. S., Huttenhain, R., Surinova, S., Gillet, L. C. J., Mouritsen, J., Brunner, R., Navarro, P., & Aebersold, R. (2013). Quantitative measurements of N-linked glycoproteins in human plasma by SWATH-MS. *Proteomics, 13*(8), 1247-1256.

Lu, J., Ren, D. F., Xue, Y. L., Sawano, Y., Miyakawa, T., & Tanokura, M. (2010). Isolation of an antihypertensive peptide from alcalase digest of Spirulina platensis. *J Agric Food Chem, 58*(12), 7166-7171.

Lu, J., Sawano, Y., Miyakawa, T., Xue, Y. L., Cai, M. Y., Egashira, Y., Ren, D. F., & Tanokura, M. (2011). One-Week Antihypertensive Effect of Ile-Gln-Pro in Spontaneously Hypertensive Rats. *J Agric Food Chem, 59*(2), 559-563.

Lupatini, A. L., Colla, L. M., Canan, C., & Colla, E. (2017). Potential application of microalga Spirulina platensis as a protein source. *J Sci Food Agric, 97*(3), 724-732.

Matos, A. P. (2017). The Impact of Microalgae in Food Science and Technology. *Journal of the American Oil Chemists Society, 94*(11), 1333-1350.

Minic, S. L., Stanic-Vucinic, D., Mihailovic, J., Krstic, M., Nikolic, M. R., & Cirkovic Velickovic, T. (2016). Digestion by pepsin releases biologically active chromopeptides from C-phycocyanin, a blue-colored biliprotein of microalga Spirulina. *J Proteomics, 147*, 132-139.

Montalvo, G. E. B., Thomaz-Soccol, V., Vandenberghe, L. P. S., Carvalho, J. C., Faulds, C. B., Bertrand, E., Prado, M. R. M., Bonatto, S. J. R., & Soccol, C. R. (2019). Arthrospira maxima OF15 biomass cultivation at laboratory and pilot scale from sugarcane vinasse for potential biological new peptides production. *Bioresour Technol, 273*, 103-113.

Montone, C. M., Capriotti, A. L., Cavaliere, C., La Barbera, G., Piovesana, S., Zenezini Chiozzi, R., & Lagana, A. (2018). Peptidomic strategy for purification and identification of potential ACE-inhibitory and antioxidant peptides in Tetradesmus obliquus microalgae. *Anal Bioanal Chem, 410*(15), 3573-3586.

Nakashima, E. M. N., Kudo, A., Iwaihara, Y., Tanaka, M., Matsumoto, K., & Matsui, T. (2011). Application of 13C stable isotope labeling liquid chromatography–multiple reaction

monitoring–tandem mass spectrometry method for determining intact absorption of bioactive dipeptides in rats. *Analytical Biochemistry, 414*(1), 109-116.

Neumann, U., Derwenskus, F., Gille, A., Louis, S., Schmid-Staiger, U., Briviba, K., & Bischoff, S. C. (2018). Bioavailability and Safety of Nutrients from the Microalgae Chlorella vulgaris, Nannochloropsis oceanica and Phaeodactylum tricornutum in C57BL/6 Mice. *Nutrients, 10*(8).

Nongonierma, A. B., & FitzGerald, R. J. (2014). An in silico model to predict the potential of dietary proteins as sources of dipeptidyl peptidase IV (DPP-IV) inhibitory peptides. *Food Chem, 165*, 489-498.

Ou, Y., Lin, L., Pan, Q., Yang, X., & Cheng, X. (2012a). 1 Preventive effect of phycocyanin from Spirulina platensis on alloxan-injured mice. *Environ Toxicol Pharmacol, 34*(3), 721-726.

Ou, Y., Lin, L., Pan, Q., Yang, X., & Cheng, X. (2012b). Preventive effect of phycocyanin from Spirulina platensis on alloxan-injured mice. *Environ Toxicol Pharmacol, 34*(3), 721-726.

Ou, Y., Lin, L., Yang, X., Pan, Q., & Cheng, X. (2013). 2 Antidiabetic potential of phycocyanin: effects on KKAy mice. *Pharm Biol, 51*(5), 539-544.

Ou, Y., Lin, L., Yang, X. G., Pan, Q., & Cheng, X. D. (2013). Antidiabetic potential of phycocyanin: Effects on KKAy mice. *Pharm Biol, 51*(5), 539-544.

Ou, Y., Ren, Z., Wang, J., & Yang, X. (2016). Phycocyanin ameliorates alloxan-induced diabetes mellitus in mice: Involved in insulin signaling pathway and GK expression. *Chem Biol Interact, 247*, 49-54.

Panchaud, A., Affolter, M., & Kussmann, M. (2012). Mass spectrometry for nutritional peptidomics: How to analyze food bioactives and their health effects. *J Proteomics, 75*(12), 3546-3559.

Phong, W. N., Show, P. L., Ling, T. C., Juan, J. C., Ng, E. P., & Chang, J. S. (2018). Mild cell disruption methods for bio-functional proteins recovery from microalgae-Recent developments and future perspectives. *Algal Research-Biomass Biofuels and Bioproducts, 31*, 506-516.

Picotti, P., Bodenmiller, B., Mueller, L. N., Domon, B., & Aebersold, R. (2009). Full dynamic range proteome analysis of S. cerevisiae by targeted proteomics. *Cell, 138*(4), 795-806.

Piovesana, S., Capriotti, A. L., Cavaliere, C., La Barbera, G., Montone, C. M., Zenezini Chiozzi, R., & Laganà, A. (2018). Recent trends and analytical challenges in plant bioactive peptide separation, identification and validation. *Anal Bioanal Chem, 410*(15), 3425-3444.

Sanchez-Rivera, L., Martínez-Maqueda, D., Cruz-Huerta, E., Miralles, B., & Recio, I. (2014). Peptidomics for Discovery, Bioavailability and Monitoring of Dairy Bioactive Peptides. *Food Research International, 63*.

Santos Ade, L., Cecilio, H. P., Teston, E. F., de Arruda, G. O., Peternella, F. M., & Marcon, S. S. (2015). Microvascular complications in type 2 diabetes and associated factors: a telephone survey of self-reported morbidity. *Cien Saude Colet, 20*(3), 761-770.

Sheih, I. C., Fang, T. J., Wu, T. K., & Lin, P. H. (2010). Anticancer and antioxidant activities of the peptide fraction from algae protein waste. *J Agric Food Chem, 58*(2), 1202-1207.

Sheih, I. C., Wu, T. K., & Fang, T. J. (2009). Antioxidant properties of a new antioxidative peptide from algae protein waste hydrolysate in different oxidation systems. *Bioresour Technol, 100*(13), 3419-3425.

Shih, J. Y. C. C. C. L. C. R. S. H. H. L. M. F. (2010). Beneficial effects of Chlorella-11 peptide on blocking LPS-induced macrophage activation and alleviating thermal injury-induced inflammation in rats. *Int. J. Immunopathol. Pharmacol., 23*(3), 10.

Soto-Sierra, L., Stoykova, P., & Nikolov, Z. L. (2018). Extraction and fractionation of microalgae-based protein products. *Algal Research-Biomass Biofuels and Bioproducts, 36*, 175-192.

Stack, J., Gouic, L., A.V., T., P.R., G., F., S., D.B.,, & FitzGerald, R. J. (2018). Protein extraction and bioactive hydrolysate generation from two microalgae, Porphyridium purpureum and Phaeodactylum tricornutum. In). International Society for Nutraceuticals and Functional Foods.

Stack, J., Le Gouic, A.*V., T., P.R., G., F., S., D.B.,,* & *FitzGerald, R. J.* (2018). Protein extraction and bioactive hydrolysate generation from two microalgae, Porphyridium purpureum and Phaeodactylum tricornutum. In). International Society for Nutraceuticals and Functional Foods.

Suetsuna, K., & Chen, J. R. (2001). Identification of antihypertensive peptides from peptic digest of two microalgae, Chlorella vulgaris and Spirulina platensis. *Mar Biotechnol (NY), 3*(4), 305-309.

Sui, Y. X., Muys, M., Vermeir, P., D'Adamo, S., & Vlaeminck, S. E. (2019). Light regime and growth phase affect the microalgal production of protein quantity and quality with Dunaliella salina. *Bioresour Technol, 275*, 145-152.

van der Spiegel, M., Noordam, M. Y., & van der Fels-Klerx, H. J. (2013). Safety of Novel Protein Sources (Insects, Microalgae, Seaweed, Duckweed, and Rapeseed) and Legislative Aspects for Their Application in Food and Feed Production. *Comprehensive Reviews in Food Science and Food Safety, 12*(6), 662-678.

Vo, T. S., & Kim, S. K. (2013). antiatherosclerotic Down-regulation of histamine-induced endothelial cell activation as potential anti-atherosclerotic activity of peptides from Spirulina maxima. *Eur J Pharm Sci, 50*(2), 198-207.

Xie, J., Chen, X., Wu, J., Zhang, Y., Zhou, Y., Zhang, L., Tang, Y. J., & Wei, D. (2018). Antihypertensive Effects, Molecular Docking Study, and Isothermal Titration Calorimetry Assay of Angiotensin I-Converting Enzyme Inhibitory Peptides from Chlorella vulgaris. *J Agric Food Chem, 66*(6), 1359-1368.

Xu, Q., Hong, H., Wu, J., & Yan, X. (2019). Bioavailability of bioactive peptides derived from food proteins across the intestinal epithelial membrane: A review. *Trends in Food Science & Technology, 86*, 399-411.

Zhao, C. J., Hu, Y., Schieber, A., & Gänzle, M. (2013). Fate of ACE-inhibitory peptides during the bread-making process: Quantification of peptides in sourdough, bread crumb, steamed bread and soda crackers. *Journal of Cereal Science, 57*(3), 514-519.

Zheng, J., Inoguchi, T., Sasaki, S., Maeda, Y., McCarty, M. F., Fujii, M., Ikeda, N., Kobayashi, K., Sonoda, N., & Takayanagi, R. (2013). Phycocyanin and phycocyanobilin from Spirulina platensis protect against diabetic nephropathy by inhibiting oxidative stress. *Am J Physiol Regul Integr Comp Physiol, 304*(2), R110-120.

Zhu, Q., Chen, X., Wu, J., Zhou, Y., Qian, Y., Fang, M., Xie, J., & Wei, D. (2017). Dipeptidyl peptidase IV inhibitory peptides from Chlorella vulgaris: in silico gastrointestinal hydrolysis and molecular mechanism. *European Food Research and Technology, 243*(10), 1739-1748.

Zhu, Q. S., Chen, X. J., Wu, J. J., Zhou, Y., Qian, Y., Fang, M., Xie, J. L., & Wei, D. Z. (2017). Dipeptidyl peptidase IV inhibitory peptides from Chlorella vulgaris: in silico gastrointestinal hydrolysis and molecular mechanism. *European Food Research and Technology, 243*(10), 1739-1748.

Part II.

Scientific contributions

CHAPTER 3

MANUSCRIPT 1

CHEMICAL AND BIOLOGICAL CHARACTERIZATION OF SPIRULINA PROTEIN HYDROLYSATES: FOCUS ON ACE AND DPP-IV ACTIVITIES MODULATION

Gilda Aiello[1], Yuchen Li[1], Giovanna Boschin[1], Carlotta Bollati[1], Anna Arnoldi[1], Carmen Lammi[1]*

[1]Department of Pharmaceutical Sciences, University of Milan, 20133 Milan, Italy

Abbreviations: ACE, angiotensin converting enzyme; ACN, Acetonitrile; BSA, bovine serum albumin; CVD, Cardiovascular; C-PC, C-phycocyanin; DH, degree of hydrolysis; DPP-IV, peptidyl-peptidase IV; GIP, glucose inhibitory polypeptide; GLP-1, glucagon-like peptide-1; HA, hippuric acid; HHL, hippuryl-histidyl-leucine; IB, inhibitor blank; IC_{50}, inhibitory concentration 50%; LC-ESI-MS/MS, liquid chromatography electrospray ionization tandem mass spectrometry; MW, molecular weight; OPA, o-phthaldialdehyde; RB, reaction blank; SDS-PAGE, sodium dodecyl sulfate-polyacrylamide gel electrophoresis; SHRs, spontaneously hypertensive rats; SP, Spirulina proteins digested by pepsin; ST, Spirulina protein digested by trypsin; Tris, tris(hydroxymethyl)aminomethane; UF, ultrafiltration.

3. Abstract

Microalgae are considered a viable source of protein and among them spirulina (*Arthrospira platensis*) stands out for its exceptionally high protein content and its potential nutraceutical properties. In the present work, peptic (SP) and tryptic (ST) protein hydrolysates were produced using pepsin and trypsin, respectively. The kinetics of peptides release from the protein were investigated and the hydrolysates composition was assessed by HPLC-ESIMS/ MS, identifying 55 and 76 species-specific peptides in the SP and ST hydrolysates, respectively. The bioactivity was investigated by performing *in vitro* experiments and cellular assays in Caco-2 cells. SP and ST inhibited *in vitro* the activity of peptidyl-peptidase IV (DPP-IV) with IC_{50} of 3.4 and 0.1 mg/mL, respectively, and of angiotensin converting enzyme (ACE) with IC50 of 3.0 and 0.28 mg/mL. Both activities were confirmed in Caco-2 cells, although their further metabolic degradation reduced their potencies.

3.1 Introduction

Hypertension and diabetes are two of the main risk factors for atherosclerosis and cardiovascular disease development. Not by chance, both diseases frequently occur together, suggesting a substantial overlap in their aetiology and disease mechanisms (Cheung & Li, 2012).

In this context, angiotensin converting enzyme (ACE, EC 3.4.15.1), a dipeptidyl-carboxypeptidase expressed in many tissues (lung, kidney, intestine), is a key enzyme for blood pressure regulation. In fact, this enzyme converts the inactive angiotensin I (Ang) into active Ang II, a vasoconstrictive octapeptide, which is responsible for the hypertension progression (Zhuo, Ferrao, Zheng, & Li, 2013). Moreover, dipeptidyl peptidase IV (DPPIV)/CD26 (EC 3.4.14.5) is an ectoenzyme expressed in several tissues (kidney, intestine, prostate), which is considered an interesting anti-diabetic target, because it plays a key role in glucose metabolism by N-terminal truncation and inactivation of the incretins glucagon-like peptide (GLP)-1 and gastrointestinal insulinotropic peptide (GIP) that together are responsible for up to 70% of post-prandial

insulin secretion (Nauck, Baller, & Meier, 2004).

Food bioactive peptides have been extensively studied for their ability to exert hypotensive and anti-diabetic activity targeting ACE and DPP-IV enzymes (Daskaya-Dikmen, Yucetepe, Karbancioglu-Guler, Daskaya, & Ozcelik, 2017; Nongonierma, Mazzocchi, Paolella, & FitzGerald, 2017). In this area, mostly milk and ham peptides have been characterized, however there is an increasing interest for investigating innovative sustainable sources of protein with nutraceutical properties, such as microalgae. Among other microalgae species, spirulina (*Arthrospira platensis, synonym Spirulina platensis*) stands out due to its exceptionally high protein content (60–70% of its dry weight). Currently, several studies have been performed on its nutraceutical properties, investigating in particular the anti-inflammatory (Romay, Gonzalez, Ledon, Remirez, & Rimbau, 2003), hypolipidemic (Torres-Duran, Ferreira-Hermosillo, & Juarez-Oropeza, 2007), hypoglycemic (Gargouri, Magne, & El Feki, 2016), antihypertensive (Torres-Duran et al., 2007), and antioxidant activities (Karkos, Leong, Karkos, Sivaji, & Assimakopoulos, 2011).

Since the bioactivity of food-derived peptides depends on their physicochemical features, such as the lengths, hydrophobicity and peptide sequences, the identification of bioactive sequences and the kinetic process by which they may be released are crucial aspects to take in account in order to produce hydrolysates with specific functionalities (Aiello, Lammi, Boschin, Zanoni, & Arnoldi, 2017; Ji et al., 2018; Soni, Sudhakar, & Rana, 2017).

The first objective of the work was to obtain a spirulina total protein extract (STPE) that was hydrolyzed using two common gastrointestinal enzymes, i.e., trypsin and pepsin, in order to produce peptic (SP) and tryptic (ST) hydrolysates. The kinetics of the peptides release was investigated and the composition of each hydrolysate was analytically assessed by HPLC-ESI-MS/MS. The potential hypotensive and anti-diabetic activities of these hydrolysates was evaluated, initially measuring the ability of SP and ST to modulate *in vitro* the ACE and DPP-IV activities and, afterwards, by carrying out experiments using Caco-2 cells, in order to measure their ability to reduce the activities of both enzymes expressed on the luminal surface of human enterocytes

(Howell, Brewis, Hooper, Kenny, & Turner, 1993).

3.2 Material and methods

3.2.1 Reagents

All chemicals and reagents were of analytical grade. Acetonitrile (ACN), tris(hydroxymethyl)aminomethane (Tris), hydrochloric acid (HCl), ammonium bicarbonate, pepsin from porcine gastric mucosa (P7012, lyophilized powder, ≥2500 units/mg protein), trypsin from bovine pancreas (T1426, lyophilized powder, ≥10,000 units/mg protein), ACE from porcine kidney (500 mU/mg of activity), hippurylhistidyl-leucine (HHL), formic acid, sodium chloride, zinc chloride were from Sigma-Aldrich (St. Louis, MO, USA). Bovine serum albumin (BSA) and β-mercaptoethanol were from Thermo Fisher Scientific (Life Technology, Milan Italy). Mini-Protean apparatus, precision plus protein standards, Bradford reagent and Coomassie Blue G-250 were purchased from Bio-Rad (Hercules, CA, USA). LC-grade H2O (18 MΩ cm) was prepared with a Milli-Q H_2O purification system (Millipore, Bedford, MA, USA).

3.2.2 Microalgae biomass

Spirulina (Spirulina platensis) dry powder was purchased from Qingdao Lang Yatai Company Limited (Qingdao, China). The manufacturer declares that they cultivate it in photoautotrophic conditions in outdoor runway pools and the dry powder is prepared by spray drying technology.

3.2.3 Ultrasound-assisted protein extraction from spirulina

Spirulina powder was defatted overnight with hexane (ratio 1:20 w/v) under magnetic stirring. After drying, the defatted powder was subjected to protein extraction. In details 0.5 g of defatted powder were suspended in 10 mL of NH_4Cl solution (0.05 M, pH 4.39) (Manirafasha et al., 2017). The mixture was treated with ultrasonic cell disruptor for 6 min, conducted for 5 s at 50 W, 23 kHz frequency pulses followed by 5 s of cool-down period in ice. Then the sonicated suspension was cleared via centrifugation at 7200 g at

4 °C for 30 min. The supernatant was collected and dialyzed against 0.01M NH4Cl and stored at -20 °C until analysis. The protein extraction protocol was evaluated by SDSPAGE. The stacking gel was composed of a 4% polyacrylamide over a 12% resolving polyacrylamide gel. The cathodic and anodic compartments were filled with Tris–glycine buffer, pH 8.3, containing 0.1% m/v SDS. The electrophoresis was conducted at 100 V until the dye front reached the gel bottom. Staining was performed with colloidal Coomassie Blue and destaining with 7% (v/v) acetic acid in water.

3.2.4 Spirulina protein hydrolysis for releasing bioactive peptides

The enzymatic hydrolysis of spirulina proteins was performed using trypsin and pepsin, dissolved in 1 mM HCl and 30 mM NaCl, respectively. For the trypsin digestion, the pH of the protein extracts was adjusted to pH 8 by adding 1 M NaOH and for the pepsin digestion it was set at pH 2-3 by adding 1 M HCl. The trypsin and pepsin solution were added to protein extracts at a 1:50 (w/w) E/S ratio. The reactions were mixed and incubated at 37 °C. For the kinetics study, 40 μL of each hydrolysis solution was pipetted out for blocking the reaction at 0, 5, 10, 20, 40, 60, 120, 180, 210 min incubation time points. After overnight incubation (16 h), all reactions were blocked: the samples digested by trypsin by heating at 95 °C for 5 min, whereas those digested with pepsin by adjusting the pH to 8. Each hydrolysate was passed through ultrafiltration (UF) membranes with a 3 kDa cut-off, using a Millipore UF system (Millipore, Bedford, MA, USA). All recovered peptides were lyophilized and store -80 °C until use. The degree of hydrolysis (DH) for each hydrolysate was detected by the OPA assay. In the presence of β-mercaptoethanol, o-phthaldialdehyde (OPA) reacts with the amino terminal of protein and peptides and the generated complex has a strong absorbance at 340 nm. By measuring the absorbance of hydrolysed and unhydrolyzed samples, the number of amino groups produced during the enzymatic reaction is measured. On this basis, the degree of hydrolysis (%) was calculated according to the equation:

$$DH\ (\%) = \frac{peptide\ content}{protein\ content} \times 100 \quad (1)$$

3.2.5 Kinetics of the protein hydrolysis

The kinetics study of hydrolysis of spirulina proteins was performed to measure the initial reaction rate and the kinetics parameters (K_m and k_{cat}) according to the following equation.

$$V = \frac{K_{cat} \times [E]_0 \times [S]}{k_m + [S]} \quad (2)$$

The reaction was initiated by adding 20 µg of each enzyme to 1 mL of protein solution at various concentrations (0.08, 0.2, 0.4, 0.8, 1.2, 1.6, 2, 3, 4, 5, 6 mg/mL). At time zero and after 60 min of incubation, aliquots of 5 µL were withdrawn and added to 200 µL of OPA. A Lineweaver-Burk plot was used to determine the reaction kinetic parameters. To determine the K_m and k_{cat}, the equation was rearranged into a linear form. For experiments at a fixed enzyme concentration, the plot of 1/V against 1/S resulted in a straight line with slope K_m/k_{cat} and intercept $1/k_{cat}$ allowing the calculation of K_m and k_{cat} values.

3.2.6 Peptide sequencing by LC-ESI-MS/MS

Peptides sequences were identified by LC-ESI-MS/MS analysis. Both peptic and tryptic hydrolysates were freeze-dried and reconstituted in 500 µL of a water solution containing 2% ACN and 0.1% formic acid. Four microliters of each hydrolysate were injected in a nano-chromatographic system, HPLC-Chip (Agilent, Palo Alto, CA, USA). The analysis was conducted on a SL Ion Trap mass spectrometer (Agilent). Each sample was loaded onto a 40 nL enrichment column (Zorbax 300SBC18, 5 µm pore size) and separated onto a 43 mm×75 µm analytical column packed (Zorbax 300SB-C18, 5 µm pore size). Separation was carried out in gradient mode at a flowrate of 500 nL/min. The LC solvent A was 95% water, 5% ACN, 0.1% formic acid; solvent B was 5% water, 95% ACN, 0.1% formic acid. The nano pump gradient program was as follows: 5% solvent B (0 min), 50% solvent B (0-50 min), 95% solvent B (50–60 min), and back to 5% in 10 min. Data acquisition occurred in positive ionization mode. Capillary voltage was -2000 V, with endplate offset -500 V. Full scan mass spectra were acquired in the mass range from *m/z* 300 to 2000 Da. LC-MS/MS analysis was

performed in data-dependent acquisition AutoMS(n) mode. In order to increase the number of identified peptides, three technical replicates (LC-ESI-MS/MS runs) were run for each hydrolysate. The MS/MS data were analysed by a Spectrum Mill Proteomics Workbench (Rev B.04.00, Agilent), consulting the *A. platensis* database (12,530 entries) downloaded from the UniProtKB/Swiss-Prot - ExPASy. Pepsin and trypsin were selected as cutting enzyme. Two missed cleavages were allowed to each enzyme used; peptide mass tolerance was set to 1.0 Da and fragment mass tolerance to 0.8 Da. Autovalidation strategy both peptide and protein polishing mode was performed using FDR cut-off ≤1.2%.

3.2.7 In vitro measurement of the ACE inhibitory activity

In order to evaluate the ACE-inhibitory activity, the hydrolysates were tested measuring the formation of hippuric acid (HA) from hippuryl-histidylleucine (HHL), a mimic substrate for Ang I (Cushman & Cheung, 1971). The experimental details have been published previously (Boschin, Scigliuolo, Resta, & Arnoldi, 2014a, 2014b). For each sample, 100 μL of 2.5 mM hippuryl-histidylleucine (HHL) in buffer 1 (100 mM Tris-HCOOH, 300 mM NaCl pH 8.3) was mixed with 30 μL of sample in buffer 1 at different concentrations. Samples were preincubated at 37 °C for 15 min, then 15 μL of ACE solution, corresponding to 3 mU of enzyme in buffer 2 (100 mM Tris-HCOOH, 300 nM NaCl, 10 μM ZnCl2, pH 8.3), were added. This reaction system was incubated for 60 min at 37 °C and then stopped with 125 μL of 0.1 M HCl. The aqueous solution was extracted twice with 600 μL of ethyl acetate. The organic phase was collected and evaporated at 95 °C. The residue was dissolved in 500 μL of buffer 1 and then analyzed by a HPLC 1200 series, equipped with an autosampler (Agilent Technologies, Santa Clara, US). A Lichrospher 100, C18 column (4.6 mm × 250 mm, 5 μm; Grace, Italy) was used with water and acetonitrile as solvent following the gradient: 0 min 5% acetonitrile, 10 min 60% acetonitrile, 12 min 60% acetonitrile, 15 min 5% acetonitrile. Injection volume was 10 μL, wavelength 228 nm, flow 0.5 mL/min. The evaluation of ACE inhibition was based on the comparison between the concentrations of HA in the

presence or absence of an estimated inhibitor. The phenomenon of autolysis of HHL to give HA was evaluated by a reaction blank, i.e., a sample with the higher evaluated inhibitor concentration and without the enzyme. The percentage of ACE inhibition was computed considering the area of HA peak with the following formula:

$$\%\ \text{ACE inhibition} = \left[\frac{(\text{AIB} - \text{AN})}{(\text{AIB} - \text{ARB})}\right] \times 100$$

where A_{IB} is the area of HA in inhibitor blank (IB) sample (i.e., sample with enzyme but without any estimated inhibitor), A_N is the area of HA in the n samples containing different amounts of the estimated inhibitor (in our case the hydrolysate), and A_{RB} is the area of HA in the reaction blank (RB) sample (i.e., sample without enzyme and with the estimated inhibitor at the highest concentration).

3.2.8 Cellular measurement of the ACE inhibitory activity

For the experiments, cells were seeded on 96-well plates at a density of 5×104 cells/well for 24 h. The following day, cells were treated with 100 µL of SP and ST hydrolysates (from 1.0 to 5.0 mg/mL) or vehicle in growth medium for 24 h at 37 °C. The ACE inhibitory activity was measured using the ACE1 Activity Assay Kit (Biovision, Milpitas Blvd., Milpitias, CA, USA) following the manufacture's protocol. Briefly, the next day, cells were scraped in 30 µL of ice-cold ACE1 lysis buffer and transferred in an ice-cold microcentrifuge tube. After centrifugation at 13,300 g for 15 min at 4 °C, the supernatant was recovered and transferred into a new ice-cold tube. Total proteins were quantified by Bradford method, and 2 µL of the supernatant (the equivalent of 2 µg of total proteins) were added to 18 µL of ACE1 lysis buffer in each well in a black 96-well plate with clear bottom. For the background control, 20 µL of ACE1 lysis buffer were added to 20 µL of ACE1 assay buffer. Then, 20 µL of diluted ACE1 substrate [o-aminobenzoyl peptide (Abz based peptide) substrate, 4% of ACE1 substrate in assay buffer] was added in each well except the background one. The active ACE, cleaving

the Abz-peptide (substrate), led to the release of the fluorophore and fluorescence signal (Ex/Em 330/430 nm) was measured in a kinetic mode for 10 min at 37 °C.

3.2.9 In vitro measurement of the DPP-IV inhibitory activity

The experiments were carried out in triplicate in a half volume 96 well solid plate (white) using conditions previously optimized (Lammi, Zanoni, Arnoldi, & Vistoli, 2016). A total of 50.0 μL of each reaction was prepared in a microcentrifuge tube adding 30.0 μL of 1×assay buffer [20mM Tris-HCl, pH 8.0, containing 100 mM NaCl, and 1 mM EDTA], 10.0 μL of SP or ST (at the final concentration of 1.0, 2.5, and 5.0 mg/mL), sitagliptin at 1.0 μM (positive control), or vehicle (C, H_2O) and 10.0 μL of purified human recombinant DPP-IV enzyme. Subsequently, reagents were transferred in each well of the plate and each reaction was started by adding 50.0 μL of substrate solution (5mM H-Gly-Pro-AMC) and incubated at 37 °C for 30 min. Fluorescence signals were measured using the Synergy H1 fluorescent plate reader from Biotek (exc/em wavelengths 360/465 nm).

3.2.10 Cellular measurement of the DPP-IV inhibitory activity

SP and ST hydrolysates were tested on Caco-2 cells (5×10^4/well in black 96-well plates) at 1.0, 2.5, and 5.0 mg/mL, sitagliptin at 1.0 μM (positive control), or vehicle in growth medium for 24 h at 37 °C, following the method previously optimized and reported (Lammi et al., 2018). On the day after the spent media were removed and cells were washed with 100 μL of PBS without Ca^{++} and Mg^{++}, and 100 μL of Gly-Pro-aminomethylcoumarin (AMC) substrate (Cayman Chemical, Ann Arbor, MI, USA) at the concentration of 50.0 μM in PBS without Ca^{++} and Mg^{++} were added in each well. Fluorescence signals (ex./em. 350/450 nm) were measured using the Synergy H1 from Biotek every 1 min for 10 min.

3.2.11 Statistical analysis of the biochemical assays

All measurements were performed in triplicate and results were expressed as the mean

± standard deviation, where p-values < 0.05 were considered to be significant. Statistical analyses were performed by one-way ANOVA (Graphpad Prism 7, GraphPad Software, La Jolla, CA, USA) followed by Brown-Forsythe's test.

3.3 Results and discussion

3.3.1 Chemical characterization of SP and ST hydrolysates

To improve the release of microalgae valuable components, spirulina cells were lysed by ultrasound-assisted extraction, a viable method, which has been recently proposed (Dey & Rathod, 2013). The efficiency of the extraction is illustrated in **Figure 3.1A**, which displays the SDS-PAGE of STPE from spirulina powder. Two intense bands were detected in the STPE lane, corresponding to the β (18.1 kDa) and α (17.6 kDa) subunit of C-phycocyanin (C-PC), which is the most abundant protein in spirulina, accounting for 20% of the dry biomass. Most of the other proteins fell in the 25-100 kDa range, where the most intense bands were detected in the range between 35 and 55 kDa. The efficiency of the hydrolysis was evaluated comparing the protein and peptide profiles of STPE and SP and ST, respectively as shown in **Figure 3.1B**. From the SDS-PAGE, it appears evident that practically all proteins, high molecular weight ones included, were completely hydrolyzed during the overnight enzymatic process. However, their susceptibility to hydrolysis varied greatly: in particular, C-PC resulted much more sensitive to pepsin than trypsin digestion as revealed by comparing lane T_0 (SP) and lane T_0 (ST) (**Figure 3.1B**). The DHs of the SP and ST hydrolysates reached 37.8% and 49.4%, respectively (**Figure 3.1C**). The common methods currently adopted for peptides release involve the use of digestive enzyme, helpful for obtaining a partial breakdown of proteins into peptides and for improving the bio-accessibility (Meade, Reid, & Gerrard, 2005). The digestive enzymes, pepsin and trypsin, which have different cleavage properties, produce peptide sequences with different structural features which are responsible for single or multiple functional activities (Ejike et al., 2017).

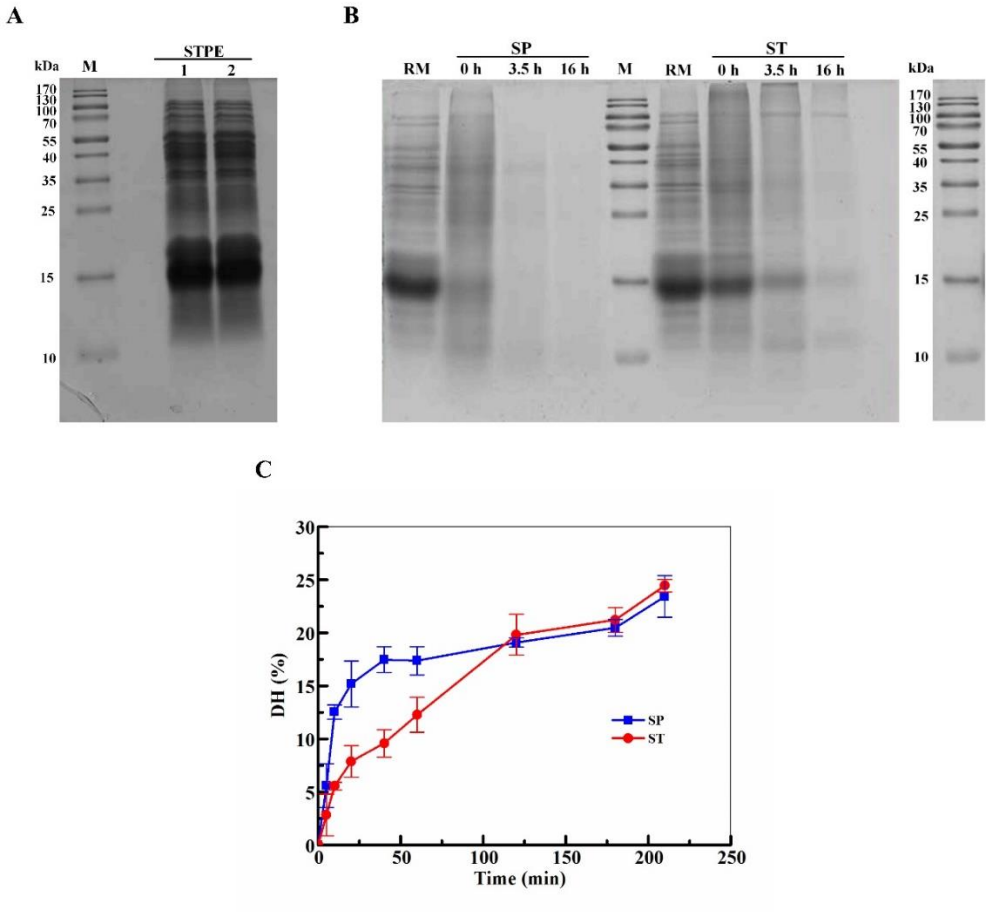

Figure 3.1 Protein profile, degree of hydrolysis (DH) trend, and digestion efficiency of spirulina protein. (A) SDS-PAGE pattern of spirulina total protein extract (STPE). Lanes number 1 and 2 are two independent extractions. (B) SDS-PAGE analysis of hydrolysates sampled at different hydrolysis time points. SP: spirulina proteins digested by pepsin, ST: spirulina protein digested by trypsin. C) DH at different time points within the first 3.5 h of *in vitro* digestion.

The hydrolysis properties of pepsin and trypsin towards spirulina protein extract were investigated via Michaelis-Menten kinetic model. The Lineweaver-Burk plots were used for calculating the kinetic parameters K_m and k_{cat} as reported in **Figure 3.2**. The results show that the constant K_m varied broadly among the different proteinases. The calculated kinetics parameters were K_m=4.33 mg/mL and k_{cat} of 0.72 min^{-1} for pepsin and K_m=56.10 mg/mL and k_{cat}=3.26 min^{-1} for trypsin. The K_m corresponds to the concentration of substrate at half- maximum velocity and its value varies widely depending on the type of substrate and experimental conditions, including pH,

temperature, ionic strength, and polarity (Marangoni, 2003). The lower the K_m, the higher the binding affinity between enzyme and substrate (Tardioli, Sousa, Giordano, & Giordano, 2005). Therefore, the lower K_m of pepsin in comparison to trypsin, proved that spirulina proteins are better substrates for pepsin than for trypsin. Pepsin is thus a more efficient enzyme for spirulina protein hydrolysis. Since the catalytic efficiency (k_{cat}/K_m) is more appropriate than K_m to compare enzyme activity (Bisswanger, 2013), it was used to investigate the substrate binding capability of pepsin and trypsin, respectively. Based on data presented in **Table 3.1**, pepsin showed higher k_{cat}/K_m for spirulina proteins. Along with K_m values, these results confirmed the faster activity of pepsin on the peptide bonds of spirulina proteins. Interestingly, a recent study has demonstrated that trypsin is more active than chymotrypsin (Sedighi, Jalili, Darvish, Sadeghi, & Ranaei-Siadat, 2019).

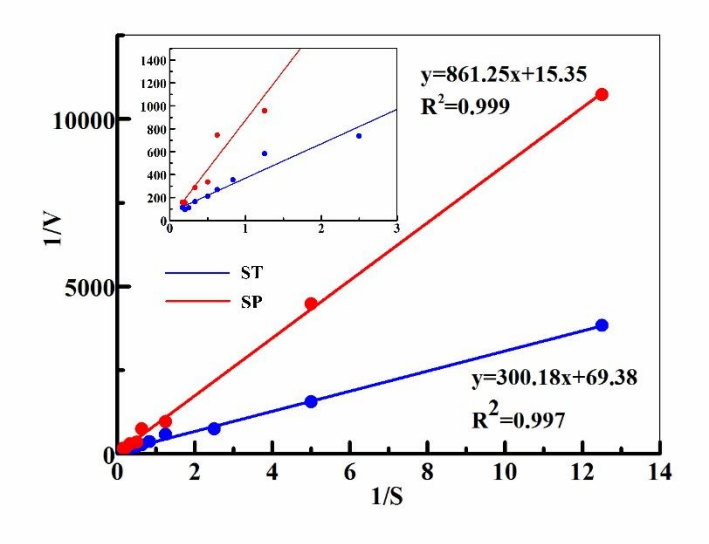

Figure 3.2 Lineweaver-Burk plots of spirulina protein hydrolysis by pepsin and trypsin.

Table 3.1 Kinetic parameters of enzymatic hydrolysis of Spirulina protein by pepsin and trypsin

	V_{max}	K_m (mg/mL)	k_{cat} (min^{-1})	k_{cat}/K_m (mg^{-1} mL mg^{-1})
ST	0.065	56.10	3.26	0.06
SP	0.014	4.33	0.72	0.17

3.3.2 Analytical characterization of SP and ST hydrolysates

The composition of both ST and SP was characterized by HPLC-ESI MS/MS. **Figure. 3.3** reports the extracted ion chromatograms for both peptic and tryptic protein hydrolysates. Using SwissProt UniProtKB *A. platensis* as reference database, a total of 76 and 55 peptides were identified in the tryptic and peptic hydrolysates, respectively (**Table 3.2**). The most frequently detected peptides in ST derived from C-PC, with the α subunit sequence covered by about 37% and the β subunit sequence covered by 35%, respectively. The fact that, instead, C-PC peptides were not identified in the peptic hydrolysates suggests that this protein is very fast digested by pepsin with the production of very small peptides undetectable by our MS method.

The molecular weights of the detected peptides in both hydrolysates fell between 1.5 and 1 kDa as reported in **Figure 3.4A**. However, it is important to underline that the SpectrumMill search engine allows the identification of peptide sequences with a number of amino acids residues higher than 4, whereas smaller peptides, such as di-tri and tetrapeptides, cannot be identified since they are not uniquely assigned to a specific protein.

Since the physical-chemical properties influence the peptide bioactivity, the distribution of peptides in ST and SP hydrolysates as a function of the length was determined and the hydrophobicity of each subgroup was calculated as indicated in **Figure 3.4B**. More in detail, the SP hydrolysate contained 27.3% peptides with a 7-10 amino acid residues length and a hydrophobicity of 14.4 kcal mol^{-1}, 38.2% peptides with a length of 11-15 amino acid residues and a hydrophobicity of 16.7 kcal mol^{-1}, and 34.5% peptides with a length of 16-23 amino acid and a hydrophobicity of 20.7 kcal mol^{-1} (**Figure 3.4B**). On the contrary, the ST hydrolysate contained 18.4% peptides with a length ranging from 7 to10 amino acid residues and a hydrophobicity of 14.5 kcal mol^{-1}, 36.8% peptides with 11-15 amino acid residues length and a hydrophobicity of 16.4 kcal mol^{-1}, and 44.8% of peptides with a length of 16-27 amino acid and a hydrophobicity of 20.9 kcal mol^{-1} (**Figure 3.4B**). Since a high hydrophobicity value corresponds to a great number of hydrophobic amino acids in the sequence, it is possible to affirm that both SP and ST hydrolysates contained a large number of hydrophobic

peptides even though the shortest peptides were more abundant in the SP hydrolysate than in the ST one.

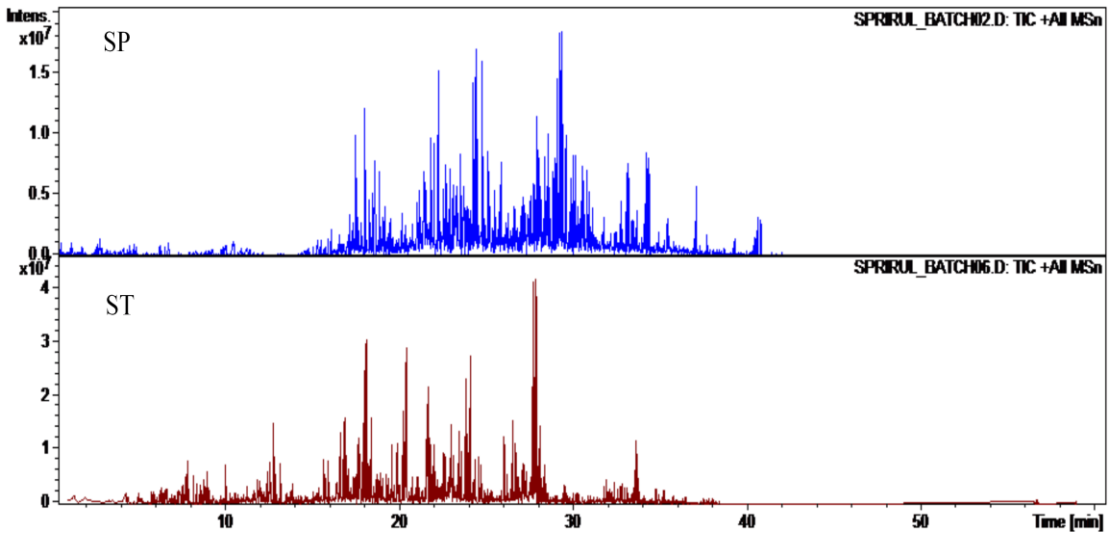

Figure 3.3 TIC MS (2) of peptic and tryptic spirulina protein hydrolysates.

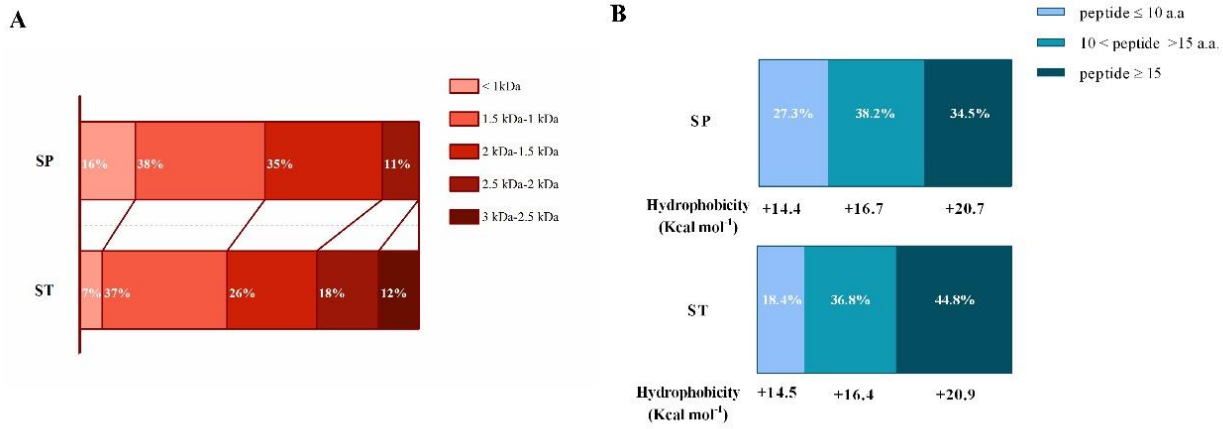

Figure. 3.4 (A) Molecular weight distribution of peptides identified in hydrolysate fraction less than 3 kDa in SP and ST groups. (B) Length and a hydrophobicity distribution among the hydrolysate ST and SP.

Table 3.2 LC-ESI-MS/MS based identification of tryptic (A) and peptic (B) peptides from spirulina protein hydrolysis.

(A)

No	Protein name [a]	Accession no [a]	m/z [b] (charge)	Start	Peptide sequence [b]	Spectra (#)	Distinct Peptides (#)	Total Protein Spectral Intensity	% AA Coverage
1	Allophycocyanin alpha subunit	D5A426	523.63 (2) 699.97 (2) 903.59 (3) 479.3 (2) 525.62 (2)	7 118 135 84 17	(K)SIVNADAEAR(Y) (K)SLGTPIEAVAEGVR(A) (K)SVATSLLSGEDAAEAGAYFDYLIGAMS(-) (R)DLDYYLR(L) (R)YLSPGELDR(I)	27	5	3.15e+009	41.6
2	Allophycocyanin beta chain	P72505	897.36 (2) 514.63 (2) 673 (2) 479.3 (2) 1096.49 (2) 594.79 (2)	1 29 40 84 114 135	(-)MQDAITSVINSSDVQGK(Y) (K)AYFATGELR(V) (R)AATTISANAANIVK(E)\ (R)DLDYYLR(Y) (K)ETYNSLGVPIGATVQAIQAMK(E) (K)EVTAGLVGADAGK(E)	38	6	4.55e+009	49.6
3	C-phycocyanin alpha subunit	D5A5N9	846.4 (3) 515.93 (3) 450.28 (2) 842.8 (2)	138 3 87 121	(K)ANHGLSGDAAVEANSYLDYAINALS(-) (K)TPLTEAVSIADSQGR(F) (R)DIGYYLR(M) (R)TFELSPSWYIEALK(Y)	46	4	4.14e+009	37.6

4	C-phycocyanin beta chain	P72508	445.12 (2) 903.84 (2) 742.01 (3) 703.33 (2)	85 115 16 44	(R)DMEIILR(Y) (R)ETYLALGTPGSSVAVGVGK(M) (R)GEMLSTAQIDALSQMVAESNK(R) (R)ITSNASTIVSNAAR(S)	34	4	2.47e+009	35.4
5	Elongation factor Tu	P13552	574.73 (2) 844.6 (2) 572.43 (2) 775.38 (3) 657.79 (2)	178 276 250 156 264	(K)ALDFLTENPK(T) (K)TLEEGMAGDNVGLLLR(G) (K)VGDTVELIGIK(D) (R)ELLSSYDFPGDDIPIVSGSALK(A) (R)TTTVTGAEMFQK(T)	20	5	1.32e+009	17.3
6	60 kDa chaperonin	D4ZWH1	759.37 (2) 531.21 (2) 750.87 (2) 882.64 (2) 599.1 (2)	327 171 455 210 105	(K)DNTTIVAEGNEAGVK(A) (K)EGVISLEEGK(S) (R)IAENAGENGAVVAER(V) (R)MEAILDEPYILLTDK(K) (R)NVAAGANPIELK(R)	25	5	5.58e+00	12.2
7	10 kDa chaperonin	D4ZWH0	579.29 (2)	29	(K)TAGGILLPDTAK(E)	9	1	3.48e+008	11.6
8	Fructose-bisphosphate aldolase	D4ZYP4	614.52 (2) 625.89 (3)	114 169	(K)TPSDFEYNVR(V) (R)DQLLTDPDQAVEFVER(T)	16	2	7.48e+008	7.2
9	Uncharacterized protein	D4ZRI3	799.31 (3) 799.27 (3) 876.35 (3)	583 2692 1045	(R)VSETSDSGDINNAIASDDSTIQR(L) (R)ISETSDSGDVNNAIASDDSTIQR(I) (R)ISETSDSGDVNNAIASTYDSPSIQR(L)	15	3	3.17e+008	2.5
10	ATP synthase subunit alpha	D5A0Q3	662.22 (2) 617.42 (2)	15 481	(K)DQIEQYGQDVK(V) (K)VLTEEAEAMLK(E)	5	2	1.14e+008	4.3

11	ATP synthase subunit beta	D4ZT81	596.91 (2)	66	(R)SVAMSGTDGLVR(G)	2	1	2.79e+007	2.4
12	Uncharacterized protein	D4ZQH6	810.54 (3) 799.07 (3)	162 40	(R)YPYLYEHCFLTDHSEIDQR(Q) (R)GLFLGEQEYQVTEVWQALER(I)	2	2	1.55e+008	9.4
13	Glyceraldehyde-3-phosphate dehydrogenase	D5A243	529.24 (2)	326	(R)VVDLAEIVAK(H)	3	1	1.66e+008	2.9
14	Ferredoxin--NADP reductase	D4ZYS5	859.97 (3)	83	(R)TQAAPENGQQSQSSGTQTPTMTQAK(A)	3	1	2.84e+007	6.2
15	50S Ribosomal protein L7/L12	D4ZXX3	645.18 (2)	14	(K)SLSLLEASELVK(Q)	2	1	4.55e+007	8.9
16	Zeta-carotene desaturase	D5A195	657.27 (3)	367	(R)SGQGSLLQLVLTPGDPFIK(Q)	2	1	3.68e+008	3.8
17	Putative peroxiredoxin	D5A2X7	601.75 (2)	63	(R)YEELYDEIK(A)	3	1	1.09e+008	5.1
18	Two-component response regulator	D4ZS72	500.68 (2)	341	(K)LQIENDLR(R)	3	1	2.92e+008	1.3
19	Phycobilisome core-membrane linker polypeptide	D4ZWE3	649.42 (2)	308	(R)AYSQGISDLESK(F)	1	1	1.16e+007	1.3
20	Inositol-5-monophosphate dehydrogenase	D4ZSU5	551.29 (3)	304	(R)GFHWGMATPSPVLPR(G)	1	1	2.77e+007	3.8
21	Uncharacterized protein	D4ZZD7	733.36 (3)	92	(R)ELANKPPEYAVASILLESPR(Y)	1	1	1.66e+008	3.4
22	UDP-glucose 6-dehydrogenase	D5A4L4	720.41 (2)	355	(R)DAPALNLIEQLSR(L)	1	1	2.68e+007	2.8
23	Putative bacterioferritin comigratory protein	D4ZR50	763.36 (2)	16	(K)DTNGNTVSLSDFAGK(T)	1	1	3.72e+007	10.4
24	Uncharacterized protein	D5A4N2	770.59 (2)	392	(K)VATTAMGAIVGHVGQK(D)	4	1	8.21e+008	2.1
25	Uncharacterized protein	D4ZV49	663.4 (3)	60	(R)VLDPAEADALTDLADESDK(H)	3	1	1.29e+008	11.8

26	D-fructose 1,6-bisphosphatase 2/sedoheptulose 1,7-bisphosphatase	D4ZR96	771.85 (3)	1	(-)MDNAIGLEIIEVVEQAAIASAR(W)	1	1	1.48e+007	6
27	Phycobilisome rod Linker polypeptide CpcH	D5A5N8	511.27 (2)	75	(R)ALAVSELYR(K)	1	1	4.36e+007	3.3
28	Putative transposase	D4ZS64	612.14 (3)	82	(K)TSAQMAELWDDDISPR(T)	1	1	2.90e+007	5.8
29	DNA helicase	D5A420	848.27 (3)	281	(R)EIWLEIEADNGINLALSVEEER(I)	1	1	9.49e+006	1.5
30	Transketolase-like protein	D4ZQU6	717.85 (2)	553	(K)STLNVVDEDMLAK(I)	1	1	4.90e+007	2
31	Thioredoxin	D4ZSU6	508.02 (2)	87	(R)VDMVVGAVPK(S)	1	1	2.35e+007	9.3
32	Glucokinase	D4ZYV1	957.39 (3)	73	(K)ACFGIAGPVVNDSCELTNLSWSLDSDR(L)	1	1	6.58e+007	7.6
33	Uncharacterized protein	D4ZPT7	794 (3)	202	(K)SVVFGWAIAVIGTSWGLTTTGGAK(G)	2	1	3.37e+008	9.1
34	Chaperone protein DnaJ	D4ZPK0	855.94 (3)	138	(K)SPGYGGFEDFTSSSSSHSGSNLETK(V)	1	1	8.94e+006	7.5
35	Uncharacterized protein	D4ZZR8	606.21 (3)	211	(R)LQNALIDGIFILPSFR(S)	1	1	2.87e+007	5.7
36	Copper-transporting P-type ATPase CtaA	D5A3X4	734.16 (3)	54	(R)VNLATEVATVECEPGTVDPQK(L)	1	1	2.00e+008	2.6
37	Photosystem I reaction center subunit II	D4ZSP4	918.65 (3)	38	(K)EQVFEMPTGGAAIMNEGENLLYLAR(K)	1	1	8.03e+006	17.6
38	Uncharacterized protein	D5A296	493.72 (3)	121	(K)SIDTQLKPCLPHK(N)	1	1	2.18e+007	9.5
39	Penicillin-binding protein	D5A2M7	761.75 (3)	556	(K)QVLDPDSTAITTWMLTHVVR(N)	1	1	1.03e+007	2.8

40	Two-component sensor histidine kinase	D4ZXQ0	582.13 (3)	205	(K)QVLLSLVDGAIAGSESGK(V)	1	1	3.13e+007	5.5
41	Mannose-1-phosphate guanyltransferase/phosphomanno mutase	D5A5P3	544.21 (2)	741	(R)TDLPHVIHR(R)	1	1	8.97e+007	1
42	Probable oxidoreductase	D4ZTW2	588.21 (3)	72	(R)DLLEYVDAVCVAVPTR(L)	1	1	5.26e+007	4.5
43	Adenylate cyclase	D5A3E2	799.32 (3)	340	(R)NAGFAGTVAESGEPLLIPFDVYK(D)	1	1	6.51e+007	2.2
44	Photosystem II protein D1	D5A686	882.48 (3)	335	(R)NVHNFPLDLASTESKPVNLVAPNIG(-)	1	1	3.13e+007	6.9
45	Uncharacterized protein	D4ZQ74	630.18 (3)	131	(R)IGGGTNMNLAVENGLSTLK(T)	1	1	1.20e+007	6.3
46	Uncharacterized protein	D4ZRX7	459.83 (2)	123	(K)GDFVEKPK(S)	1	1	2.35e+007	3.9
47	Twitching motility protein	D5A0P9	706.91 (2)	161	(R)LIGATILTLEQLK(L)	1	1	5.15e+007	3.1
48	Probable protein phosphatase	D5A2Y1	706.64 (3)	132	(K)ATILGMTIALSGGMIIGLADAK(L)	1	1	6.05e+007	7

(B)

No	**Protein name [a]**	**Accession no [a]**	**m/z [b] (charge)**	**Start**	**Peptide sequence [b]**	**Spectra (#)**	**Distinct Peptides (#)**	**Total Protein Spectral Intensity**	**% AA Coverage**
1	Uncharacterized protein	D5A518	499.78 (2)	45	(E)IQKPGSVIR(I)	3	1	4.08e+08	1.6
2	Uncharacterized protein	D4ZU53	732.11 (3)	81	(E)FPKTDRQTDKTDSRNRND(Y)	3	1	9.79e+008	9.5
3	Uncharacterized protein	D4ZRL9	447.08 (2)	5	(L)FNSASSPAI(I)	4	1	4.79e+007	1.9
4	Malonyl CoA-acyl carrier	D5A3C0	426.17 (3)	117	(E)LMDKAAGGQMAAL(I)	1	1	1.07e+007	4.4

	protein transacylase								
5	Uncharacterized protein	D5A2Y4	615.91 (3)	482	(E)IGRQAAQVSSTAFGLPSR(I)	1	1	4.18e+007	3
6	o-succinylbenzoate synthase	D4ZX99	499.69 (2)	201	(F)LEQPLGVNE(L)	1	1	1.27e+008	2.8
7	Polyketide synthase ketosynthase domain	Q32Z17	381.23 (3)	159	(L)WGNGVGLVVLK(L)	1	1	2.29e+007	4.6
8	Two-component sensor histidine kinase	D4ZXA8	467.73 (2)	1	(-)MPTSQDQK(I)	4	1	1.79e+008	2.2
9	Uncharacterized protein	D4ZRB6	515.86 (3)	537	(S)IGIALADTAETRAED(L)	1	1	2.51e+007	1.8
10	Acetyl-CoA synthetase	D5A1V4	452.92 (3)	790	(K)LSSRTGHEPMSR(L)	1	1	9.05e+006	1.3
11	Uncharacterized protein	D5A488	439.18 (3)	61	(R)LGEVQRNPTMGI(-)	2	1	2.08e+007	16.6
12	Uncharacterized protein	D5A621	609.18 (3)	186	(Q)LRSHGNADPAVSEAWSK(L)	1	1	3.63e+007	7.7
13	Probable transglycosylase	D4ZYP1	755.73 (2)	536	(S)LSRRNDPEEHQE(Y)	1	1	5.50e+007	1.6
14	UPF0182 protein NIES39_H00340	D4ZT44	470.01 (3)	555	(T)LSPVNKVAEGGLPK(Y)	1	1	2.69e+007	1.3
15	Uncharacterized protein	D4ZUH0	616.96 (3)	214	(I)LAGSAAALNAIANVYGRDT(L)	2	1	9.51e+007	7.9
16	Transaldolase	D4ZMW4	503.14 (3)	301	(K)LEEGIKGFSKALES(L)	1	1	8.75e+007	4.2
17	Trehalose synthase	D5A0I1	410.1 (3)	950	(K)ITGLRTRCHGD(Y)	1	1	2.71e+007	0.9
18	Glucose-1-phosphate adenylyltransferase	D4ZPK2	574.28 (3)	360	(Q)YGLEKGSVPIGIGNNTT(I)	1	1	7.36e+007	3.9
19	Uncharacterized protein	D4ZU16	580.62 (2)	86	(I)IPPGGDNPLGSH(W)	1	1	4.24e+007	7.8
20	WD-40 repeat protein	D4ZRA1	617.16 (2)	193	(L)IKDKNRTPFN(I)	1	1	6.14e+007	0.8
21	Uncharacterized protein	D4ZS12	497.74 (3)	269	(R)FSVRDTGIGISPEN(I)	1	1	2.41e+007	3.9
22	Uncharacterized protein	D4ZNJ6	457.09 (3)	149	(C)LKSQEVYQCDR(L)	1	1	5.90e+007	2.6
23	DNA mismatch repair protein MutL	D4ZXL7	617.39 (3)	531	(Q)WVSTRSPRTCPHGRPI(F)	1	1	3.73e+007	2.8

24	Uncharacterized protein	D5A6C7	698.76 (3)	374	(Q)FSTQTVVVTGGNQGDRVVTE(I)	1	1	6.90e+007	5
25	Uncharacterized protein	D4ZSH9	696.12 (3)	110	(R)WNQPIDVKPQMTSDEVAK(F)	4	1	6.28e+008	10
26	30S ribosomal protein S7	D4ZUX9	823.68 (3)	62	(L)FEKAVRNATPLVEVKARRVGGAT(Y)	1	1	9.30e+006	14.7
27	GTP cyclohydrolase 1	D5A155	752.4 (3)	184	(S)WTSTSAVRGVFSEDAKTRQE(F)	1	1	8.16e+007	9.3
28	Uncharacterized protein	D5A594	306.37 (3)	147	(N)LQRSERE(L)	1	1	2.38e+007	1.3
29	Two-component hybrid sensor and regulator	D4ZT35	571.84 (3)	445	(Q)IKQTAIKRGICQPEE(L)	1	1	3.13e+007	1.7
30	Protein translocase subunit SecE	D4ZXX8	457.27 (3)	29	(E)LDKVVWPTRQQ(L)	1	1	5.28e+007	14.8
31	Uncharacterized protein	D4ZXB8	552.3 (3)	249	(Q)IPITRTGSPLDRVGAT(L)	1	1	1.35e+008	1
32	Uncharacterized protein	D4ZUL0	637.6 (3)	1	(-)MVRNEPIGLPLTAITRE(L)	1	1	6.69e+007	32
33	Glutaminase	D4ZPR9	598.39 (3)	225	(W)IEPCRQVKALMMTCGL(Y)	1	1	9.79e+007	5.2
34	Uncharacterized protein	D5A1P8	500.76 (2)	263	(Y)FQAAGHSVAL(Y)	1	1	4.43e+007	3.4
35	Uncharacterized protein	D4ZNL8	789.28 (2)	98	(W)LTGIPNRVGYAGSSGE(I)	1	1	1.67e+008	5
36	Probable D-amino acid oxidase	D4ZXC9	514.79 (3)	258	(L)IVLGATAENVGFHKS(L)	1	1	2.00e+007	4
37	Uncharacterized protein	D4ZQG9	547.77 (2)	324	(E)YAGTKGQGRR(L)	1	1	3.99e+007	2.2
38	Transglutaminase-like domain	D5A0B7	826.54 (2)	86	(R)YDTVYVCRGAFVGDS(I)	1	1	1.09e+008	2.6
39	Aminopeptidase P	D5A239	499.5 (2)	289	(C)IEQVKPGVE(Y)	1	1	1.33e+008	1.9
40	Type I restriction enzyme R Protein	D5A254	500.09 (2)	141	(Y)INGIAVAVLE(L)	1	1	2.10e+007	0.9
41	Uncharacterized protein	D4ZRC4	467.64 (3)	522	(D)YGTKRDVYAQSN(F)	1	1	5.65e+007	2.1
42	ATP synthase subunit beta	D4ZT81	503.19 (2)	161	(L)FGGAGVGKTVI(I)	1	1	3.27e+008	2.2
43	Uncharacterized protein	D4ZTN5	457.81 (3)	30	(T)LACEALVSKVLPQ(Y)	1	1	5.23e+007	3.7
44	Nitrate reductase	D5A461	617.72 (3)	305	(M)WSMGINQSSEGTAKVRT(L)	1	1	5.66e+006	2.3
45	Dihydroorotate dehydrogenase	D4ZZW9	467.49 (3)	259	(M)LMAGAKVTHVCSAL(L)	1	1	3.14e+007	4.1

46	Uncharacterized protein	D4ZZP3	503.09 (2)	324	(S)LPDATETKM(I)	1	1	1.99e+008	1.6
47	6,7-dimethyl-8-ribityllumazine synthase	D4ZN11	817.02 (3)	121	(I)LTTDSMQQALERAGIKSNKGWD(Y)	1	1	9.56e+007	10.9
48	Uncharacterized protein	D4ZPS2	467.49 (2)	207	(T)LTMRSDVL(F)	1	1	4.61e+007	3.7
49	PQQ repeat protein	D5A6C9	955.46 (2)	346	(R)FRTQAVIGSSPAVSAGVVY(F)	1	1	5.45e+007	3.5
50	DNA repair protein RadA	D4ZWV4	660.27 (3)	156	(L)WNAQSVANVADDDGDGDDD(L)	1	1	4.70e+007	3.2
51	Histidine kinase	D4ZRT5	488.27 (2)	1181	(T)LEAVGRMAK(I)	1	1	1.27e+007	0.6
52	Uncharacterized protein	D4ZTF8	928.7 (2)	15	(I)WRTEPAPAKKPPPPKR(F)	1	1	7.89e+007	28
53	Uncharacterized protein	D4ZWF1	447.61 (2)	102	(D)FGSATQVAN(F)	1	1	1.14e+007	4.1
54	Serine/threonine protein kinase with WD-40 repeats	D4ZZ44	539.76 (2)	352	(I)LAIAFSRDGK(L)	1	1	2.92e+007	1.6
55	Uncharacterized protein	D4ZWX7	491.14 (3)	304	(Y)FVLEADSGYGKTAI(L)	1	1	1.20e+007	2.1

3.3.3 In vitro and cellular DPP-IV inhibitory activity of SP and ST hydrolysates

In vitro experiments were carried out in order to assess the inhibitory activity of SP and ST hydrolysates against human recombinant DPP-IV using the fluorescent substrate H-Gly-Pro-AMC. The enzymatic reaction was monitored by measuring the fluorescence signals due to the release of the free AMC group after the cleavage of the peptide HGly-Pro by DPP-IV and using sitagliptin (sita) at the final concentration of 1.0 μM, as positive control, which inhibited the enzyme activity by 88.9 ± 1.9%. The activity of SP and ST were screened at the final concentration of 1.0, 2.5, and 5.0 mg/mL. **Figure 3.5A** and B suggests that both SP and ST diminished the DPP-IV activity *in vitro*: SP dropped the enzyme by 15.2 ± 0.9%, 42.0 ± 1.7%, and 64.6 ± 0.5% displaying an IC_{50} value equal to 3.4 mg/mL (**Figure 3.5A** and **B**), while ST by 14.6 ± 1.0%, 55.3 ± 3.3% and 74.2 ± 2.9% at 1.0, 2.5, and 5.0 mg/mL, with an IC_{50} of 3.0 mg/mL (**Figure 3.5B**). Our findings are in line with the bioactivity of other food protein hydrolysates (Power, Nongonierma, Jakeman, & FitzGerald, 2014). In particular, an Atlantic salmon skin gelatin hydrolysate, obtained using Flavorzyme®, diminished the DPP-IV activity by 45.0% at 5.0 mg/mL (Li-Chan, Hunag, Jao, Ho, & Hsu, 2012), whereas a tryptic hydrolysate of amaranth proteins had an IC_{50} value between 1.2 and 2.0 mg/mL (Velarde-Salcedo et al., 2013). Moreover, a Japanese rice bran peptide mixture obtained using Umanizyme G® reduced the DPP-IV activity with an IC_{50} equal to 2.3 mg/mL (Hatanaka et al., 2012). Finally, both peptic and tryptic hempseed hydrolysates (HP and HT) and soybean hydrolysates impaired the DPP-IV activity *in vitro* with a comparable potency. More in details, peptic soybean hydrolysate reduced the DPPIV activity by 16.3 ± 3.0% and 31.4 ± 0.12% at 1.0 and 2.5 mg/mL, respectively, whereas tryptic soybean hydrolysate by 15.3 ± 11.0% and 11.0 ± 0.30% at 1.0 and 2.5 mg/mL, respectively (Lammi, Arnoldi, & Aiello, 2019), whereas HT and HP hydrolysates inhibited the DPP-IV activity by 17.5 ± 2.7% and 32.0 ± 6.2%, respectively, at 1.0 mg/mL (Lammi, Bollati, Gelain, Arnoldi, & Pugliese, 2019).

The luminal surface of the enterocytes expresses DPP-IV in a great quantity and therefore, before being absorbed, any potential inhibitor deriving from food digestion

is likely to interact with intestinal DPP-IV and other intestinal peptidases. This certainly exposes the peptides to the risk of secondary metabolic degradation before being released into circulation, where they can interact with the soluble and vascular endothelial form of DPP-IV. Taking into account all these aspects, another specific feature of this work is the employment of an intestinal cell-based assay for evaluating the inhibition of DPP-IV. In particular, Caco-2 cells were treated with 1.0, 2.5, and 5.0 mg/mL of SP and ST hydrolysates for 24 h, then the AMC-Gly-Pro substrate (50.0 μM) was added, and the fluorescence signals were detected and quantified. Experiments were performed using sitagliptin (1 μM) as reference compound. **Figure 3.5C** and **D** shows that SP reduces cellular the DPP-IV activity by 19.3 ± 9.4%, 29.0 ± 12.1%, and 31.7 ± 5.8%, whereas ST by 21.1 ±, 22.6 ±, 39.8 ± at 1.0, 2.5, and 5.0 mg/mL, respectively. These results clearly suggest that both hydrolysates are less active at cellular than *in vitro* levels, confirming their susceptibility to metabolic degradation by intestinal cells. However, at the maximum tested concentration (5.0 mg/mL), ST is more active than SP at cellular than *in vitro* level, indicating that the metabolic activity of intestinal cells can actively modulate the intrinsically bioactivity of complex hydrolysates. Based on these evidences, the application of a simple biochemical tool to screen the activity of peptides is clearly unrealistic, whereas the cellular characterization provides a more physiological environment, which takes into account the metabolic effect exerted by the lumen surface of intestinal cells. In line with these results, recently, it has been demonstrated that the incubation with the Caco-2 cells slightly impairs the inhibitory potencies of hempseed hydrolysates (Lammi, Bollati, et al., 2019) and similar metabolic effects have been observed also in case of soybean hydrolysates (Lammi, Bollati, et al., 2019). Moreover, it is useful to observe that also the tryptic hydrolysates from soybean proteins ST were more active than the peptic hydrolysate SP at cellular level. This phenomenon may be explained considering that the tryptic hydrolysate contains a greater number of long peptides in respect to the peptic hydrolysate. Probably, the metabolic effects exerted by Caco-2 cell cleave the peptic peptides to very short sequences that are devoid of any inactivity.

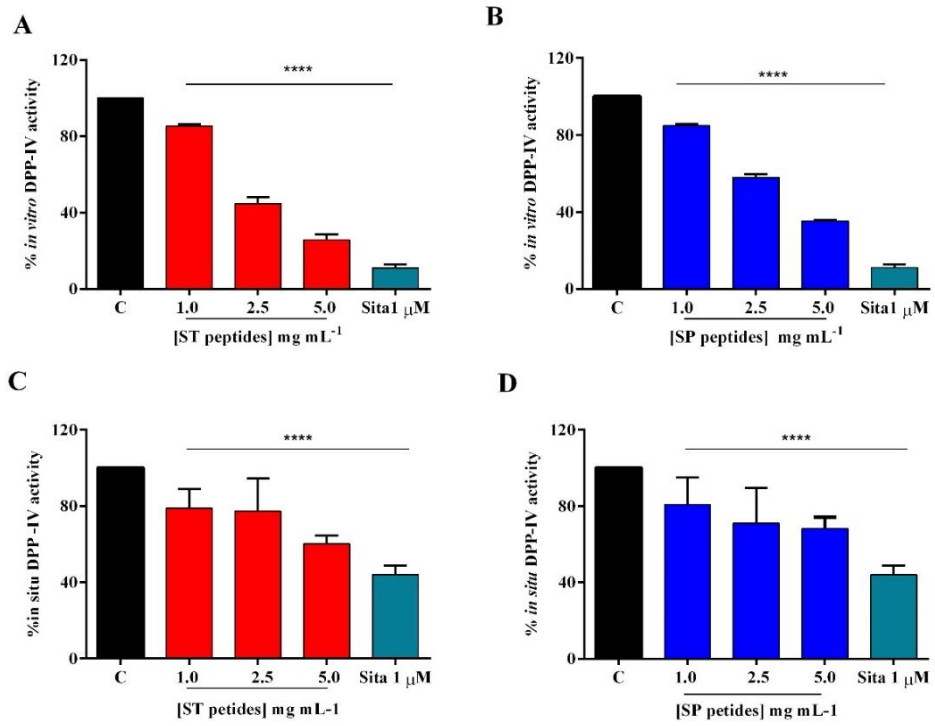

Figure 3.5 Effects of ST and SP protein hydrolysates on DPP-IV activity. (A and B) *in vitro* activity of human recombinant DPP-IV, (C and D) cellular activity of DPP-IV expressed on Caco-2 cell membranes after treatment with ST and SP, respectively. Bars represent the average ± sd of 3 independent experiments in duplicate. ****p < 0.0001, versus untreated sample (C). sita: sitagliptin, positive control, at 1.0 μM.

3.3.4 SP and ST hydrolysates modulate the in vitro and cellular ACE activity

Considering that the enzymatic hydrolysis of total protein extracts generates thousands of peptides out of which numerous may be active, it appears feasible to hypothesize that these hydrolysates may show a multifunctional behavior. Therefore, both SP and ST hydrolysates were assessed in order to investigate their potential hypotensive effect targeting ACE activity. *In vitro* experiments were realized using purified recombinant porcine kidney ACE and testing the hydrolysates in the concentration range from 0.08 to 1.0 mg/mL. Both SP and ST hydrolysates dropped the *in vitro* ACE activity with a dose-response trend and IC_{50} values equal to 0.1 ± 0.04 mg/mL and 0.28 ± 0.03 mg/mL, respectively. This means that *in vitro* SP is 3 times more active than ST (**Figure 3.6A**). This result may be explained by the different composition and physical-chemical properties of the two hydrolysates, which both contain numerous hydrophobic peptides

even though short peptides are more abundant in the SP hydrolysate than in the ST one. This suggests that the shortest peptides are more active than the longest one.

Our findings are in line with previous studies, in which total spirulina proteins have been hydrolyzed with other enzymes. For example, the hydrolysate obtained with alcalase inhibited the ACE activity with an IC_{50} value equal to 0.23 mg/mL (Lu et al., 2010), whereas spirulina peptides, generated after the hydrolysis with Protamex and SM98011, inhibited the ACE activity with an IC_{50} value smaller than 0.5 mg/mL (He et al., 2007). Moreover, hydrolysates produced by alcalase and flavourzyme dropped the enzyme activity with IC_{50} values in the range of 1.0–2.0 mg/mL (He et al., 2007).

Literature reports also some *in vivo* studies. In spontaneously hypertensive rats (SHRs), the oral administration of a peptic fraction (200 mg/kg) derived by the hydrolysis of spirulina caused a significant reduction to 39.5 mmHg at 2 h with a continuous antihypertensive effect for 4 h (Suetsuna & Chen, 2001). Specifically, peptides AQL, IAPG, and VAF detected in this study showed IC_{50} values equal to 34.7 μM, 11.4 μM and 35.8 μM, respectively.

The evaluation of the *in vitro* ACE activity, however, does not provide a comprehensive picture of the phenomenon. Therefore, another objective of this work was to evaluate the ACE activity inhibition in a more realistic way using an assay based on human intestinal Caco-2 cells. Besides being the first physiological barrier that food-derived peptides encounter, the intestine expresses good levels of ACE. We have therefore treated Caco-2 cells with both SP and ST (0.5–5.0 mg/mL) for 24 h. Afterwards, cells were lysated and the ACE activity measured in the presence of a fluorescent substrate. In this assay, both hydrolysates inhibited cellular the ACE activity with a dose-response trend and IC_{50} values equal to 2.7 ± 0.3 mg/mL and 2.8 ± 0.9 mg/mL for SP and ST, respectively (**Figure 3.6B**). Surprisingly, at cellular level both hydrolysates displayed a comparable inhibitory potency, even though drastically affected by active peptidase expressed on the surface of the apical side of the intestinal cells. Also in this case the further metabolic degradation preserve better the activity of the tryptic peptides as already observed while commenting the DPP-IV activity.

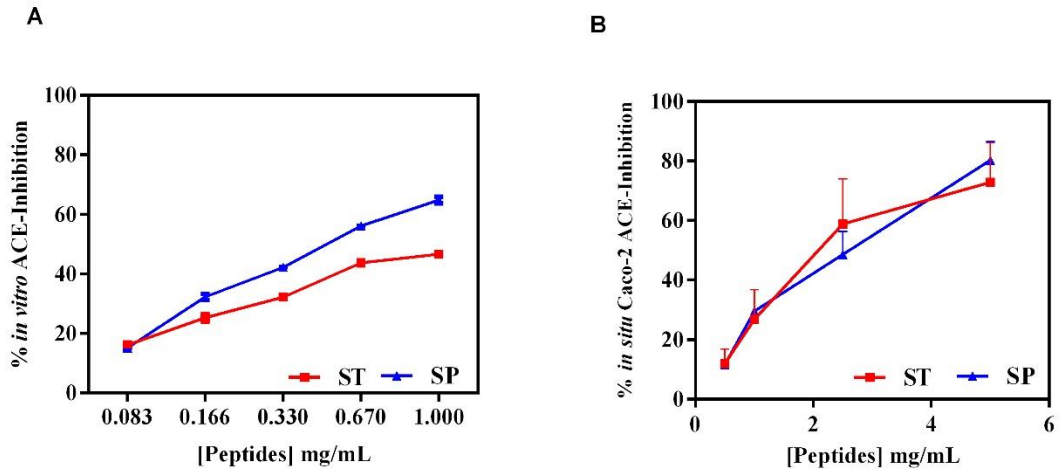

Figure 3.6 Effects of ST and SP protein hydrolysates on ACE activity. (A) *in vitro* activity of ACE, (B) cellular activity of ACE expressed on Caco-2 cell membranes after treatment with ST and SP. Bars represent the sd of 3 independent experiments in duplicate.

3.4 Conclusion

In conclusion, this study has provided a comprehensive investigation on the *in vitro* hypotensive and anti-diabetic activities of spirulina protein hydrolysates targeting ACE and DPP-IV. Briefly, we have demonstrated that both peptic and tryptic spirulina hydrolysates inhibit the *in vitro* activity of ACE and DPP-IV enzyme. In particular, SP drops the ACE and DPP-IV activities with IC_{50} values equal to 3.4 and 0.1 mg/mL, respectively, whereas ST reduces the same activities with IC_{50} values of 3.0 and 0.28 mg/mL, respectively. These findings, obtained using biochemical tools, clearly suggest that both hydrolysates are stronger ACE than DPPIV inhibitors. The application of a simple biochemical tool to screen the activity of peptides is clearly unrealistic, whereas a cellular characterization provides a more physiological environment, which takes into account the metabolic effects exerted by the lumen surface of intestinal cells. In fact, the results of the cellular experiments in human intestinal cells highlight the different bioactivity profiles of each hydrolysate against the ACE and DPP-IV enzymes.

Food bioactive peptides represent a dynamic topic, although many efforts are still necessary for a concrete exploitation in dietary supplements and functional foods. In

this panorama, spirulina protein hydrolysates are doubtlessly a promising source of peptides with multifunctional activities. Further work will be necessary for the identification of multifunctional bioactive peptides discriminating them from peptides endowed with a single activity. To achieve this goal, we will evaluate also their ability to be absorbed at intestinal level.

References

Aiello, G., Lammi, C., Boschin, G., Zanoni, C., & Arnoldi, A. (2017). Exploration of potentially bioactive peptides generated from the enzymatic hydrolysis of hempseed proteins. Journal of Agricultural and Food Chemistry, 65(47), 10174–10184.

Bisswanger, H. (2013). Practical Enzymology.

Boschin, G., Scigliuolo, G. M., Resta, D., & Arnoldi, A. (2014a). ACE-inhibitory activity of enzymatic protein hydrolysates from lupin and other legumes. Food Chemistry, 145, 34–40.

Boschin, G., Scigliuolo, G. M., Resta, D., & Arnoldi, A. (2014b). Optimization of the enzymatic hydrolysis of lupin (Lupinus) proteins for producing ACE-inhibitory peptides. Journal of Agricultural and Food Chemistry, 62(8), 1846–1851.

Cheung, B. M. Y., & Li, C. (2012). Diabetes and hypertension: Is there a common metabolic pathway? Current Atherosclerosis Reports, 14(2), 160–166.

Cushman, D. W., & Cheung, H. S. (1971). Spectrophotometric assay and properties of the angiotensin-converting enzyme of rabbit lung. Biochemical Pharmacology, 20(7), 1637–1648.

Daskaya-Dikmen, C., Yucetepe, A., Karbancioglu-Guler, F., Daskaya, H., & Ozcelik, B. (2017). Angiotensin-I-Converting Enzyme (ACE)-inhibitory peptides from plants. Nutrients, 9(4).

Dey, S., & Rathod, V. K. (2013). Ultrasound assisted extraction of β-carotene from Spirulina platensis. Ultrasound Sonochemistry, 20(1), 271–276.

Ejike, C., Collins, S. A., Balasuriya, N., Swanson, A. K., Mason, B., & Udenigwe, C. C. (2017). Prospects of microalgae proteins in producing peptide-based functional foods for promoting cardiovascular health. Trends in Food Science & Technology, 59, 30–36.

Gargouri, M., Magne, C., & El Feki, A. (2016). Hyperglycemia, oxidative stress, liver damage and dysfunction in alloxan-induced diabetic rat are prevented by Spirulina supplementation.

Nutrition Research, 36(11), 1255–1268.

Hatanaka, T., Inoue, Y., Arima, J., Kumagai, Y., Usuki, H., Kawakami, K., ... Mukaihara, T. (2012). Production of dipeptidyl peptidase IV inhibitory peptides from defatted rice bran. Food Chemistry, 134(2), 797–802.

He, H. L., Chen, X. L., Wu, H., Sun, C. Y., Zhang, Y. Z., & Zhou, B. C. (2007). High throughput and rapid screening of marine protein hydrolysates enriched in peptides with angiotensin-I-converting enzyme inhibitory activity by capillary electrophoresis. Bioresource Technology, 98(18), 3499–3505.

Howell, S., Brewis, I. A., Hooper, N. M., Kenny, A. J., & Turner, A. J. (1993). Mosaic expression of membrane peptidases by confluent cultures of Caco-2 cells. FEBS Letters, 317(1–2), 109–112.

Ji, C. F., Han, J., Zhang, J. B., Hu, J., Fu, Y. H., Qi, H., ... Yu, C. X. (2018). Omicsprediction of bioactive peptides from the edible cyanobacterium Arthrospira platensis proteome. Journal of the Science of Food and Agriculture, 98(3), 984–990.

Karkos, P. D., Leong, S. C., Karkos, C. D., Sivaji, N., & Assimakopoulos, D. A. (2011). Spirulina in clinical practice: Evidence-based human applications. Evidence-Based Complementary and Alternative Medicine, 2011, 531053.

Lammi, C., Arnoldi, A., & Aiello, G. (2019). Soybean peptides exert multifunctional bioactivity modulating 3-hydroxy-3-methylglutaryl-CoA reductase and dipeptidyl peptidase-IV targets *in vitro*. Journal of Agricultural and Food Chemistry, 67(17), 4824–4830.

Lammi, C., Bollati, C., Ferruzza, S., Ranaldi, G., Sambuy, Y., & Arnoldi, A. (2018). Soybean- and lupin-derived peptides inhibit DPP-IV activity on *in situ* human intestinal Caco-2 cells and ex vivo human serum. Nutrients, 10(8).

Lammi, C., Bollati, C., Gelain, F., Arnoldi, A., & Pugliese, R. (2019). Enhancement of the stability and anti-DPPIV activity of hempseed hydrolysates through self-assembling peptide-based hydrogels. Frontiers in Chemistry, 6, 670.

Lammi, C., Zanoni, C., Arnoldi, A., & Vistoli, G. (2016). Peptides derived from soy and lupin protein as Dipeptidyl-Peptidase IV inhibitors: *In vitro* biochemical screening and in silico molecular modeling study. Journal of Agricultural and Food Chemistry, 64(51), 9601–9606.

Li-Chan, E. C., Hunag, S. L., Jao, C. L., Ho, K. P., & Hsu, K. C. (2012). Peptides derived from atlantic salmon skin gelatin as dipeptidyl-peptidase IV inhibitors. Journal of Agricultural and Food

Chemistry, 60(4), 973–978.

Lu, J., Ren, D. F., Xue, Y. L., Sawano, Y., Miyakawa, T., & Tanokura, M. (2010). Isolation of an antihypertensive peptide from alcalase digest of Spirulina platensis. Journal of Agricultural and Food Chemistry, 58(12), 7166–7171.

Manirafasha, E., Murwanashyaka, T., Ndikubwimana, T., Yue, Q., Zeng, X. H., Lu, Y. H., & Jing, K. J. (2017). Ammonium chloride: A novel effective and inexpensive salt solution for phycocyanin extraction from Arthrospira (Spirulina) platensis. Journal of

Applied Phycology, 29(3), 1261–1270. Marangoni, A. G. (2003). Enzyme kinetics: A modern approach. John Wiley & Sons. Meade, S. J., Reid, E. A., & Gerrard, J. A. (2005). The impact of processing on the nutritional quality of food proteins. Journal of AOAC International, 88(3), 904–922.

Nauck, M. A., Baller, B., & Meier, J. J. (2004). Gastric inhibitory polypeptide and glucagon-like peptide-1 in the pathogenesis of type 2 diabetes. Diabetes, 53(Suppl 3), S190–196.

Nongonierma, A. B., Mazzocchi, C., Paolella, S., & FitzGerald, R. J. (2017). Release of dipeptidyl peptidase IV (DPP-IV) inhibitory peptides from milk protein isolate (MPI) during enzymatic hydrolysis. Food Research International, 94, 79–89.

Power, O., Nongonierma, A. B., Jakeman, P., & FitzGerald, R. J. (2014). Food protein hydrolysates as a source of dipeptidyl peptidase IV inhibitory peptides for the management of type 2 diabetes. Proceedings of the Nutrition Society, 73(1), 34–46.

Romay, C., Gonzalez, R., Ledon, N., Remirez, D., & Rimbau, V. (2003). C-phycocyanin: A biliprotein with antioxidant, anti-inflammatory and neuroprotective effects. Current Protein & Peptide Science, 4(3), 207–216.

Sedighi, M., Jalili, H., Darvish, M., Sadeghi, S., & Ranaei-Siadat, S. O. (2019). Enzymatic hydrolysis of microalgae proteins using serine proteases: A study to characterize kinetic parameters. Food Chemistry, 284, 334–339.

Soni, R. A., Sudhakar, K., & Rana, R. S. (2017). Spirulina - From growth to nutritional product: A review. Trends in Food Science & Technology, 69, 157–171.

Suetsuna, K., & Chen, J. R. (2001). Identification of antihypertensive peptides from peptic digest of two microalgae, Chlorella vulgaris and Spirulina platensis. Marine Biotechnology (NY), 3(4), 305–309.

Tardioli, P. W., Sousa, R. S., Giordano, R. C., & Giordano, R. L. C. (2005). Kinetic model of the

hydrolysis of polypeptides catalyzed by Alcalase((R)) immobilized on 10% glyoxyl-agarose. Enzyme and Microbial Technology, 36(4), 555–564.

Torres-Duran, P. V., Ferreira-Hermosillo, A., & Juarez-Oropeza, M. A. (2007). Antihyperlipemic and antihypertensive effects of Spirulina maxima in an open sample of Mexican population: A preliminary report. Lipids in Health and Disease, 6.

Velarde-Salcedo, A. J., Barrera-Pacheco, A., Lara-Gonzalez, S., Montero-Moran, G. M., Diaz-Gois, A., Gonzalez de Mejia, E., & Barba de la Rosa, A. P. (2013). *In vitro* inhibition of dipeptidyl peptidase IV by peptides derived from the hydrolysis of amaranth (Amaranthus hypochondriacus L.) proteins. Food Chemistry, 136(2), 758–764.

Zhuo, J. L., Ferrao, F. M., Zheng, Y., & Li, X. C. (2013). New frontiers in the intrarenal Renin-Angiotensin system: a critical review of classical and new paradigms. Front Endocrinol (Lausanne), 4, 166.

CHAPTER 4

MANUSCRIPT 2

PHYCOBILIPROTEINS FROM ARTHROSPIRA PLATENSIS (SPIRULINA): A NEW SOURCE OF PEPTIDES WITH DIPEPTIDYL PEPTIDASE-IV INHIBITORY ACTIVITY

Yuchen Li[1], Gilda Aiello[1], Carlotta Bollati[1], Martina Bartolomei[1], Anna Arnoldi[1] and Carmen Lammi[1*]

[1]Department of Pharmaceutical Sciences, University of Milan, 20133 Milan, Italy

Abbreviations: ACE, angiotensin converting enzyme; ACN, acetonitrile; AMC, 7-Amido-4-methylcoumarin; APC, allophycocyanin; BSA, bovine serum albumin; C-PC, C-phycocyanin; DH, degree of hydrolysis; DMEM, Dulbecco Minimum Essential Medium; DMSO, dimethyl sulfoxide; DPP-IV, dipeptidyl peptidase IV; FBS, fetal bovine serum; GIP, insulinotropic peptide; GLP-1, glucagon-like peptide; HMGCoAR; 3-hydroxy-3-methyl-glutaryl-coenzyme A reductase, HPLC-ESI-MS/MS, High-performance liquid chromatography electrospray ionization tandem mass spectrometry; INS-1 β-cells, rat insulinoma beta cells; MTT, 3-(4,5-dimethylthiazol-2-yl)-2,5-diphenyltetrazolium bromide; MW, molecular weight; OPA, o-phthaldialdehyde; PBP, phycobiliproteins; PBS, phosphate buffered saline; SDS-PAGE, sodium dodecyl sulphate-polyacrylamide gel electrophoresis; T2D, type 2 diabetes; TIC, total ion chromatogram; UF, ultrafiltration.

4. Abstract

Arthrospira platensis (spirulina) is a cyanobacterium, which contains mainly two phycobiliproteins (PBP), i.e., C-phycocyanin (C-PC) and allophycocyanin (APC). In this study, PBP were hydrolyzed using trypsin, and the composition of the hydrolysate was characterized by HPLC-ESI-MS/MS. Furthermore, the potential anti-diabetic activity was assessed by using either biochemical or cellular techniques. Findings suggest that PBP peptides inhibit DPP-IV activity *in vitro* with a dose-response trend and an IC_{50} value falling in the range between 0.5 and 1.0 mg/mL. A lower inhibition of the DPP-IV activity expressed by Caco-2 cells was observed, which was explained by a secondary metabolic degradation exerted by the same cells.

4.1 Introduction

Arthrospira platensis (spirulina) is a cyanobacterium, which contains mainly two phycobiliproteins (PBP), namely C-phycocyanin (C-PC) and allophycocyanin (APC) (Patil, Chethana, Madhusudhan, & Raghavarao, 2008). Both phycobiliproteins are water-soluble, brightly colored, and highly fluorescent, and are used for numerous applications, such as fluorescent markers in biomedical research (Glazer, 1994), nutrient ingredients, and natural dyes for food and cosmetics (Yoshida, Takagaki, & Nishimune, 1996), as well as potentially therapeutic agents in oxidative stress-induced diseases (Bhat & Madyastha, 2001). Recently, some angiotensin converting enzyme (ACE) inhibitory peptides have been described, derived from either C-PC or APC (Cermeno, Stack, Tobin, O'Keeffe, Harnedy, Stengel, et al., 2019; Furuta, Miyabe, Yasui, Kinoshita, & Kishimura, 2016). Moreover, numerous biological effects of C-PC have been reported, such as anti-inflammatory (Cherng, Cheng, Tarn, & Chou, 2007), anti-apoptotic (Romay, Gonzalez, Ledon, Remirez, & Rimbau, 2003), antioxidant (Piñero Estrada, Bermejo Bescós, & Villar del Fresno, 2001), and hypolipidemic activities (Nagaoka, Shimizu, Kaneko, Shibayama, Morikawa, Kanamaru, et al., 2005). In addition, the literature provides some evidence on the *in vivo* hypoglycemic activity exerted by C-PC peptides in different animal models (Yu Ou, Lin, Pan, Yang, & Cheng, 2012; Y. Ou, Lin, Yang, Pan, & Cheng, 2013). In particular, a recent study has shown that C-PC peptides activate the insulin signaling pathway and glucokinase expression

in the pancreas and liver of diabetic mice (Y. Ou, Ren, Wang, & Yang, 2016). Moreover, the treatment of insulin-secreting INS-1 β-cells, a common model for diabetes research, with C-PC peptides induces an interesting protective mechanism (Gao, Liao, Xiang, Yang, Cheng, & Ou, 2016). Briefly, C-PC was capable to protect INS-1 pancreatic β-cells against methylglyoxal-induced cell dysfunction through modulating the PI3K/Akt pathway and the downstream FoxO1, which leads to the improvement of insulin secretion.

Dipeptidyl peptidase IV (DPP-IV) (EC 3.4.14.5), a serine exopeptidase belonging to the prolyl oligopeptidase family, is considered an interesting therapeutic target for the management of type 2 diabetes (T2D), because it plays a key role in glucose metabolism by the N-terminal truncation and inactivation of the incretins glucagon-like peptide 1 (GLP-1) and gastrointestinal insulinotropic peptide (GIP) that together are responsible for up to 70% of post-prandial insulin secretion (Nauck, Baller, & Meier, 2004). The inhibition of DPP-IV represents a new strategy for T2D treatment, and some therapeutic agents, also known as gliptins, are already available on the market. However, there is also lively research activity on food peptides as innovative DPP-IV inhibitors, since several studies have demonstrated that the ingestion of food protein-derived hydrolysates and peptides inhibits DPP-IV activity, either *in vitro* or in small animal models (Lacroix & Li-Chan, 2016; Nongonierma & FitzGerald, 2016). However, no specific DPP-IV inhibitory hydrolysates have been submitted to clinical studies for investigating their anti-diabetic properties, suggesting that human interventions should be performed in the near future in order to demonstrate the relevance of current research.

Considering that there is an increasing interest for underexploited sustainable sources of proteins, such as microalgae, in a preceding paper, we investigated the inhibitory activity of a peptic and a tryptic hydrolysate from a total protein extract from spirulina and observed that, *in vitro*, the tryptic hydrolysate is a much better inhibitor of DPP-IV activity (IC_{50} = 0.1 mg/mL) than the peptic hydrolysate (IC_{50} = 3.4 mg/mL) (Gilda Aiello, Li, Boschin, Bollati, Arnoldi, & Lammi, 2019). In view of these results, the present study was aimed at investigating the potential ability of a tryptic PBP hydrolysate to modulate DPP-IV activity. The first objective was the optimization of PBP hydrolysis using trypsin and the characterization of the hydrolysate composition by HPLC-ESI-MS/MS analysis. The second objective was the evaluation of the potential anti-diabetic activity, which was carried out by measuring the effects on *in vitro* DPP-IV activity, as well as by performing experiments on Caco-2 cells, in order

to measure the reduction of the enzymatic activity expressed on the cellular membranes of human enterocytes (Howell, Brewis, Hooper, Kenny, & Turner, 1993).

4.2 Materials and Methods

4.2.1 Reagents

All chemicals and reagents were of analytical grade. LC-grade H_2O (18 MΩ cm) was prepared with a Milli-Q H_2O purification system (Millipore, Bedford, MA, USA). Acetonitrile (ACN), ammonium bicarbonate, and trypsin from bovine pancreas (T1426, lyophilized powder, ≥ 10,000 BAEE unit/mg protein) were provided by Sigma-Aldrich (St. Louis, MO, USA). Bovine serum albumin (BSA) and β-mercaptoethanol were from Thermo Fisher Scientific (Life Technology, Milan Italy). The Mini-Protean apparatus, Precision Plus protein standards, Bradford reagent, and Coomassie Blue G-250 were purchased from Bio-Rad (Hercules, CA, USA).

4.2.2 Microalgae Biomass

Purified PBP dry powder was provided by Fuqing King Dnarmsa Spirulina CO., LTD. (Fujian, China), and was a material that had been purified and concentrated by microfiltration and ultrafiltration from crude protein extracts from *A. platensis*, cultivated in photoautotrophic conditions in an outdoor runway pool. Spray drying technology had been applied by the manufacturer to produce both the dry spirulina powder and dry PBP powder. This PBP was not as pure as the analytical grade C-PC and APC but it satisfied the demand of this study since it is aimed to understand the bioactivity of PBP peptides regarding it as a dietary source. Before preparing the peptides, we evaluated the purity of PBP by SDS-PAGE and in-gel digestion. The same amount of protein samples was loaded to perform SDS-PAGE. As shown in **Figure 4.1**, compared with the lanes of total spirulina protein extracts, lanes of PBP presents less bands of unwanted protein but much more intense bands of PBP alpha and beta subunit (band 3 and 4, 17-18 kDa). After in-gel digestion and LC-MS/MS identification, we identified band 3 and 4 were exactly the mixture of alpha and beta subunits from C-PC and APC. As to band 2, two subunits of C-PC and APC were also identified as the main protein, from which we supposed band 2 was the PBP heterodimers composed of alpha and beta subunits (around 35 kDa). The present of heterodimers could be due to the

uncompleted reduced reaction between the PBP and the reduced loading buffer, so that the thioether bonds linking alpha and beta subunits were not destroyed completely. A few unwanted proteins present in band 1 and 2 showed much lower spectrum intensity compared with that of PBP. Hence, PBP were considered to have a proper purity and met the requirement of this study.

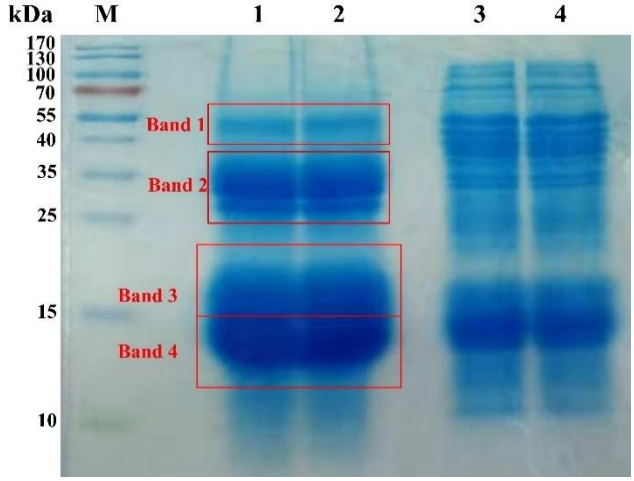

Figure 4.1 SDS-PAGE of purified PBP and total spirulina protein extracts. M-marker; Lane 1 and 2 - two parallels of purified PBP; 3 and 4 -two parallels of total spirulina protein extracts.

4.2.3 Enzymatic Hydrolysis of PBP

The protease used for the hydrolysis was trypsin from bovine pancreas. Pure PBP (0.4 g) was suspended in 40 mL of Milli-Q H_2O, the pH was adjusted to 8 with 1 M NaOH, and trypsin was added in a 1:50 ratio of E/S (*w/w*). The reaction mixture was then mixed and incubated at 37 °C for different times. The sample (40 μL) was pipetted out for the immediate blocking of the reaction at the 0, 5, 10, 20, 40, 60, 120, 180, and 210 min incubation time points. In this non-physiological way, the *in vitro* tryptic digestion of PBP was kept going overnight (16 h). After that, all of the hydrolyses were blocked by heating at 95 °C for 5 min, and then they were passed through ultrafiltration (UF) membranes (with a molecular weight (MW) cut-off of 3 kDa) using a Millipore UF system (Millipore, Bedford, MA, USA). All of the recovered peptides were lyophilized and stored at -80 °C until use. The degree of hydrolysis (DH) was measured by the o-phthaldialdehyde (OPA) assay, following a procedure previously described (G. Aiello, Lammi, Boschin, Zanoni, & Arnoldi, 2017).

The SDS-PAGE analyses were performed on gels composed of a 4% polyacrylamide stacking gel (125 mM Tris-HCl, pH 6.8, 0.1%, m/v, SDS) over a 12% resolving polyacrylamide gel (375 mM Tris-HCl, pH 8.8, 0.1%, m/v, SDS buffer). Electrophoresis was performed with a Mini-Protean III vertical apparatus (Bio-Rad Lab, Hercules, Calif., U.S.A.) at 100 V until the dye front reached the gel bottom. The resolved protein bands were stained by immersing the gel in a solution containing 45% methanol, 10% glacial acetic acid, and 0.25% Coomassie Brilliant Blue R-250. To visualize the bands, the gels were destained in a solution containing 45% methanol and 10% glacial acetic acid until they were clearly visible.

4.2.4 Analysis of the Hydrolysate by LC-ESI-MS/MS

The lyophilized tryptic hydrolysate was reconstituted in 500 μL of water solution containing 2% ACN and 0.1% formic acid, and 4 μL were injected into a HPLC-Chip system equipped with a SL IT mass spectrometer (Agilent Technologies Inc., Palo Alto, CA, USA). Each sample was loaded onto a 40 nL enrichment column (Zorbax 300SB-C18, 5 μm pore size), and separated onto a 43 mm × 75 μm analytical column (Zorbax 300SB- C18, 5 μm pore size). The separations were carried out in gradient mode at a flow rate of 500 nL/min. The elution solvent A was 95% water, 5% ACN, and 0.1% formic acid; solvent B was 5% water, 95% ACN, and 0.1% formic acid. The nano pump gradient program was as follows: 5% solvent B (0 min), 50% solvent B (0–50 min), 95% solvent B (50–60 min), and back to 5% for 10 min.

Data acquisition occurred in positive ionization mode. The capillary voltage was -2000 V, with an endplate offset of -500 V. Full scan mass spectra were acquired in the mass range from m/z 300 to 2000 Da. LC-MS/MS analysis was performed in data-dependent acquisition AutoMS(n) mode. In order to increase the number of identified peptides, three technical replicates (LC-MS/MS runs) were run for each hydrolysate. The MS/MS data were analyzed by the Spectrum Mill Proteomics Workbench (Rev B.04.00, Agilent), consulting the *A. platensis* database (12,530 entries) downloaded from UniProtKB/Swiss-Prot - ExPASy. Trypsin was selected as the cutting enzyme, two missed cleavages were allowed for each enzyme used, and the peptide mass tolerance was set to 1.0 Da and the fragment mass tolerance to 0.8 Da. An auto-validation strategy for both the peptide and protein polishing modes was performed using an FDR cut-off ≤1.2%.

4.2.5 In Vitro DPP-IV Activity of Tryptic PBP Peptides

The *in vitro* experiments were carried out in triplicate in a half volume 96 well solid plate (white). Each reaction (100 µL) was prepared by adding the reagents in a micro centrifuge tube in the following order: 1 × assay buffer [20 mM Tris-HCl, pH 8.0, containing 100 mM NaCl, and 1 mM EDTA]; PBP hydrolysate with a final concentration of 0.1, 0.5, 1.0, 2.5, or 5.0 mg/mL, or vehicle; and finally, the purified human DPP-IV enzyme (10 µL, from Cayman Chemical Company, Michigan, US). Subsequently, the samples were mixed, and 50 µL of each reaction were transferred into each plate well. Each reaction was started by adding 50 µL of substrate solution (200 µM H-Gly-Pro-7-amido-4-methylcoumarin (AMC)) to each well and incubated at 37 °C for 30 min. Fluorescence signals were measured using the Synergy H1 fluorescent plate reader (Biotek, Bad Friedrichshall, Germany) (excitation and emission wavelengths 360 and 465 nm, respectively).

4.2.6 Cell Culture

Caco-2 cells, obtained from INSERM (Paris, France), were routinely sub-cultured at 50% density [21], and were maintained at 37 °C in a 90% air, 10% CO_2 atmosphere, in Dulbecco Minimum Essential Medium (DMEM) containing 25 mM glucose, 3.7 g/L $NaHCO_3$, 4 mM stable L-glutamine, 1% nonessential amino acids, 100 U/L penicillin, and 100 µg/L streptomycin (complete medium), supplemented with 10% heat-inactivated fetal bovine serum (FBS Hyclone Laboratories, Logan, UT, USA).

4.2.7 MTT Assay

A total of 3 x 10^4 Caco-2 cells/well were seeded in 96-well plates and treated with 0.1, 0.5, 1.0, 2.5, and 5 mg mL^{-1} of tryptic PBP peptides and/or vehicle (H_2O) in complete growth medium for 48 h at 37 °C under a 5% CO_2 atmosphere, following the procedure previously reported (C. Lammi, Zanoni, Scigliuolo, D'Amato, & Arnoldi, 2014).

4.2.8 Evaluation of the Inhibitory Effect of PBP Peptides on the In Situ DPP-IV Activity Expressed by Caco-2 cells

A total of 5 x 10^4 Caco-2 cells/well were seeded in black 96-well plates with clear bottoms. The second day after seeding, spent medium was discarded, and Caco-2 cells were treated with 0.1, 0.5, 1.0, 2.5, and 5 mg/mL of tryptic PBP peptides and/or vehicle

in growth medium for 30 min and 1, 3, 6, and 24 h at 37 °C. Afterwards, the treatments were removed, and the Caco-2 cells were washed once with 100 µL of PBS w/o Ca^{++} and Mg^{++}. Thus, 40 µL of Gly-Pro-AMC substrate at the concentration of 20.0 µM in PBS w/o Ca^{++} and Mg^{++} were added into each well, and the fluorescence signals (ex./em. 350/450 nm) were measured using the Synergy H1 microplate reader every 1 min for 10 min.

4.2.9 Statistical Analysis

All measurements were performed in triplicate and the results are expressed as the mean ± standard deviation (SD) of six independent experiments, each performed in triplicate, where p-values < 0.05 were considered to be significant. Statistical analyses were performed by one-way and two-way ANOVA (Graphpad Prism 8.3, GraphPad Software, La Jolla, CA, USA), followed by Dunnett's and Tukey's tests, respectively.

4.3 Results

4.3.1 PBP *In Vitro* Digestion and Peptide Identification by Nano ESI-MS/MS

In order to release the peptides with potential health benefits from PBP, a non-physiological *in vitro* digestion was performed using trypsin. **Figure 4.2a** shows the increasing trend of DH in the first 3.5 h of reaction, which reached a value of 24.7%, suggesting an efficient digestion. The process was continued overnight (16 h), reaching a final DH value of 47.0% (data not shown). The SDS-PAGE analysis (**Figure 4.2b**) indicated that the PBP band-including the C-PC alpha and beta subunits, as well as the APC alpha and beta subunits, all of which have MWs of 17-18 kDa- was less intense at the end than at the beginning of hydrolysis (time 0 h), even though this band was still detectable after 16 h of treatment.

The peptide composition of PBP hydrolysates was analyzed by LC-ESI-MS/MS. **Figure 4.2c** presents the total ion chromatogram (TIC) of the sample, whereas the overall identified peptides are reported in **Table 4.1**. In total, 26 unique sequences were identified as peptides produced by the tryptic hydrolysis. The length of those peptides ranged from 7 to 27 amino acids. Among these, seven were from the C-PC alpha chain, six from the C-PC beta chain, and five and eight from the APC alpha and beta subunits, respectively. The sequence coverages (%AA) of each identified protein were 65.4%,

45.3%, 41.6%, and 65.8%, respectively. Based on the MS/MS results, the length distribution of peptides derived from the tryptic PBP hydrolysate (**Figure 4.2d**) and the average hydrophobicity of peptides in each subgroup were calculated (**Figure 4.2d**). The peptides composed of 7-10 amino acids accounted for 28% of the PBP hydrolysate and had an average hydrophobicity of 13.7 kcal mol^{-1}, the peptides containing 11-14 amino acid residues accounted for 24% of the hydrolysate and had an average hydrophobicity of 14.4 kcal mol^{-1}, and the peptides with a length of 15-27 amino acids were 48% of the total and had an average hydrophobicity of 18.1 kcal mol^{-1}.

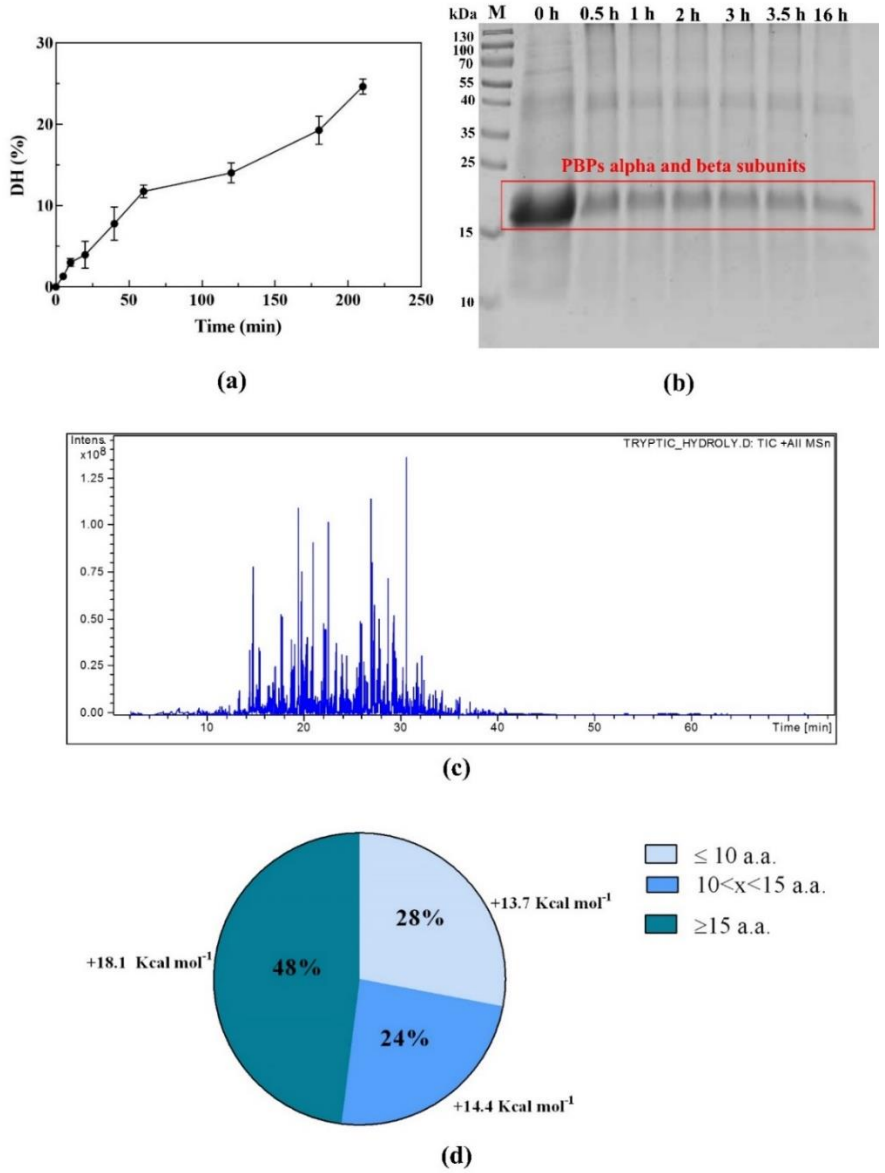

Figure 4.2 The preparation and analysis of the tryptic PBP hydrolysate. (a) The trend of degree of hydrolysis (DH) versus time in the first 3.5 h of digestion with trypsin. (b) The SDS-PAGE analysis of the hydrolysis sampled at different time points. (c) The total ion chromatogram (TIC) of the phycobiliprotein (PBP) hydrolysate. (d) The length and hydrophobicity distribution of the peptides from the PBP hydrolysate.

Table 4.1 HPLC-Chip-ESI-MS/MS based identification of peptides in the tryptic PBP hydrolysate

No	Protein name [a]	Accession no [a]	m/z [b] (charge)	Start	MH^+ Matched (Da)	Peptide sequence [b]	Spectra (#)	Distinct Peptides (#)	Total Protein Spectral Intensity	% AA Coverage
1	C-phycocyanin alpha subunit	D5A5N9	846.28(3)	138	2536,20	(K)ANHGLSGDAAVEANSYLDYAINALS(-)	42	7	8.74e+09	65.4
			503.44(3)	48	1507,77	(K)ADSLISGAAQAVYNK(F)				
			994.71(2)	63	1987,89	(K)FPYTTQMQGPNYAADQR(G)				
			515.69(3)	3	1544,79	(K)TPLTEAVSIADSQGR(F)				
			727.97(2)	18	1454,76	(R)FLSSTEIQVAFGR(F)				
			842.49(2)	121	1683,86	(R)TFELSPSWYIEALK(Y)				
			899.45(1)	87	899,46	(R)DIGYYLR(M)				
2	C-phycocyanin beta chain	P72508	741.96(3)	16	2223,06	(R)GEMLSTAQIDALSQMVAESNK(R)	14	6	2.30e+09	45.3
			938.86(2)	92	1875,91	(R)YVTYAVFAGDASVLEDR(C)				
			703.25(2)	44	1404,74	(R)ITSNASTIVSNAAR(S)				
			602.8(3)	115	1805,97	(R)ETYLALGTPGSSVAVGVGK(M)				
			445.25(2)	85	889,48	(R)DMEIILR(Y)				
			569.45(3)	21	1705,84	(R)TAQIDALSQMVAESNK(R)				
3	Allophycocyanin alpha subunit	D5A426	904.04(3)	135	2709,26	(K)SVATSLLSGEDAAEAGAYFDYLIGAMS(-)	14	5	1.37e+09	41.6
			700.15(2)	118	1398,76	(K)SLGTPIEAVAEGVR(A)				
			523.42(2)	7	1045,53	(K)SIVNADAEAR(Y)				
			525.36(2)	17	1049,53	(R)YLSPGELDR(I)				

			479.24(2)	84	957,47	(R)DLDYYLR(L)				
4	Allophycocyanin beta chain	D5A425	598.62(3)	1	1792,88	(-)MQDAITSVINSSDVQGK(Y)	20	8	3.28e+09	65.8
			731.37(3)	114	2191,14	(K)ETYNSLGVPIGATVQAIQAMK(E)				
			514.74(2)	29	1027,52	(K)AYFATGELR(V)				
			594.36(2)	135	1187,63	(K)EVTAGLVGADAGK(E)				
			504.81(2)	18	1008,54	(K)YLDASAIQK(L)				
			479.24(2)	84	957,47	(R) DLDYYLR (Y)				
			629.41(3)	91	1885,90	(R)YATYAMLAGDPSILDER(V)				
			672.78(2)	40	1344,75	(R)AATTISANAANIVK(E)				

4.3.2 PBP Peptides Inhibit DPP-IV Activity *in Vitro* and at Cellular Level

In order to assess the ability of tryptic PBP peptides to modulate DPP-IV activity, preliminary *in vitro* experiments were performed using the purified recombinant DPP-IV enzyme. The enzyme was incubated with the PBP peptides in the concentration range of 0.1-5.0 mg/mL and the fluorescent substrate, H-Gly-Pro-AMC, for 30 min at 37 °C. The reaction was monitored by measuring the fluorescence signals (465 nm) due to the release of the free AMC group after the cleavage of the peptide H-Gly-Pro, catalyzed by DPP-IV. Sitagliptin was used as a reference compound. **Figure 4.3a** shows that the tryptic PBP hydrolysate reduces DPP-IV activity *in vitro* by 11.9% ± 2.8%, 40.5% ± 7.6%, 62.1% ± 1.3%, 82.9% ± 0.7%, and 95.8% ± 0.3%, at 0.1, 0.5, 1.0, 2.5, and 5.0 mg/mL, respectively, whereas sitagliptin (1 µM) inhibits the enzyme activity by 79.5% ± 2.5%.

The inhibitory activity was then evaluated *in situ* using Caco-2 cells, which express high levels of DPP-IV on their cellular membranes (Howell, Brewis, Hooper, Kenny, & Turner, 1993). Firstly, in order to exclude any potential cytotoxic effects exerted by PBP peptides, MTT experiments were performed after 48 h of cellular treatment in a 0.1 - 5.0 mg/mL concentration range. The results of this experiment showed that the PBP hydrolysate was safe for the Caco-2 cells at each dose tested (data not shown). Therefore, the cell experiments for measuring the *in situ* DPP-IV activity were carried out at the same concentrations applied in the biochemical assay. Namely, Caco-2 cells were treated with PBP peptides in the range of concentrations 0.1 - 5.0 mg/mL, and their effects on cellular enzyme activity were evaluated using the same fluorescent substrate for 30 min at 37 °C, and again, sitagliptin was used as a reference compound. **Figure 4.3b** indicates that the PBP hydrolysate inhibited cellular DPP-IV activity by 9.3% ± 4.1%, 16.4% ± 7.4%, 29.2% ± 1.3%, 34.6% ± 2.7%, and 44% ± 5.4%, at 0.1, 0.5, 1, 2.5, and 5 mg/mL, respectively, whereas sitagliptin did such by 89.6% ± 0.9% at 1.0 µM.

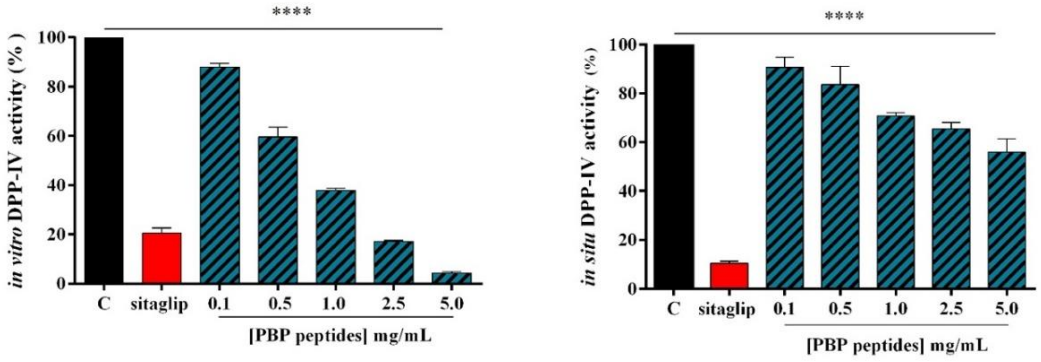

(a) **(b)**

Figure 4.3 Evaluation of the inhibitory activity of the tryptic PBP hydrolysate on DPP-IV: (a) the in vitro inhibition of the activity of human recombinant DPP-IV; (b) the in-situ inhibition of the DPP-IV activity expressed by non-differentiated Caco-2 cells, after 30 min of treatment. The data are represented as the means ± SD of six independent experiments, performed in triplicate. Statistical analysis was performed by one-way ANOVA, followed by Dunnett's test (****) $p<0.0001$.

4.3.3 Kinetics of the Inhibition of DPP-IV Activity Expressed by Caco-2 Cells Induced by the PBP Hydrolysate

In order to evaluate the kinetics of DPP-IV inhibition by PBP peptides in a cellular system, Caco-2 cells were treated with the PBP hydrolysate at 0.1, 0.5, 1.0, 2.5, and 5.0 mg/mL for 0.5, 1, 3, 6, and 24 h. This experiment allowed us to evaluate the potential transient DPP-IV inhibitory nature of the PBP hydrolysate. At each time point, the sample inhibitory activity was assessed by measuring the fluorescence signals due to the release of the free AMC group after the cleavage of the peptide H-Gly-Pro, catalyzed by cellular DPP-IV. **Figure 4.4** shows the curves of the dependence of the enzyme activity on time, obtained at the different concentrations of the PBP hydrolysate. In detail, after 0.5 h incubation, the hydrolysate inhibited DPP-IV activity by 9.3% ± 4.1%, 16.4% ± 7.4%, 29.2% ± 1.3%, 34.6% ± 2.7%, and 44% ± 5.4%; after 1 h of incubation by 15.3% ± 0.3%, 24.4% ± 2.9%, 32.7% ± 2.5%, 43.7% ± 1.9%, and 49.5% ± 1.1%; after 3 h by 11.9% ± 5.7%, 24.8% ± 2.5%, 38.1% ± 3.1%, 49.9% ± 2.0%, and 63.1% ± 1.6%; after 6 h by 9.3% ± 5.4%, 24.1% ± 4.3%, 32% ± 2.6%, 47.2% ± 6.0%, and 52.7% ± 3.5%; and after 24 h by 6.3% ±0.3%, 10.4% ±0.1%, 18.7% ±0.02%, 28.3% ±0.6%, and 27.9% ±0.5%; at 0.1, 0.5, 1.0, 2.5, and 5.0 mg/mL, respectively. The

maximum reductions of DPP-IV activity were observed at around 1 h for the treatments at 0.1 and 0.5 mg/mL, and at around 3 h for the treatments at 1.0, 2.5, and 5.0 mg/mL.

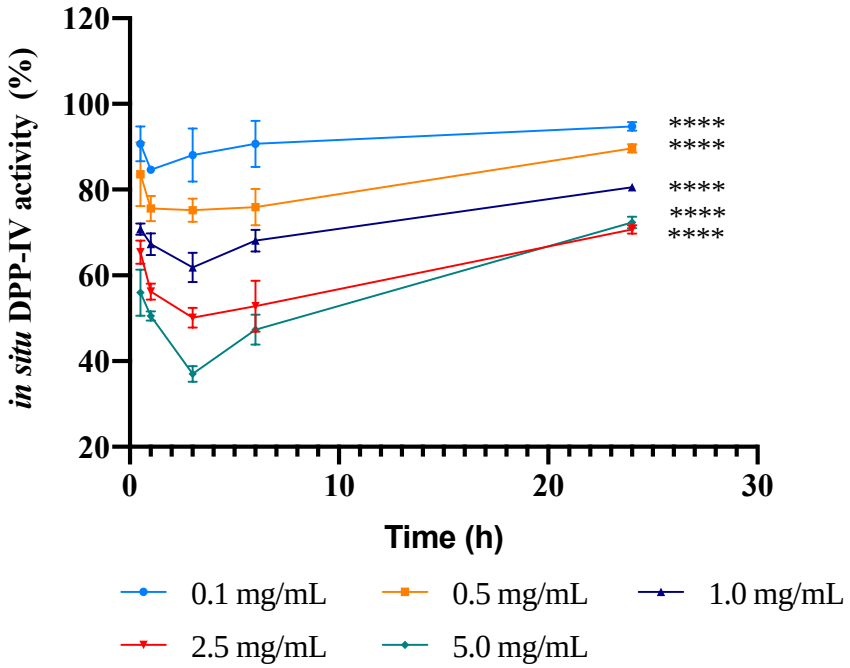

Figure 4.4 The kinetics of the inhibition of in situ DPP-IV activity after incubating Caco-2 cells with the PBP hydrolysate at different concentrations. The data are represented as the means ± SD of six independent experiments, performed in triplicate. Multiple comparisons by two-way ANOVA were performed, comparing within each concentration, each time point, and comparing within each time point, each concentration. (****) $p < 0.0001$.

4.4 Discussion

For the first time, this study provides new evidence regarding the ability of tryptic PBP to modulate DPP-IV activity *in vitro* on human recombinant enzyme, and *in situ* on the cellular intestinal membrane level. In a previous study, we reported the DPP-IV inhibitory activity of a tryptic hydrolysate derived from a spirulina total protein extract (Gilda Aiello, Li, Boschin, Bollati, Arnoldi, & Lammi, 2019). In total, 78 peptides were identified, out of which 19 individual sequences were attributed to C-PC or APC, i.e., four to the C-PC alpha subunit, four to the C-PC beta subunit, five to the APC alpha subunit, and six to the APC beta subunit, corresponding to sequence coverages of 37.6%, 35.4%, 41.6%, and 49.6%, respectively. The sequence coverages of identified C-PC alpha and beta subunits, and APC alpha and beta subunits from PBP digests were higher than those obtained from spirulina total protein hydrolysates, obviously reflecting that the accuracy of the LC-MS/MS analysis was improved after PBP

purification. In the same study, it was also shown that the spirulina hydrolysate exerts a potential hypoglycemic effect, targeting DPP-IV activity either *in vitro* or in a cellular system (Gilda Aiello, Li, Boschin, Bollati, Arnoldi, & Lammi, 2019). Those results stimulated the present investigation focused on a tryptic PBP hydrolysate. The chemical analysis of this material permitted the detection of 26 peptides, out of which 13 peptides were assigned to C-PC and 13 to APC (**Table 4.1**), reflecting the specificity of trypsin, which generally cleaves peptide chains at the carboxyl side of lysine or arginine. Interestingly, all the peptides previously identified in the spirulina hydrolysate were also detected in the PBP hydrolysate. In addition, the evaluation of the PBP peptide distribution as a function of length and hydrophobicity may be doubly useful. Firstly, hydrophobicity may positively contribute to peptide bioavailability after oral ingestion. Even though the molecular mechanism involved in food bioactive peptide absorption across the intestinal epithelium has not been elucidated yet, transcytosis is an energy-dependent transcellular transport pathway, which favors the transport of bioactive peptides with long chains and high hydrophobicity (Sun, Acquah, Aluko, & Udenigwe, 2020). Moreover, it has also been established that hydrophobic peptides are more prone to exert inhibitory activity against DPP-IV (Nongonierma & FitzGerald, 2016).

Discussing now the inhibitory effects exerted by the tryptic PBP hydrolysate on DPP-IV activity, the *in vitro* screening suggested that it inhibits the enzyme with a dose-response trend, and an IC_{50} value between 0.5 and 1.0 mg/mL (**Figure 4.3a**). This means that the tryptic PBP hydrolysate is about three-fold more active than the tryptic spirulina hydrolysate, which reduces the enzyme activity by 55.3% at 2.5 mg/mL. Since 19 peptides out of the 26 peptides identified in the PBP hydrolysate had been also identified in the spirulina hydrolysate, it seems reasonable to formulate the hypothesis that the PBP peptides have a relevant role in the DPP-IV inhibitory activity of the spirulina hydrolysate, whose lower activity may probably be explained by the unfavorable effects of numerous inactive or poorly active peptides present in its complex composition.

This PBP hydrolysate is more active than the previously reported tryptic hydrolysates, such as those from soybean and hempseed. In fact, the soybean hydrolysate inhibits DPP-IV activity by 15.3% ± 11.0% and 11.0% ± 0.30% at 1.0 and 2.5 mg/mL, respectively (C. Lammi, Arnoldi, & Aiello, 2019), whereas the hempseed does so by 32.0% ± 6.2% at 1.0 mg/mL (C Lammi, Bollati, Gelain, Arnoldi, & Pugliese, 2019). Our results are also in line with the activities of other food protein hydrolysates (Power,

Nongonierma, Jakeman, & FitzGerald, 2013), such as of marine, plant, bovine meat, and egg proteins, which have been widely investigated as sources of DPP-IV inhibitory peptides. Particularly good results have been obtained especially with milk proteins, since a caprine casein hydrolysate, a bovine milk protein isolate, and a camel milk hydrolysate have shown IC_{50} values equal to 0.8, 0.8, and 0.5 mg/mL, respectively (Nongonierma, Mazzocchi, Paolella, & FitzGerald, 2017; Nongonierma, Paolella, Mudgil, Maqsood, & FitzGerald, 2017; Zhang, Chen, Zuo, Ma, Zhang, & Chen, 2016). However, it is important to underline that all those studies have been carried out exclusively using biochemical tools based on purified enzyme. This traditional approach doubtlessly represents a great limitation for a more realistic characterization of the hydrolysates with DPP-IV inhibitory activity. In light of these observations, a specific feature of our work was the employment of an intestinal cell-based assay for measuring the enzymatic activity, which represents a complementary and cost-effective strategy for a more efficient discovery of food-derived DPP-IV inhibitors (C. Lammi, Bollati, Ferruzza, Ranaldi, Sambuy, & Arnoldi, 2018). In fact, the enterocyte luminal surface expresses a great quantity of DPP-IV: this means that, before absorption, any potential inhibitor deriving from food digestion is likely to interact with intestinal DPP-IV and other intestinal peptidases. This exposes the peptides to the risk of secondary metabolic degradation, which may dynamically modify the composition of the hydrolysate, modulating its intrinsic bioactivity. In the case of an extensive secondary metabolic degradation, a drastic reduction of the bioactivity might also take place. In order to check this hypothesis, Caco-2 cells were treated with the same PBP hydrolysate concentrations used in the *in vitro* test (0.1–5 mg/mL) for 30 min at 37 °C. The results indicate that even though a certain bioactivity is maintained, a significant reduction is observed (**Figure 4.3b**). This outcome may be explained by considering that the metabolic effects exerted by Caco-2 cells cleave the PBP peptides into shorter sequences that are characterized by a reduced activity. A similar metabolic degradation and consequent reduction of DPP-IV inhibition have been observed when testing the spirulina hydrolysate at the cellular level (Gilda Aiello, Li, Boschin, Bollati, Arnoldi, & Lammi, 2019).

This hypothesis is reinforced by the kinetic study of the *in situ* DPP-IV activity after incubation of the Caco-2 cells with the PBP hydrolysate at different concentrations as a function of time (**Figure 4.4**). As expected, the PBP hydrolysate reduces the cellular DPP-IV activity with an effectiveness that depends on the concentration. Interestingly,

the curves at the lower doses are characterized by a maximum that is achieved after 1 h treatment, and those of the higher doses have a maximum that is achieved after 3 h of treatment (**Figure 4.4**). After the maximum, the secondary metabolic activity of Caco-2 cells prevails, and the changing composition of the hydrolysate has an unfavorable effect on the bioactivity. The susceptibility to gastrointestinal peptidase degradation is generally considered a weakness of bioactive food peptides. However, the maxima in these curves suggest that, at least at the beginning of the treatment, the secondary metabolic degradation exerted by intestinal cells may produce a favorable effect on the bioactivity, whereas only when the degradation is much more extensive does it induce a substantial limitation of the inhibitory activity.

In conclusion, this work provides new insights on the ability of tryptic PBP hydrolysate to modulate DPP-IV activity in Caco-2 cells. These results draw attention to the possibility of exploiting a tryptic PBP hydrolysate as a new source of peptides for the development of nutraceuticals or functional foods. Moreover, they underline the dynamic nature of bioactive food hydrolysates that may be modulated by the biological systems with whom they get in touch. In this direction, future investigations will be planned to simulate sequential human-like gastrointestinal digestion and the absorption of PBP and total spirulina peptides together, and further experiments will be carried out for confirming their biological activities as DPP-IV inhibitors, also assessing the effects on GLP-1 levels and stability.

References

Aiello, G., Lammi, C., Boschin, G., Zanoni, C., & Arnoldi, A. (2017). Exploration of Potentially Bioactive Peptides Generated from the Enzymatic Hydrolysis of Hempseed Proteins. *J Agric Food Chem, 65*(47), 10174-10184.

Aiello, G., Li, Y., Boschin, G., Bollati, C., Arnoldi, A., & Lammi, C. (2019). Chemical and biological characterization of spirulina protein hydrolysates: Focus on ACE and DPP-IV activities modulation. *Journal of Functional Foods, 63*, 103592.

Bhat, V. B., & Madyastha, K. M. (2001). Scavenging of peroxynitrite by phycocyanin and phycocyanobilin from Spirulina platensis: Protection against oxidative damage to DNA. *Biochemical and Biophysical Research Communications, 285*(2), 262-266.

Cermeno, M., Stack, J., Tobin, P. R., O'Keeffe, M. B., Harnedy, P. A., Stengel, D. B., & FitzGerald, R. J. (2019). Peptide identification from a Porphyra dioica protein hydrolysate with antioxidant, angiotensin converting enzyme and dipeptidyl peptidase IV inhibitory activities. *Food Funct, 10*(6), 3421-3429.

Cherng, S.-C., Cheng, S.-N., Tarn, A., & Chou, T.-C. (2007). Anti-inflammatory activity of c-phycocyanin in lipopolysaccharide-stimulated RAW 264.7 macrophages. *Life Sciences, 81*(19), 1431-1435.

Furuta, T., Miyabe, Y., Yasui, H., Kinoshita, Y., & Kishimura, H. (2016). Angiotensin I Converting Enzyme Inhibitory Peptides Derived from Phycobiliproteins of Dulse Palmaria palmata. *Mar Drugs, 14*(2).

Gao, Y., Liao, G., Xiang, C., Yang, X., Cheng, X., & Ou, Y. (2016). Effects of phycocyanin on INS-1 pancreatic beta-cell mediated by PI3K/Akt/FoxO1 signaling pathway. *Int J Biol Macromol, 83*, 185-194.

Glazer, A. N. (1994). PHYCOBILIPROTEINS - A FAMILY OF VALUABLE, WIDELY USED FLUOROPHORES. *Journal of Applied Phycology, 6*(2), 105-112.

Howell, S., Brewis, I. A., Hooper, N. M., Kenny, A. J., & Turner, A. J. (1993). MOSAIC EXPRESSION OF MEMBRANE PEPTIDASES BY CONFLUENT CULTURES OF CACO-2 CELLS. *Febs Letters, 317*(1-2), 109-112.

Lacroix, I. M. E., & Li-Chan, E. C. Y. (2016). Food-derived dipeptidyl-peptidase IV inhibitors as a potential approach for glycemic regulation - Current knowledge and future research considerations. *Trends in Food Science & Technology, 54*, 1-16.

Lammi, C., Arnoldi, A., & Aiello, G. (2019). Soybean Peptides Exert Multifunctional Bioactivity Modulating 3-Hydroxy-3-Methylglutaryl-CoA Reductase and Dipeptidyl Peptidase-IV Targets in Vitro. *J Agric Food Chem, 67*(17), 4824-4830.

Lammi, C., Bollati, C., Ferruzza, S., Ranaldi, G., Sambuy, Y., & Arnoldi, A. (2018). Soybean- and Lupin-Derived Peptides Inhibit DPP-IV Activity on In Situ Human Intestinal Caco-2 Cells and Ex Vivo Human Serum. *Nutrients, 10*(8).

Lammi, C., Bollati, C., Gelain, F., Arnoldi, A., & Pugliese, R. (2019). Enhancement of the stability and anti-DPPIV activity of hempseed hydrolysates through self-assembling peptide-based hydrogels. *Frontiers in Chemistry, doi: 10.3389/fchem.2018.00670*.

Lammi, C., Zanoni, C., Scigliuolo, G. M., D'Amato, A., & Arnoldi, A. (2014). Lupin peptides lower low-density lipoprotein (LDL) cholesterol through an up-regulation of the LDL receptor/sterol regulatory element binding protein 2 (SREBP2) pathway at HepG2 cell line. *J Agric Food Chem, 62*(29), 7151-7159.

Nagaoka, S., Shimizu, K., Kaneko, H., Shibayama, F., Morikawa, K., Kanamaru, Y., Otsuka, A., Hirahashi, T., & Kato, T. (2005). A Novel Protein C-Phycocyanin Plays a Crucial Role in the Hypocholesterolemic Action of Spirulina platensis Concentrate in Rats. *The Journal of Nutrition, 135*(10), 2425-2430.

Natoli, M., Leoni, B. D., D'Agnano, I., D'Onofrio, M., Brandi, R., Arisi, I., Zucco, F., & Felsani, A. (2011). Cell growing density affects the structural and functional properties of Caco-2 differentiated monolayer. *J Cell Physiol, 226*(6), 1531-1543.

Nauck, M. A., Baller, B., & Meier, J. J. (2004). Gastric Inhibitory Polypeptide and Glucagon-Like Peptide-1 in the Pathogenesis of Type 2 Diabetes. *Diabetes, 53*(suppl 3), S190.

Nongonierma, A. B., & FitzGerald, R. J. (2016). Structure activity relationship modelling of milk protein-derived peptides with dipeptidyl peptidase IV (DPP-IV) inhibitory activity. *Peptides, 79*, 1-7.

Nongonierma, A. B., Mazzocchi, C., Paolella, S., & FitzGerald, R. J. (2017). Release of dipeptidyl peptidase IV (DPP-IV) inhibitory peptides from milk protein isolate (MPI) during enzymatic hydrolysis. *Food Research International, 94*, 79-89.

Nongonierma, A. B., Paolella, S., Mudgil, P., Maqsood, S., & FitzGerald, R. R. (2017). Dipeptidyl peptidase IV (DPP-IV) inhibitory properties of camel milk protein hydrolysates generated with trypsin. *Journal of Functional Foods, 34*, 49-58.

Ou, Y., Lin, L., Pan, Q., Yang, X., & Cheng, X. (2012). Preventive effect of phycocyanin from Spirulina platensis on alloxan-injured mice. *Environ Toxicol Pharmacol, 34*(3), 721-726.

Ou, Y., Lin, L., Yang, X. G., Pan, Q., & Cheng, X. D. (2013). Antidiabetic potential of phycocyanin: Effects on KKAy mice. *Pharm Biol, 51*(5), 539-544.

Ou, Y., Ren, Z., Wang, J., & Yang, X. (2016). Phycocyanin ameliorates alloxan-induced diabetes mellitus in mice: Involved in insulin signaling pathway and GK expression. *Chem Biol Interact, 247*, 49-54.

Patil, G., Chethana, S., Madhusudhan, M. C., & Raghavarao, K. (2008). Fractionation and purification of the phycobiliproteins from Spirulina platensis. *Bioresour Technol*, *99*(15), 7393-7396.

Piñero Estrada, J. E., Bermejo Bescós, P., & Villar del Fresno, A. M. (2001). Antioxidant activity of different fractions of Spirulina platensis protean extract. *Il Farmaco*, *56*(5), 497-500.

Power, O., Nongonierma, A. B., Jakeman, P., & FitzGerald, R. J. (2013). Food protein hydrolysates as a source of dipeptidyl peptidase IV inhibitory peptides for the management of type 2 diabetes. *Proceedings of the Nutrition Society*, *73*(1), 34-46.

Romay, C., Gonzalez, R., Ledon, N., Remirez, D., & Rimbau, V. (2003). C-phycocyanin: A biliprotein with antioxidant, anti-inflammatory and neuroprotective effects. *Current Protein & Peptide Science*, *4*(3), 207-216.

Sun, X., Acquah, C., Aluko, R. E., & Udenigwe, C. C. (2020). Considering food matrix and gastrointestinal effects in enhancing bioactive peptide absorption and bioavailability. *Journal of Functional Foods*, *64*, 103680.

Yoshida, A., Takagaki, Y., & Nishimune, T. (1996). Enzyme immunoassay for phycocyanin as the main component of Spirulina color in foods. *Bioscience Biotechnology and Biochemistry*, *60*(1), 57-60.

Zhang, Y., Chen, R., Zuo, F., Ma, H., Zhang, Y., & Chen, S. (2016). Comparison of dipeptidyl peptidase IV-inhibitory activity of peptides from bovine and caprine milk casein by in silico and in vitro analyses. *International Dairy Journal*, *53*, 37-44.

CHAPTER 5

MANUSCRIPT 3

INVESTIGATION OF *CHLORELLA PYRENOIDOSA* PROTEIN AS A SOURCES OF NOVEL ANGIOTENSIN I-CONVERTING ENZYME (ACE) AND DIPEPTIDYL PEPTIDASE- IV (DPP-IV) INHIBITORY PEPTIDES

Yuchen Li[1], Gilda Aiello[2], Patrizia Locatelli[3], Giovanna Boschin[1], Anna Arnoldi[1], Giovanni Grazioso[1], Carmen Lammi[1*]

[1]Department of Pharmaceutical Sciences, University of Milan, 20133 Milan, Italy

[2]Department of Human Science and Quality of Life Promotion, Telematic University San Raffaele, Rome, Italy

[3]Department of Pharmaceutical Sciences, University of Pavia, 27100 Pavia, Italy

Abbreviations:

ACE, angiotensin I-converting enzyme; DPP-IV, dipeptidyl peptidase- IV; CVD, cardiovascular diseases; GLP-1, glucagon-like peptide-1; GIP, glucose-dependent insulinotropic polypeptide; MD, molecular dynamics; GI, gastrointestinal; HHL, hippuryl-histidyl-leucine; BSA, bovine serum albumin; DH, degree of hydrolysis; OPA, o-phthaldialdehyde; HA, hippuric acid; CP, chlorella proteins digested by pepsin; CT, chlorella proteins digested by trypsin; AMC, 7-amido-4-methylcoumarin; RCSB PDB, Research Collaboratory for Structural Bioinformatics Protein Data Bank; RMSD, root mean square deviation; MM/GBSA, Molecular Mechanics/ Generalized Born surface area; AP, apical.

5. Abstract

Chlorella pyrenoidosa (*C. pyrenoidosa*) is a microalgae species with a remarkably high protein content that may potentially become a source of hypotensive and hypoglycemic peptides. In this study, *C. pyrenoidosa* proteins were extracted and hydrolyzed overnight with pepsin and trypsin with final degrees of hydrolysis of 18.7% and 35.5%, respectively. By LC-MS/MS, 47 valid peptides were identified in the peptic hydrolysate (CP) and 66 in the tryptic one (CT). At the concentration of 1.0 mg/mL, CP and CT hydrolysates inhibit *in vitro* the angiotensin converting enzyme (ACE) activity by 84.2 ± 0.37 % and 78.6 ± 1.7 %, respectively, whereas, tested at cellular level at the concentration of 5.0 mg/mL, they reduce the ACE activity by 61.5 ± 7.7% and 69.9±0.8%, respectively. At the concentration of 5.0 mg/mL, they decrease *in vitro* the DPP-IV activity by 63.7% and 69.6% and in Caco-2 cells by 38.4% and 42.5%, respectively. Short peptides (≤ 10 amino acids) were selected for investigating the potential interaction with ACE and DPP-IV by using molecular modeling approaches and four peptides were predicted to block both enzymes. Finally, the stability of these peptides was investigated against gastrointestinal digestion.

5.1 Introduction

Hypertension and diabetes type 2 are two of the main risk factors for the development of cardiovascular diseases (CVD) that occur frequently together and share a substantial overlap of pathogenesis (Cheung & Li, 2012). Angiotensin-converting enzyme (ACE, EC 3.4.15.1) and dipeptidyl peptidase-IV (DPP-IV, EC 3.4.14.5) are crucial enzymes involved in hypertension and diabetes, respectively. Expressed in many human tissues, ACE is associated to elevated blood pressure and is responsible to cleave a dipeptide (HL) from the decapeptide angiotensin I to form the potent vasoconstrictor, angiotensin II. Furthermore, ACE inhibits and degrades bradykinin, a potent vasodilator (Riordan, 2003). On the other hand, DPP-IV, a metabolic serine peptidase widely distributed in several tissues, causes the degradation and inactivation of glucagon-like peptide-1 (GLP-1) and glucose-dependent insulinotropic polypeptide (GIP), which are incretin

hormones responsible for stimulating the secretion of insulin (Lambeir, Durinx, Scharpé, & De Meester, 2003).

In the field of bioactive food peptides, ACE and DPP-IV inhibitory activity have been studied extensively (Liu, Cheng, & Wu, 2019; Martin & Deussen, 2019) and many hypotensive and hypoglycemic peptides have been identified from different food matrices, such as milk, egg, ham, hempseed, lupin, and soybean, whereas only a few from microalgae, such as *Arthrospira platensis* (spirulina) (de Castro & Sato, 2015; Singh, Vij, & Hati, 2014).

Among the microalgae species available on the market, *Chlorella pyrenoidosa* stands out for the high protein content (55-60% of biomass) and balanced amino acid composition. These features indicate that this species is a sustainable food alternative as well as a potential source of bioactive peptides (Li, Lammi, Boschin, Arnoldi, & Aiello, 2019). Several biological effects of chlorella derived protein hydrolysates and peptides have been reported, such as antioxidant, anti-inflammatory, antihypertensive, and immunostimulant activities (Fan, Bai, Zhu, Yang, & Zhang, 2014). Although experimental and clinical studies have shown that the consumption of *C. pyrenoidosa* reduces high blood pressure, serum cholesterol, and glucose levels while it improves the immune functions (Cherng & Shih, 2005; Merchant & Andre, 2001; Senthilkumar, Sangeetha, & Ashokkumar, 2012), the peptides of this microalga are not sufficiently investigated yet.

In light of these considerations, the first objective of this work was to obtain a total protein extract of *C. pyrenoidosa* that was hydrolyzed using two common gastrointestinal enzymes, i.e., pepsin and trypsin, in order to produce a peptic (CP) and a tryptic (CT) hydrolysate. The composition of each hydrolysate was assessed by HPLC-ESI-MS/MS, using a peptidomic approach, and the potential hypotensive and hypoglycemic activities were evaluated, initially measuring the ability of both hydrolysates to inhibit *in vitro* the ACE and DPP-IV activities and, afterwards, by carrying out experiments using Caco-2 cells that express both enzymes. The positive results obtained in these experiments suggested the presence of some very active multifunctional peptides within both hydrolysates. In order to identify the active species,

docking and molecular dynamics (MD) tools were applied to simulate the interaction between the peptides and the protein targets and to hierarchize the most promising ones. Finally, the hydrolysates were submitted to simulated gastrointestinal digestion (GI) in order to verify whether the candidate peptides were sufficiently stable to digestion.

5.2 Material and Methods

5.2.1 Reagents.

All chemicals and reagents were of analytical grade and from commercial sources. Acetonitrile (ACN), tris(hydroxymethyl)aminomethane (Tris), hydrochloric acid (HCl), ammonium bicarbonate, pepsin from porcine gastric mucosa (P7012, lyophilized powder, ≥ 2,500 units/mg protein), trypsin from bovine pancreas (T1426, lyophilized powder, ≥ 10,000 units/mg protein), ACE from porcine kidney, hippuryl-histidyl-leucine (HHL), formic acid, sodium chloride, zinc chloride were from Sigma-Aldrich (St. Louis, MO, USA). Bovine serum albumin (BSA) and β-mercaptoethanol were from Thermo Fisher Scientific (Life Technology, Milan Italy). Bradford reagent and Coomassie Blue G-250 were purchased from Bio-Rad (Hercules, CA, USA). LC-grade H_2O (18 MΩ cm) was prepared with a Milli-Q H_2O purification system (Millipore, Bedford, MA, USA). Dulbecco's modified Eagle's medium (DMEM), L-glutamine, fetal bovine serum (FBS), phosphate buffered saline (PBS), penicillin/streptomycin and 96-well plates were purchased from Euroclone (Milan, Italy). Sitagliptin and Gly-Pro-amido-4-methylcoumarin hydrobromide (Gly-Pro-AMC) were from Sigma-Aldrich (St. Louis, MO, USA). ACE1 Activity Assay Kit was from Biovision (Milpitas Blvd., Milpitas, CA, USA).

5.2.2 Microalgae biomass.

C. pyrenoidosa dry powder was purchased from Qingdao Lang Yatai Company Limited (Qingdao, China). The manufacturer declares that they had cultivated it in photoautotrophic conditions in outdoor runway pools and that the dry powder had been prepared by spray drying.

5.2.3 Ultrasound-assisted and heating protein extraction.

C. pyrenoidosa powder was defatted overnight with hexane (ratio 1:20 w/v) under magnetic stirring. After drying, the defatted powder (0.5 g) was suspended in 10 mL of lysis buffer (8 M urea, 1% CHAPS, 20 mM DTT in 0.1 M of NH_4HCO_3). The mixture was placed in ice and treated with ultrasonic cell disruptor for 6 min (5 s at 50 W, 23 kHz frequency pulses followed by 5 s of cool-down period). Then the sonicated suspension was heated for 15 min and cleared via centrifugation at 7200 g (4 °C, 30 min). The supernatant was collected and dialyzed against ddH_2O at 4 °C for 48 h and then stored at -20 °C until analysis. By SDS-PAGE, the chlorella protein extract was profiled as previously reported (G. Aiello, Y. C. Li, G. Boschin, C. Bollati, A. Arnoldi, & C. Lammi, 2019).

5.2.4 C. pyrenoidosa protein hydrolysis and peptide sequencing by LC-ESI MS/MS.

The enzymatic hydrolysis of *C. pyrenoidosa* proteins was performed using trypsin and pepsin. For the trypsin and pepsin digestion, the pH of the protein extracts was adjusted to pH 8 and 2, respectively, by adding 1 M NaOH or 1 M HCl. The trypsin and pepsin solutions were added to the protein extracts at a 1:50 (w/w) E/S ratio. After overnight digestion (16 h), trypsin was inactivated by heating at 95 °C for 5 min, whereas the peptic digestion was blocked by adjusting the pH to 8. Each hydrolysate was passed through ultrafiltration membranes with a 3 kDa cut-off, using a Millipore UF system (Millipore, Bedford, MA, USA). Recovered peptides were lyophilized and stored at -80 °C until use. The degree of hydrolysis (DH) of each hydrolysate was measured by the o-phthaldialdehyde (OPA) assay (G. Aiello, Y. C. Li, G. Boschin, C. Bollati, A. Arnoldi, & C. Lammi, 2019). CT and CP hydrolysates were analyzed by HPLC-CHIP-ESI-MS/MS as previously reported (G. Aiello, Y. Li, G. Boschin, C. Bollati, A. Arnoldi, & C. Lammi, 2019). For the peptide identification, the MS/MS data were analyzed by a Spectrum Mill Proteomics Workbench (Rev B.04.00, Agilent), consulting the *C. vulgaris* database (310 entries) downloaded from the UniProtKB-SwissProt. The use of

this database instead of *C. pyrenoidosa* is justified by the phylogenetic proximity of these microalgae. Pepsin and trypsin were selected as cutting enzymes, respectively. Two missed cleavages were allowed to each enzyme used; peptide mass tolerance was set to 1.0 Da and fragment mass tolerance to 0.8 Da. Auto-validation strategy both peptide and protein polishing mode was performed using FDR cut-off ⩽1.2%.

5.2.5 Biological evaluation of the peptic and tryptic hydrolysates

5.2.5.1 *In vitro* measurement of the ACE inhibitory activity.

In order to assess the ACE-inhibitory activity, the peptic and tryptic hydrolysates were tested by using HHL as a mimic substrate for angiotensin 1 and the produced hippuric acid (HA) was analyzed by HPLC, as previously reported (Boschin, Scigliuolo, Resta, & Arnoldi, 2014).

5.2.5.2 *In vitro* measurement of the DPP-IV inhibitory activity.

The in vitro experiments were carried out in a half volume 96 well solid plate (white) using conditions previously optimized by (Lammi, Zanoni, Arnoldi, & Vistoli, 2016). Further details are provided in section **3.2.9**

5.2.5.3 Cell cultures

Caco-2 cells, obtained from INSERM (Paris, France), were routinely sub-cultured at 50% density and maintained at 37 °C in a 90% air/10% CO_2 atmosphere in DMEM containing 25 mM of glucose, 3.7 g/L of NaHCO3, 4 mM of stable L-glutamine, 1% nonessential amino acids, 100 U/L of penicillin, and 100 µg/L of streptomycin (complete medium), supplemented with 10% heat-inactivated fetal bovine serum.

5.2.5.4 Cellular measurement of the ACE inhibitory activity.

A total of 5×10^4 Caco-2 cells /well were seeded in 96-well plates for 24 h. In the following day, cells were treated with 100 µL of hydrolysates from chlorella proteins digested by pepsin (CP) and trypsin (CT) (in the concentration range from 1.0 to 5.0 mg/mL) or vehicle in growth medium for 24 h at 37 °C. Afterwards, the ACE1 Activity Assay Kit (Biovision, Milpitas Blvd., Milpitas, CA, USA) was used to evaluate the ACE inhibitory activity. The procedure is described in detail in section **3.2.8**.

5.2.5.5 Cellular measurement of DPP-IV inhibitory activity.

Caco-2 cells (5×10^4/well) were seeded in black 96-well plates with clear bottoms and cultured for 24 h. Afterwards, spent media was removed and CP and CT hydrolysates (1.0, 2.5, and 5.0 mg/mL), sitagliptin at 1.0 μM (positive control), or vehicle in growth medium were separately used to treat Caco-2 cells for 24 h at 37 °C. Then the treatment media were removed and cells were washed with 100 μL of PBS without Ca^{++} and Mg^{++}, and 100 μL of Gly-Pro-AMC substrate (Cayman Chemical, Ann Arbor, MI, USA) at the concentration of 50.0 μM in PBS without Ca^{++} and Mg^{++} were added in each well. Fluorescence signals (ex./em. 350/450 nm) were detected using the Synergy H1 fluorescent plate reader from Biotek every 1 min for 10 min.

5.2.6 In silico molecular docking and MD of the inhibitory peptides on ACE and DPP-IV.

The molecular modeling study aimed at describing the interaction of CT and CP peptides with both the N and C domains of human ACE and DPP-IV. The study relied on model preparation, docking studies, and molecular dynamic (MD) simulations, as detailed below.

5.2.6.1 Preparation of receptors and ligands.

Before performing molecular docking, protein molecules and peptides are prepared separately to minimize docking errors resulted from the incorrect assignments. Protein Preparation Wizard from Maestro was used for protein model preparation. The model for C and N domains of human ACE and DPP-IV derived from the three-dimensional structures were imported from the protein molecules of ACE and DPP-IV from PDB (http://www.rcsb.org), i.e. the X-ray crystallographic structures of human-testicular ACE-captopril complex (PDB ID: 1UZF) and human DPP-IV in complex with Diprotin A(IPI) (PDB ID: 1NU8 (Natesh, Schwager, Evans, Sturrock, & Acharya, 2004; Thoma, Loffler, Stihle, Huber, Ruf, & Hennig, 2003). The protein preparation involved the following steps: 1) pre-processing the imported protein structure with the defaults that are recommended for the minimal processing; 2) modifying the structure by removing

all the water molecules and undesired chains and ligands; 3) for H-bond assignment, optimizing automatically the hydroxyl, Asn, Gln, and His states at a given pH of 7.0; 4) finally performing the restrained minimization of the protein structure to specify the root mean square deviation (RMSD) of the heavy-atom displacement below 0.3 Å, compared with the input geometry. The force field was set as OPLS3. To prepare the ligands, Captopril and Diprotin A (IPI) were extracted from the imported structure of ACE-captopril complex and DPP-IV-diprotin A (IPI) complex, respectively. 3D builder was applied to build the extended conformation of the eleven selected peptides from the sequence. For each ligand, LigPrep was used to produce one output structure with low energy for docking analysis. Possible ionization and tautomeric states at target pH 7.0 +/-2.0 were generated by means of Epik. The specified chirality of the peptides was retained to guarantee they were from the natural protein source.

5.2.6.2 Molecular modeling of ACE and DPP-IV binding interactions with peptides.

GLIDE was employed to perform the docking. First the receptor grids were generated in the prepared protein structure of ACE and DPP-IV, respectively. Next, the docking between two receptors and each ligand were carried out with the default docking parameters while the precision was set as standard precision (SP) for peptide. Peptides were docked softly into the protein binding site (ligand sampling: flexible). The docked structures were further optimized by the "Perform post-docking minimization" option in which bond lengths, bond angles, as well as torsion angles are optimized in the context of the protein. Finally, five docking poses per ligand were produced and the one with lowest docking score was firstly considered for MD.

5.2.6.3 MD analysis.

A solvent system of each ligand-protein complex was prepared by building an orthorhombic TIP3P box of water molecule with 10 Å in all three dimensions. The complex system was then submitted to MD analysis with an NPT ensemble at the temperature of 300 K, pressure of 1.01325 bar. A trajectory for each complex was recorded during the total simulation time of 200 ns, wherein the snapshots of complex were extracted at every 1 ns, producing 200 snapshots totally. The MD trajectories were visualized with the VMD program. By analyzing the backbone RMSD changes of one

trajectory, the successive stable snapshots within 1 Å changes were extracted for free binding energy calculation based on MM/GBSA (Molecular Mechanics/ Generalized Born Surface Area) methodology. The final binding free energy presents as an average of the binding free energies of snapshots.

5.2.7 Evaluation of peptide stability toward simulated gastrointestinal digestion

After having shifted the pH to 2.0, the CP and CT solutions were added with pepsin (4 mg/mL in NaCl using E/S ratio 1:100) and incubated at 37 °C for 60 min under continuous shaking. Then, the pH was adjusted to 8.0 with 1 M NaOH and pancreatin (4 mg/mL in ddH2O) was added (E/S ratio 1:100) for performing the digestion at 37 °C for 15 min. The enzymatic reaction was blocked by heating at 95 °C for 10 min and the enzymes were completely removed by centrifugal ultrafiltration (3 kDa cutoff). This process was repeated without adding pepsin and pancreatin in order to prepare the controls. The stability of the four screened peptides was assessed through multiple reaction monitoring (MRM) mass spectrometry. The injected samples were eluted as following gradients: 5% solvent B (0 min), 70% solvent B (0-10 min), and back to 5% in 5 min. The drying gas temperature was set at 300 °C, flow rate 3 L/min (nitrogen). Data acquisition was carried out in positive ionization mode. Capillary voltage was -2000 V, with endplate offset -500 V. Full scan mass spectra were acquired in the mass range from 100 to 850 Da. Capillary voltage was −2000 V, with endplate offset −500 V, skimmer -40 V, drying gas flow 5 L/min, drying gas temperature 300 °C. The targeted assay was performed by targeting the precursor ions at *m/z* 474.0 for Pep2 (FLKPLGSGK), *m/z* 601.3 for Pep8 (FLFVAEAIYK) and *m/z* 281 for both Pep7 (QIYTMGK) and Pep10(QHAGTKAK), respectively. Peptides were targeted through matching the retention time, MS profiles and MS/MS fragmentation spectra. For Pep2 and Pep8, intensity of their MS profiles was acquired to monitor the peptide stability, instead, for Pep7 and Pep10, since their m/z are quite similar, the intensity of typical fragment ions at m/z 167.9, 319.0 for Pep7 and m/z 197.4, 394.1 for Pep10 were employed.

5.2.8 Statistical analysis

All liquid chromatography−mass spectrometry (LC−MS) analyses were run in triplicate. For the experiments aimed at evaluating the bioactivities, all measurements were performed in triplicate and results were expressed as the mean ± standard deviation, where p-values < 0.05 were significant. Statistical analyses were performed by one-way ANOVA (GraphPad Prism 7, GraphPad Software, La Jolla, CA, USA) followed by Tukey's post-hoc test.

5.3 Results

5.3.1 Optimization of the protein extraction and hydrolysis

In order to improve the protein extraction from the *C. pyrenoidosa* matrix, a protocol with specific conditions was optimized (data not shown). At the end of this investigation, a highly concentrated urea solution (8 M) buffer coupled with ultrasonication and heating permitted to achieve the best protein yield. With this optimized method, the concentration of total protein extract from *C. pyrenoidosa* was 18.34 mg/mL. For the hydrolysis, two enzymes, i.e., trypsin and pepsin were employed, whose effectiveness was monitored by detecting the DH (%). **Figure 5.1A** shows the trend of the DH during the first 3.5 h, indicating that in both cases the maximum rate of hydrolysis was achieved in the first 30 min. After overnight digestion (16 h), the final DH of the CP and CT reached 18.7% and 31.8%, respectively. Correspondingly, SDS-PAGE was used to compare the protein profile of raw and enzymatically digested samples for both CP and CT group. In **Figure 5.1B**, the RM lane shows the protein composition of raw total protein extracts without the addition of enzymes. The most intense protein bands were detected in the range between 25–170 kDa. During both hydrolysis, these intense protein bands almost disappeared already at time 3.5 h.

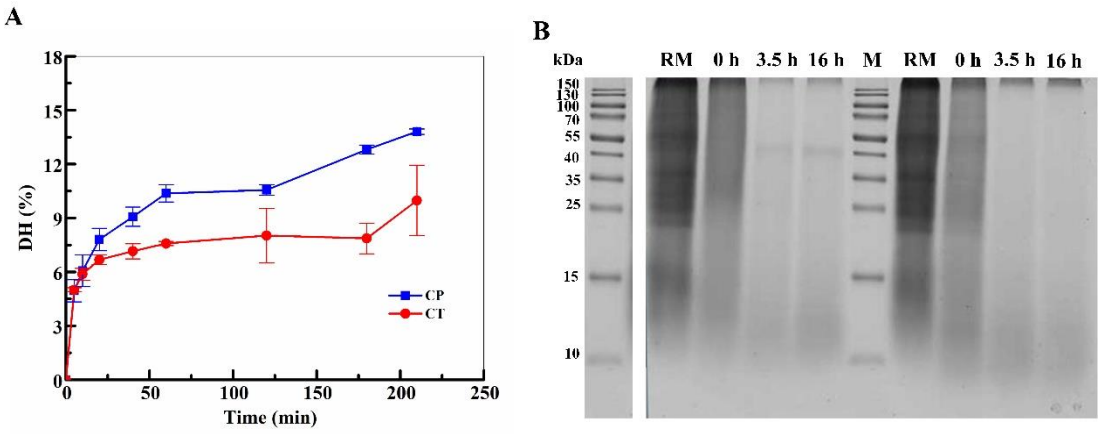

Figure 5.1 Degree of hydrolysis (DH) trend and digestion efficiency of protein from *C. pyrenoidsa*. A) DH at different time points within the first 3.5 h of enzymatic digestion. B) SDS-PAGE analysis of hydrolysates sampled at different hydrolysis time points. RM: raw protein extract; CP: *C. pyrenoidsa* proteins digested by pepsin; ST: *C. pyrenoidsa* protein digested by trypsin.

5.3.2 Peptide profile by LC-MS/MS

The peptide profiles of CP and CT were characterized by nano-ESI-MS/MS. In total, 47 peptides were identified in the CP sample and 66 in the CT sample (**Table 5.1**). Since several studies have demonstrated that significant biological effects are exerted by low molecular weight peptides, short peptides (aa ≤10) were selected as a targeted dataset for further investigations (Zou, He, Li, Tang, & Xia, 2016). **Table 5.2** lists the identified peptide sequences with the number of amino acids (aa) ≤10, among which 5 were from the CP sample and 6 from the CT sample. All the peptides were numbered as Pep1 to Pep11. Among these short peptides, 6 peptides (Pep1, Pep4, Pep6, Pep7, and Pep11) were abundant, since they showed high spectrum intensity (>10^8), accounting for the main percentage of the protein hydrolysates. Hydrophobicity of each selected peptide was calculated by Wimley-White scale. Five peptides (Pep2, Pep3, Pep7, Pep9, and Pep10) showed relatively high hydrophobicity, with values equal to +12.19, +18.27, +10.37, +26.37, +19.00 Kcal/mol, respectively.

Table 5.1 LC-ESI-MS/MS based identification of tryptic (A) and peptic (B) peptides from *C. pyrenoidosa* protein hydrolysis.

(A)

No	Protein name	Accession no	m/z (charge)	Start	Peptide sequence	Spectrum Intensity	% AA Coverage
1	Leucine-tRNA ligase	A0A087SIG7	540.19	172	(Q)YAIQTGTHPAATTATN(I)	2.84E+07	1.2
2	CTP synthase	A0A1D1ZND9	646.42	386	(K)IAAAQYARTHGVPYFGIC(L)	3.93E+07	3
3	Expressed protein	E1ZPI4	672.68	88	(M)WALGARHLVDHNATELVN(L)	3.14E+07	3.9
4	Uncharacterized protein	E1ZHY9	891.37	709	(L)LGALRGDEDGGGGGGGGSWRGRGRKGTE(-)	1.20E+07	3.8
5	Uncharacterized protein	E1ZF52	967.68	375	(F)YAPCLANRPKGDEPPQASGPGLESFPDS(L)	1.20E+07	5.9
6	Uncharacterized protein	A0A087SUF8	473.63	1	(-)MSANHDAGGS(Y)	1.24E+07	3.8
7	Uncharacterized protein (Fragment)	E1ZS03	563.12	916	(E)LMQQLEAAAAVVGEKE(L)	1.08E+07	1.6
8	Carboxypeptidase	E1ZNB5	647.06	2350	(C)YLNLPEVQEALGVAPGLR(F)	2.97E+07	3.2
9	Uncharacterized protein	M1HUP1	887.93	5	(T)FAPRFNDGRSTAREDFHEPLPVC(L)	1.39E+07	5.9
10	Glucose-methanol-choline oxidoreductase	A0A248QE08	658.71	264	(T)FQVMQDKGTRADMYRQ(Y)	3.01E+07	2.4
11	Serine/threonine-protein kinase	M1HU78	473.99	5	(T)FLKPLGSGK(Y)	2.75E+07	2.8
12	Uncharacterized protein (Fragment)	A0A1D2A4B0	661.47	1148	(D)LGGRCAGEAGALCPPRDLLN(L)	6.71E+07	1.3
13	Uncharacterized protein	A0A087SFH1	690.05	12	(T)LCRLPRGEHHPVSKPTQL(F)	3.14E+07	13.3
14	Uncharacterized protein	E1ZHZ3	615.36	18	(R)LTDRRIDGSLAAAKGTAE(L)	1.45E+07	4.4
15	TGACG-sequence-specific DNA-binding protein TGA-1B	A0A087SLT2	960.21	35	(H)LVVLEDVRASPSASAVQFPLTHQALDD(L)	1.54E+07	5.5
16	Uncharacterized protein	A0A1D1ZZN7	686.95	213	(H)LGRLLVAGAYPVAIAWQME(Y)	2.19E+07	6

17	Uncharacterized protein	A0A1D2A7Q0	922.44	81	(F)LCVAAATVPGGWAFTHPDECTCGGISAM(L)	7.44E+07	7
18	ABC transporter A family member 2	A0A087SS55	702.68	680	(H)LHVFAAIKGIPAATRAAEAAK(L)	1.22E+07	2
19	Putative sugar phosphate/phosphate translocator	A0A087S9M6	837.29	114	(T)YENPALPLPTPPLTSLPPPNPFH(L)	6.77E+07	10
20	Cation/calcium exchanger 4	A0A087SNT9	856.45	263	(L)LDPRVMHAPPLAAFEVRGRYRD(L)	2.31E+07	3.8
21	Cytosine-specific methyltransferase	M1HEI8	989.07	229	(E)WKPNGYSVNGVISTFHIKHPTRSPEN(I)	1.36E+07	7.5
22	Uncharacterized protein	E1ZTT2	948.67	695	(L)LGWSLSDGVAQTEAPQGGASHMVRFAGN(L)	8.37E+06	3.5
23	Uncharacterized protein	M1HE87	280.94	254	(Q)LLTKS(I)	2.72E+07	1.7
24	Uncharacterized protein	E1ZIX6	785.38	61	(I)LDQDVSGFAAAAAAAAAERGPVAAPQ(L)	2.81E+07	4.5
25	Uncharacterized protein	E1ZIV7	841.11	45	(F)ILSVMGVLDTGKGLIREGSGSAVFN(L)	1.34E+07	14.3
26	Glycosyl transferase	M1IGC6	900.21	84	(Y)IDSAAVFERPITPYAEHVTDEKPI(L)	2.10E+07	2.8
27	Broad-range acid phosphatase DET1	A0A087SH24	281.04	445	(R)LLGRC(L)	5.09E+08	0.6
28	Uncharacterized protein	A0A1D2ABY3	864.85	595	(Y)LDRGKTVIVYCDTRESPEACAHE(I)	1.70E+07	2.1
29	LAGLIDADG homing endonuclease	A0A1Z1GBL4	578.56	125	(K)WKKHSKAIRFCTDN(F)	1.06E+07	6.8
30	Uncharacterized protein C9orf78	A0A087SE57	541.66	13	(T)LDEAHESGEEDAPPK(L)	1.92E+07	5.9
31	Uncharacterized protein PDC1	E1ZFT1	926.51	113	(R)LKMISCCNELNAGYAADGYGRANGIAC(L)	1.84E+07	4.2
32	Hypoxanthine phosphoribosyltransferase	E1ZD74	887.38	77	(S)YGAGTVSSGKVALTMVGGTDVKGRHVL(L)	1.58E+07	14.4
33	GIY-YIG catalytic domain-containing endonuclease	M1HCV1	281.64	488	(C)LLSKT(W)	5.31E+08	1.5
34	Type I inositol 1,4,5-trisphosphate 5-phosphatase 12	A0A087SPV7	917.24	117	(M)LRLIALAQSEHPFTSKNADVALSPAT(W)	2.48E+07	2.1

35	Glucosamine--fructose-6-phosphate aminotransferase	M1I2B0	961.26	174	(K)YKSPLVIGMNADGSICIASDPIATTTDK(I)	3.48E+07	4.7
36	Uncharacterized protein	E1ZL33	591.15	290	(I)WDTQPPQPTITTSGGGK(F)	6.82E+06	0.7
37	Uncharacterized protein	E1ZLR1	805.23	7	(S)WRPCKSDTVVERRVATAAPRD(W)	3.21E+07	2.7
38	Uncharacterized protein	E1ZND2	857.67	462	(L)LEVFARMYNQRPAVDYAVVAQM(L)	9.82E+06	2.8
39	Uncharacterized protein (Fragment)	A0A1D1ZUE1	941.25	36	(S)WGTCARCSGPLTGALWTSGLVCVLLSGI(L)	1.56E+07	7.2
40	Uncharacterized protein	E1Z5N4	846.75	882	(E)LWRDPNCAGSLTAAAQAAPDTPAGAL(F)	3.52E+07	1.8
41	Palmitoyl-monogalactosyldiacylglycerol delta-7 desaturase, chloroplastic	A0A087SFK9	991.24	499	(W)FVNSAAHVWGSQSYRTGD(L)	8.78E+06	3
42	Uncharacterized protein	E1ZHA1	843.2	216	(L)LNDQSTILPSGAKEPD(Y)	4.68E+07	2.5
43	Uncharacterized protein	E1ZK58	883.58	644	(S)LSCFADGTPVFALADADGAFASTVFR(L)	1.80E+07	2.7
44	Uncharacterized protein	E1ZIM1	867.57	732	(Q)LLPLADQHLRVEATGAAQQARVLM(L)	1.18E+07	2
45	Enhancer of polycomb-like protein	E1Z3I7	814.44	1	(-)MSRAFRARPLDVSRPLELIVD(L)	2.26E+07	2.8
46	Uncharacterized protein	E1Z511	938.57	752	(M)LNHGPAAAANAAFDMCPLPAALPPSLQR(Y)	1.80E+07	2.8
47	Uncharacterized protein	E1ZMI6	941.39	134	(Y)FEKRQPFNPIAFLKTPYGMMGAFM(L)	1.99E+07	11.7

(B)

No	Protein name	Accession no	m/z (charge)	Start	Peptide sequence	Spectrum Intensity	% AA Coverage
1	ATP synthase subunit beta	F2YGR0	747.35	256	(K)QDVLLFIDNIFR(F)	1.92E+08	2.4
2	ATP synthase subunit beta	A0A087SBN0	955.5	259	(R)DEEGQDVLLFVDNIFR(F)	1.19E+08	1.1

3	Elongation factor 1-alpha	A0A087SK74	622.45	42	(R)LLFELGGIPER(E)	1.41E+07	2.3
4	Acyl carrier protein	E1Z5W8	595.97	75	(K)ISTVQEAADLIAAQIDK(-)	2.21E+07	18.6
5	Elongation factor Tu, chloroplastic	P56292	723.83	216	(R)ETEKPFLMAVEDVFSITGR(G)	1.40E+08	4.6
6	Photosystem II CP47 reaction center protein	A0A2I4S6M8	929.56	311	(R)YQWDLGFFQQEIER(R)	2.62E+07	2.5
7	Uncharacterized protein	E1Z395	874.89	19	(K)AAGIEVEPYWPGLFAK(L)	2.74E+07	17.3
8	Chlorophyll a-b binding protein, chloroplastic	E1ZLI4	820.73	59	(K)GEFPGDYGWDTAGLSADPETFAR(Y)	1.63E+07	8.9
9	3-ketoacyl-CoA thiolase 2, peroxisomal	A0A087SPH9	685.8	106	(K)DTPVDDLIAAVLK(D)	3.52E+07	2.8
10	Ribulose bisphosphate carboxylase large chain	F2YGL1	601.28	218	(R)FLFVAEAIYK(S)	2.78E+07	2.1
11	Expressed protein	E1ZAF0	713.34	333	(K)LDAAPEDDHITLMRNGTLR(L)	5.65E+07	2.6
12	Uncharacterized protein	E1Z7I0	917.42	707	(R)ATAAAGDVDSVLAGIDRFAGYYPMYR(S)	4.50E+07	2.6
13	Uncharacterized protein	E1ZJA2	737.01	31	(R)GITFGRAGFTTGTGDGLVVVQR(Y)	7.15E+07	7.8
14	DNA excision repair protein ERCC-6-like protein	A0A087SA08	916.63	311	(R)LLAGGYSFEIQEHLAHASFIPGFSR(A)	4.54E+07	1.6
15	WD repeat-containing protein 74	A0A087SLF6	697.1	131	(R)QPDDGAWAEAWRWQAACK(E)	5.92E+07	5.6
16	Uncharacterized protein	E1ZA50	916.79	71	(K)SGGCHSDHSTPGSSGSAAAHGAAHGPPPPR(Q)	5.55E+07	4.3
17	Expressed protein	E1Z3R5	903.94	229	(R)QELRCQGSCHSDTIDCMRFLPGGR(L)	1.85E+07	5.8
18	Putative histone-lysine N-methyltransferase ATXR3	A0A087SSG3	686.73	342	(R)DAWGMDCYTRR(N)	3.82E+07	0.8
19	Uncharacterized protein	E1Z1Z7	891.36	134	(R)DYFLPIVADAEAGFGGPLNAYELTK(H)	6.00E+07	5.9
20	Putative polygalacturonase	A0A087SUF0	700.16	139	(R)ALVDWADPSCPVPSECRPR(L)	3.77E+07	4.3

21	Uncharacterized protein	E1Z9B3	700.16	12	(R)GEEDLLKIQQLLDEALDR(R)	3.85E+07	5.2
22	Uncharacterized protein (Fragment)	E1ZMP5	809.48	272	(K)GLLNLIDLAGSERLSRSAVTGER(L)	7.36E+06	6
23	DNA polymerase epsilon catalytic subunit A	A0A087SA98	745.04	1923	(R)LLQTHGEKLEVSAEELNAPR(F)	2.76E+07	0.9
24	Uncharacterized protein	E1ZBW6	773.42	633	(R)GPFKGGGGGGGGSGARGSGVEAAGQER(D)	9.52E+06	4
25	Thymidylate synthase	M1IKB3	801.03	162	(K)ESARMVLPMSSPTTIYMTGTAR(S)	9.81E+06	9.7
26	Uncharacterized protein	E1ZQZ4	617.97	22	(R)LEQAQSEHSQLKEAVR(S)	3.87E+07	4.6
27	Biotin carboxyl carrier protein of acetyl-CoA carboxylase	A0A087SAZ6	698.86	189	(R)VGKGPLAAAGDSVKK(G)	6.59E+07	6.3
28	Uncharacterized protein	A0A1D1ZW70	840.83	383	(R)LYRVDIQLAFPEASTKALTAGVR(Q)	1.24E+07	3
29	Uncharacterized protein (Fragment)	A0A1D1ZQ66	855.86	160	(R)LGGHGGARARHHAAHHAGGDADALPR(G)	4.04E+07	6.3
30	PBCV-specific basic adaptor domain-containing protein	M1HTF0	972.53	205	(K)INIQGTNTGAFKKVYSNFIFPIQTSK(G)	1.28E+07	5.2
31	Uncharacterized protein Z225R	A7K8I5	637.27	146	(K)DTIQRFAREQLNDFR(Y)	3.86E+07	4.3
32	Uncharacterized protein	E1ZTL8	654.31	59	(R)IVAGYQLNLATEEVERR(L)	9.71E+06	7.7
33	Pre-mRNA-splicing factor SYF1	A0A087SH90	926.15	394	(K)QILCYTEAVRTVDPDK(A)	1.18E+08	1.7
34	Uncharacterized protein b105L	A7IVY0	942.22	75	(R)QASRLIGIAREAILFSIDNLSSHGTR(N)	2.64E+07	11.3
35	Prostaglandin E synthase 2	A0A087SK04	923.61	131	(K)TPLPLPESIVLYQYEVCPFCCKVK(A)	6.66E+07	8.4
36	Uncharacterized protein	E1ZP51	281.11	175	(R)LLSTK(A)	5.17E+08	2.1
37	Uncharacterized protein	E1Z860	713.91	208	(R)VMPLREGGADIPVTEENRR(E)	6.35E+07	4.8
38	Uncharacterized protein	M1HZD6	775.8	236	(K)ILAETDDVSADVAPAIQIILEK(T)	4.98E+06	7.3
39	Uncharacterized protein	E1ZDE7	922.88	207	(K)IEALRAIMERPVAANGATLHFVDDR(Y)	4.00E+07	8
40	Uncharacterized protein M629L	A7IV09	831.93	199	(R)EHNTAGGFLDHLVSSIAGEVERR(L)	6.09E+06	9.9

41	Elongation factor G, mitochondrial	E1Z1Z5	781.03	362	(R)VLLPCSKTGPLVALAFKLEEGR(F)	4.88E+07	2.8
42	Uncharacterized protein	M1HK68	812.2	190	(K)RAFSLVRPFDNSLVTTEIVDR(N)	3.57E+07	8
43	Putative serine/threonine-protein kinase GCN2	A0A087SFY1	576.18	105	(R)DVAHEMALKREAEAR(R)	1.67E+07	1.1
44	Uncharacterized protein (Fragment)	A0A1D1ZYR9	280.96	1	(-)QIYTMGK(D)	7.32E+08	1.2
45	Uncharacterized protein	E1Z459	792.23	1755	(R)QAADGPAGGGGVVVDLVGGGAAPVRVK(R)	1.10E+08	1.4
46	Abnormal spindle-like microcephaly-associated protein-like protein	A0A087SMF7	836.46	252	(R)LVDALTGRPGLALQTEIDRLAAGR(G)	1.90E+07	2
47	Protein arginine N-methyltransferase	A0A087SR29	967.19	371	(R)MYAVEKNPNAIVTLSHRVETEWQGK(V)	2.11E+07	4
48	Uncharacterized protein	E1Z6X6	630.59	250	(R)NREALYAVSGALERAAAK(R)	1.35E+07	3.4
49	Uncharacterized protein	A0A1D2A538	838.43	1	(-)MALGPTVIRGNASEIMALASLGGER(T)	5.89E+07	11.7
50	Uncharacterized protein	A0A1D2ACR1	990.94	32	(R)SITVPRPISAPTYAPEDPKGRSFVQTR(Y)	6.68E+06	6.6
51	Gene, similar to reverse transcriptase genes of various retrotransposons	O64463	713.62	56	(R)LIDAAAEFCEQTGMVISVDK(T)	8.21E+07	10.4
52	Transmembrane protein 56-A	A0A087SMF8	923.57	260	(R)TLKPEELDSSIGAAFGAPRHDVSKDK(D)	6.83E+06	13.4
53	Uncharacterized protein	E1ZE84	926.51	712	(K)IPVSPEEHQPALPPATLRPETAAEAR(A)	3.59E+07	2.8
54	Uncharacterized protein	E1ZJF1	906.17	201	(K)LRAEVAAAEGAWLPPWAAASLGPALAR(T)	2.14E+07	6.3
55	Uncharacterized protein	E1ZCL5	474.11	472	(R)EAERGGDGR(G)	2.00E+07	1.6
56	Uncharacterized protein	A0A1D2AD70	684.99	327	(R)KLIIGSLPVSLFCSGQTYK(E)	1.43E+07	2.9
57	Uncharacterized protein	E1ZFA8	280.96	267	(R)ILGCR(F)	2.01E+09	0.4
58	Chaperone protein dnaJ 10	A0A087SRC2	988.59	197	(R)FQRLGQAYQVLGNPDLR(A)	1.49E+07	4

59	Uncharacterized protein	A0A1D2A1J8	941.35	229	(R)LLQTAPQLLPAAVEAFYYRDLDDAK(A)	1.40E+07	4
60	Hydrogenase	E7BYE2	617.29	200	(K)QGEADREWFNTTGLAR(D)	2.72E+07	3.6
61	Protein DGCR14	A0A087SQK6	871.89	178	(K)SAAGPRPTDGFGTGGQPSDRLVQWR(Y)	3.81E+07	7.2
62	Uncharacterized protein	E1ZPJ5	663.54	110	(K)QQEEGERLRAEGDGGGDGK(G)	1.22E+07	5.2
63	Peptidyl-prolyl cis-trans isomerase, chloroplastic	A0A087SB74	955.91	46	(R)YALPIHNTPIRQVQESLESISEALR(I)	7.00E+07	2.5
64	Uncharacterized protein	E1Z9J7	886.15	39	(K)IVVVGGQSSGKSSVLEAVVGRDFLPR(G)	1.98E+07	4.2
65	Phosphatidylserine synthase 2	A0A087SSA8	280.93	420	(R)QHAGTKAK(A)	2.68E+07	1.8
66	Uncharacterized protein	A0A1D1ZZN9	706.3	889	(R)QWGGAAQREASASPAEASTSR(A)	8.03E+07	1.9

Table 5.2 Short peptides (≤10 aa) identified from CP and CT by LC-MS/MS

	Peptides	Spectrum Intensity	m/z (charge)	MW (Da)	Hydrophobicity (Kcal/mol) [a]	Protein precursor
	From CP					
Pep1	LLGRC	5.09E+08	281.04 (2)	561.318	+8.34	Broad-range acid phosphatase DET1
Pep2	FLKPLGSGK	2.75E+07	473.99 (2)	946.573	+12.19	Serine/threonine-protein kinase
Pep3	MSANHDAGGS	1.24E+07	473.63 (2)	946.369	+18.27	Uncharacterized protein
Pep4	LLSKT	5.31E+08	281.64 (2)	561.361	+8.91	GIY-YIG catalytic domain-containing endonuclease
Pep5	LLTKS	2.72E+07	280.94 (2)	561.361	+8.91	Uncharacterized protein
	From CT					
Pep6	ILGCR	2.01E+09	280.96 (2)	561.318	+8.47	Uncharacterized protein
Pep7	QIYTMGK	7.32E+08	280.96 (3)	840.429	+10.37	Uncharacterized protein (Fragment)
Pep8	FLFVAEAIYK	2.78E+07	601.28 (2)	1200.667	+8.37	Ribulose bisphosphate carboxylase large chain
Pep9	EAERGGDGR	2.00E+07	474.11 (2)	946.434	+26.37	Uncharacterized protein
Pep10	QHAGTKAK	2.68E+07	280.93 (3)	840.469	+19.00	Phosphatidylserine synthase 2
Pep11	LLSTK	5.17E+08	281.11 (2)	561.361	+8.91	Uncharacterized protein

a: Hydrophobicity was calculated by PepDraw tool (http://www.tulane.edu/~biochem/WW/PepDraw/), according to the method of Wimley-White scale, 1996.

5.3.3 In vitro and cellular ACE inhibitory activity

The inhibitory effects of CP and CT hydrolysates (0.08 -1.0 mg/mL) on the *in vitro* ACE activity were evaluated using the porcine recombinant form of the enzyme. **Figure 5.2A-B** shows that both CP and CT hydrolysates efficiently inhibited the ACE activity by 84.2 ± 0.37 % and 78.6 ± 1.7 %, respectively, at 1.0 mg/mL. The CP hydrolysate was more active having a better IC_{50} than CT (0.21 mg/mL versus 0.32 mg/mL). In order to assess the effects of the CP and CT hydrolysate at cellular level, human intestinal Caco-2 cells were treated with both hydrolysates (at 1.0 – 5.0 mg/mL) for 24 h. After cell lysis, the ACE activity was measured in the presence of a fluorescent substrate. In this assay, both hydrolysates inhibited the cellular ACE activity with a dose-response trend. More in details, CP hydrolysate reduces the enzyme activity by 32.6±5.6%, 48.9±4.9, and 61.5±7.7%, respectively, at 1.0, 2.5, and 5.0 mg/mL (**Figure 5.2C**), whereas CT hydrolysate by 49±12.7%, 67.1±2.0%, 69.9±0.8%, respectively, at the same concentrations (**Figure 5.2D**).

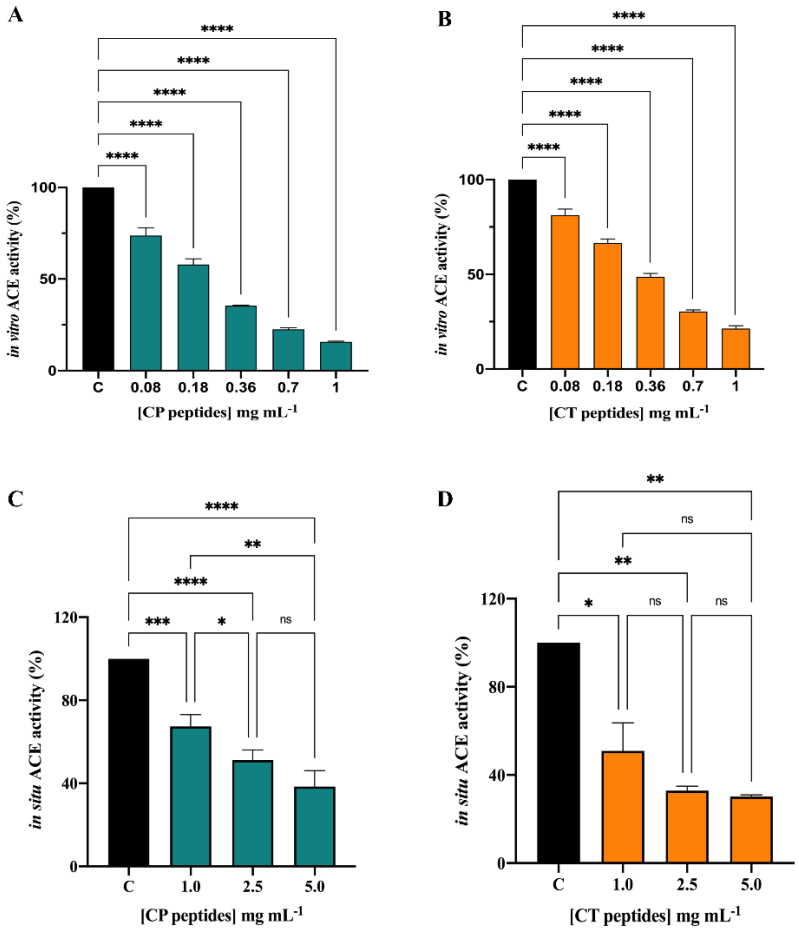

Figure 5.2 Evaluation of the inhibitory effects of CP and CT hydrolysates on ACE. (A) in vitro inhibition of ACE; (B) inhibition of ACE expressed on Caco-2 cell membranes. Bars represent the average ± SD of 3 independent experiments in duplicates. ****p<0.0001, ***p<0.001, **p<0.01.

5.3.4 In vitro and cellular DPP-IV inhibitory activity

For evaluating the DPP-IV inhibitory activity of the hydrolysates, in vitro experiments were preliminarily performed by using the purified recombinant DPP-IV enzyme and H-Gly-Pro-AMC as a substrate. The reaction was monitored by measuring the fluorescence signals (465 nm) deriving from the release of a free AMC group after the cleavage of H-Gly-Pro-AMC catalyzed by DPP-IV. **Figure 5.3A** indicates that both CP and CT hydrolysates significantly inhibited the DPP-IV activity in vitro: CP reduced the DPP-IV activity by 21.3 ± 2.9, 41.5 ± 0.9, and 63.7 ± 0.5 %, respectively, at 1.0, 2.5, and 5.0 mg/mL, whereas CT by 13.7 ± 0.8, 43.1 ± 5.4, and 69.6 ± 1.4 %, respectively, at the same concentrations. Then, the DPP-IV inhibitory activity was assessed in cellular experiments, using Caco-2 cells that are an improved tool for the screening of DPP-IV inhibitors, since they are a reliable model of intestinal epithelial cells and express high levels of DPP-IV (Caron, Domenger, Dhulster, Ravallec, & Cudennec, 2017). The same concentrations applied in the in vitro assay were used here. By monitoring the same fluorescent reaction, clear DPP-IV inhibitory effects were observed as shown by **Figure 5.3B**. The CP hydrolysate dropped the cellular DPP-IV activity by 25.3 ± 7.9, 20.5 ± 5.7, and 38.4 ± 3.4% at 1.0, 2.5, and 5.0 mg/mL, respectively, and CT by 22.3 ± 9.8, 20.5 ± 5.7, and 42.5 ± 5.7% at 1.0, 2.5, and 5 mg/mL, respectively. These results indicate that both hydrolysates are less active at cellular level than *in vitro*.

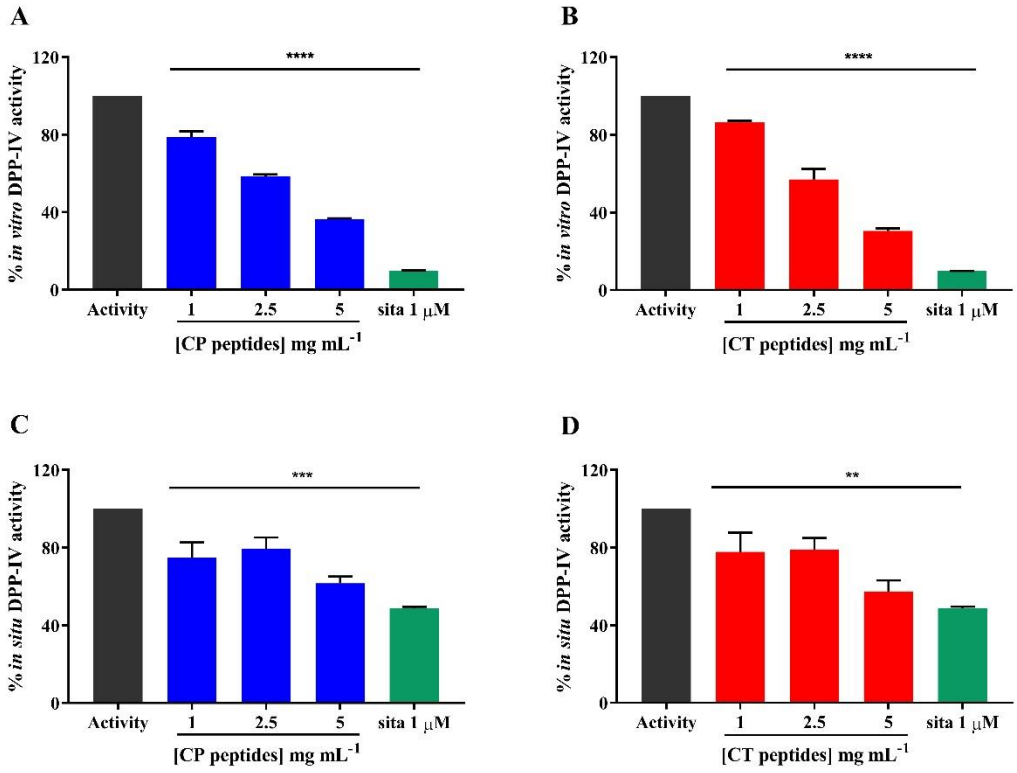

Figure 5.3 Evaluation of the inhibitory effects of CP and CT hydrolysates on DPP-IV. A and B: in vitro inhibitory activity on human recombinant DPP-IV; C and D cellular inhibitory activity on DPP-IV expressed on Caco-2 cell membranes. Bars represent the average ± SD of 3 independent experiments in duplicates. ****p<0.0001, ***p<0.001, **p<0.01 versus untreated sample (Activity). sita: sitagliptin, positive control, at 1.0 μM.

5.3.5 In silico molecular docking and dynamics of ACE and DPP-IV inhibitory activity and selected peptides

After having identified by LC-MS/MS the most abundant among short peptides, it was decided to submit them to an in silico molecular docking study. The Schrodinger software was applied to predict and evaluate the interactions of these short peptides with ACE and DPP-IV. The strategy of molecular modelling includes two stages: 1) the validation step and 2) docking and MD analysis of the peptides with ACE/DPP-IV.

The first step was necessary to improve the accuracy of docking method. Captopril and Diprotin A (IPI) were used as referenced inhibitor for ACE and DPP-IV interaction, respectively (Ondetti & Cushman, 1977). Each docking step was optimized and

validated by making the docking poses of captopril-ACE and IPI-DPP-IV close to their corresponding crystal structure as far as possible. To evaluate the predicted conformation against experimentally solved complex structures, RMSD between simulated and native ligands and ligand-receptor binding sites were considered as two important criteria. For each complex (captopril-ACE, IPI-DPP-IV), **Figure 5.4** shows the comparison between their docking pose and crystal structure. With the modified docking method, the captopril-ACE presents an excellent RMSD of 0.7640 Å against the reported crystal structure while IPI-DPP-IV docking complex got a slightly higher RMSD of 2.7390 Å against the crystal structure (**Figure 5.4A**, **D**), indicating the docking method was reasonable since typically predictions within an RMSD of 2 Å are considered successful, whereas values higher than 3 Å indicate docking failure. In addition, the binding sites of each docking structure (captopril-ACE, IPI-DPP-IV) were highly in line with that of the corresponding crystal structures as shown clearly in the 2D interaction view. In both crystal structure (**Figure 5.4B**) and docking pose (**Figure 5.4C**), residue GLN281, TYR520 were bond to carboxyl of captopril by hydrogen bond and LYS511 by salt bridge; His353 and His513 interact with carbonyl by hydrogen bond. Particularly, in the docking pose, salt bridge was generated between zinc and reduced thiol group of captopril, like the situation in the crystal structure, where zinc is occupied by thiol group of captopril through metal coordination and salt bridge, greatly contributing to the inhibition of enzyme activity since ACE is a zinc-dependent dipeptidyl carboxypeptidase and zinc directly participates in the catalysis (Bunning & Riordan, 1985; Natesh, Schwager, Evans, Sturrock, & Acharya, 2004). Although the metal coordination was not predicted by Ligand docking, RMSD between zinc and captopril (2.34 Å) was really close to that of the crystal structure (2.37 Å). In terms of IPI-DPP-IV complex (**Figure 5.4D**), all the binding sites in the native complex were involved in the docking pose: TYR547, TYR 631 were bond to the oxyanion of IPI by hydrogen bonds, just as ASN710, working on another carboxylate oxygen (**Figure 5.4E-F**). Carboxyl groups of Glu205/206 interact with the N terminus of IPI via salt bridge and hydrogen bond, which served as a large network to stabilize the complex (Thoma, Loffler, Stihle, Huber, Ruf, & Hennig, 2003). ARG125 acts on the C-terminal

carboxyl group while binding types between docking and native structure are different. Considering the passable RMSD value and the pretty similar binding mode. we approved of the method of docking ligands to ACE and DPP-IV.

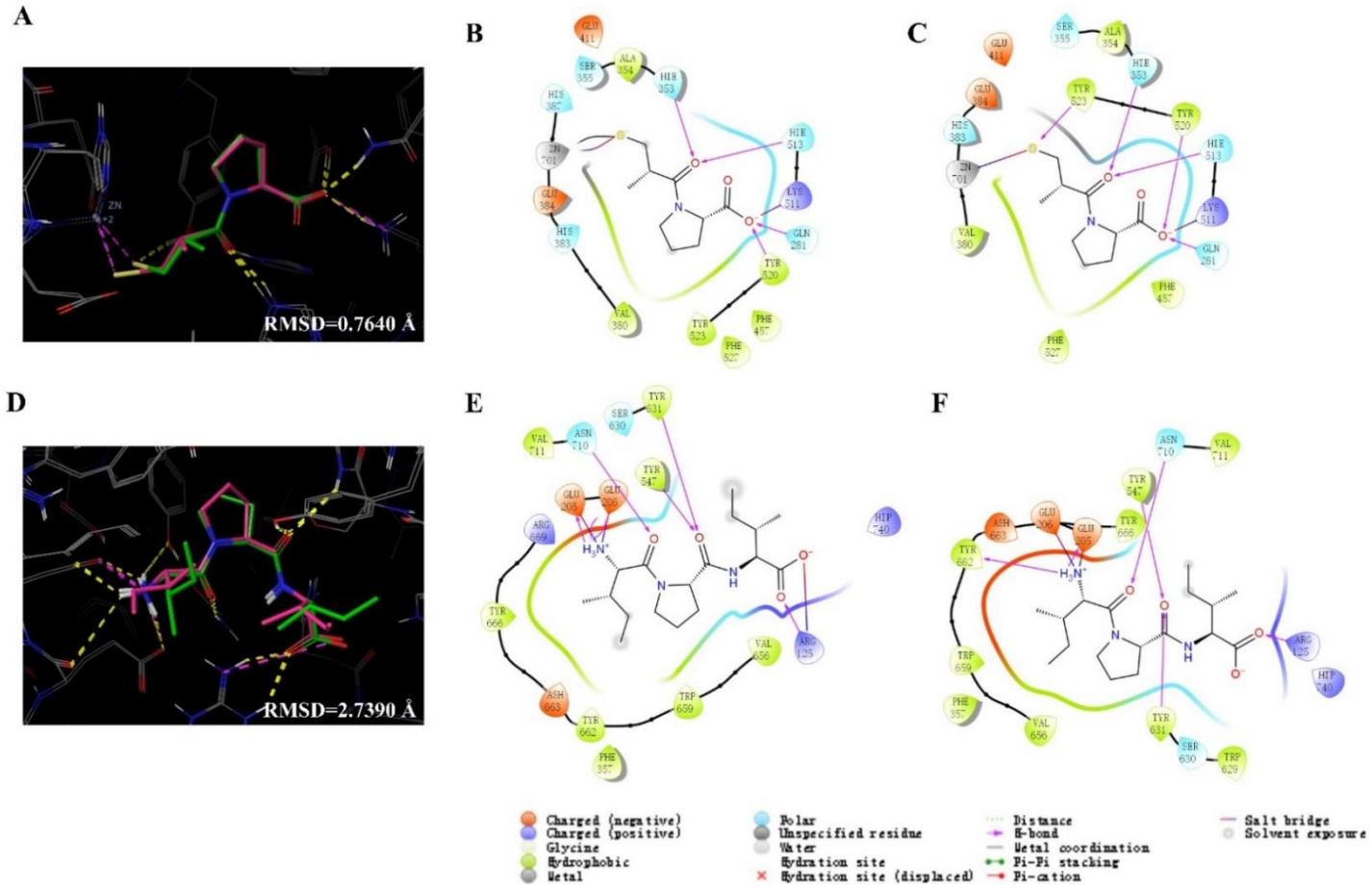

Figure 5.4 Validation of the molecular docking by comparing the docking pose and crystal structure of ACE-captopril and DPP-IV-IPI complexes, respectively. For ACE: (A) the alignment of docking pose (green) and crystal structure of captopril (pink); (B) binding sites between ACE and captopril in crystal structure; (C) predicted binding sites between ACE and captopril in the docked complex. For DPP-IV: (D) the alignment of docking pose (green) and crystal structure of captopril (pink); (E) binding sites between DPP-IV and IPI in crystal structure; (F) predicted binding sites between DPP-IV and IPI in docked complex. In (A) and (D) figures, hydrogen bond is present as yellow line and salt bridge is purple line.

By using the validated docking method, the poses of each peptide to ACE and DPP-IV were obtained. For every complex, the pose with the lowest negative value of the docking score was selected as the best one for further molecular dynamics analysis and free binding energy calculation. **Table 5.3** summarizes the free binding energies and docking scores of the docked peptide-ACE and peptide-DPP-IV complexes. For each receptor, the peptides were ranked by the value of free binding energy regardless of the docking score, because the former was obtained from the dynamic interaction of the ligands and receptors, providing more detailed information in terms of the complex energy and stability. Generally, the more negative the free binding energy, the better stability and binding affinity between the docked peptides and proteins were, indicating the higher potential of ACE/DPP-IV inhibiting effects (Du, Li, Xia, Ai, Liang, Sang, et al., 2016). Hence, according to the data, -50 kJ/mol of free binding energy was set as a threshold to screen peptides as the potential inhibitors to ACE/DPP-IV, i.e., the peptides making the free binding energy lower than -50 kJ/mol for the corresponding docked complexes. In this way, four peptides (Pep2, Pep 7, Pep8, and Pep10) satisfied the criterion for both ACE and DPP-IV receptor, indicating that these peptides were potentially multifunctional, since they exhibited inhibitory effects on two enzymes involved in different pathologies.

Table 5.3 Free binding energy and docking score for the best poses obtained by molecular docking and dynamics analysis of Chlorella-derived peptides interacting with ACE and DPP-IV enzymes

A) ACE as the receptor

Peptide			Free binding energy (kJ/mol)	Docking score
CT	**Pep8**	**FLFVAEAIYK**	**-101.6274**	-7.415
CT	**Pep7**	**QIYTMGK**	**-83.3382**	-10.807
CP	**Pep2**	**FLKPLGSGK**	**-81.115**	-11.458
CP	Pep3	MSANHDAGGS	-78.8264	-8.997
CT	Pep11	LLSTK	-53.8706	-10.601
CT	**Pep10**	**QHAGTKAK**	**-51.9093**	-6.411
CP	Pep5	LLTKS	-49.5414	-9.605
CT	Pep6	ILGCR	-47.9379	-9.179
CT	Pep9	EAERGGDGR	-46.4674	-7.712
CP	Pep1	LLGRC	-32.7801	-8.297
CP	Pep4	LLSKT	-9.1555	-9.354

B) DPP-IV as the receptor

Peptide			Free binding energy (kJ/mol)	Docking score
CT	**Pep10**	**QHAGTKAK**	**-74.1281**	-2.918
CT	**Pep7**	**QIYTMGK**	**-64.3836**	-7.503
CP	**Pep2**	**FLKPLGSGK**	**-60.2365**	-8.099
CT	**Pep8**	**FLFVAEAIYK**	**-59.8946**	-8.415
CP	Pep1	LLGRC	-56.0812	-7.61
CP	Pep5	LLTKS	-53.405	-6.566
CP	Pep4	LLSKT	-47.6713	-8.139
CT	Pep9	EAERGGDGR	-46.822	-6.777
CT	Pep11	LLSTK	-45.4348	-7.565
CP	Pep3	MSANHDAGGS	-43.2775	-9.345
CT	Pep6	ILGCR	-35.1571	-4.632

Figure 5.5 presents a 2D view of the interaction between each candidate peptide and ACE or DPP-IV. Peptides were stabilized in the complexes by binding to the amino acid residues/metal cofactor of protein mainly via hydrogen bonds and electrostatic interactions. Some protein amino acid residues/metal cofactor, which did not generate bonds to the docked peptides but stay around within 3.5 Å, are also shown in **Figure 5.5,** since atomic interactions within this distance also contribute to the stability of ligand-receptor complex (He, Aluko, & Ju, 2014).

As it shown in **Figure 5.5A-D**, the simulated structures indicate that these four peptides were docked into a hydrophobic pocket via multiple binding sites, some of which are critical active sites in the catalysis: His353, Ala354, and Tyr523 were bound by Pep2 (FLKPLGSGK), Glu162, Glu384, His353, His513, and Glu411 by Pep7 (QIYTMGK), His353 and Tyr523 by Pep8 (FLFVAEAIYK), Glu162, Gln281, Ala354, and His387 by Pep10 (QHAGTKAK), which mechanically illustrated how peptides effectively inhibit the activity of ACE. Some competitive ACE-inhibiting drugs also works by occupying the above-mentioned residues, for example, captopril binds to Gln281, His353, Lys511, His513, Tyr520, whereas lisinopril binds to His353, Ala354, Glu384, Lys511, His513, Tyr520, and Tyr523. This enhances the possibility that the four docked peptides inhibit ACE activity by competitively blocking the catalytic domain of ACE structure (Natesh, Schwager, Evans, Sturrock, & Acharya, 2004; Tzakos, Galanis, Spyroulias, Cordopatis, Manessi-Zoupa, & Gerothanassis, 2003). Moreover, the zinc ion stayed around the Pep2, Pep7, and Pep10 within 3.5 Å and especially generated salt bridge to Pep7 with -2.300 kJ/mol (Glide metal) of contribution to the final docking score.

Figure 5.5E-H shows the docking complexes between each peptide and DPP-IV, revealing the key ionic interactions, i.e., Pep2 was bound to Glu205, Glu206, Tyr547, and Trp629, Pep7 to Glu205, Glu206, Arg125, Ser630, Tyr662, and Tyr547, Pep8 to Arg125, Tyr666, and Trp629, and Pep10 to Ser209, Trp629, Arg125, and Tyr547. Glu205 and Glu206, reported as an important double Glu motif, generate a network with residue Arg125, essentially being responsible for the substrate recognition and specialty. Other critical binding sites, i.e., Tyr547, Trp629, Ser630, Tyr662, and Tyr666, play essential roles in the catalytic mechanism of DPP-IV (Bjelke, Christensen, Branner,

Wagtmann, Olsen, Kanstrup, et al., 2004; Lambeir, Durinx, Scharpé, & De Meester, 2003). On this basis, it was possible to hypothesize that these potent inhibitors probably act by blocking the substrate recognition and catalytic function of DPP-IV, with a mechanism similar to that of Diprotin A (IPI) and some DPP-IV inhibitory drugs, such as linagliptin and sitxagliptin (Metzler, Yanchunas, Weigelt, Kish, Klei, Xie, et al., 2008; Nabeno, Akahoshi, Kishida, Miyaguchi, Tanaka, Ishii, et al., 2013).

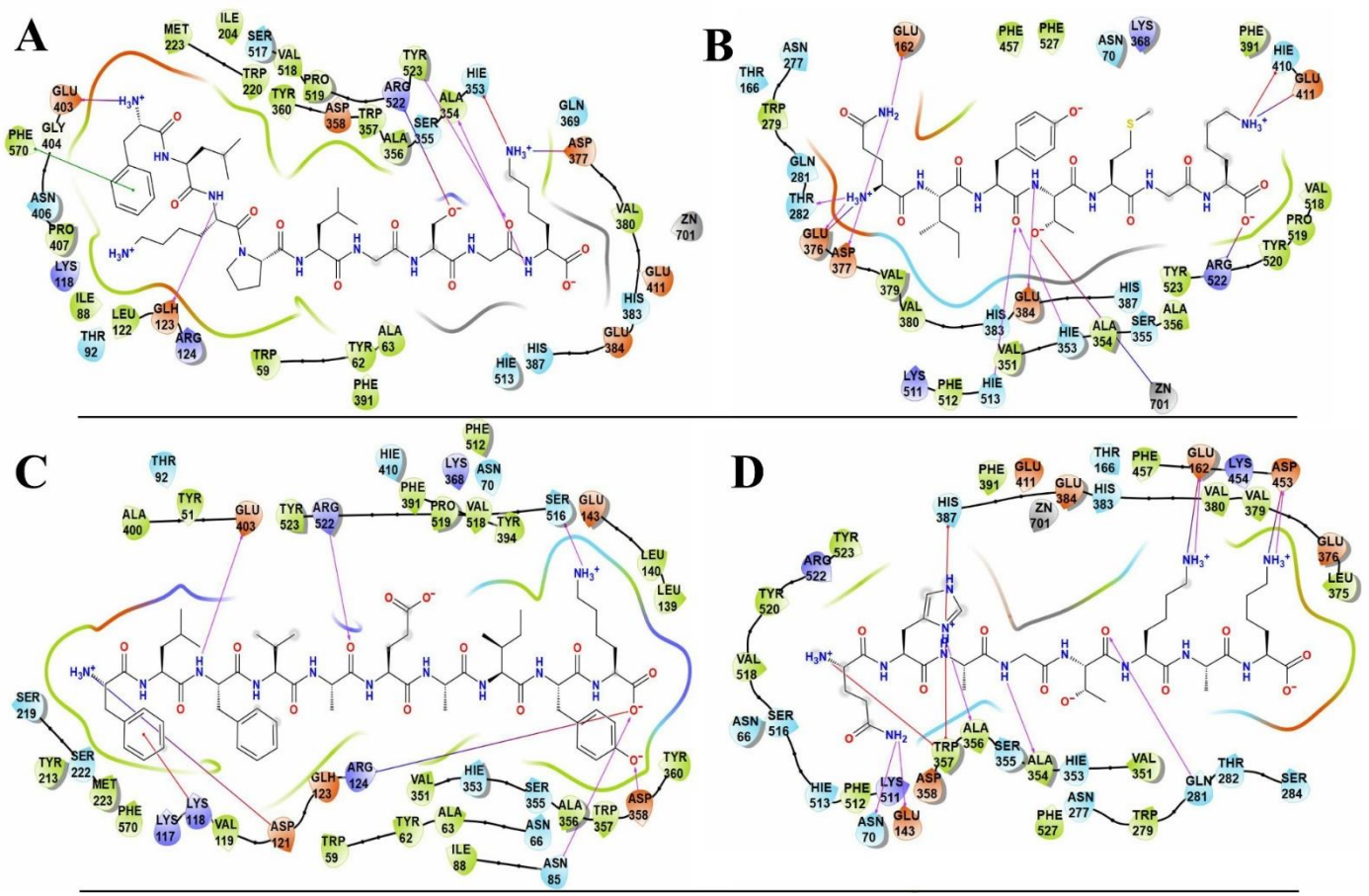
A
B
C
D

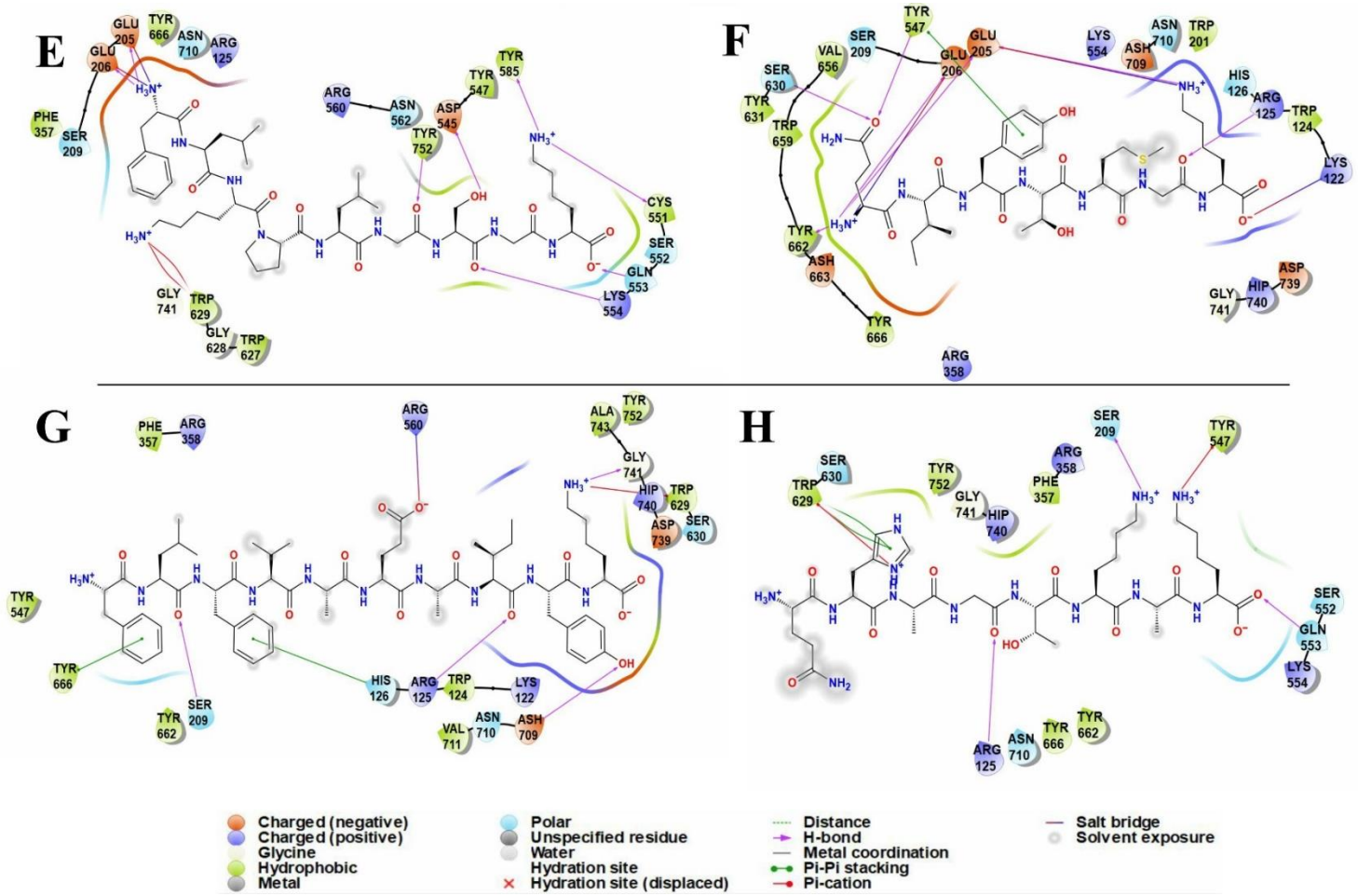

Figure 5.5 2D views of the predicted interaction between *C. pyrenoidsa* derived peptides and ACE/DPP-IV, respectively. Pep2 (FLKPLGSGK) (A), Pep7 (QIYTMGK) (B), Pep8 (FLFVAEAIYK) (C), and Pep10 (QHAGTKAK) (D) interacted with ACE; Pep2 (FLKPLGSGK) (E), Pep7 (QIYTMGK) (F), Pep8 (FLFVAEAIYK) (G), and Pep10 (QHAGTKAK) (H) interacted with DPP-IV.

5.3.6 Evaluation of the stability of the peptides towards simulated gastro intestinal (GI) digestion

To evaluate the stability of the target peptides, the CP and CT hydrolysates were submitted to simulated GI digestion with pepsin and pancreatin and the resulting solutions were analyzed by a targeted MRM assay, in comparison with the undigested samples. Whereas all four peptides were detected in the undigested samples (control) as shown by their MS/MS fragmentation spectra shown in **Figure 5.6**, their behaviors in the digested samples were diverging. In fact, Pep7 and Pep10 were easily identified in the digested samples, whereas no traces of Pep2 and Pep8 could be detected. **Figure 5.7** indicates that, after the digestion with pepsin and pancreatin, the intensities of Pep7 and P10 were decreased by 9.5 ± 5.8% and 11.1 ± 2.1%, respectively, compared to the undigested control group.

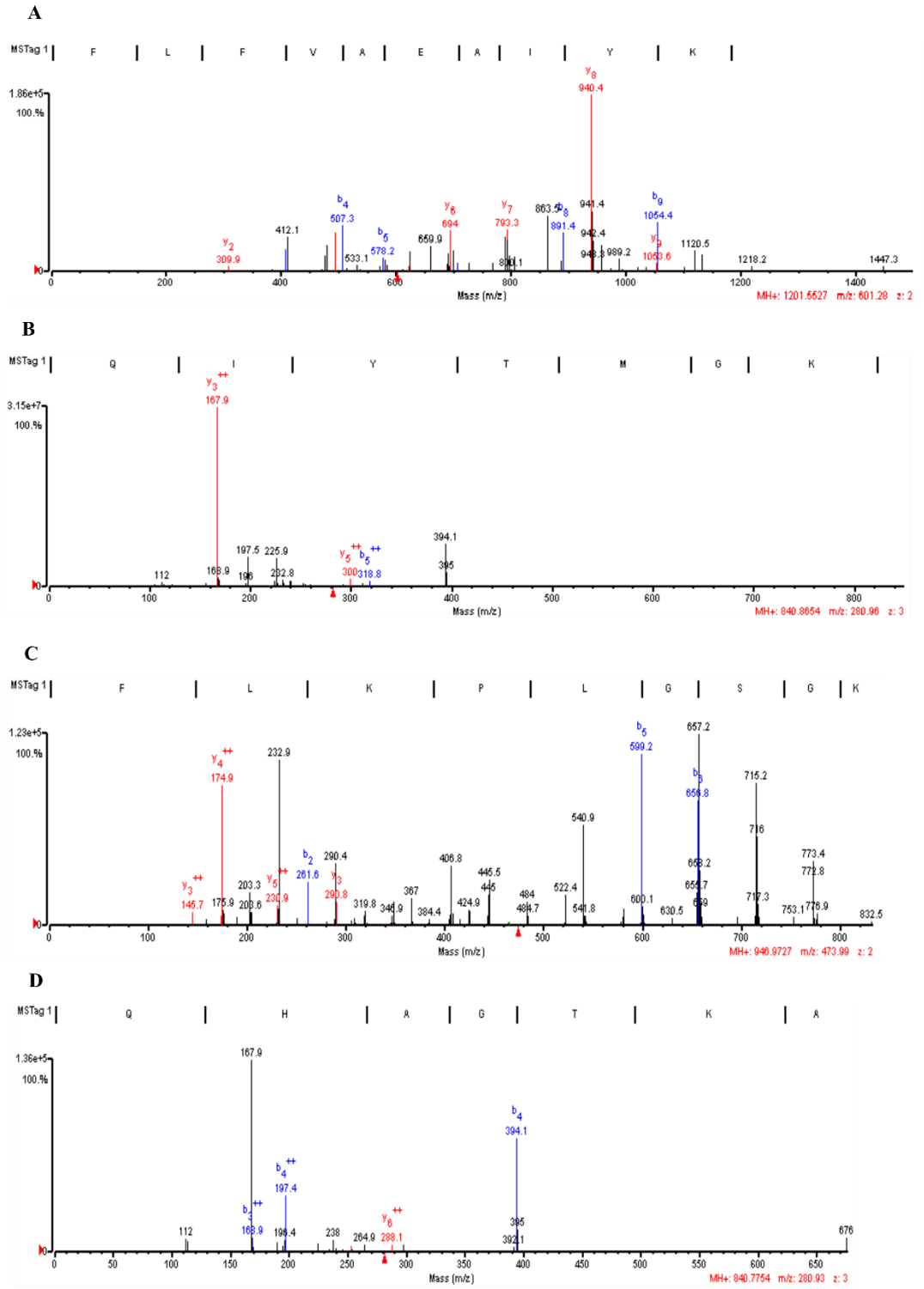

Figure 5.6 Electrospray ionization-tandem mass spectrometry spectra of $[M+H]^+$ ions of (A) Pep2, (B) Pep 7, (C) Pep8 and (D) Pep10, respectively.

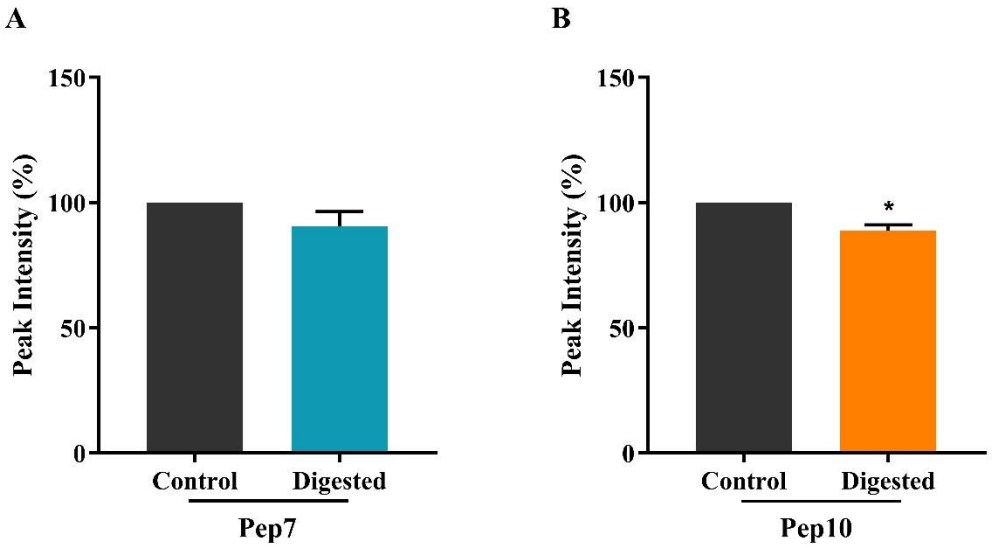

Figure 5.7 Evaluation of the stability of Pep7 (A) and Pep10 (B) by *in vitro* simulated GI digestion. Bars represent the average ± SD of 3 independent experiments in duplicates. *p<0.05 versus undigested samples (control).

5.4 Discussion

Using a multidisciplinary strategy, *C. pyrenoidosa* protein was investigated as a source of peptides active against ACE and DPP-IV targets, in line with the preclinical and clinical evidences suggesting that the consumption of *C. pyrenoidosa* may be useful for the prevention of cardiovascular disease.

Both CP and CT hydrolysates drop in vitro the ACE activity with a dose-response trend, although CP is slightly more active than CT. Both hydrolysates display also a comparable inhibitory activity at cellular level, but less efficiently than in vitro which indicates that they are affected by the peptidases expressed on the membrane of intestinal cells.

Owing to the complex composition of these protein hydrolysates, it may be presumed that they contain peptides with different biological activities (Lammi et al., 2019). In fact, the activity of a protein hydrolysate depends on its total composition, including active and inactive species, and on possible synergistic or antagonist effects. This may explain why these hydrolysates are active on two different targets such as ACE and DPP-IV. The reduced activity in the cellular assays is probably explained by

degradation induced by Caco-2 cells (Aiello, Ferruzza, Ranaldi, Sambuy, Arnoldi, Vistoli, et al., 2018). In fact, the intestinal brush border is a very complex physiological environment where a many active proteases and peptidases are expressed that might metabolize food peptides modulating their bioactivity. Therefore, this organ acts not only as a major physiological barrier against the external environment permitting the absorption of valuable nutrients, but also actively participate to the modulation of the physico-chemical profiles of food protein hydrolysates, through the metabolic activity of its proteases. Similar results have previously been obtained on peptic (SP) and tryptic (ST) hydrolysates of spirulina protein. SP and ST hydrolysates inhibit in vitro the ACE activity with IC_{50} of 0.1 and 0.28 mg/mL, and on Caco-2 cells with IC_{50} of 2.7 and 2.8 mg/mL, respectively. In addition, SP reduces the DPP-IV activity by 64.6% in vitro and 31.7% on Caco-2 cells, while ST by 74.2% in vitro and 39.8% on Caco-2 cells (at the dose of 5 mg/mL) (G. Aiello, Y. Li, G. Boschin, C. Bollati, A. Arnoldi, & C. Lammi, 2019). In addition, the tryptic digest of phycobiliprotein purified from spirulina inhibits the DPP-IV activity by 95.8% in vitro, whereas by 44% in situ at 5 mg/mL (Li, Aiello, Bollati, Bartolomei, Arnoldi, & Lammi, 2020).

It is also possible to compare these results with those obtained testing hempseed and soybean protein hydrolysates produced with the same enzymes (pepsin and trypsin) and in the same conditions. More in details, at 1.0 mg/mL, the tryptic (HT) and peptic (HP) hydrolysates from hempseed proteins inhibit in vitro the DPPIV activity by 17.5±2.7% and 32.0±6.2%, respectively, and at cellular level by 15.5±1.8% and by 22.5±0.19%, respectively (Lammi et al., 2019). A peptic soybean hydrolysate (SoP) reduces in vitro the DPP-IV activity by 16.3±3.0% and 31.4±0.12%, respectively, at 1.0 and 2.5 mg/mL, whereas a tryptic one (SoT) by 15.3±11.0% and 11.0±0.30%, respectively at 1.0 and 2.5 mg/mL. The SoP hydrolysate is 2-times less active on Caco-2 cells (37% inhibition at 5.0 mg/mL) than in vitro on the DPP-IV enzyme (31.4% inhibition at 2.5 mg/mL).

The favorable activity observed suggested to develop an *in silico* strategy to identify at least some potential bioactive peptides. Among commonly used in silico methods, molecular docking permits to evaluate the interaction between peptides and complex proteins, in order to predict the binding energy and binding sites (San Pablo-Osorio,

Mojica, & Urias-Silvas, 2019). A similar work-flow has been applied for discovering novel ACE inhibitory peptides from stone fish protein hydrolysates (Auwal, Zainal Abidin, Zarei, Tan, & Saari, 2019). Besides the molecular docking study, here also a MD analysis was performed in order to evaluate the stability of the complex during a specified simulation time, improving greatly the accuracy of prediction.

In this way, four peptides (Pep2, Pep7, Pep8, and Pep10) were finally selected as the best candidates for the biological activity, since they form stable complexes with ACE and DPP-IV. Their substructures composed by three or more amino acid residues were searched by in the SciFinder database (https://scifinder.cas.org/). Pep2 (FLKPLGSGK) contains two reported ACE-inhibitory motifs, i.e., PLG and LKP. The former, isolated from Alaskan pollack skin, is an ACE inhibitory peptide with an in vitro IC_{50} value equal to 4.74 mM (Byun & Kim, 2002), whereas the latter, released from dried bonito as well as chicken, was reported to be a ACE inhibitor with a good in vitro activity (IC_{50} 0.32 μM), which also effectively decreases the systolic blood pressure in spontaneously hypertensive rat (SHR) (Fujita, Yokoyama, & Yoshikawa, 2000; Ryan, Ross, Bolton, Fitzgerald, & Stanton, 2011). Within Pep8 (FLFVAEAIYK), the fragment AIYK has been identified in a peptic hydrolysate from wakame protein, and shown to reduce the ACE activity in vitro with an IC_{50} of 213 μM and to induce a significant decrease of blood pressure in SHR (Suetsuna & Nakano, 2000). Interestingly, some the AIYK fragments, i.e. IYK, YK, IY, are also in vitro ACE inhibitors, with IC_{50} values of 177, 610, 2.65 μM, respectively (Suetsuna & Nakano, 2000). Using BIOPEP database (http://www.uwm.edu.pl/biochemia/index.php/pl/biopep), it was confirmed that Pep2 and Pep8 contain specific motifs within their own sequences that account for the ACE inhibitory activity. Contextually, the same peptides contain also some DPP-IV inhibitory fragments; i.e., KP, FL, and PL for Pep2 and VA, FL, AE, and YK for Pep8. In addition, the potential activities of the selected peptides may be supported by their structural features. In fact, to be a potent ACE/DPP-IV inhibitor, a short peptide with 2-10 amino acids is preferred. In addition, the presence of numerous hydrophobic amino acid residues is suggested to be important, since the hydrophobic property can always enhance the interaction between peptides and the functional hydrophobic pocket

in ACE and DPP-IV enzymes. In line with this principle, Pep2, Pep7, and Pep10 have relatively high calculated hydrophobicity values (**Table 5.1**). Moreover, peptides with an aromatic residue (Trp, Tyr, Pro, and Phe), positive charged residue (His, Arg, and Lys), or branched side chain (Leu, Ile, and Val) as their C-terminal amino acids are very likely to be good ACE inhibitors. Indeed, all selected peptides have a positive charged Lys residue as their C-terminal amino acid. Instead, to be potent DPP-IV inhibitors, the peptides should respect the following rules: 1) contain a Pro residues (at the first, second, third, or fourth N-terminal position), flanked by Leu, Val, Phe, Ala, and Gly (a rule followed by Pep2, FLKPLGCGK); 2) have a hydrophobic or aromatic amino acid at N-terminus (as in Pep2, FLKPLGCGK, and Pep8, FLFVAEAIYK).

It is important to underline that, containing domains which may be responsible either of the ACE and DPP-IV inhibitory activities, it is highly probable that these are multifunctional peptides (Lammi, Aiello, Boschin, & Arnoldi, 2019). The evaluation of the gastrointestinal stability has shown that Pep7 and Pep10 are probably the most interesting species for possible future exploitation. Finally it is useful to underline that this is the first study that has investigate the potential of using *C. pyrenoidosa* protein to generate antihypertensive and hypoglycemic peptides targeting ACE and DPP-IV activities.

Reference

Aiello, G., Ferruzza, S., Ranaldi, G., Sambuy, Y., Arnoldi, A., Vistoli, G., & Lammi, C. (2018). Behavior of three hypocholesterolemic peptides from soy protein in an intestinal model based on differentiated Caco-2 cell. *Journal of Functional Foods, 45*, 363-370.

Aiello, G., Li, Y., Boschin, G., Bollati, C., Arnoldi, A., & Lammi, C. (2019). Chemical and biological characterization of spirulina protein hydrolysates: Focus on ACE and DPP-IV activities modulation. In): Journal of Functional Foods.

Aiello, G., Li, Y. C., Boschin, G., Bollati, C., Arnoldi, A., & Lammi, C. (2019). Chemical and biological characterization of spirulina protein hydrolysates: Focus on ACE and DPP-IV activities modulation. *Journal of Functional Foods, 63*.

Auwal, S. M., Zainal Abidin, N., Zarei, M., Tan, C. P., & Saari, N. (2019). Identification, structure-activity relationship and in silico molecular docking analyses of five novel angiotensin I-converting enzyme (ACE)-inhibitory peptides from stone fish (Actinopyga lecanora) hydrolysates. *PLoS One, 14*(5), e0197644.

Bjelke, J. R., Christensen, J., Branner, S., Wagtmann, N., Olsen, C., Kanstrup, A. B., & Rasmussen, H. B. (2004). Tyrosine 547 constitutes an essential part of the catalytic mechanism of dipeptidyl peptidase IV. *Journal of Biological Chemistry, 279*(33), 34691-34697.

Boschin, G., Scigliuolo, G. M., Resta, D., & Arnoldi, A. (2014). Optimization of the Enzymatic Hydrolysis of Lupin (Lupinus) Proteins for Producing ACE-Inhibitory Peptides. *J Agric Food Chem, 62*(8), 1846-1851.

Bunning, P., & Riordan, J. F. (1985). THE FUNCTIONAL-ROLE OF ZINC IN ANGIOTENSIN CONVERTING ENZYME - IMPLICATIONS FOR THE ENZYME MECHANISM. *Journal of Inorganic Biochemistry, 24*(3), 183-198.

Byun, H. G., & Kim, S. K. (2002). Structure and activity of angiotensin I converting enzyme inhibitory peptides derived from Alaskan pollack skin. *Journal of Biochemistry and Molecular Biology, 35*(2), 239-243.

Caron, J., Domenger, D., Dhulster, P., Ravallec, R., & Cudennec, B. (2017). Using Caco-2 cells as novel identification tool for food-derived DPP-IV inhibitors. *Food Res Int, 92*, 113-118.

Cherng, J. Y., & Shih, M. F. (2005). Preventing dyslipidemia by Chlorella pyrenoidosa in rats and hamsters after chronic high fat diet treatment. *Life Sciences, 76*(26), 3001-3013.

Cheung, B. M. Y., & Li, C. (2012). Diabetes and Hypertension: Is There a Common Metabolic Pathway? *Current Atherosclerosis Reports, 14*(2), 160-166.

de Castro, R. J. S., & Sato, H. H. (2015). Biologically active peptides: Processes for their generation, purification and identification and applications as natural additives in the food and pharmaceutical industries. *Food Research International, 74*, 185-198.

Du, X., Li, Y., Xia, Y. L., Ai, S. M., Liang, J., Sang, P., Ji, X. L., & Liu, S. Q. (2016). Insights into Protein-Ligand Interactions: Mechanisms, Models, and Methods. *Int J Mol Sci, 17*(2).

Fan, X. D., Bai, L., Zhu, L., Yang, L., & Zhang, X. W. (2014). Marine Algae-Derived Bioactive Peptides for Human Nutrition and Health. *J Agric Food Chem, 62*(38), 9211-9222.

Fujita, H., Yokoyama, K., & Yoshikawa, M. (2000). Classification and antihypertensive activity of angiotensin I-converting enzyme inhibitory peptides derived from food proteins. *Journal of Food Science, 65*(4), 564-569.

He, R., Aluko, R. E., & Ju, X. R. (2014). Evaluating molecular mechanism of hypotensive peptides interactions with Renin and Angiotensin converting enzyme. *PLoS One, 9*(3), e91051.

Lambeir, A. M., Durinx, C., Scharpé, S., & De Meester, I. (2003). Dipeptidyl-peptidase IV from bench to bedside: an update on structural properties, functions, and clinical aspects of the enzyme DPP IV. *Crit Rev Clin Lab Sci, 40*(3), 209-294.

Lammi, C., Aiello, G., Boschin, G., & Arnoldi, A. (2019). Multifunctional peptides for the prevention of cardiovascular disease: A new concept in the area of bioactive food-derived peptides. *Journal of Functional Foods, 55*, 135-145.

Lammi, C., Zanoni, C., Arnoldi, A., & Vistoli, G. (2016). Peptides derived from soy and lupin protein as Dipeptidyl-Peptidase IV inhibitors: *In vitro* biochemical screening and *in silico* molecular modeling study. *J Agric Food Chem, 64*(51), 9601-9606.

Li, Y. C., Aiello, G., Bollati, C., Bartolomei, M., Arnoldi, A., & Lammi, C. (2020). Phycobiliproteins from Arthrospira Platensis (Spirulina): A New Source of Peptides with Dipeptidyl Peptidase-IV Inhibitory Activity. *Nutrients, 12*(3).

Li, Y. C., Lammi, C., Boschin, G., Arnoldi, A., & Aiello, G. (2019). Recent Advances in Microalgae Peptides: Cardiovascular Health Benefits and Analysis. *J Agric Food Chem, 67*(43), 11825-11838.

Liu, R., Cheng, J., & Wu, H. (2019). Discovery of Food-Derived Dipeptidyl Peptidase IV Inhibitory Peptides: A Review. *Int J Mol Sci, 20*(3), 463.

Martin, M., & Deussen, A. (2019). Effects of natural peptides from food proteins on angiotensin converting enzyme activity and hypertension. *Crit Rev Food Sci Nutr, 59*(8), 1264-1283.

Merchant, R. E., & Andre, C. A. (2001). A review of recent clinical trials of the nutritional supplement Chlorella pyrenoidosa in the treatment of fibromyalgia, hypertension, and ulcerative colitis. *Alternative Therapies in Health and Medicine, 7*(3), 79-+.

Metzler, W. J., Yanchunas, J., Weigelt, C., Kish, K., Klei, H. E., Xie, D. L., Zhang, Y. Q., Corbett, M., Tamura, J. K., He, B., Hamann, L. G., Kirby, M. S., & Marcinkeviciene, J. (2008). Involvement

of DPP-IV catalytic residues in enzyme-saxagliptin complex formation. *Protein Science, 17*(2), 240-250.

Nabeno, M., Akahoshi, F., Kishida, H., Miyaguchi, I., Tanaka, Y., Ishii, S., & Kadowaki, T. (2013). A comparative study of the binding modes of recently launched dipeptidyl peptidase IV inhibitors in the active site. *Biochemical and Biophysical Research Communications, 434*(2), 191-196.

Natesh, R., Schwager, S. L. U., Evans, H. R., Sturrock, E. D., & Acharya, K. R. (2004). Structural details on the binding of antihypertensive drugs captopril and enalaprilat to human testicular angiotensin I-converting enzyme. *Biochemistry, 43*(27), 8718-8724.

Ondetti, M. A., & Cushman, D. W. (1977). DESIGN OF SPECIFIC INHIBITORS OF ANGIOTENSIN-CONVERTING ENZYME - NEW CLASS OF ORALLY ACTIVE ANTIHYPERTENSIVE AGENTS. *Science, 196*(4288), 441-444.

Riordan, J. F. (2003). Angiotensin-I-converting enzyme and its relatives. *Genome Biol, 4*(8), 225.

Ryan, J. T., Ross, R. P., Bolton, D., Fitzgerald, G. F., & Stanton, C. (2011). Bioactive peptides from muscle sources: meat and fish. *Nutrients, 3*(9), 765-791.

San Pablo-Osorio, B., Mojica, L., & Urias-Silvas, J. E. (2019). Chia Seed (Salvia hispanica L.) Pepsin Hydrolysates Inhibit Angiotensin-Converting Enzyme by Interacting with its Catalytic Site. *Journal of Food Science, 84*(5), 1170-1179.

Senthilkumar, T., Sangeetha, N., & Ashokkumar, N. (2012). Antihyperglycemic, antihyperlipidemic, and renoprotective effects of Chlorella pyrenoidosa in diabetic rats exposed to cadmium. *Toxicology Mechanisms and Methods, 22*(8), 617-624.

Singh, B. P., Vij, S., & Hati, S. (2014). Functional significance of bioactive peptides derived from soybean. *Peptides, 54*, 171-179.

Suetsuna, K., & Nakano, T. (2000). Identification of an antihypertensive peptide from peptic digest of wakame (Undaria pinnatifida). *Journal of Nutritional Biochemistry, 11*(9), 450-454.

Thoma, R., Loffler, B., Stihle, M., Huber, W., Ruf, A., & Hennig, M. (2003). Structural basis of proline-specific exopeptidase activity as observed in human dipeptidyl peptidase-IV. *Structure, 11*(8), 947-959.

Tzakos, A. G., Galanis, A. S., Spyroulias, G. A., Cordopatis, P., Manessi-Zoupa, E., & Gerothanassis, I. P. (2003). Structure-function discrimination of the N- and C-catalytic domains of human

angiotensin-converting enzyme: implications for Cl- activation and peptide hydrolysis mechanisms. *Protein Engineering, 16*(12), 993-1003.

Zou, T. B., He, T. P., Li, H. B., Tang, H. W., & Xia, E. Q. (2016). The Structure-Activity Relationship of the Antioxidant Peptides from Natural Proteins. *Molecules, 21*(1), 72.

Part III.

Concluding Remarks

GENERAL CONCLUSIONS AND PERSPECTIVES

The present thesis provides a comprehensive investigation on the in vitro hypotensive and anti-diabetic activities of microalgae protein hydrolysates targeting ACE and DPP-IV, crucially focusing on the acquisition and discovery of promising peptide sequences, as well as understanding the possible action mechanisms of the microalgae bioactive peptides toward the therapeutic agents.

In particular, the key achievements of my PhD study are described as below:

- It was verified that spirulina and chlorella are promising sources of producing peptides with cardiovascular-promoting benefits, which endows these microalgae more prospects to be exploited as nutraceuticals and pharmaceuticals.
- For the first time, this study provides new evidence regarding the ability of tryptic PBP to modulate DPP-IV activity in vitro on human recombinant enzyme, and in situ on the cellular intestinal membrane level.
- Peptide sequences within different protein hydrolysates from spirulina, PBP and chlorella were profiled by nano LC-MS/MS, providing a dataset for further discovery and analysis of bioactive peptides.
- A multidisciplinary approach combining peptidomics, biochemical assays, and bioinformatic tools was adopted in this study to screen potential bioactive peptides, which overcomes the difficulty of isolating single peptides from complex matrix by classical fractionation method.

In the present study, the protein hydrolysates from spirulina, PBP and chlorella generally presented significant ACE and/or DPP-IV inhibitory activities. By comparison, peptic hydrolysate of spirulina protein showed the best in vitro inhibiting effect on ACE with IC_{50} value of 0.1 ± 0.04 mg/mL while the tryptic hydrolysate of PBP stands out with the lowest IC_{50} value of DPP-IV inhibition (0.5 – 1.0 mg/mL). Noticeably, when working on the intestinal Caco-2 cells, all the hydrolysates turned to be less bioactive than in vitro, indicating their susceptibility to metabolic degradation

by intestinal cells. This is further in line with the kinetics of DPP-IV inhibition of PBP tryptic hydrolysate working on the intestinal cells, which showed the decreasing trend of its bioactivity after incubation with Caco-2 cells for 3 h. This reflects the issue of peptide bioavailability, which could be stressed in further studies. Moreover, peptides Pep2 (FLKPLGSGK), Pep7 (QIYTMGK), Pep8 (FLFVAEAIYK), and Pep10 (QHAGTKAK) were screened from hydrolysates of chlorella protein by peptidomics combined with docking and MD. The modelling results indicated that they may block the important domain of both ACE and DPP-IV and generate dynamically stable peptide-ACE/DPP-IV complexes. Based on this theoretical evidence, further study will focus on the verification of their actual bioactivity by biochemical approaches.

In conclusion, the bioactivity investigation of microalgae protein hydrolysates provides new evidence that microalgae protein are great sources to produce peptides with health-promoting properties. The exclusive data of peptide characterization makes a foundation to isolate single bioactive peptides as well as offers useful structural and functional implications for food ingredient formulation or pharmacological use.

Appendix

In addition to the main researches focused on microalgae bioactive peptides, I had the possibility to participate to two different projects on proteins and peptides from other foods, giving my scientific contribution. The former project employed different mass spectrometry techniques to analyze the narrow-leaf lupin proteins in the lupin-enriched pasta, whereas the latter tried to explore the physicochemical and conformational changes of the proteins extracted from soybean okara byproducts using ultrasound treatments at different energies and temperatures. The efforts made on these projects have deepened my understanding of the importance of exploiting protein and peptides in food development, and expanded my skills of protein analysis, such as shotgun proteomics and physicochemical assays. I was very happy to participate to these projects that are focused on some key issues of the current food industry development.

1 Development of innovative functional food

Functional food development has enjoyed increasing interest from researchers, market, and governments, since substantial diet-disease links have been revealed over the past decades. With the incorporation of bioactive food components or nutrients enrichment, functional foods provide additional functional capacity to promote health benefits beyond the provision of essential nutrients, resulting in the prevention of certain diseases increasing the life in the general population. To meet the huge demand of the consumers and market, the development of innovative functional food needs extensive efforts. In this context, Project I focused on a newly developed lupin-enriched pasta, with the aim to evaluate the effect of narrow-leaf lupin flour supplementation on the quality of pasta protein. Briefly, the aims of the project include:

- Investigation of the protein profile of the lupin-enriched pasta samples by an optimized proteomic approach based on the untargeted MS method.

- Optimization of a targeted proteomics method based on MRM analysis to quantitatively measure the protein γ-conglutin in the pasta, which is reported to be a potent blood glucose-reducing component.

2 Utilization of food by-products

Food processing by-products are a kind of common industrial discards, which lead to economic loss and environmental problems. Hence, the alternative uses and exploitation of food by-products are recently a global issue. Among the various food by-products, soybean okara, the ground residue remaining after soymilk or soybean curd production, is produced in huge amounts owing to the great consumption of these soybean derived foods. Having a relatively high nutritional value, soybean okara is a hot topic for circular economy. For this reason, Project II was dedicated to provide new information of the physicochemical and conformational changes of protein extracted from okara with innovative methods in order to evaluate their nutritional and technological values for new food applications. Technically, Project II employed an integrated strategy including different techniques, such as mass spectrometry, biochemical assays and optical analysis, to assessed the changes in the protein profile, physicochemical and conformational properties as well as antioxidant activity in comparison with the untreated okara sample.

Project I

ANALYSIS OF NARROW-LEAF LUPIN PROTEINS IN LUPIN-ENRICHED PASTA BY UNTARGETED AND TARGETED MASS SPECTROMETRY

Gilda Aiello [1, 2, *], Yuchen Li [2], Giovanna Boschin [2], Marco Stanziale [3], Carmen Lammi [2] and Anna Arnoldi [2]

[1] Department of Human Science and Quality of Life Promotion, Telematic University San Raffaele, 00166 Rome, Italy

[2] Department of Pharmaceutical Sciences, University of Milan, 20133 Milan, Italy

[3] Department of Research and Development, Rustichella d'Abruzzo S.p.a., 65019 Pianella (PE), Italy

Abbreviations

ACN, acetonitrile; BSA, bovine serum albumin; DTT, 1,4-dithiothreitol; DW, durum wheat flour (DW); FDR, false discovery rate; HCA, Hierarchical clustering analysis; HCl, hydrochloric acid (HCl); HPLC-ESI-MS/MS, High-performance liquid chromatography electrospray ionization tandem mass spectrometry; iBAQ, intensity-based absolute quantification; IAM, 2-iodoacetamide; MRM, multiple reactions monitoring; LOD, limit of detection; LOQ limit of quantification; LK, lupin kernel; MW, molecular weight; RDS%, standard deviation percentage; SDS-PAGE, sodium dodecyl sulphate-polyacrylamide gel electrophoresis; TIC, total ion chromatogram; Tris-HCl, tris(hydroxymethyl)aminomethane.

I. Abstract:

The supplementation of different food items with grain legumes and, in particular, with lupin has been demonstrated to provide useful health benefits, especially in the area of cardiovascular disease prevention. In this work, label free quantitative untargeted and targeted approaches based on liquid chromatography–electrospray ionization–tandem mass spectrometry (LC-ESI-MS/MS) for investigating the protein profile of three pasta samples containing different percentages of narrow-leaf lupin flour were carried out. The untargeted method permitted the identification of the main acidic globulins (α-conglutin, β-conglutin, and γ-conglutin) and the comparison of their profile with raw lupin flour. The targeted method, based on high-performance liquid chromatography electrospray ionization tandem mass spectrometry HPLC-Chip-Multiple Reaction Monitoring (MRM) mode, allowed the quantification of γ-conglutin, the main hypoglycemic component of lupin protein: its concentration was around 2.25 mg/g in sample A, 2.16 mg/g in sample D, and 0.57 mg/g in sample F.

I-1. Introduction

The role of foods and food components in the prevention of several diseases is increasingly being acknowledged worldwide. For this reason, many food companies have plans for improving the nutraceutical properties of their products or developing innovative functional foods, especially targeting hypercholesterolemia, hypertension, diabetes, obesity, and metabolic syndrome. Furthermore, food industries are also constantly developing strategies to improve the nutritional quality of their products, particularly by incorporating low-glycemic index ingredients to address the demand for healthy products and to foster the particular niche of consumers with diabetes mellitus (Kumar & Prabhasankar, 2014).

During the past 15 years, lupin flour has been increasingly used as a food ingredient because of its interesting nutritional and techno-functional properties (Saleh, Al-Ismail, & Ajo, 2017). Out of the four domesticated species, the commercially available raw materials derive from *Lupinus albus* (white lupin) and *Lupinus angustifolius* (narrow-

leaf lupin). Due to its high protein content, various researchers have recently investigated the addition of lupin flour in a variety of cereal-based products, like cakes, pancakes, biscuits, or brioche (LampartSzczapa, Obuchowski, Czaczyk, Pastuszewska, & Buraczewska, 1997), as well as spaghetti, pasta, and crisps [4]. In addition, lupin flour is also used as a protein-rich ingredient in gluten-free items because it does not contain any gluten (Scarafoni, Ronchi, & Duranti, 2009).

Besides its useful nutritional features, numerous studies have shown that lupin provides interesting health benefits (Arnoldi, Boschin, Zanoni, & Lammi, 2015), particularly in the area of hyperglycemia control (Duranti, Consonni, Magni, Sessa, & Scarafoni, 2008; Lovati, Manzoni, Castiglioni, Parolari, Magni, & Duranti, 2012), hypertension prevention (Boschin, Scigliuolo, Resta, & Arnoldi, 2014), and cholesterol reduction (Lammi, Zanoni, Aiello, Arnoldi, & Grazioso, 2016; C. R. Sirtori, Triolo, Bosisio, Bondioli, Calabresi, De Vergori, et al., 2012; Zanoni, Aiello, Arnoldi, & Lammi, 2017). Protein seems to play a main beneficial role in these effects (Arnoldi, Zanoni, Lammi, & Boschin, 2015), a fact that points out the importance of the validation of adequate techniques for the assessment of the quality of the protein profile in processed food products. Although the technologies for pasta production are certainly well established, the enrichment of traditional pasta with other ingredients, such as lupin flour, may lead to an alteration of the quality of pasta, influencing the final composition as well as the texture and techno-functional properties, such as firmness, hardness, and cohesiveness. The need to establish food quality in terms of protein content after the addition of new ingredients is a fundamental prerequisite for food industries. On this basis, the first goal of this work was to optimize a proteomic approach based on mass spectrometry (MS) for evaluating the protein profile of some lupin-enriched pasta samples produced using different raw materials and food processing conditions. Shotgun proteomics, which is currently considered a fast and effective screening method, was selected for the characterization of these products. In details, based on the intensity-based absolute quantification (iBAQ), the changes of soluble lupin proteins among lupin-enriched pasta in comparison to raw materials were explored. Despite the fact that some MS-methods have already been developed for detecting and quantifying the main storage

proteins of white lupin in beverages and protein isolates (Arnoldi, Zanoni, Lammi, & Boschin, 2015), as well as in pasta and biscuits using rapid shotgun proteomics methods (Mattarozzi, Bignardi, Elviri, & Careri, 2012), literature does not report any methodology for the detection of narrow-leaf lupin protein in the final products. In addition, there are no reports aimed at evaluating how the lupin protein profile is modified by food processing techniques. In order to overcome this limit, the untargeted method based on high pressure liquid chromatography-tandem mass spectrometry (HPLC-MS/MS) analysis, implemented by software-based data mining and complementary bioinformatics evaluation, as a tool for the rapid detection of the total profile of narrow-leaf lupin proteins in some lupin-enriched pasta samples were presented. The selectivity and the specificity of shotgun proteomics, however, was implemented by the optimization of a method for the quantitative measurement of narrow-leaf lupin γ-conglutin in pasta based on multiple reactions monitoring (MRM). When compared to white bread, the consumption of bread enriched with narrow-leaf lupin flour reduces the post-prandial glucose response in healthy adults, mediated by an increased insulin response (Hall, Thomas, & Johnson, 2005). Among the lupin proteins, γ-conglutin certainly has a crucial role in this activity since pasta supplemented with isolated γ-conglutin reduces plasma glucose concentration in rats after glucose overload trial (Capraro, Magni, Scarafoni, Caramanico, Rossi, Morlacchini, et al., 2014) as well as in humans (Bertoglio, Calvo, Hancke, Burgos, Riva, Morazzoni, et al., 2011). Having specific and selective analytical tools aimed at quantifying even low levels of proteins, such as γ-conglutin, in lupin-enriched foods, as well as for the assessment of its integrity when it is incorporated into complex food matrices is an increasingly strong demand from industries. The only methods described in literature have been developed for the analysis of white lupin γ-conglutin in lupin protein extracts (Resta, Brambilla, & Arnoldi, 2012) or in pasta and biscuits (Mattarozzi, Bignardi, Elviri, & Careri, 2012). In spite of this interest about *L. albus*, little is known about the γ-conglutin from narrow-leaf lupin kernel. Moreover, the complexity of the γ-conglutin in the range of lupin species in terms of gene structure, phylogenetic relationships, and the protein abundance during seed development support the MRM-

method development for γ-conglutin quantification. The accurate quantification of multiple target proteins in a very complex mixture, such as pasta, is a challenging issue that requires highly sensitive and high-throughput assays like those provided by MRM analysis (Boja & Rodriguez, 2012; Picotti & Aebersold, 2012).

I-2. Materials and Methods

I-2.1 Chemicals, Enzymes, and Solvents

All chemicals and reagents were of analytical grade. LC-grade H_2O (18 MΩ cm) was prepared with a Milli-Q H_2O purification system (Millipore, Bedford, MA, USA). Acetonitrile (ACN), tris(hydroxymethyl)aminomethane (Tris-HCl), hydrochloric acid (HCl), ammonium bicarbonate, 2-iodoacetamide (IAM), 1,4-dithiothreitol (DTT), trypsin from bovine pancreas (T1426, lyophilized powder, ≥10,000 units/mg protein), and pepsin from porcine gastric mucosa (P7012, lyophilized powder, ≥2500 units/mg protein) were from Sigma-Aldrich (St. Louis, MO, USA). Bovine serum albumin (BSA), Mini-Protean apparatus, precision plus protein standards, Bradford reagent, and Coomassie Blue G-250 were purchased from Bio-Rad (Hercules, CA, USA).

I-2.2 Analyzed Samples

All samples were provided by the company Rustichella d'Abruzzo (Pianella (PE), Italy), an artisanal pasta factory. They were unprocessed raw materials (flours), i.e., narrow-leaf lupin kernel flour (LK), durum wheat flour (DW), Mix (consisting of 58% of lupine flour, 33% of durum wheat, 5% of atomized lemon juice, 2% of vegetal fiber, and 2% of carob flour), as well as three samples of lupin enriched pasta products (samples A, D, and F). All pasta products were produced by adding lupin ingredients to DW in order to ensure a desired texture and cooking quality for the products. Specifically, sample A was constituted of 56% of LK and 44% of DW; sample D was constituted of 58% of LK and 42% of DW. Sample F was made of 100% Mix. During the processing phase, the temperature of the water used to knead the dough of samples A and D was 28 °C, while for sample F, the temperature was 38 °C. Pasta samples A and D were then dried

for about 16 h at 52 °C, whereas pasta sample F was dried for 16 h at 56 °C.

I-2.3 Protein Extraction and Sodium Dodecyl Sulphate-Polyacrylamide Gel Electrophoresis (SDS-PAGE)

The raw materials were extracted as such, whereas sample A, D, and F were previously manually ground to obtain a fine and homogeneous powder. To remove lipids, 5 g of each sample was defatted with 100 mL of hexane overnight under magnetic stirring. After drying at room temperature, 1 g of defatted material was suspended in 10 mL of Tris-HCl 100 mM/NaCl buffer (0.5 M, pH 8.2) and the protein extraction was carried out at 60 °C for 6 h under magnetic stirring. The solid residue was eliminated by centrifugation at 5800×g at 4 °C for 30 min and the supernatant was dialyzed against 100 mM Tris-HCl buffer, pH 8.0, at 4 °C for 36 h. The protein concentration was determined by the colorimetric Bradford. Analyses were carried out at a wavelength λ = 595 nm. To determine protein concentration, a standard curve based on BSA was employed. The efficiency of protein extraction was evaluated by SDS-PAGE. Then, 12% of polyacrylamide was used with Tris–glycine buffer (pH 8.3, 0.1% SDS).

I-2.4 Tryptic and Peptic Digestions

In order to improve the efficiency of the enzymatic digestion, the samples were previously heated at 60 °C for 45 min to unfold the protein structure. The reduction and alkylation processed was similar to those reported previously (Mattarozzi, Bignardi, Elviri, & Careri, 2012). Two different enzymatic digestions were employed. The tryptic digestion, used for untargeted MS analysis, was performed by adding 5 µL of 2 mg/mL trypsin solution to 100 µL of purified protein extract (protein/trypsin ratio of 50:1) and carried out at 37 °C overnight. The digestion reaction was stopped with 1% formic acid. In parallel, the peptic digestion was employed to hydrolyze the γ-conglutin that was subsequently quantified by MRM-MS. The peptic digestion was performed by changing the pH of the protein extract to 2 by adding 0.1 M HCl. Then, 5 µL of 2 mg/mL pepsin were added to 100 µL of the purified protein extract (protein/trypsin

ratio of 50:1) and carried out at 37 ℃ overnight. The digestion reaction was quenched by changing the pH to neutral.

I-2.5 Untargeted Shotgun Analysis by LC-ESI-MS/MS and Data Processing

Digested samples were purified using SepPak C18 cartridges (Thermo Fisher Scientific, Life Technology, Milan, Italy), dried in a Speed-Vac (Martin Christ, Germany) and then reconstituted with 50 μL of a solution of 98% water and 2% ACN containing 0.1% formic acid. Aliquots of 5 μL of tryptic peptides were injected in a nano-chromatographic system, HPLC-Chip (Agilent Palo Alto, CA, USA). The analysis was conducted on a SL IT mass spectrometer. LC-MS/MS analysis was performed in data-dependent acquisition AutoMS (n) mode. In order to increase the number of identified peptides, three technical replicates (LC-MS/MS runs) were run for each hydrolysate. Both the detailed chromatographic separation conditions and the MS parameters used are reported in the Supplementary Materials. PEAKS Studio 8.5 software (Bioinformatics Solutions Inc., Waterloo, ON, Canada) was used for the automated peptide identification from tandem mass spectrogram. The *Viridiplantae* protein sequences database downloaded from SwissProt Uniprot (2018) was consulted. Carbamidomethylation was chosen as a fixed modification. Parent mass and fragment mass error tolerance were set at 1.2 and 0.8 Da, respectively. Protein confidence levels were set to a 1% false discovery rate (FDR) and at least ≥2 peptide/protein with 1% FDR at the peptide level were used to filter out inaccurate proteins for the PEAKS search. “De novo only” analysis was also included in the search. A –10lgP > 20 indicated that the detected proteins were relatively high in confidence, as it targeted very few decoy matches above that threshold. The hierarchical clustering analysis (HCA) and its visualization were performed using Cluster 3.0 and Java TreeView, respectively. The complete linkage method was then used in the assignment of clusters.

I-2.6 Label Free Quantification

Protein quantification was established on the intensity-based absolute quantification

(iBAQ) method provided by Scaffold (Schwanhäusser, Busse, Li, Dittmar, Schuchhardt, Wolf, et al., 2011). Protein intensities were provided by PEAKs as the sum of all the identified peptide intensities per protein. The iBAQ values were obtained by dividing the protein intensities by the number of theoretically observable peptides of each protein (calculated by in silico protein digestion). The tryptic peptides taken in account had lengths between 6 and 30 amino acids (Arike, Valgepea, Peil, Nahku, Adamberg, & Vilu, 2012; Nagaraj, Wisniewski, Geiger, Cox, Kircher, Kelso, et al., 2011). The average of iBAQ values of the three technical replicates for each protein was considered as the "protein abundance", providing an accurate determination of the relative abundance of all proteins identified in each sample.

I-2.7 MRM Method Optimization and Validation for the γ-Conglutin Quantification

The quantification of γ-conglutin was performed by analyzing the peptic digests through multiple reaction monitoring (MRM) mass spectrometry, monitoring two diagnostic peptides, PNNIQ (control peptide) and NIHKRTPL (quantification peptide), both belonging univocally to γ-conglutin. Two transitions were monitored for each peptide as reported in the "Results" section. Both peptides were eluted applying the following gradient: 20% solvent B (0 min), 95% solvent B (0–30 min), and back to 5% in 5 min. The drying gas temperature was set at 300 °C, flow rate 3 L/min (nitrogen). Data acquisition was carried out in positive ionization mode. Capillary voltage was –1970 V, with endplate offset –500 V. Full scan mass spectra were acquired in the mass range from m/z 300 to 2000 Da. Three technical replicates (LC–MS/MS runs) were run for each hydrolysate. Analytical parameters, i.e., LOQ and LOD, were measured to ensure appropriate performance of the developed method. The accuracy of the assay was assessed, spiking DW flour with the standard peptide PNNIQ at 25 μg/mL. The sensitivity of the method was calculated by the LOQ's [signal-to-noise (S/N) = 10] and LOD's (S/N = 3). The analytical validation study evaluated the assay accuracy, precision (intra- and inter-day repeatability), linearity, and recovery.

I-2.8 Statistical Analysis

From a statistical point of view, both the extraction of proteins from each sample and the protein digestion were performed three times. The peptides obtained from each independent digestion (i.e., tryptic and peptic) were then pooled and analyzed by MS with three technical replicates (n = 3), respectively, and the results are represented as mean ± SD unless otherwise mentioned.

I-3 Results

I-3.1 Qualitative Comparison of the Protein Profile of the Pasta Samples by SDS-PAGE and MS Analysis

Acidic globulins and albumins, in respect to wheat prolamins and glutelins, were extracted from the raw materials and pasta samples by using an alkaline buffer containing NaCl. The concentration of the soluble protein in each sample was assessed by the Bradford method. The soluble protein content of the starting materials was as follows: DW 4.57 ± 0.5 μg/μL, LK 5.05 ± 0.2 μg/μL, and Mix 0.78 ± 0.2 μg/μL. The low value of the last sample probably depended on an inefficient extraction, possibly caused by the presence of the carob flour and vegetal fiber that hindered the protein extraction. The protein contents of the pasta samples A, D, and F were equal to 3.5 ± 0.3, 3.8 ± 0.4, and 2.7 ± 0.3μg/μL, respectively, indicating that samples A and D have similar protein contents, whereas sample F has a much lower protein content, possibly linked to the inclusion of Mix in its formulation.

Aiming to deeply investigate the differences in protein composition among the lupin-enriched pasta samples and the raw materials, a proteomic approach based on SDS-PAGE, after sulfur bridges reduction, was selected as a tool for a visual screening of the molecular weight protein distribution among the samples. The results of this analysis are shown in **Figure I-1**. Starting from the raw materials, the samples Mix and DW showed very similar protein bands due to the high prevalence of wheat proteins, whereas LK had a completely different pattern, where lupin legumins and vicilins are easily recognized (Duranti, Consonni, Magni, Sessa, & Scarafoni, 2008). In fact, the

protein profile of narrow-leaf lupin is characterized by the presence of proteins with molecular weights falling in the range of 68 to 15 kDa (E. Sirtori, Resta, Brambilla, Zacherl, & Arnoldi, 2010). The intense bands around 53–74 kDa indicate the presence of the acid and basic subunits of α-conglutin (legumins or 11S globulins). On the contrary, β-conglutin (vicilins or 7S globulins), which does not contain any disulfide bridge, is a very heterogeneous protein fraction that produces numerous bands falling in the range 15–72 kDa (Muranyi, Volke, Hoffmann, Eisner, Herfellner, Brunnbauer, et al., 2016). Finally, the intense band at 16 kDa may be attributed to the small subunit of γ-conglutin (E. Sirtori, Resta, Brambilla, Zacherl, & Arnoldi, 2010). Considering now the pasta samples, lupin proteins are clearly visible in the SDS-PAGE of A and D, which are very similar, whereas the profile of sample F is very different, with the absence of α-conglutin and the low presence of β-conglutin.

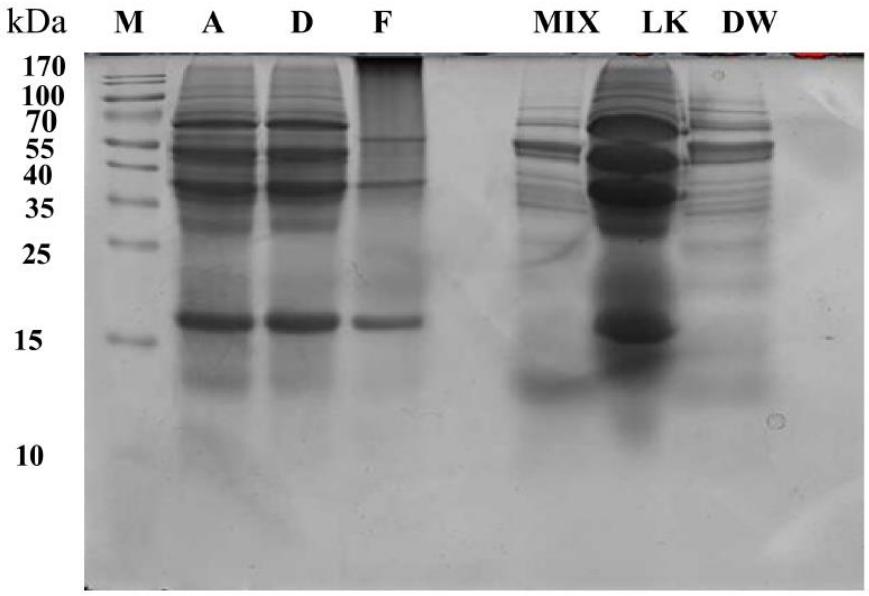

Figure I-1 Reduced SDS-PAGE protein profile of lupin-enriched pasta samples and raw materials; M, pre-stained molecular marker; A, D, and F lupin-based pasta samples; Mix, LK: lupin kernel, and DW: durum wheat. Each sample (10 μL) was added to 10 μL of loading buffer, loading 20 μL for each well.

To get a deeper characterization of the protein composition of each sample, a shotgun proteomic approach was adopted, since comparative proteomics currently represents

the most up-to-date method for characterizing proteome changes consequent to food processing (Mora, Gallego, & Toldra, 2018). The peptide obtained by tryptic digestion was analyzed by nano-electrospray ionization tandem mass spectrometry nESI-LC-MS/MS. Data obtained by Data-Dependent-Acquisition (DDA) mode were analyzed to identify lupin tryptic peptides assessing the sequence coverage for each conglutin. In particular, by comparing MS/MS data against Viridiplantae database, α, β, and γ-conglutin from *L. angustifolius* were easily identified (several isoforms were detected for each protein), whereas no peptides belonging to γ-conglutin could be found. This phenomenon may be explained by the well-known resistance of γ-conglutin to tryptic hydrolysis (Magni, Sessa, Accardo, Vanoni, Morazzoni, Scarafoni, et al., 2004). Besides proteins belonging to the Lupinus genus, proteins belonging to different phylogenetic species were identified, including monogalactosidase glycerol synthase 2 type B; uncharacterized protein (*Oryza sativa* subsp. Japonica); protein synthesis inhibitor I (*Hordeum vulgare*); Rho GTPase-activating protein 5 (*Arabidopsis thaliana*); legumin (*Phaseolus vulgaris*); and auxin response factor (*Spinacea oleracea*). **Table I-S1** reports the peptides and proteins identified in each analyzed sample.

The subsequent quantitative evaluation was focused only on the proteins belonging to *L. angustifolius*. With the aim of highlighting the similarities between the pasta samples and the raw materials, it was decided to use hierarchical clustering analysis (HCA), which allows the presentation of cluster results in a dendrogram, where the similarity among the samples is shown by a smaller distance at which they join in a single cluster. By plotting –10LgP for each identified protein across the samples, the heatmap reported in **Figure I-2** clearly shows the correlation in terms of composition existing between sample A and D, which form a very narrow cluster. Both are then correlated with LK, whereas sample F and Mix fall at a wider distance, indicating a very different protein composition in respect to LK.

Figure I-2 Hierarchical clustering analysis (HCA) with the dendrogram of the identified protein in lupin-based pasta samples and raw materials. Individual proteins are given in columns. Heat map colors are bases on values of -10LgP (protein confidence score), combined with hierarchical clustering of samples.

I-3.2. Quantitative Comparison of Lupin-Based Pasta Samples and Raw Materials by an MS Label-Free Method

Trustworthy quantitative methods to determine the total protein content of foods and food ingredients are widely used, not only to guarantee the quality and safety of food, but also to get a comprehensive view of how technological processes change the protein profile of treated foods. Common processing-induced changes include variations in molecular weight distribution following hydrolysis, racemization, and/or oxidation of amino acids and protein cross-linking (Horneffer, Foster, & Velikov, 2007). For example, label-free quantification methods have been widely used to highlight the differences in the peptide profile of Spanish Teruel, Italian, and Belgian dry-cured ham (Mora, Escudero, & Toldra, 2016).

With the aim to get a relative quantification of lupin proteins in each pasta sample, an

MS label-free method was adopted for protein quantification. The protein abundance was calculated by applying the iBAQ methodology, which has been described to have a good correlation with known relative protein amounts over at least four orders of magnitude (Schwanhäusser, et al., 2011). It estimates protein abundance as the sum of intensities of all tryptic peptides identified for each protein divided by the theoretically observable peptides, obtained by in silico digestion, taking into account only peptides consisting of 6–30 amino acid residues. In this work, the resulting iBAQ intensities were used to provide an accurate determination of the relative abundance of all identified proteins.

Most of the selected proteins were present at higher concentrations in the raw material LK, whereas they decreased in the processed samples, as reported in **Figure I-3A**, which shows the trend of α, β, and γ-conglutin isoforms, respectively, in lupin-enriched pasta samples and LK. The three graphs show substantial protein differences among the samples. In order to highlight the variation in the relative abundance of each identified protein between processed lupin-enriched pasta and raw LK, the Log2 ratio was plotted as reported in **Figure I-3B**. The higher the observed value of Log2 ratio, the higher the protein yields in the samples. **Table I-1** reports the relative percentages of each identified protein in pasta samples in comparison to those detected in raw LK. Specifically, conglutin α1 (F5B8V6) was detected as the most abundant protein in sample D, characterized by a 74% content in respect to LK, whereas the highest reduction in concentration was observed for conglutin α-2 (F5B8V7) in sample F, where its yield slumps to 4.63% versus LK (**Figure I-3B**). On the contrary, sample F was characterized by the highest content of conglutin γ-2 large chain (F5B8W8), corresponding to 69% (**Figure I-3B**). Overall, it is possible to affirm that A and D are the richest in lupin proteins, i.e., 11S α-conglutin and 7S β-conglutin, whereas F is the richest in the conglutin γ-2 large chain. The pasta samples described here have a very high lupin protein content in respect to literature where all the formulations comprise lupin ingredient percentages ranging from <5% to 30% (Albuja-Vaca, Yepez, Vernaza, & Navarrete, 2020; Doxastakis, Papageorgiou, Mandalou, Irakli, Papalamprou, D'Agostina, et al., 2007; Lucas, Stoddard, Annicchiarico, Frias, Martinez-Villaluenga,

Sussmann, et al., 2015). The iBAQ strategy thus permits one to calculate the relative percentages of proteins in the samples. Here, it was used to monitor the impact of the different raw materials and processing conditions on the final protein composition. The rapidity of the untargeted method represents the main advantage in respect to the methods available in the literature which make use of the more elaborated MRM approach, even to detect abundant proteins that are easily identifiable with untargeted MS (Mattarozzi, Bignardi, Elviri, & Careri, 2012).

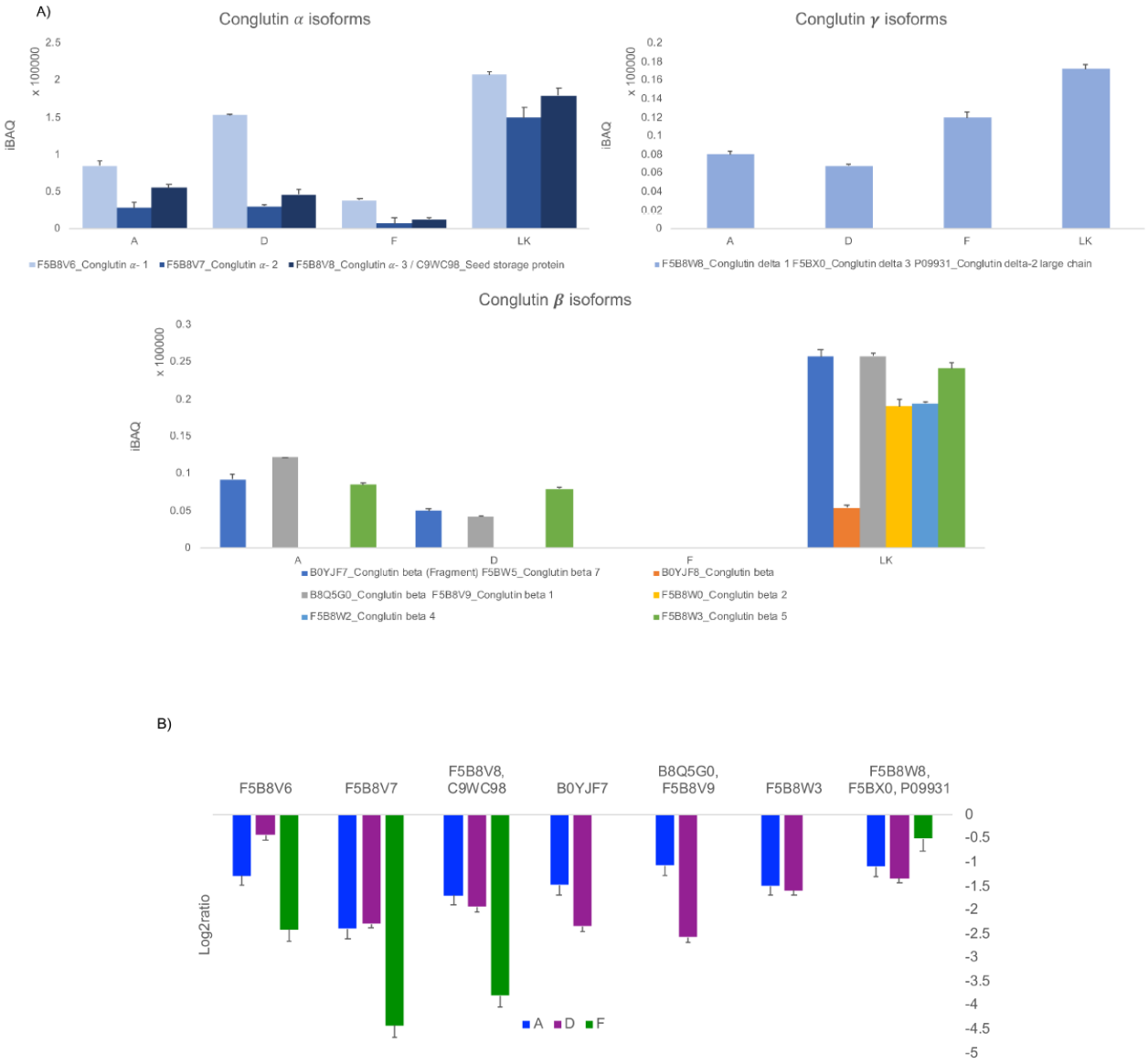

Figure I-3 (A) iBAQ values of α, β, and γ-conglutin isoforms in samples A, D, F, and LK. (B) The log2 fold-changes of the protein levels in A, D, and F versus raw lupin flour (LK).

Table I-1. iBAQ values and relative percentage of lupin protein identified in lupin-enriched pasta.

Protein Name Accession N.	A ± SD (iBAQ)	D ± SD (iBAQ)	F ± SD (iBAQ)	LK ± SD (iBAQ)	%A	%D	%F
Conglutin α-1_F5B8V6_LUPAN	$(8.45 \pm 0.74) \times 10^4$	$(1.53 \pm 0.18) \times 10^5$	$(3.88 \pm 0.14) \times 10^4$	$(2.07 \pm 0.04) \times 10^5$	40.82	73.91	18.74
Conglutin α-2_F5B8V7_LUPAN	$(2.83 \pm 0.73) \times 10^4$	$(3.05 \pm 0.22) \times 10^4$	$(6.94 \pm 0.74) \times 10^3$	$(1.50 \pm 0.11) \times 10^5$	18.87	20.33	4.63
Conglutin α-3_F5B8V8_LUPAN	$(5.52 \pm 0.52) \times 10^4$	$(4.66 \pm 0.73) \times 10^4$	$(1.28 \pm 0.26) \times 10^4$	$(1.79 \pm 0.11) \times 10^5$	30.84	26.03	7.15
Conglutin β (Fragment)_B0YJF7_LUPAN	$(9.18 \pm 0.66) \times 10^3$	$(5.04 \pm 0.24) \times 10^3$		$(2.57 \pm 0.09) \times 10^4$	35.72	19.61	
Conglutin β-1_F5B8V9_LUPAN	$(1.22 \pm 0.54) \times 10^4$	$(4.31 \pm 0.43) \times 10^3$		$(2.58 \pm 0.46) \times 10^4$	47.29	16.71	
Conglutin β-2_F5B8W0_LUPAN				$(1.90 \pm 0.09) \times 10^4$			
Conglutin β-4_F5B8W2_LUPAN				$(1.94 \pm 0.02) \times 10^4$			
Conglutin β-5_F5B8W3_LUPAN	$(8.47 \pm 0.35) \times 10^3$	$(7.92 \pm 0.23) \times 10^3$		$(2.41 \pm 0.08) \times 10^4$	35.15	32.86	
Conglutin β-_B0YJF8_LUPAN				$(5.38 \pm 0.34) \times 10^3$			
Conglutin δ-2 large chain _F5B8W8_LUPAN	$(8.00 \pm 0.4) \times 10^3$	$(6.76 \pm 0.1) \times 10^3$	$(1.20 \pm 0.06) \times 10^4$	$(1.72 \pm 0.05) \times 10^4$	46.51	39.30	69.77

I-3.3 Development of a Targeted MRM-Assay for the Absolute Quantification of γ-Conglutin

Since the untargeted MS method used for profiling the differences among processed samples and raw ingredients did not provide any information about γ-conglutin, a specific targeted MRM assay was developed. It is well known that the γ-conglutin protein fraction of *L. angustifolius* is highly resistant to tryptic hydrolysis. Its insensitivity has been explained in (Czubinski, Siger, & Lampart-Szczapa, 2016). However, the quantification of this protein in lupin-enriched food items is fundamental, since it is one of the main hypoglycemic lupin components. In order to increase the accuracy of γ-conglutin determination, it was decided to develop a sensitive MRM assay that is widely adopted for monitoring peptide integrity in nutritional investigations (Aiello, Ferruzza, Ranaldi, Sambuy, Arnoldi, Vistoli, et al., 2018).

The development consisted of three main steps: (1) selection of proteotypic peptides through in silico pepsin hydrolysis by PeptideCutter of γ-conglutin; (2) hydrolysis of the extracted proteins with pepsin; (3) method refinement by analyzing peptic hydrolysates of crude proteins extracted from pasta. In order to guarantee the specificity

of the method, two peptides, i.e., PNNIQ and NIHKRTPL belonging to γ-conglutin 2 (F5B8W7, CONG2_LUPAN_SwissProt_Uniprot), were selected as proteotypic peptides to be monitored. Both met the stringent criteria required for this technique, i.e., good ESI ionization and no post-translational modifications, and 0 missed cleavage (Koeberl, Clarke, & Lopata, 2014). The adopted MS/MS strategy was suitable for the unambiguous determination and quantification of γ-conglutin in the complex pasta matrix, since the selected peptides belong univocally to *L. angustifolius* γ-conglutin. The absence of the selected prototypic peptide signals in a real food matrix was checked by analyzing DW (data not shown). The specificity and uniqueness of the selected marker peptides were verified by blasting, comparing the peptide sequences against the online accessible protein databases (SwissProt, Uniprot). With the aim to ensure greater specificity, the LC-MRM analysis was performed, monitoring two diagnostic transitions for each peptide. In order to obtain highly sensitive measurements, robust MS/MS transitions with high specificity and intensity for each peptide were monitored. The MRM transitions for PNNIQ were those from the mono-charged precursor ion $[M + H]^+$ (m/z 585.3) to product-ions b4 and b5 with m/z 439.0 and 568.2, respectively. The MRM transitions for NIHKRTPL were from the mono-charged precursor ion $[M+H]^+$ (m/z 978.6) to product-ions y5 and b8 with m/z 614.3 and 960.6, respectively, as shown in **Figure I-4**. The peak areas of all monitored transitions from parent to product ions of NIHKRTPL were integrated and used for the quantification.

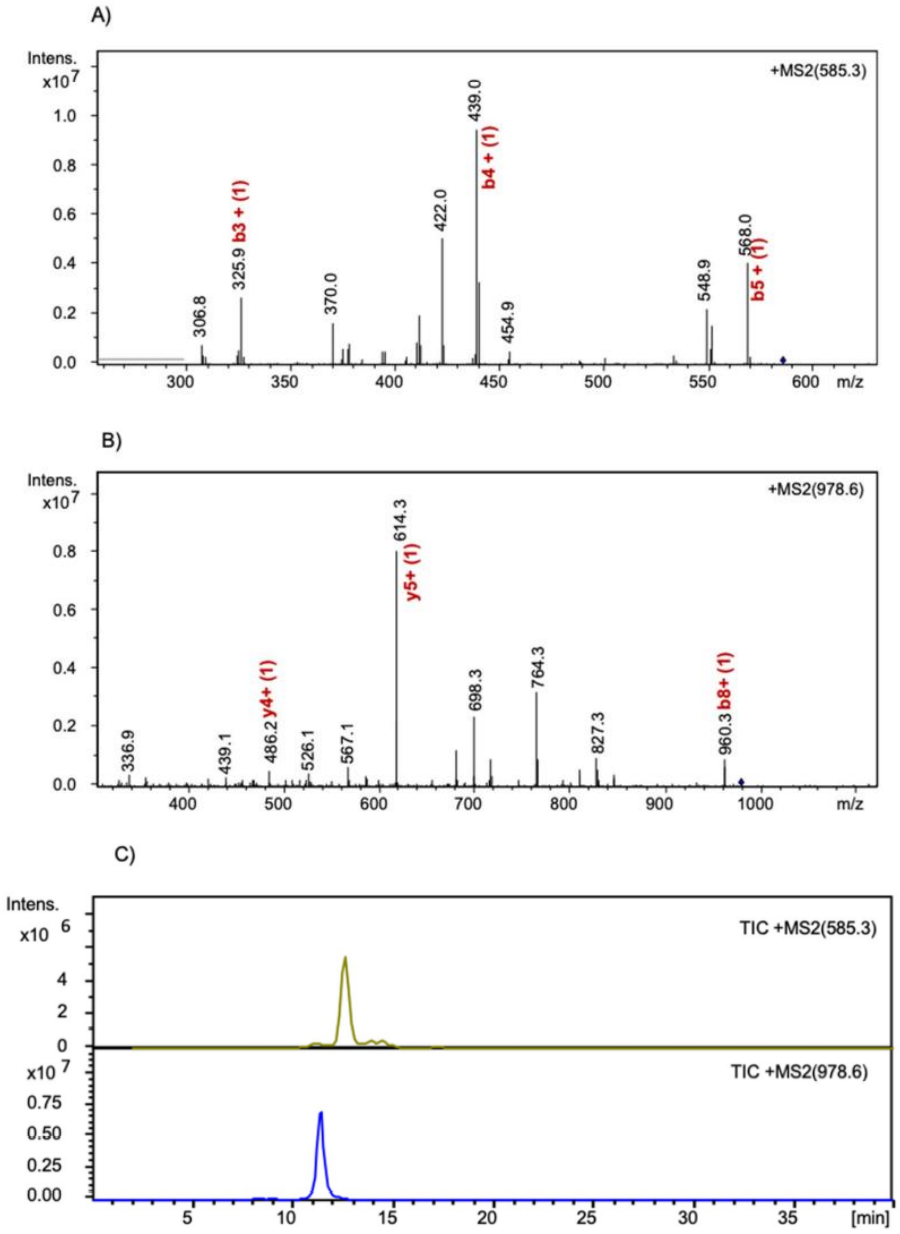

Figure I-4 Electrospray ionization-tandem mass spectrometry spectra of $[M + H]^+$ ions of (**A**) PNNIQ and (**B**) NIHKRTPL, respectively; (**C**) Total ion chromatograms (TIC) of PNNIQ (m/z 585.23) and NIHKRTPL (m/z 978.6).

I-3.4 Validation of the Analytical Parameters: Range of Linearity, Sensitivity, LOQ, and LOD of -Conglutin

Quantification in Lupin Based-Pasta The linearity of the method was assessed in the concentration range, spanning three different orders of magnitude. Therefore, six different concentrations of standard peptide NIHKRTPL ranging from 25, 50, 250, 500,

1000, 2000, and 4000 µg/mL were analyzed in three replicates. To determine the relation between the peak area under the curves and the concentration of peptides, the calibration curve was built by plotting the mean response factor (peak area) against the respective concentrations of NIHKRTPL. The linearity of the method was determined by the correlation coefficient. A correlation coefficient greater than 0.95 and an intercept not significantly different from zero was accepted as criteria for a good standard regression curve. All peak area values were linear (R2 > 0.99) and the RDS% values were in all cases under 12%, thus showing good repeatability of the measurement. The accuracy of MRM assay was verified by adding known quantities of NIHKRTPL to the blank matrix (DW) at 250 µg/mL. The accuracy was detected as higher than 95%. LOQ was 0.25 mg/g, whereas LOD was detected equal to 0.20 mg/g. The developed approach was then applied to the lupin-enriched pasta samples. Exemplary extracted ion chromatograms of NIHKRTPL in A, D, and F samples are shown in **Figure I-5**. The amounts of -conglutin detected in A, D, and F samples, obtained by interpolating the signal of the targeted peptide over the calibration curve, are reported in **Table I-2**. The highest -conglutin concentration was found in pasta sample A, containing 2.25 mg/g of -conglutin/pasta, followed by samples D (2.16 mg/g), and F (0.57 mg/g). Again, the fibers of samples F impaired the γ-conglutin detection. These results are in line with those reported in other commercial food products (Mattarozzi, Bignardi, Elviri, & Careri, 2012).

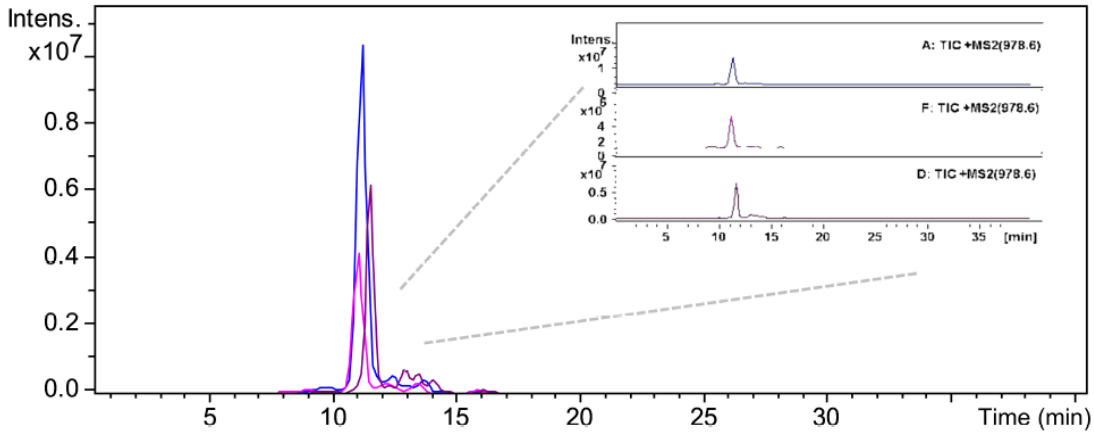

Figure I-5 Extracted ion chromatograms of NIHKRTPL after mass spectrometry (MS) analysis in

A, D, and F pasta samples.

Table I-2. Amount of -conglutin found in lupin-based pasta.

Sample	Amount of γ-Conglutin (mg/g)	RSD%
A	2.25	12.2
D	2.16	3.5
F	0.57	11.3

I-4. Conclusions

To the best of our knowledge, this is the first study on the effect of narrow-leaf lupin flour supplementation on the quality of pasta proteins. These integrated methods, based on either untargeted or targeted approaches, have a high potential for exploitation for the simultaneous detection of additional protein sources in various foods. The untargeted LC-MS/MS procedure enabled the estimation of the relative changes in protein abundance in all the examined samples. In addition, the sensitivity and selectivity obtained by the targeted proteomic-based MRM-LC-ESI-MS/MS approach allowed us to propose a useful quantitative method for the detection of a specific nutraceutical protein fraction in pasta supplemented with narrow-leaf lupin flour. Both the untargeted and targeted methods were demonstrated to be useful tools for investigating protein composition in lupin supplemented pasta. Finally, it is important to underline that the described pasta samples contain very large amounts of lupin protein, which has never been described before in literature.

SUPPORTING INFORMATION

Table II-S1. Proteins and peptides identified in samples A, D, F, and LK

Sample A	Protein Name and Acc.	-10lgP	P-value	Coverage (%)	MW	Peptide	Unique	-10lgP	m/z	z	Intensity	iBAQ
1	**Conglutin alpha 1 OS=Lupinus angustifolius**	**125.07**	**3.11172E-13**	**25**	**57793**							**4.84E+06**
	F5B8V6_LUPAN					K.TNDIPQIAALAGLTSSIR.A	Y	59.65	921.28	2	1.20E+07	
						K.SLDDNFSYVAFK.T	Y	45.62	703.25	2	1.84E+06	
						R.ALPLDVVAHAF.N	Y	41.6	576.94	2	5.72E+07	
						N.GLEETLC(+57.02)TLK.L	Y	32.29	582.43	2	2.14E+06	
						R.FYLSGNQEQEFLQY.Q	Y	27.84	883.60	2	5.92E+05	
						R.WLGLAAEHGSIY.K	Y	26.94	658.82	2	3.12E+05	
						R.EGDIIAVPTGVPF.W	Y	26.59	1314.62	1	6.68E+06	
						K.TLTSLDFPILR.W	Y	25.9	638.61	2	2.36E+07	
						K.FLVPPPQSQLR.A	Y	16.9	641.31	2	5.82E+05	
						K.SEAGTIETWNPNNDQLR.C	Y	16.87	972.85	2	1.63E+06	
2	**Conglutin alpha 3 OS=Lupinus angustifolius**	**105.64**	**2.72898E-11**	**19**	**67381**							**1.13E+06**
	tr|F5B8V8|F5B8V8_LUPAN					R.VQVVNSQGNSVFNDDLR.R	Y	46.61	945.89	2	9.77E+05	
						R.GIPAEVLANAFR.L	Y	41.78	629.43	2	2.06E+07	
						R.VEEGLGVISPK.W	Y	35.12	564.61	2	9.92E+05	
						R.LSLNQVSELK.Y	Y	31.94	565.89	2	1.55E+06	
						N.GLEETIC(+57.02)TAILR.E	Y	30.96	688.78	2	6.67E+06	

						R.GIPAEVLANAF.R	N	28.67	551.23	2	5.62E+04	
						R.RGQLLVVPQNF.V	N	21.68	635.97	2	2.41E+06	
						K.NNILSGFDPQFLSQALNIDED TVHK.L	Y	21.35	939.22	3	8.94E+04	
						R.EGDILVIPPGTPY.W	Y	15.33	686.33	2	5.86E+05	
3	**Seed storage protein OS=Lupinus angustifolius**	**105.64**	**2.72898E-11**	**23**	**57124**							**1.41E+06**
	tr|C9WC98|C9WC98_LUPAN					R.VQVVNSQGNSVFNDDLR.R	Y	46.61	945.89	2	9.77E+05	
						R.GIPAEVLANAFR.L	Y	41.78	629.43	2	2.06E+07	
						R.VEEGLGVISPK.W	Y	35.12	564.61	2	9.92E+05	
						R.LSLNQVSELK.Y	Y	31.94	565.89	2	1.55E+06	
						N.GLEETIC(+57.02)TAILR.E	Y	30.96	688.78	2	6.67E+06	
						R.GIPAEVLANAF.R	N	28.67	551.23	2	5.62E+04	
						R.RGQLLVVPQNF.V	N	21.68	635.97	2	2.41E+06	
						K.NNILSGFDPQFLSQALNIDED TVHK.L	Y	21.35	939.22	3	8.94E+04	
						R.EGDILVIPPGTPY.W	Y	15.33	686.33	2	5.86E+05	
4	**Conglutin alpha 2 OS=Lupinus angustifolius**	**74.32**	**3.69828E-08**	**10**	**74194**							**2.86E+05**
	tr|F5B8V7|F5B8V7_LUPAN					R.LVAINLLDTTSLLNQLDPSPR. R	Y	46.08	1147.32	2	6.09E+06	
						R.GIPAEVLANAF.G	N	28.67	551.23	2	5.62E+04	
						R.LNALEPDNRVESEGGVTETW .N	Y	25.42	1108.81	2	3.14E+05	
						R.RGQLLVVPQNF.V	N	21.68	635.97	2	2.41E+06	

5	**Conglutin beta 1 OS=Lupinus angustifolius**	**71.05**	**7.85236E-08**	**8**	**71926**							**4.95E+05**
	F5B8V9|CONB1_LUPAN					R.NFLAGSEDNVIK.Q	Y	39.53	653.85	2	2.83E+06	
						K.ELTFPGSIEDVER.L	Y	34.34	746.50	2	8.42E+06	
						R.LLGFGINANENQR.N	N	26.72	723.71	2	3.88E+05	
						K.GDVFIIPAGHPL.S	Y	21.73	618.50	2	6.69E+06	
6	**Conglutin beta OS=Lupinus angustifolius**	**71.05**	**7.85236E-08**	**8**	**71896**							**4.95E+05**
	tr|B8Q5G0|B8Q5G0_LUPAN					R.NFLAGSEDNVIK.Q	Y	39.53	653.85	2	2.83E+06	
						K.ELTFPGSIEDVER.L	Y	34.34	746.50	2	8.42E+06	
						R.LLGFGINANENQR.N	N	26.72	723.71	2	3.88E+05	
						K.GDVFIIPAGHPL.S	Y	21.73	618.50	2	6.69E+06	
7	**Conglutin beta (Fragment) OS=Lupinus angustifolius**	**64.51**	**3.53997E-07**	**6**	**61469**							**4.99E+05**
	tr|B0YJF7|B0YJF7_LUPAN					R.NFLAGSEDNVISQLDR.E	Y	51.15	889.77	2	1.56E+07	
						R.LLGFGINANENQR.N	N	26.72	723.71	2	3.88E+05	
8	**Conglutin beta 7 OS=Lupinus angustifolius**	**64.51**	**3.53997E-07**	**5**	**71605**							**4.43E+05**
	F5B8W5|CONB7_LUPAN					R.NFLAGSEDNVISQLDR.E	Y	51.15	889.77	2	1.56E+07	
						R.LLGFGINANENQR.N	N	26.72	723.71	2	3.88E+05	
9	**Conglutin beta 5 OS=Lupinus angustifolius**	**62.05**	**6.23735E-07**	**4**	**75207**							**2.92E+05**
	F5B8W3|CONB5_LUPAN					R.NFLAGSEDNVIR.Q	Y	41.38	667.87	2	1.92E+06	
						R.LSEGDILVIPAGHPL.S	Y	41.34	765.99	2	9.17E+06	
10	**Conglutin delta 3 OS=Lupinus angustifolius**	**58.63**	**1.37088E-06**	**21**	**17406**							**6.96E+05**

	tr|F5B8X0|F5B8X0_LUPAN					R.ALQQIYESQSEQC(+57.02)EGR.Q	Y	49.82	963.50	2	3.39E+06	
						R.QQEQQLEGELEKLPR.I	Y	17.61	609.39	3	2.88E+06	
11	**Conglutin delta 1 OS=Lupinus angustifolius**	**58.63**	**1.37088E-06**	**20**	**17752**							**6.96E+05**
	tr|F5B8W8|F5B8W8_LUPAN					R.ALQQIYESQSEQC(+57.02)EGR.Q	Y	49.82	963.50	2	3.39E+06	
						R.QQEQQLEGELEKLPR.I	Y	17.61	609.39	3	2.88E+06	
12	**Conglutin delta-2 large chain OS=Lupinus angustifolius**	**58.63**	**1.37088E-06**	**39**	**9400**							**1.25E+06**
	P09931|CGD2L_LUPAN					R.ALQQIYESQSEQC(+57.02)EGR.Q	Y	49.82	963.50	2	3.39E+06	
						R.QQEQQLEGELEKLPR.I	Y	17.61	609.39	3	2.88E+06	

D	**Protein Name**	**-10lgP**		**Coverage (%)**	**Avg. Mass**	**Peptide**	**Unique**	**-10lgP**	**m/z**	**z**	**Intensity**	**iBAQ**
1	**Seed storage protein OS=Lupinus angustifolius**	**114.55**	**3.50752E-12**	**15**	**57124**							**3.56E+06**
	tr|C9WC98|C9WC98_LUPAN					R.VQVVNSQGNSVFNDDLR.R	Y	62.49	946.49	2	1.31E+06	
						R.GIPAEVLANAFR.L	Y	38.03	629.71	2	1.38E+07	
						R.VEEGLGVISPK.W	Y	35.04	564.66	2	1.13E+06	
						N.GLEETIC(+57.02)TAILR.E	Y	32.45	688.25	2	4.57E+07	
						R.LSLNQVSELK.Y	Y	26.85	565.86	2	1.13E+06	
						R.GQLLVVPQNF.V	N	26.08	1115.20	1	3.65E+06	
						R.GIPAEVLANAF.R	N	24.78	551.26	2	1.86E+07	

2	**Conglutin alpha 3 OS=Lupinus angustifolius**	**114.55**	**3.50752E-12**	**12**	**67381**							**2.84E+06**
	tr|F5B8V8|F5B8V8_LUPAN					R.VQVVNSQGNSVFNDDLR.R	Y	62.49	946.49	2	1.31E+06	
						R.GIPAEVLANAFR.L	Y	38.03	629.71	2	1.38E+07	
						R.VEEGLGVISPK.W	Y	35.04	564.66	2	1.13E+06	
						N.GLEETIC(+57.02)TAILR.E	Y	32.45	688.25	2	4.57E+07	
						R.LSLNQVSELK.Y	Y	26.85	565.86	2	1.13E+06	
						R.GQLLVVPQNF.V	N	26.08	1115.20	1	3.65E+06	
						R.GIPAEVLANAF.R	N	24.78	551.26	2	1.86E+07	
3	**Conglutin alpha 1 OS=Lupinus angustifolius**	**107.59**	**1.74181E-11**	**22**	**57793**							**7.73E+06**
	tr|F5B8V6|F5B8V6_LUPAN					R.WLGLAAEHGSIYK.N	Y	45.92	722.86	2	2.50E+05	
						R.ALPLDVVAHAF.N	Y	40.68	576.88	2	3.37E+07	
						R.FYLSGNQEQEFLQY.Q	Y	37.33	883.43	2	2.11E+06	
						K.TLTSLDFPILR.W	Y	34.67	638.78	2	6.10E+07	
						N.GLEETLC(+57.02)TLK.L	Y	33.77	582.47	2	4.57E+07	
						R.EGDIIAVPTGVPF.W	Y	28.97	658.19	2	2.52E+07	
						K.FLVPPPQSQLR.A	Y	23.6	641.29	2	3.20E+05	
						K.SEAGTIETWNPNNDQLR.C	Y	22.44	972.87	2	7.99E+05	
						R.RPFYTNAPQEIY.I	Y	22.09	749.81	2	1.10E+06	
4	**Conglutin alpha 2 OS=Lupinus angustifolius**	**93.59**	**4.37522E-10**	**19**	**74194**							**1.45E+06**
	tr|F5B8V7|F5B8V7_LUPAN					R.LVAINLLDTTSLLNQLDPSPR.R	Y	42.64	1147.04	2	1.53E+07	
						R.ISSVNSLTLPILR.W	Y	34.51	706.91	2	3.45E+06	

						R.LNALEPDNRVESEGGVTETW.N	Y	34.02	1109.10	2	1.23E+06	
						N.GLEETIC(+57.02)TAR.L	Y	27.8	575.37	2	3.88E+05	
						R.GQLLVVPQNF.V	N	26.08	1115.20	1	3.65E+06	
						R.GIPAEVLANAF.G	N	24.78	551.26	2	1.86E+07	
						R.FYIAGNPEEEHPETQEQQGQQR.E	Y	23.96	872.67	3	2.00E+06	
						D.PQFLTQAFNVDEEIINR.L	Y	21	1017.28	2	3.14E+05	
5	**Conglutin beta 5 OS=Lupinus angustifolius F5B8W3|CONB5_LUPAN**	**71.3**	**7.4131E-08**	**6**	**75207**							**3.53E+05**
						R.LLGFGINADENQR.N	Y	44.02	723.99	2	2.23E+06	
						R.NFLAGSEDNVIR.Q	Y	37.28	667.86	2	4.48E+06	
						R.LSEGDILVIPAGHPL.S	Y	25.89	766.05	2	6.71E+06	
6	**Conglutin beta 1 OS=Lupinus angustifolius F5B8V9|CONB1_LUPAN**	**69.09**	**1.2331E-07**	**6**	**71926**							**8.78E+05**
						K.ELTFPGSIEDVER.L	Y	40.5	746.96	2	9.24E+06	
						R.NFLAGSEDNVIK.Q	Y	37.6	654.31	2	2.81E+06	
						K.GDVFIIPAGHPL.S	Y	29.36	618.55	2	2.04E+07	
7	**Conglutin beta OS=Lupinus angustifolius tr|B8Q5G0|B8Q5G0_LUPAN**	**69.09**	**1.2331E-07**	**6**	**71896**							**2.50E+05**
						K.ELTFPGSIEDVER.L	Y	40.5	746.96	2	9.24E+06	
						R.NFLAGSEDNVIK.Q	Y	37.6	654.31	2	2.81E+06	
						K.GDVFIIPAGHPL.S	Y	29.36	618.55	2	2.04E+07	
8	**Conglutin delta-2 large chain OS=Lupinus angustifolius**	**61.09**	**7.78037E-07**	**49**	**9400**							**5.16E+05**

	P09931|CGD2L_LUPAN					R.ALQQIYESQSEQC(+57.02)EGR.Q	Y	36.78	963.82	2	1.13E+06	
						R.IC(+57.02)GFGPLR.R	Y	31.89	460.23	2	4.52E+05	
						R.QQEQQLEGELEKLPR.I	Y	25.08	609.14	3	9.92E+05	
9	**Conglutin delta 3 OS=Lupinus angustifolius**	**61.09**	**7.78037E-07**	**26**	**17406**							**2.86E+05**
	tr|F5B8X0|F5B8X0_LUPAN					R.ALQQIYESQSEQC(+57.02)EGR.Q	Y	36.78	963.82	2	1.13E+06	
						R.IC(+57.02)GFGPLR.R	Y	31.89	460.23	2	4.52E+05	
						R.QQEQQLEGELEKLPR.I	Y	25.08	609.14	3	9.92E+05	
10	**Conglutin delta 1 OS=Lupinus angustifolius**	**61.09**	**7.78037E-07**	**26**	**17752**							**2.86E+05**
	tr|F5B8W8|F5B8W8_LUPAN					R.ALQQIYESQSEQC(+57.02)EGR.Q	Y	36.78	963.82	2	1.13E+06	
						R.IC(+57.02)GFGPLR.R	Y	31.89	460.23	2	4.52E+05	
						R.QQEQQLEGELEKLPR.I	Y	25.08	609.14	3	9.92E+05	
11	**Conglutin beta (Fragment) OS=Lupinus angustifolius**	**36.6**	**0.000218776**	**3**	**61469**							**3.33E+05**
	tr|B0YJF7|B0YJF7_LUPAN					R.NFLAGSEDNVISQLDR.E	Y	36.6	889.44	2	1.06E+07	
12	**Conglutin beta 7 OS=Lupinus angustifolius**	**36.6**	**0.000218776**	**3**	**71605**							**2.96E+05**
	F5B8W5|CONB7_LUPAN					R.NFLAGSEDNVISQLDR.E	Y	36.6	889.44	2	1.06E+07	
13	**11S globulin isoform 2 OS=Castanea sativa**	**27.83**	**0.001648162**	**2**	**60739**							**9.29E+05**
	tr|E3SET9|E3SET9_CASSA					R.AIPADVLANAF.Q	Y	27.83	551.60	2	1.95E+07	

14	**11S globulin isoform 1 OS=Castanea sativa tr|E3SET8|E3SET8_CASSA**	**27.83**	**0.001648162**	**2**	**60840**	R.AIPADVLANAF.Q	Y	27.83	551.60	2	1.95E+07	**9.29E+05**
15	**11S globulin isoform 3 OS=Castanea sativa tr|R4IW40|R4IW40_CASSA**	**27.83**	**0.001648162**	**2**	**61016**	R.AIPADVLANAF.Q	Y	27.83	551.60	2	1.95E+07	**9.29E+05**

F	Protein Name and Acc.	-10lgP	P-value	Coverage (%)	Avg. Mass	Peptide	Unique	-10lgP	m/z	z	Intensity	iBAQ
1	**Seed storage protein OS=Lupinus angustifolius tr|C9WC98|C9WC98_LUPAN**	**103.76**	**4.20727E-11**	**15**	**57124**	R.GIPAEVLANAFR.L	Y	51.72	629.89	2	7.94E+06	**5.41E+05**
						R.VEEGLGVISPK.W	Y	46.95	564.90	2	4.06E+05	
						R.LSLNQVSELK.Y	Y	31.56	565.85	2	4.54E+05	
						N.GLEETIC(+57.02)TAILR.E	Y	27.03	688.49	2	9.50E+05	
						R.RGQLLVVPQNF.V	N	25.5	636.04	2	2.09E+06	
						R.FYLAGNPEEEYPETQQQR.Q	Y	23.76	734.02	3	3.02E+05	
						R.GIPAEVLANAF.R	N	15.55	1101.55	1	8.37E+05	
2	**Conglutin alpha 3 OS=Lupinus angustifolius tr|F5B8V8|F5B8V8_LUPAN**	**103.76**	**4.20727E-11**	**13**	**67381**	R.GIPAEVLANAFR.L	Y	51.72	629.89	2	7.94E+06	**4.33E+05**
						R.VEEGLGVISPK.W	Y	46.95	564.90	2	4.06E+05	
						R.LSLNQVSELK.Y	Y	31.56	565.85	2	4.54E+05	
						N.GLEETIC(+57.02)TAILR.E	Y	27.03	688.49	2	9.50E+05	
						R.RGQLLVVPQNF.V	N	25.5	636.04	2	2.09E+06	
						R.FYLAGNPEEEYPETQQQR.Q	Y	23.76	734.02	3	3.02E+05	

						R.GIPAEVLANAF.R	N	15.55	1101.55	1	8.37E+05	
3	**Conglutin alpha 1 OS=Lupinus angustifolius**	**97.86**	**1.63682E-10**	**12**	**57793**							**8.09E+05**
	tr|F5B8V6|F5B8V6_LUPAN					R.ALPLDVVAHAF.N	Y	50.86	577.37	2	1.25E+07	
						K.TNDIPQIAALAGLTSSIR.A	Y	47.4	921.15	2	1.52E+05	
						K.TLTSLDFPILR.W	Y	36.33	638.37	2	5.08E+06	
						N.GLEETLC(+57.02)TLK.L	Y	26.8	581.93	2	1.08E+05	
						R.EGDIIAVPTGVPF.W	Y	22.42	657.79	2	5.83E+06	
4	**Conglutin alpha 2 OS=Lupinus angustifolius**	**33.28**	**0.000469894**	**3**	**74194**							**6.79E+04**
	tr|F5B8V7|F5B8V7_LUPAN					R.RGQLLVVPQNF.V	N	25.5	636.04	2	2.09E+06	
						R.GIPAEVLANAF.G	N	15.55	1101.55	1	1.21E+04	
5	**Conglutin delta-2 large chain OS=Lupinus angustifolius**	**31.29**	**0.000743019**	**28**	**9400**							**3.45E+05**
	P09931|CGD2L_LUPAN					R.QQEQQLEGELEKLPR.I	Y	21.38	609.16	3	1.25E+06	
						R.IC(+57.02)GFGPL.R	Y	19.82	763.31	1	4.73E+05	
6	**Conglutin delta 3 OS=Lupinus angustifolius**	**31.29**	**0.000743019**	**15**	**17406**							**1.92E+05**
	tr|F5B8X0|F5B8X0_LUPAN					R.QQEQQLEGELEKLPR.I	Y	21.38	609.16	3	1.25E+06	
						R.IC(+57.02)GFGPL.R	Y	19.82	763.31	1	4.73E+05	
7	**Conglutin delta 1 OS=Lupinus angustifolius**	**31.29**	**0.000743019**	**14**	**17752**							**1.92E+05**
	tr|F5B8W8|F5B8W8_LUPAN					R.QQEQQLEGELEKLPR.I	Y	21.38	609.16	3	1.25E+06	
						R.IC(+57.02)GFGPL.R	Y	19.82	763.31	1	4.73E+05	
8	**Monogalactosyldiacylglycerol synthase 2 type B**	**20.27**	**0.009397233**	**1**	**53969**							**3.90E+02**

	tr|S6BK49|S6BK49_SESIN					K.FMVKH.V	Y	20.27	660.76	1	1.21E+04	

MIX	**Protein Name and Acc.**	**-10lgP**	**P-value**	**Coverage (%)**	**Avg. Mass**	**Peptide**	**Unique**	**-10lgP**	**m/z**	**z**	**Intensity**	**iBAQ**
1	**Uncharacterized protein OS=Oryza sativa subsp. japonica**	**22.63**	**0.005457579**	**1**	**43113**							**1.80E+04**
	tr|B9FHE0|B9FHE0_ORYSJ					MAQIID.G	Y	22.63	690.58	1	5.57E+05	
2	**Protein synthesis inhibitor II OS=Hordeum vulgare**	**22.63**	**0.005457579**	**6**	**29863**							**2.23E+04**
	P04399|RIP2_HORVU					R.DLLGDTDKLTNVALGR.Q	Y	22.63	851.43	2	3.79E+05	
3	**Protein synthesis inhibitor I OS=Hordeum vulgare**	**22.63**	**0.005457579**	**6**	**29973**							**2.23E+04**
	P22244|RIP1_HORVU					R.DLLGDTDKLTNVALGR.Q	Y	22.63	851.43	2	3.79E+05	
4	**Putative uncharacterized protein OS=Selaginella moellendorffii**	**22.5**	**0.005623413**	**2**	**84461**							**4.37E+04**
	tr|D8RC85|D8RC85_SELML					A.KLLEKLLVDTPAC(+57.02)K.A	Y	22.5	814.99	2	2.32E+06	
5	**Rho GTPase-activating protein 5 OS=Arabidopsis thaliana**	**20.94**	**0.008053784**	**2**	**36830**							**9.93E+04**
	Q6NKT5|RGAP5_ARATH					MDIGGPT.N	Y	20.94	690.33	1	1.69E+06	

LUPIN KERNEL	**Protein Name and Acc.**	**-10lgP**	**P-value**	**Coverage (%)**	**Avg. Mass**	**Peptide**	**Unique**	**-10lgP**	**m/z**	**z**	**Intensity**	**iBAQ**
1	**Seed storage protein OS=Lupinus angustifolius**	**142.01**	**6.29506E-15**	**15**	**57124**							**7.90E+06**
	tr|C9WC98|C9WC98_LUPAN					R.VQVVNSQGNSVFNDDLR.R	Y	77.12	946.39	2	1.88E+06	

						R.GIPAEVLANAFR.L	Y	49.71	629.51	2	3.04E+07	
						R.VEEGLGVISPK.W	Y	43.86	564.52	2	2.18E+06	
						N.GLEETIC(+57.02)TAILR.E	Y	41.31	688.73	2	1.22E+08	
						R.LSLNQVSELK.Y	Y	32.12	565.96	2	1.45E+06	
						R.GIPAEVLANAF.R	N	30.85	551.22	2	2.64E+07	
						R.GQLLVVPQNF.V	N	24.57	1114.47	1	5.21E+06	
2	**Conglutin alpha 3 OS=Lupinus angustifolius tr|F5B8V8|F5B8V8_LUPAN**	**142.01**	**6.29506E-15**	**12**	**67381**							**6.32E+06**
						R.VQVVNSQGNSVFNDDLR.R	Y	77.12	946.39	2	1.88E+06	
						R.GIPAEVLANAFR.L	Y	49.71	629.51	2	3.04E+07	
						R.VEEGLGVISPK.W	Y	43.86	564.52	2	2.18E+06	
						N.GLEETIC(+57.02)TAILR.E	Y	41.31	688.73	2	1.22E+08	
						R.LSLNQVSELK.Y	Y	32.12	565.96	2	1.45E+06	
						R.GIPAEVLANAF.R	N	30.85	551.22	2	2.64E+07	
						R.GQLLVVPQNF.V	N	24.57	1114.47	1	5.21E+06	
3	**Conglutin alpha 2 OS=Lupinus angustifolius tr|F5B8V7|F5B8V7_LUPAN**	**132.42**	**5.72796E-14**	**23**	**74194**							**4.39E+06**
						R.WFQLSADYVNLYR.N	Y	65.36	837.78	2	1.39E+07	
						R.LVAINLLDTTSLLNQLDPSPR.R	Y	48.04	1147.08	2	2.79E+07	
						K.NNVLSGFDPQFLTQAFNVDEEIINR.L	Y	42.98	960.79	3	6.17E+06	
						R.ISSVNSLTLPILR.W	Y	40.92	707.18	2	3.30E+07	
						R.GIPAEVLANAF.G	N	30.85	551.22	2	2.64E+07	
						K.YSGNQGPLVSPQSESED.H	Y	29.63	897.84	2	1.69E+06	
						R.GQLLVVPQNF.V	N	24.57	1114.47	1	5.21E+06	

						R.LNALEPDNRVESEGGVTETW.N	Y	16.38	1108.34	2	4.72E+05	
						R.EGDIIAIPPGIPYWTY.N	Y	16.34	903.18	2	2.12E+07	
4	**Conglutin alpha 1 OS=Lupinus angustifolius**	**127.02**	**1.98609E-13**	**23**	**57793**							**9.36E+06**
	tr|F5B8V6|F5B8V6_LUPAN					R.FYLSGNQEQEFLQY.Q	Y	52.89	883.52	2	9.79E+06	
						R.ALPLDVVAHAF.N	Y	44.94	576.96	2	3.56E+07	
						K.TLTSLDFPILR.W	Y	43.47	638.77	2	1.26E+08	
						N.GLEETLC(+57.02)TLK.L	N	38.25	582.42	2	6.45E+05	
						K.TNDIPQIAALAGLTSSIR.A	Y	35.43	921.44	2	3.82E+06	
						R.RFYLSGNQEQEFLQY.Q	Y	35.28	961.32	2	9.79E+06	
						K.SEAGTIETWNPNNDQLR.C	Y	34.45	973.33	2	6.85E+06	
						R.GIFGLIFPGC(+57.02)R.E	Y	31.95	618.98	2	7.90E+06	
						R.RPFYTNAPQEIY.I	Y	28.05	749.89	2	1.92E+06	
						K.FLVPPPQSQLR.A	Y	26.01	641.35	2	3.80E+06	
5	**Conglutin beta (Fragment) OS=Lupinus angustifolius**	**91.52**	**7.04693E-10**									**2.02E+06**
	tr|B0YJF7|B0YJF7_LUPAN					R.NFLAGSEDNVISQLDR.E	Y	49.06	889.87	2	5.71E+07	
						K.ELTFPGSAQDVER.L	Y	46.99	725.26	2	3.90E+06	
						R.LLGFGINANENQR.N	N	41.98	723.80	2	1.79E+06	
						F.IVVVDEGEGNYELVGIR.D	N	19.88	930.46	2	1.79E+06	
6	**Conglutin beta OS=Lupinus angustifolius**	**88.72**	**1.34276E-09**	**12**	**71896**							**1.10E+06**
	tr|B8Q5G0|B8Q5G0_LUPAN					R.LLGFGINANENQR.N	N	41.98	723.80	2	1.79E+06	
						R.IIEFQSKPNTL.I	N	39.35	645.35	2	6.58E+05	
						K.GDVFIIPAGHPL.S	Y	30.85	618.97	2	3.62E+07	

						K.LYDFYPSTTK.D	N	30.27	617.94	2	8.48E+05	
						R.NFLAGSEDNVIK.Q	Y	29.46	653.89	2	7.92E+05	
						F.IVVVDEGEGNYELVGIR.D	N	19.88	930.46	2	3.10E+05	
7	**Conglutin beta 1 OS=Lupinus angustifolius**	**88.72**	**1.34276E-09**	**12**	**71926**							**1.10E+06**
	F5B8V9|CONB1_LUPAN					R.LLGFGINANENQR.N	N	41.98	723.80	2	1.79E+06	
						R.IIEFQSKPNTL.I	N	39.35	645.35	2	6.58E+05	
						K.GDVFIIPAGHPL.S	Y	30.85	618.97	2	3.62E+07	
						K.LYDFYPSTTK.D	N	30.27	617.94	2	8.48E+05	
						R.NFLAGSEDNVIK.Q	Y	29.46	653.89	2	7.92E+05	
						F.IVVVDEGEGNYELVGIR.D	N	19.88	930.46	2	3.10E+05	
8	**Conglutin delta-2 large chain OS=Lupinus angustifolius**	**86.81**	**2.08449E-09**	**30**	**9400**							**2.15E+06**
	P09931|CGD2L_LUPAN					R.ALQQIYESQSEQC(+57.02)EGR.Q	Y	70.96	963.74	2	8.88E+06	
						R.IC(+57.02)GFGPLR.R	Y	31.69	460.26	2	1.85E+06	
9	**Conglutin delta 3 OS=Lupinus angustifolius**	**86.81**	**2.08449E-09**	**16**	**17406**							**1.19E+06**
	tr|F5B8X0|F5B8X0_LUPAN					R.ALQQIYESQSEQC(+57.02)EGR.Q	Y	70.96	963.74	2	8.88E+06	
						R.IC(+57.02)GFGPLR.R	Y	31.69	460.26	2	1.85E+06	
10	**Conglutin delta 1 OS=Lupinus angustifolius**	**86.81**	**2.08449E-09**	**16**	**17752**							**1.19E+06**
	tr|F5B8W8|F5B8W8_LUPAN					R.ALQQIYESQSEQC(+57.02)EGR.Q	Y	70.96	963.74	2	8.88E+06	
						R.IC(+57.02)GFGPLR.R	Y	31.69	460.26	2	1.85E+06	

11	**Conglutin beta 2 OS=Lupinus angustifolius**	**80.9**	**8.12831E-09**	**8**	**70701**							**3.52E+05**
	F5B8W0|CONB2_LUPAN					R.LLGFGINADENQR.N	N	47.14	723.97	2	1.00E+06	
						R.NFLAGSEDNVIR.Q	N	37.47	668.32	2	1.23E+07	
						K.QLTFPGSVEDVER.L	Y	30.33	738.88	2	3.34E+05	
						R.IVEFQSKPNTL.I	N	19.65	638.75	2	1.15E+05	
12	**Conglutin beta 5 OS=Lupinus angustifolius**	**79.91**	**1.02094E-08**	**6**	**75207**							**5.83E+05**
	F5B8W3|CONB5_LUPAN					R.LLGFGINADENQR.N	N	47.14	723.97	2	1.00E+06	
						R.LSEGDILVIPAGHPL.S	Y	40.55	765.91	2	8.88E+06	
						R.NFLAGSEDNVIR.Q	N	37.47	668.32	2	1.23E+07	
13	**Conglutin beta 4 OS=Lupinus angustifolius**	**77.05**	**1.97242E-08**	**8**	**69407**							**3.65E+05**
	F5B8W2|CONB4_LUPAN					R.LLGFGINADENQR.N	N	47.14	723.97	2	1.00E+06	
						R.NFLAGSEDNVIR.Q	N	37.47	668.32	2	1.23E+07	
						R.IVEFQSKPNTL.I	N	19.65	638.75	2	1.15E+05	
						K.GLTFPGSTEDVER.L	Y	18.47	704.80	2	1.04E+05	
14	**Conglutin beta OS=Lupinus angustifolius**	**75.67**	**2.71019E-08**	**7**	**54300**							**8.14E+04**
	tr|B0YJF8|B0YJF8_LUPAN					R.VLLGDDELQEN(+.98).E	Y	45.9	622.74	2	8.55E+05	
						R.IIEFQSKPNTL.I	N	39.35	645.35	2	6.58E+05	
						K.LYDFYPSTTK.D	N	30.27	617.94	2	8.48E+05	
15	**Legumin OS=Phaseolus vulgaris**	**61.83**	**6.56145E-07**	**7**	**68724**							**2.97E+05**
	tr|F8QXP7|F8QXP7_PHAVU					N.GIEETLC(+57.02)TLK.L	N	38.25	582.42	2	6.45E+05	
						K.GQLLVVPQNF.M	N	24.57	1114.47	1	5.21E+06	

						R.ELEC(+57.02)AGVTF(+31.99)SR(+14.02)R.T	Y	19.53	736.37	2	1.39E+06	
						K.T(+79.97)NPNAVTSYLK(+27.99).D	Y	19.12	658.18	2	2.55E+06	
16	**Auxin response factor OS=Spinacia oleracea tr|A0A0K9QSD3|A0A0K9QSD3_SPIOL**	**21.43**	**0.00719449**	**1**	**97053**							**1.37E+03**
						R.SIDVTSYK.D	Y	21.43	456.62	2	4.39E+04	
17	**Auxin response factor OS=Gossypium raimondii tr|A0A0D2TMS8|A0A0D2TMS8_GOSRA**	**21.43**	**0.00719449**	**1**	**110946**							**1.37E+03**
						R.SIDVTSYK.N	Y	21.43	456.62	2	4.39E+04	

References

Aiello, G., Ferruzza, S., Ranaldi, G., Sambuy, Y., Arnoldi, A., Vistoli, G., & Lammi, C. (2018). Behavior of three hypocholesterolemic peptides from soy protein in an intestinal model based on differentiated Caco-2 cell. *Journal of Functional Foods, 45*, 363-370.

Albuja-Vaca, D., Yepez, C., Vernaza, M. G., & Navarrete, D. (2020). Gluten-free pasta: development of a new formulation based on rice and lupine bean flour (Lupinus Mutabilis) using a mixture-process design. *Food Science and Technology, 40*(2), 408-414.

Arike, L., Valgepea, K., Peil, L., Nahku, R., Adamberg, K., & Vilu, R. (2012). Comparison and applications of label-free absolute proteome quantification methods on Escherichia coli. *J Proteomics, 75*(17), 5437-5448.

Arnoldi, A., Boschin, G., Zanoni, C., & Lammi, C. (2015). The health benefits of sweet lupin seed flours and isolated proteins. *J Funct Foods, 18*, 550-563.

Arnoldi, A., Zanoni, C., Lammi, C., & Boschin, G. (2015). The role of grain legumes in the prevention of hypercholesterolemia and hypertension. *Critical Reviews in Plant Sciences, 34*(1-3), 144-168.

Bertoglio, J. C., Calvo, M. A., Hancke, J. L., Burgos, R. A., Riva, A., Morazzoni, P., Ponzone, C., Magni, C., & Duranti, M. (2011). Hypoglycemic effect of lupin seed γ-conglutin in experimental animals and healthy human subjects. *Fitoterapia, 82*(7), 933-938.

Boja, E. S., & Rodriguez, H. (2012). Mass spectrometry-based targeted quantitative proteomics: Achieving sensitive and reproducible detection of proteins. *Proteomics, 12*(8), 1093-1110.

Boschin, G., Scigliuolo, G. M., Resta, D., & Arnoldi, A. (2014). ACE-inhibitory activity of enzymatic protein hydrolysates from lupin and other legumes. *Food Chem, 145*, 34-40.

Capraro, J., Magni, C., Scarafoni, A., Caramanico, R., Rossi, F., Morlacchini, M., & Duranti, M. (2014). Pasta supplemented with isolated lupin protein fractions reduces body weight gain and food intake of rats and decreases plasma glucose concentration upon glucose overload trial. *Food & Funct, 5*(2), 375-380.

Czubinski, J., Siger, A., & Lampart-Szczapa, E. (2016). Digestion susceptibility of seed globulins isolated from different lupin species. *European Food Research and Technology, 242*(3), 391-403.

Doxastakis, G., Papageorgiou, M., Mandalou, D., Irakli, M., Papalamprou, E., D'Agostina, A., Resta, D., Boschin, G., & Arnoldi, A. (2007). Technological properties and non-enzymatic browning of white lupin protein enriched spaghetti. *Food Chem, 101*(1), 57-64.

Duranti, M., Consonni, A., Magni, C., Sessa, F., & Scarafoni, A. (2008). The major proteins of lupin seed: Characterisation and molecular properties for use as functional and nutraceutical ingredients. *Trends in Food Science & Technology, 19*(12), 624-633.

Hall, R. S., Thomas, S. J., & Johnson, S. K. (2005). Australian sweet lupin flour addition reduces the glycaemic index of a white bread breakfast without affecting palatability in healthy human volunteers. *Asia Pacific Journal of Clinical Nutrition, 14*(1), 91-97.

Horneffer, V., Foster, T. J., & Velikov, K. P. (2007). Fast characterization of industrial soy protein isolates by direct analysis with matrix-assisted laser desorption ionization time-of-flight mass Spectrometry. *J Agric Food Chem, 55*(26), 10505-10508.

Koeberl, M., Clarke, D., & Lopata, A. L. (2014). Next Generation of Food Allergen Quantification Using Mass Spectrometric Systems. *Journal of Proteome Research, 13*(8), 3499-3509.

Kohajdova, Z., Karovicova, J., & Schmidt, S. (2011). Lupin Composition and Possible Use in Bakery-A Review. *Czech Journal of Food Sciences, 29*(3), 203-211.

Kumar, S. B., & Prabhasankar, P. (2014). Low glycemic index ingredients and modified starches in wheat based food processing: A review. *Trends in Food Science & Technology, 35*(1), 32-41.

Lammi, C., Zanoni, C., Aiello, G., Arnoldi, A., & Grazioso, G. (2016). Lupin Peptides Modulate the Protein-Protein Interaction of PCSK9 with the Low Density Lipoprotein Receptor in HepG2 Cells. *Sci Rep, 6*, 29931.

LampartSzczapa, E., Obuchowski, W., Czaczyk, K., Pastuszewska, B., & Buraczewska, L. (1997). Effect of lupine flour on the quality and oligosaccharides of pasta and crisps. *Nahrung-Food, 41*(4), 219-223.

Lovati, M. R., Manzoni, C., Castiglioni, S., Parolari, A., Magni, C., & Duranti, M. (2012). Lupin seed gamma-conglutin lowers blood glucose in hyperglycaemic rats and increases glucose consumption of HepG2 cells. *British Journal of Nutrition, 107*(1), 67-73.

Lucas, M. M., Stoddard, F. L., Annicchiarico, P., Frias, J., Martinez-Villaluenga, C., Sussmann, D., Duranti, M., Seger, A., Zander, P. M., & Pueyo, J. J. (2015). The future of lupin as a protein crop in Europe. *Frontiers in Plant Science, 6*.

Magni, C., Sessa, F., Accardo, E., Vanoni, M., Morazzoni, P., Scarafoni, A., & Duranti, M. (2004). Conglutin gamma, a lupin seed protein, binds insulin in vitro and reduces plasma glucose levels of hyperglycemic rats. *Journal of Nutritional Biochemistry, 15*(11), 646-650.

Mattarozzi, M., Bignardi, C., Elviri, L., & Careri, M. (2012). Rapid Shotgun Proteomic Liquid Chromatography-Electrospray Ionization-Tandem Mass Spectrometry-Based Method for the Lupin (Lupinus albus L.) Multi-allergen Determination in Foods. *J Agric Food Chem, 60*(23), 5841-5846.

Mora, L., Escudero, E., & Toldra, F. (2016). Characterization of the peptide profile in Spanish Teruel, Italian Parma and Belgian dry-cured hams and its potential bioactivity. *Food Research International, 89*, 638-646.

Mora, L., Gallego, M., & Toldra, F. (2018). New approaches based on comparative proteomics for the assessment of food quality. *Current Opinion in Food Science, 22*, 22-27.

Muranyi, I. S., Volke, D., Hoffmann, R., Eisner, P., Herfellner, T., Brunnbauer, M., Koehler, P., & Schweiggert-Weisz, U. (2016). Protein distribution in lupin protein isolates from Lupinus angustifolius L. prepared by various isolation techniques. *Food Chem, 207*, 6-15.

Nagaraj, N., Wisniewski, J. R., Geiger, T., Cox, J., Kircher, M., Kelso, J., Pääbo, S., & Mann, M. (2011). Deep proteome and transcriptome mapping of a human cancer cell line. *Molecular systems biology, 7*, 548-548.

Picotti, P., & Aebersold, R. (2012). Selected reaction monitoring–based proteomics: workflows, potential, pitfalls and future directions. *Nature Methods, 9*(6), 555-566.

Resta, D., Brambilla, F., & Arnoldi, A. (2012). HPLC-Chip-Multiple Reaction Monitoring (MRM) method for the label-free absolute quantification of gamma-conglutin in lupin: Proteotypic peptides and standard addition method. *Food Chem, 131*(1), 126-133.

Saleh, M., Al-Ismail, K., & Ajo, R. (2017). Pasta quality as impacted by the type of flour and starch and the level of egg addition. *Journal of Texture Studies, 48*(5), 370-381.

Scarafoni, A., Ronchi, A., & Duranti, M. (2009). A real-time PCR method for the detection and quantification of lupin flour in wheat flour-based matrices. *Food Chem, 115*(3), 1088-1093.

Schwanhäusser, B., Busse, D., Li, N., Dittmar, G., Schuchhardt, J., Wolf, J., Chen, W., & Selbach, M. (2011). Global quantification of mammalian gene expression control. *Nature, 473*(7347), 337-342.

Sirtori, C. R., Triolo, M., Bosisio, R., Bondioli, A., Calabresi, L., De Vergori, V., Gomaraschi, M., Mombelli, G., Pazzucconi, F., Zacherl, C., & Arnoldi, A. (2012). Hypocholesterolaemic effects of lupin protein and pea protein/fibre combinations in moderately hypercholesterolaemic individuals. *British Journal of Nutrition, 107*(8), 1176-1183.

Sirtori, E., Resta, D., Brambilla, F., Zacherl, C., & Arnoldi, A. (2010). The effects of various processing conditions on a protein isolate from Lupinus angustifolius. *Food Chem, 120*(2), 496-504.

Zanoni, C., Aiello, G., Arnoldi, A., & Lammi, C. (2017). Investigations on the hypocholesterolaemic activity of LILPKHSDAD and LTFPGSAED, two peptides from lupin beta-conglutin: Focus on LDLR and PCSK9 pathways. Journal of Functional Foods, 32, 1-8.

Project II

ASSESSMENT OF THE PHYSICOCHEMICAL AND CONFORMATIONAL CHANGES OF ULTRASOUND-DRIVEN PROTEINS EXTRACTED FROM SOYBEAN OKARA BYPRODUCT

Gilda Aiello[1], Raffaele Puglieseb[2], Lukas Ruller[3], Carlotta Bollati[4], Martina Bartolomei[4], Yuchen Li[4], Josef Robert[3], Anna Arnoldi[4], Carmen Lammid[*]

[1] Department of Human Science and Quality of Life Promotion, Telematic University San Raffaele, Rome, Italy

[2] NeMO Lab, ASST Grande Ospedale Metropolitano Niguarda, Milan, Italy

[3] Fraunhofer Institute for Environmental, Safety and Energy Technology UMSICHT, Oberhausen, Germany

[4] Department of Pharmaceutical Sciences, University of Milan, 20133 Milan, Italy

Abbreviations

1,4-dithiothreitol (DTT), 2-iodoacetamide (IAM), 2,2-diphenyl-1-picrylhydrazyl (DPPH), 5,5- dithio-bis-(2-nitrobenzoic acid) (DTNB), Acetonitrile (ACN), Atomic Force Microscopy (AFM), Circular dichroism spectroscopy (CD), Disulfide bonds (S-S), Ethylenediaminetetraacetic acid (EDTA), Free-sulfhydryl group (SH), Hydrochloric acid (HCl), Mass spectrometry (MS), Phytic acid (PA), Scanning electron microscopy (SEM), Storage modulus G', Sulfate-polyacrylamide gel electrophoresis (SDS-PAGE), Total ion current (TIC), Tris(hydroxymethyl)aminomethane (Tris- HCl), Tryptophan (Trp), Tyrosine (Tyr), Water binding capacity (WBC).

II. Abstract

This study is aimed at the valorization of the okara byproduct deriving form soy food manufacturing, by using ultrasound at different temperatures for extracting the residual proteins. The physicochemical and conformational changes of the extracted proteins were investigated in order to optimize the procedure. Increasing the temperature from 20 up to 80 °C greatly enhanced the yields and the protein solubility without affecting the viscosity. The protein secondary and tertiary structure was also gradually modified in a significant way. After the ultrasonication at the highest temperature, a significant morphological transition from well-defined single round structures to highly aggregated ones, was observed, which was confirmed by measuring the water contact angles and wettability. After the ultrasound process, the improvement of peptides generation and the different amino acid exposition within the protein led to an increase of the antioxidant properties. The integrated strategy applied in this study allows to foster the okara protein obtained after ultrasound extraction as valuable materials for new applications.

II-1. INTRODUCTION

Soybean (*Glycine max*) is a protein-rich oilseed widely employed in the food industry for producing soy foods and beverages. Thanks to its nutrient content, soybean is used in several dishes as a valid alternative to meat and it is added in various vegan-friendly food and beverages (Rizzo Baroni, 2018). Soybean stands out not only for its nutritional value, but also for the health benefits it provides (i.e., lowering of blood cholesterol level, increasing of bone density, and minimization of the risk of cancer development) (Messina & Messina, 2010).

The rising demand for plant-based foods is strengthening the growth of the soy food market across the globe. In fact, the global soy food market was worth US$ 38.7 billion in 2018 and is expected to reach the value of 53.1 US$ billion by 2024, registering a compound annual growth rate (CAGR) of around 5% during 2019-2024. In general, soybeans with a high protein content are chosen for the preparation of soymilk,

compared to those utilized for oil extraction.

During soymilk and tofu production, soybeans are milled under hot (>80 °C) and alkaline (pH 8.0) conditions to guarantee a protein solubilization as well as to inactivate trypsin inhibitors and the enzyme lipoxygenase (Vishwanathan, Singh, & Subramanian, 2011). Insoluble materials are removed from the slurry using centrifugation: this process results in the production of a soy base, which is the precursor of soymilk or tofu, and a solid by-product generally named with the Japanese word okara, which contains about 50% dietary fibers, 25% protein, 10% lipid, and other nutrients (Colletti, Attrovio, Boffa, Mantegna, & Cravotto, 2020; Li, Qiao, & Lu, 2012). Due to this interesting composition, okara byproducts have been already assessed for the extraction of fibers (Fan, Chang, Lin, Zhao, Zhang, Li, et al., 2020) and polysaccharides (Villanueva-Suárez, Pérez-Cózar, & Redondo-Cuenca, 2013) as well as for the manufacture of snack (Katayama & Wilson, 2008). Although it would be certainly advisable to extract the residual proteins for human use, this is impaired by the okara structure. A specific sustainable protein extraction methodology is thus required to reach this goal.

The ultrasound technology has been widely studied in the food industry for aiding the extraction of components of interest from plant starting materials (Chemat, Zill e, & Khan, 2011; Esclapez, Garcia-Perez, Mulet, & Carcel, 2011; Shirsath, Sonawane, & Gogate, 2012). The ultrasound technology shows promise as a green technology within the field of extraction, reasons including reductions in extraction times, solvent use, and more effective energy utilization, as well as improvement of the quality of the product (Chemat, Rombaut, Sicaire, Meullemiestre, Fabiano-Tixier, & Abert-Vian, 2017; Jacotet-Navarro et al., 2016; Sicaire, Vian, Fine, Carre, Tostain, & Chemat, 2016). The success of ultrasound is attributed to the cavitation phenomenon. In fact, upon asymmetric bubble collapse, liquid jets are formed that can disrupt cells upon contact with cell walls (Li, Pordesimo, & Weiss, 2004), causing the release of intracellular compounds.

Within the storage cells of soybean, protein is organized in 5-20 μm protein bodies, surrounded by a cytoplasmic network containing oil bodies in the size range of 0.2-0.5

μm stabilized by proteinaceous oleosins (Rosenthal, Pyle, & Niranjan, 1998).

Different methods are applied for the protein extraction of soybean and okara. More specifically, the extraction of proteins is carried out using acid and alkaline conditions (Ma, Liu, Kwok, & Kwok, 1996; Vishwanathan, Govindaraju, Singh, & Subramanian, 2011), enzyme assisted extractions (Fischer, Kofod, Schols, Piersma, Gruppen, & Voragen, 2001; Sari, Bruins, & Sanders, 2013), and more recently with the aid of ultrasonication technology (Chemat et al., 2017), which is nevertheless still rarely employed. The complexity of soybean cellular microstructure influences the protein extraction in normal conditions, but thanks to the cavitation phenomenon, an improvement of extraction yields from hexane-defatted soy flakes is achievable at lab-scale. Protein functionality improvement from soybean protein isolate and concentrates has also been reported with positive results in protein solubility and particle size reduction (Tian et al., 2020). In addition, the ultrasound treatment significantly increases the solubility of isolated soy proteins in water (Jambrak, Lelas, Mason, Kresic, & Badanjak, 2009; Sun et al., 2014).

In light with these observations, this study is aimed at assessing the physicochemical and conformational changes of ultrasound-driven extracted proteins from soybean okara processing materials. To achieve this goal, the protein extraction was carried out using ultrasound at 20, 60, and 80 °C obtaining the samples named SoK_U20, SoK_U60, and SoK_U80, respectively. The high temperature limit was chosen taking into account that temperatures up to 80 °C are used in the processes where okara is produced as byproduct. The assessment of the changes in the protein profile, concentration, secondary and tertiary structure, hydrophobicity, solubility, antioxidant capacity, rheological and morphological features was performed in comparison with untreated soy okara protein (SoK_nU). Herein, a combination of different techniques and an integrated strategy was applied in order to fostering the okara protein samples obtained after ultrasound extraction as valuable and high-quality products for new applications and to providing, therefore, a more sustainable way to solve the environmental criticism related to the huge quantities of okara produced annually, which pose a significant disposal problem.

II-2. Material and methods

II-2.1 Reagents

All chemicals and reagents were of analytical grade. LC-grade H_2O (18 MΩ cm) was prepared with a Milli-Q H_2O purification system (Millipore, Bedford, MA, USA). Acetonitrile (ACN), tris(hydroxymethyl)aminomethane (Tris-HCl), hydrochloric acid (HCl), 2-iodoacetamide (IAM), 1,4-dithiothreitol (DTT), NaCl, 3 kDa molecular weight cut-off membranes (Amicon® Ultra, Millipore, Billerica, MA, USA), 5,5-dithio-bis-2-nitrobenzoic acid (DTNB), ethylenediaminetetraacetic acid (EDTA) 2,2-diphenyl-1-picrylhydrazyl (DPPH), phytic acid (PA), $FeCl_3.6H_2O$, sulfosalicylic acid and trypsin from bovine pancreas (T1426, lyophilized powder, ≥10,000 units/mg protein) were from Sigma-Aldrich (St. Louis, MO, USA). Bovine serum albumin (BSA), Mini-Protean apparatus, precision plus protein standards, Bradford reagent, and Coomassie Blue G-250 were purchased from Bio-Rad (Hercules, CA, USA).

II-2.2 Samples and ultrasonic system

The experimental investigations were performed with an ultrasonic batch system (TC 10, BSONIC GmbH, Germany) that allows power inputs of up to 4 kW at a frequency of 18 kHz and an oscillation amplitude of 45 – 60 µm. The probe tip has a diameter of 41.75 mm. Regulation of power input and recording of process parameters is done via PC. Berief Food GmbH, Germany, supplies the soy okara samples as frozen 3 kg units directly from the production process. For the liquid mixture of soy okara, tap water is used.

II-2.3 Ultrasound-assisted processing of okara

Experiments of ultrasound-assisted extraction of proteins were performed at Fraunhofer UMSICHT, Germany, using the materials and ultrasonic system mentioned above. A defined ratio of 1:2.5 of soy okara and water was heated up to the experimental temperature of 20 °C (SoK_U20), 60 °C (SoK_U60), and 80 °C (SoK_U80), respectively, with continuous stirring. The ratio of 1:2.5 has been defined in previous

experimental investigations, which are part of a separate publication (Chemat et al., 2017). This ratio was selected as optimum concerning an effective protein extraction, the disintegration of okara, and the minimization of total treatment volume. The pH of the mixture was 6.5 (± 0.14) at 20 °C. The ultrasound treatment was controlled and measured via PC and was conducted by immerging the ultrasound sonotrode into the beaker containing the samples (5 L). Ultrasound parameters of power input (4 kW), correlating oscillation amplitude (μm), and the treatment time of 0.5 min were fixed. Hence, the total energy input for all samples was 24 kJ/ L. These ultrasound treatment parameters have been defined ahead as part of a separate publication (Chemat et al., 2017) showing that they allow the best protein extraction yield. Directly after the ultrasound treatment, the processed samples were centrifuged at 12,298 g for 15 min (Avanti JXN-26, Beckmann Coulter) to separate solid and liquid fractions. Both fractions were separately freeze-dried (Alpha 2–4 LSC plus, Christ) in order to allow a simpler storage and delivery of the samples. The protein extraction yields were determined bu kjeldahl analysis.

II-2.4 Soy okara protein extraction

Proteins from sonicated okara were extracted by modifying a method previously described (Aiello, Lammi, Boschin, Zanoni, & Arnoldi, 2017). Briefly 1 g of each sample was suspended in 10 mL of 100 mM Tris−HCl/0.5 M NaCl buffer at pH 8.0. The extraction was performed in a batch at 4 °C overnight. The solid residue was eliminated by centrifugation at 10,000 rpm for 30 min at 4 °C. The protein content of each sample was assessed according to Bradford method using BSA as standard for calibration curve.

II-2.5 Molecular weight distribution and MS analysis

The molecular weight distribution of untreated and sonicated okara proteins was determined using reducing dodecyl sulfate-polyacrylamide gel electrophoresis (SDS-PAGE). The protein samples were prepared by mixing 15 μL of each sample with 10

μL of Laemmli buffer (4% SDS, 20% glycerol, 10%, 0.004% bromophenol blue, and 0.125 M Tris–HCl, pH 6.8). The mixtures were boiled for 5 min at 95 °C, and 25 μL of the mixture was loaded into each lane. The gel was composed of a 4% polyacrylamide stacking gel over a 12% resolving polyacrylamide gel. The electrophoresis was conducted at 100 V until the dye front reached the gel bottom. Staining was performed with colloidal Coomassie Blue and destaining with 7% (v/v) acetic acid in water. The gel image was acquired by using the Bio-Rad GS800 densitometer and analyzed by using the software quantity One 1-D. Gel bands for the SoK_U20, SoK_U60, and SoK_U80 lane were sliced, digested with trypsin according to a preceding paper (Aiello et al., 2016), and analyzed by nano-HPLC-CHIP-ESI Ion Trap using the same experimental conditions previously reported (Aiello et al., 2017). The MS data were analyzed by Spectrum Mill Proteomics Workbench (Rev B.04.00, Agilent), consulting the Glycine max (251326 entries) protein sequences database downloaded from the National Center for Biotechnology Information (NCBI) (Lammi, Arnoldi, & Aiello, 2019). For MS/MS search the oxidation of methionine residues was set as variable modifications.

II-2.6 Peptidomic profiles

The peptidomic profiles of the samples were obtained after ultrafiltration through 3 kDa molecular eight cut-off membranes (Amicon® Ultra, Millipore, Billerica, MA, USA). The recovered peptides were analyzed by nano LC–MS/MS analysis according to the chromatographic and MS condition reported in the material and methods. Figure II-S1 shows the MSn TIC of Sok_U80, Sok_U60, Sok_U20. The MS data were analyzed by Spectrum Mill Proteomics Workbench (Rev B.04.00, Agilent), consulting the Glycine max (251326 entries) protein sequences database downloaded from the National Center for Biotechnology Information (NCBI) (Lammi, Arnoldi, & Aiello, 2019). For MS/MS analysis and searching against a polypeptide sequence database, a non-enzyme specific search considering all of the possible proteolytic cleavages was selected as criteria.

II-2.7 Protein solubility and water binding capacity

Protein solubility was determined according to a method described previously (Hu et al., 2015) with some slight modifications. Each sonicated sample (1 g) was dispersed into 9 mL deionized water to obtain the protein solution (1 wt%). Protein solutions were stirred for 2 h and centrifuged at 10,000 rpm for 20 min at 4 °C. The protein concentration in the samples before centrifugation and in the supernatants after centrifugation was determined according to the Bradford assay using BSA as a standard. The protein solubility was expressed as grams of soluble protein per 100 g of protein. All determinations were conducted in triplicate. The water binding capacity (WBC) was assessed according to a literature method with slight modifications (Malomo, He, & Aluko, 2014). Briefly, 1 g of sample was dispersed in 10 mL distilled water in a 15 mL pre-weighed centrifuge tube. The dispersions were stirred for 30 min and then centrifuged at 7000 g for 25 min at room temperature. The supernatant was discarded, and the tubes was weighed to determine the amount of retained water per gram of sample.

II-2.8 Free sulfhydryl group determination

The sulfhydryl groups at the surface of the proteins were determined according to a method described previously (Zhao, Liu, Zhao, Ren, & Yang, 2011) with some modification. Briefly, Ellman's reagent was prepared as follows: 4 mg of DTNB reagent were added to 1 mL of Tris-glycine buffer (0.086M Tris, 0.09M glycine, 4mM EDTA, pH7.0). SoK_U20, SoK_U60, SoK_U80 and SoK_nU protein solutions were diluted in Tris-glycine buffer (w/v 0.15%). Then 5 μL of Ellman's reagent was added into 200 μL of protein suspension. The resultant protein suspensions were incubated at 25±1 °C for 15 min under shaking and then centrifuged at 10,000 g for 10 min at room temperature. The absorbance was then recorded at 412 nm. A buffer solution without proteins was used as a reagent blank.

II-2.9 Intrinsic fluorescence spectroscopy

The intrinsic fluorescence spectrum of each sample was obtained using a fluorescence spectrophotometer (Synergy H1, Biotek). The samples were diluted in phosphate-buffered saline (PBS, 10 mM, pH 7.0) in order to reach the equal concentration of 0.05 mg/ml and transferred in Greiner UV-Star® 96 well plates flat bottom clear cyclic olefin copolymer (COC) wells (cycloolefine). The excitation wavelength was set as 280 nm, while the excitation and emission slit widths were each set as 5 nm. The emission wavelength range was set up from 300 nm to 450 nm and the scanning speed was 10 nm/s.

II-2.10 Circular dichroism (CD) spectroscopy

CD spectra were recorded in continuous scanning mode (190-300 nm) at 25 °C using Jasco J-810 (Jasco Corp., Tokyo, Japan) spectropolarimeter. All spectra were collected using a 1 mm path- length quartz cell and averaged over three accumulations (speed: 10 nm min-1). A reference spectrum of distilled water was recorded and subtracted from each spectrum. The estimation of the peptide secondary structure was achieved by using a literature method (Raussens, Ruysschaert, & Goormaghtigh, 2003).

II-2.11 Water contact angle measurements

Contact angle measurements were performed on a Krüss Easy Drop instrument using freshly distilled water passed through a milliQ apparatus. Sample powders were deposited on glass slides according to a literature procedure (Nowak, Combes, Stitt, & Pacek, 2013). An 8 µL drop was produced and placed on the surface. Videos with 25 fps resolution were recorded. For each sample 2 to 3 measurements were performed, determining the first measurable contact angle and the total time needed for the droplet complete absorption.

II-2.12 Rheological test

Rheological properties of soy okara proteins were tested using a stress/rate-controlled

Kinexus DSR Rheometer (Netzsch) equipped with a parallel plate geometry (acrylic diameter, 20 mm; gap, 34 μm). All measurements were obtained at 25 °C using a Peltier cell in the lower plate of the instrument to control the temperature during each test. The viscosity of okara proteins was measured using a flow step program, at increasing shear rate (0.01-1,000 s^{-1}), to evaluate their non- Newtonian behavior. Afterwards, to evaluate the storage (G') and loss moduli (G''), frequency sweep experiments were recorded as a function of angular frequency (0.1-100 Hz) at a fixed strain of 0.1%. Each experiment was performed in triplicate. Data were processed using Origin™ 8 software.

II-2.13 Atomic force microscopy (AFM)

AFM measurements were captured in tapping mode by using a Tosca system (Anton Paar) using single-beam silicon cantilever probes (Bruker RFESP-75 0.01–0.025 Ohm-cm Antimony (n) doped Si, cantilever f_0, resonance frequency 75 kHz, constant force 3 N m^{-1}). AFM images were taken by depositing 3 μL solutions (final concentration of 0.1 mg ml-1) onto freshly cleaved mica. The samples were kept on the mica for 5 min; subsequently they were rinsed with distilled water to remove loosely bound peptides, and then dried under ambient conditions for 24 h. The morphological parameter analysis of the AFM data was performed using the Matlab-based open- source software FiberApp.

II-2.14 Scanning electron microscopy (SEM)

Scanning electron microscopy (SEM) was performed with a Vega-3 microscope from TESCAN GmbH, Germany, at 20 kV acceleration voltage under high vacuum. To guarantee a high resolution the images were taken with a secondary-electron detector (SE). Freeze-dried samples were fixed on a special two-sided adhesive tape and coated by a 10 nm gold surface in order to prevent electrostatic charging.

II-2.15 Determination of the scavenging activity by the DPPH assay

The DPPH assay to determine the antioxidant activity in vitro was performed by a

standard method with slight modifications (Lammi et al., 2020). The DPPH solution (45 µL, 0.0125 mM in methanol) was added to 15 µL of each sample at the concentration of 100 µg/mL. The reaction for scavenging the DPPH radicals was performed in the dark at room temperature (RT) and the absorbance was measured at 520 nm after 30 min incubation.

II-2.16 Phytic acid (PA) determination

Lyophilized samples were used for phytic acid determination, following the modified colorimetric method (Gao et al., 2007). Aqueous phytic acid (PA) standards in concentrations of 0–100 µg/mL were used for quantification. Aliquots of 100 µL of samples and standards were diluted 25 times with 2.4 mL of H_2O; 600 µL of the diluted samples and standards were combined with 200 µL of modified Wade reagent (0.03% of $FeCl_3$ $6H_2O$ and 0.3% of sulfosalicylic acid), and the absorbance was measured at 500 nm.

II-2.17 Statistic analysis

Data are presented as mean ± s.d. using GraphPad Prism 8 (GraphPad, La Jolla, CA, USA). Statistical analyses were carried out by t student test and ANOVA. P-values < 0.05 were considered to be significant.

II-3. Results and discussions

II-3.1 Effect of ultrasound treatments on the morphology of soy cells in okara

Proteins are largely responsible for the main features of most foods, since their composition influences nutritional, rheological, and sensory properties. The new process may induce chemical modifications in the protein, impacting on the nutritional and technological features of the final products. The experimental setup used for the ultrasound-assisted processing of okara is illustrated in **Figure II-S1**, while the features of obtained samples are reported in **Table I-1**. Low ultrasound frequency at 18 kHz was used in order to guarantee an effective acoustic cavitation. In case of low frequencies,

the periods of positive and negative pressure changes within the mechanical ultrasound wave are longer. Therefore, the growth process of the cavitation bubble is more effective and higher bubble diameters can occur. Thus, the bubble implosion takes place with higher forces and results in a more disruptive cell disintegration in comparison to higher frequencies (Chemat et al., 2017). Accordingly, the oscillation amplitude is responsible for the net pressure change within the sonicated liquid. With higher amplitude, the pressure difference is higher and acoustic cavitation bubbles are likely to increase in size. Therefore, a frequency of 18–22 kHz at a maxium oscillation amplitude is favorable for ultrasound desintegration and defines the ultrasound power input. Energy input is the product of power input and treatment time in relation to the sonicated volume. High energy input correlates with a high rate of disintegrated cells. However, treatment time should be minimized in order be able to convert the disintegration process into an industrial scale. Previous investigations that are part of a separate publication have shown that the selected ultrasound conditions guarantee an optimum of protein extraction and feasibility for potential industrial scale-up.

Table II-1. Sample description

Sample ID	T (°C)	Ultrasound	Treatment Time (min)	Energy input (kJ/L)
SoK_nU	20	-	-	-
SoK_U20	20	4.0 kW	0,5	24
SoK_U60	60	4.0 kW	0,5	24
SoK_U80	80	4.0 kW	0,5	24

In order to evaluate the effect of ultrasonication coupled to the temperature gradient on the structure and morphology of soybean cells, scanning electron microscope analysis was carried out. **Figure II-1** shows that there are clear differences among the structures of the untreated and ultrasound treated samples. While both disrupted and intact cells co-exist in the sample treated with ultrasound at 20 °C (SoK_U20), the treatment at 60 °C (SoK_U60) and 80 °C (SoK_U80) produce visible disruptions of the cell structures. Since palisade-like cell structures contain a significant amount of protein bodies, an effective disruption of cells is indispensable for an efficient protein recovery

(the protein extraction yields from SoK_U80, SoK_U60, and SoK_U20 were 23.5%, 14.9%, and 10.2%, respectively)

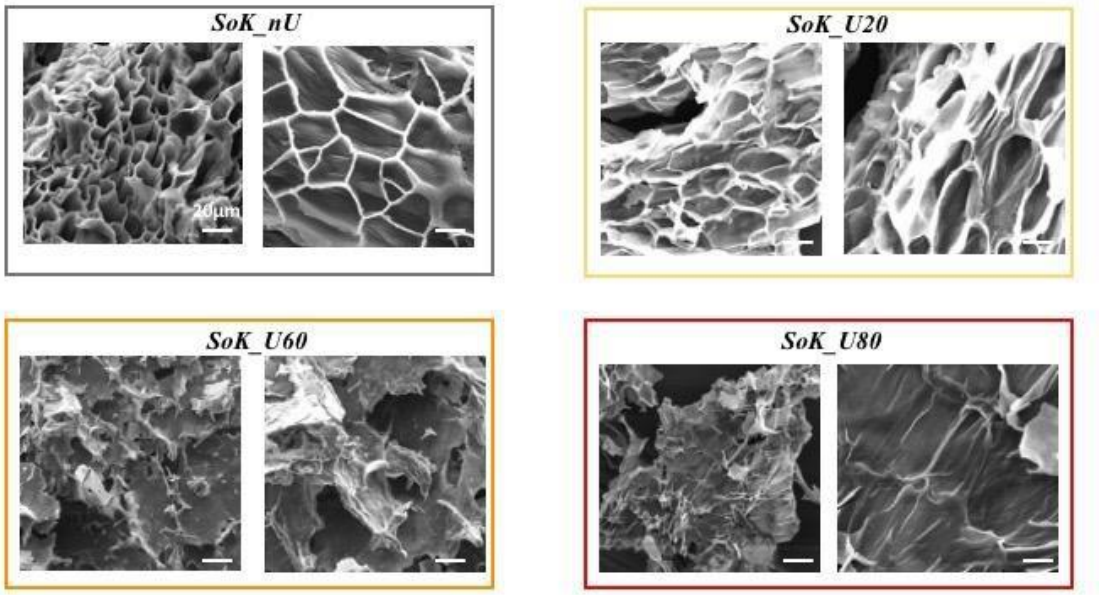

Figure II-1 SEM of protein okara obtained with and without the ultrasound treatments. *Scheme 1600*x, r.: 4000x), Sok_U20 (ultrasonicated at 20°C, magn.: l.: 800x, r.: 1600x), Sok_U60 (ultrasonicated at 60°C, magn.: l.: 160x, r.: 400x) and Sok_U80 (ultrasonicated at 80°C, magn.: l.: 400x, r.: 1600x).

II-3.2 Effect of ultrasound treatments on the molecular weight distribution of extracted proteins

The effects of ultrasound treatments on the molecular properties of extracted proteins were explored by evaluating their molecular weight profile using reducing electrophoresis. **Figure II-2A** shows the SDS-PAGE profile of the untreated control and sonicated protein samples. Under reducing conditions, four intense bands were observed for all the samples, with molecular weight ranges of 70-100 kDa, 40-55 kDa, 25-30 kDa, ~18 kDa, respectively. The identified proteins for each band are reported in **Table II-S1**. Specifically, alpha and beta-subunits of conglycinin were identified at 70 kDa and 50 kDa, respectively. These findings are in line with those reported by other authors according to which no changes in the molecular weight profiles of squid mantle

proteins (Higuera- Barraza, Torres-Arreola, Ezquerra-Brauer, Cinco-Moroyoqui, Figueroa, & Marquez-Rios, 2017), walnut protein isolate (Zhu et al., 2018), and soybean proteins were observed after sonication (Hu, Li-Chan, Wan, Tian, & Pan, 2013). The intensity of the electrophoretic bands of sonicated samples at different temperature was greater than that of the untreated sample, which may be attributed to the greater water-solubility of the sonicated proteins (see paragraph 3.6). This evidence was confirmed also by Bradford assay according to which the detected amounts of protein were 4.31 ± 0.03, 3.22 ± 0.01, 2.85 ± 0.1, and 0.36 ± 0.04 mg/mL for SoK_80, SoK_60, SoK_20 and SoK_nU, respectively. Therefore, the ultrasound process performed at room temperature (SoK_U20) leads to an improvement of protein extraction yield by up to 6.9-fold versus SoK_nU (**Figure II-2B**). This result is in agreement with other studies that have shown that ultrasound improves protein extraction yield from soybeans in a lab-scale system (Preece, Hooshyar, Krijgsman, Fryer, & Zuidam, 2017). The study on the impact of the temperature on the ultrasound aided protein extraction indicated that in SoK_U60 and SoK_U80 the protein extraction yields were increased by 13.0% and 51.2%, respectively, vs SoK_U20. This high recovery yield was in agreement with SEM investigation that highlighted the progressive destruction of the cell structure in ultrasound treated samples as a function of the temperature leading to an improvement of released proteins.

After 3 kDa cut-off filtration, each sample was submitted to a peptidomic investigation. The MS/MS analysis revealed that the ultrasonication induced a progressively greater peptide release that proportional to the increasing temperature (**Figure II-S2**). In agreement with the degree of hydrolysis (data not shown), the peptide sequences identified after ultrasound treatments increased also as a function of the temperature (**Table II-S2**): in fact, 24, 30, and 37 different peptides were identified in Sok_U20, Sok_U60, and Sok_U80 samples, respectively. Interestingly, in all samples the peptide lengths were similar, ranging from 6 to 29 amino acid residues, and the pI values were comprised between 3.8 and 9.9.

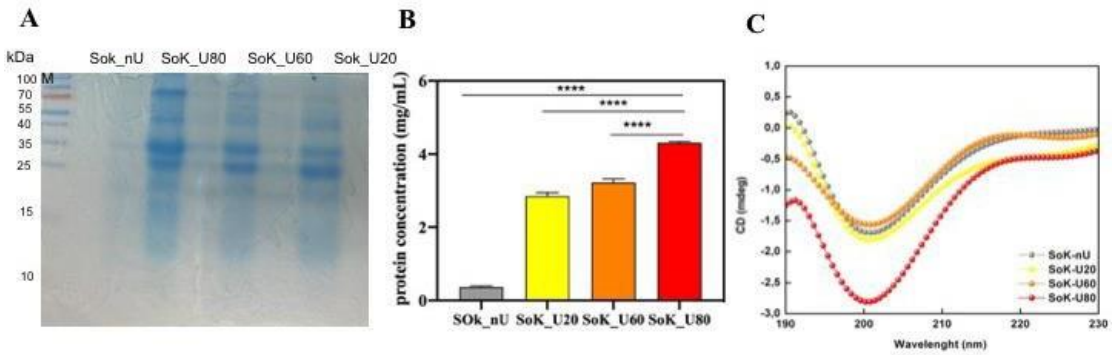

Figure II-2 Protein profile, concentration, and CD spectra. A) Reduced SDS-PAGE protein profile of ultrasonicated and untreated proteins (M, pre-stained molecular marker). B) Determination of the protein concentration by the Bradford assay. C) CD spectra of okara proteins. SoK_nU (control, untreated), Sok_U20 (ultrasonicated at 20°C), Sok_U60 (ultrasonicated at 60°C), and Sok_U80 (ultrasonicated at 80°C).

II-3.3 Circular dichroism (CD) of okara proteins

To investigate the effect of ultrasound treatment and temperature combination on the secondary structure of extracted proteins, CD spectra in the far UV region of 190-230 were recorded (**Figure II-2C**). One positive and one negative Cotton effect at 193 and 200 nm, respectively, were observed for SoK_nU, suggesting an α-helix rich conformation. Increasing the temperature of the ultrasound treatment from 20 and 60 °C, the intensity of the Cotton effect peaks was greatly decreased, suggesting a structural transition from α-helix into β-sheet rich conformations. The latter conformation was clearly visible in the SoK_U80 sample, where one maximum peak at 195 nm and one minimum peak at 200 nm were observed, demonstrating a redshift of the maximum peak, thus indicating a highly ordered β-sheet rich structures after heating the sample at 80 °C (**Figure II-2C**).

To gain further information about the secondary structure of soybean okara proteins, the Raussens and coworkers' tool was applied (Raussens et al., 2003). Results, summarized in **Table II-2**, suggest that a reduction of the percentage of α-helices and an improvement of β-sheet were obtained for the proteins after ultrasound treatment (Sok_U20) vs control sample (SoK_nU). Clearly the increase of temperature coupled

to ultrasonication induced a significant secondary structure variation. Overall, reductions of α-helices up to 11.3% and -1.1% at 60 and 80°C, respectively vs SoK_U20 (26.7%), were observed. In addition, increases of β-sheet up to 33.2% and 37.7% at 60 and 80 °C, respectively, vs SoK_U20 (28.1%) were observed. An overall slight improvement of random coil was also observed for each experimental condition.

Table II-2 Percentage of secondary structure composition of soybean okara proteins

Secondary Structure	SoK_nU	SoK_U20	SoK_U60	SoK_U80
Helix (%)	**32.4**	**26.7**	**11.3**	**1.1**
Beta (%)	**18.5**	**28.1**	**33.2**	**37.7**
Turn (%)	**12.5**	**12.5**	**12.5**	**12.5**
Random (%)	**37.6**	**38.2**	**39.5**	**42.0**

II-3.4 Free-sulfhydryl group (SH) content

Sulfhydryl groups (SH) and disulfide bonds (S-S) are important chemical bonds that stabilize the conformation of protein molecules and play very important roles in functional properties, such as foaming and emulsifying abilities. The measurement of the content of free-SH groups located on the surface of okara proteins was used to provide further insights into the ability of sonication to cause changes in the protein tertiary structure.

Figure II-3A shows significant reductions in free SH content of the extracted proteins after sonication. In details, the free SH contents of SoK_nU was 59.4±3.1 μmol/g and the ultrasonication at 20 °C led to a reduction of the free SH content up to 7.4±0.6 μmol/g. These findings clearly indicate that the ultrasonication determines a significant effect on the structure of the protein with a reduction of the exposition of the hydrophobic amino acids containing thiol groups, probably due to the formation of intermolecular disulfide bonds (S-S), which modulates the folding of the extracted proteins. Moreover, the findings suggest that an increment of the temperature induced an additional decrease of the free SH content by 28.4% and 60.8% for SoK_U60 (5.3±0.8 μmol/g) and SoK_U80 (2.9±0.6 μmol/g), respectively, versus SoK_U20.

These data underline the effects of two different factors: i) the ultrasonication process and ii) the increasing temperature that induces extensive modifications of the protein structures. the ultrasonication process and the increasing temperature that induces extensive modifications of the protein structures. This phenomenon may be possibly due to the generation of radical species during the sonication process, which may oxidize susceptible functional groups such the thiol group, leading to the formation of intermolecular disulfide bonds (S-S). Indeed, the thermolysis induced by cavitation may produce hydroxyl radicals and hydrogen atoms that can induce the formation of radical species (Gulseren, Guzey, Bruce, & Weiss, 2007). However, other researchers have reported that the sonication can increase the free SH content of egg and soy proteins (Xiong et al., 2016). The protein type, the solutions, and the processing conditions may produce these different outcomes.

II-3.5 Intrinsic fluorescence

More information regarding the effect of ultrasound at different temperature on the protein structural changes were obtained by applying intrinsic fluorescence spectroscopy, a technique that can be used to monitor alterations in protein tertiary structure due to the sensitivity of the protein amino acid residues to the polarity of the microenvironment (Vera, Valenzuela, Yazdani-Pedram, Tapia, & Abugoch, 2019). Since the intrinsic fluorescence is mainly due to the presence of tryptophan (Trp) and tyrosine (Tyr) residues, which have strong fluorescence quantum yield, after excitation at 280 nm, the fluorescence spectrum of each sample was recorded in the wavelength range 310-450 nm. An improvement of fluorescence intensity was detected as a function of the temperature reached during the ultrasound-assisted protein extraction from okara (**Figure II-3B**). The SoK_U20 had a significant 5.7% increase of fluorescence intensities compared to the untreated sample (SoK_nU). In SoK_U60 and SoK_U80 the fluorescent intensity was increased by 43.5% and 103.2%, respectively, compared to SoK_U20. The increased fluorescence intensity is correlated to an increase in the number of exposed Trp residues. Similar trends have been observed also in

soybean and chicken plasma proteins submitted to ultrasound extraction (Tian et al., 2020; Zou et al., 2019). In particular, a recent paper has shown that in soybean all sonication conditions induce a significant 13-41% increase of the fluorescence intensities compared to the control without ultrasound treatments (Tian et al., 2020).
The changes of protein tertiary structure may be determined by monitoring fluorescence intensity at the maximum wavelength (λ_{max}) (Zou et al., 2018). In these experiments, SoK_U60 reached the λ_{max} at 332 nm, whereas all the other samples displayed a λ_{max} at 340 nm. Trp resides can be classified into three types based on their different λ_{max} values [39]: i) buried Trp residue at λ_{max} between 330 and 332 nm, ii) exposed Trp with limited water contact at λ_{max} between 340 and 342 nm, and iii) exposed Trp residue at λ_{max} between 350 and 353 nm. Hence, Trp is exposed with limited water contact in SoK_nU, SoK_U20, and SoK_U80, whereas it is buried in SoK_U60. The slight shift in λ_{max} from 332 nm to 340 nm of SoK_U60 indicates a different behavior of this sample, since the Trp residues have shifted from being exposed with limited water contact to be buried.

II-3.6 Protein hydrophobicity after ultrasound treatments

In order to assess the variation of the hydrophobicity, the water contact angle was measured for each sample (**Figure II-3C-D**). Briefly, sample powders were deposited on glass slides and a drop of water was produced and fell on the surface. As shown in the videos (see supporting information), the proteins extracted with ultrasound coupled to the temperature gradient have an improved ability to absorb the water drop in comparison with the untreated sample (SoK_nU). Moreover, SoK_nU demonstrates a slower ability to absorb water and an improved ability to swell. On the contrary, SoK_U20, SoK_U60, and SoK_U80 absorbed the water drop faster without swelling **(Figure II-3C-D**) suggesting an improvement of their wettability. Precisely, the water contact angle (θ) of SoK_U20, SoK_U60, and SoK_U80 were the 42.7 ± 2.1%, 67.2 ± 4.5% and 68.9 ± 5.2%, respectively, versus SoK_nU (**Figure II-3C**). Therefore, all values were smaller than that of the untreated sample, but slight improvements were detected increasing the temperature of the ultrasound treatment. Notably, the water drop

was absorbed in 16 s by SoK_nU, whereas in 0.6 s, 0.9 s, and 1.2 s by SoK_U20, SoK_U60 and SoK_ U80, respectively (**Figure II-3D**).

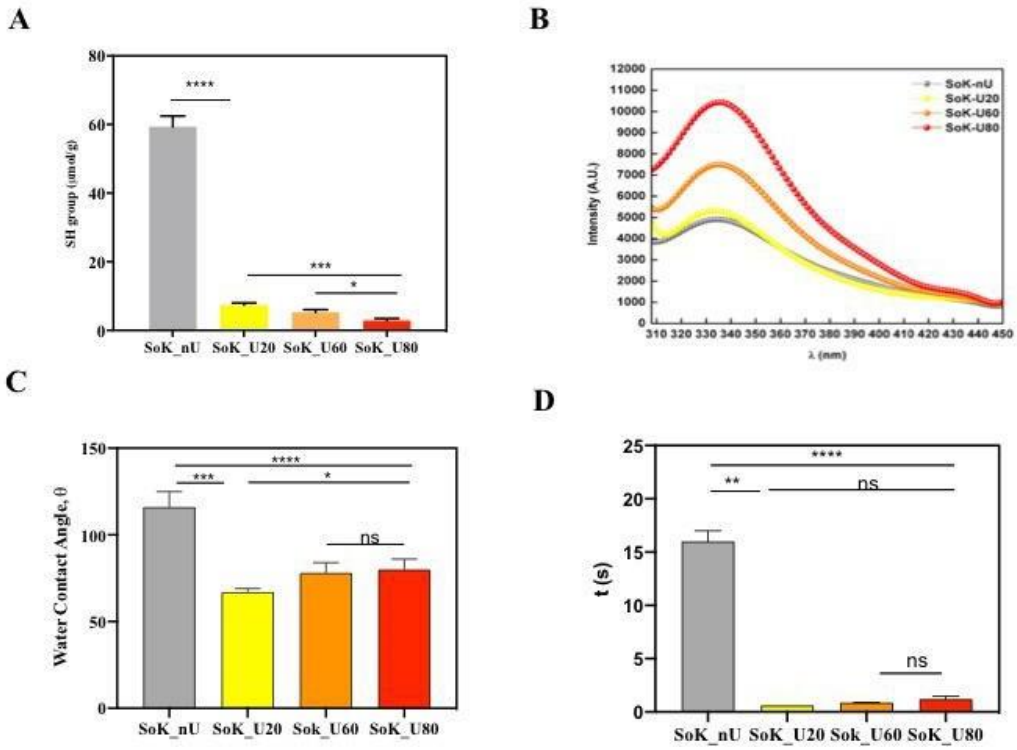

Figure II-3 Tertiary structure analysis. A) Free SH group determination. B) Intrinsic fluorescence signal detection. C) Water contact angle. D) Time (s) of water absorption of proteins extracted with and without ultrasound and temperature treatments. SoK_nU (control, untreated), Sok_U80 701 (ultrasonicated at 80 °C), Sok_U60 (ultrasonicated at 60 °C), and Sok_U20 (ultrasonicated at 20 °C). Statistical analysis was performed by one-way ANOVA (*) $p<0.5$, (**) $p<0.01$, (***) $p<0.001$, and (****) $p<0.0001$, ns: not significant. The data are represented as the means ± s.d. of three independent experiments.

II-3.7 Morphological analysis

To investigate the effect of the ultrasound and heat treatments on the extracted proteins, the morphologies of the samples were studied by AFM (**Figure II-4A**). Well-defined single round structures were observed for SoK_nU alone, with an average height of 1.6 ± 0.9 nm (**Figure II-S2**), and no obvious changes of aggregates were found in SoK_U20 (2.0 ± 1.7 nm). Instead, SoK_U60 showed unevenly distributed aggregated structures, with a slightly increased height compared to SoK_nU and SoK_U20, namely

5.6 ± 1.7 nm. Conversely, in sample SoK_U80 a significant morphological transition from well-defined single round structures to highly aggregated structures was observed. The size of the structures was increased compared to that of SoK_nU alone and SoK_U20, with a height of 47 ± 10.9 nm, indicating that the ultrasound coupled with an 80 °C temperature strongly contributed to the formation of these large aggregates. These data are in good agreement with those obtained through the turbidity assay (**Figure II-4B**), where an increase in turbidity values was observed following heating of the samples, suggesting that the higher temperature led to a significant increase in the size of the protein aggregates.

In addition, rheological experiments were performed to investigate the storage (G') and loss (G") moduli in the function of angular frequency (1–100 Hz). All samples exhibited a G'/G" profile almost unchanged along the tested frequency range (**Figure II-4C**). However, the ultrasound treated samples displayed higher G' values (≈25 Pa) compared to the untreated sample (SoK_nU, G' = 0.2 Pa); this behavior may indicate different networks of nano/microstructures inside the extracted protein, thus potentially influencing their mechanical properties.

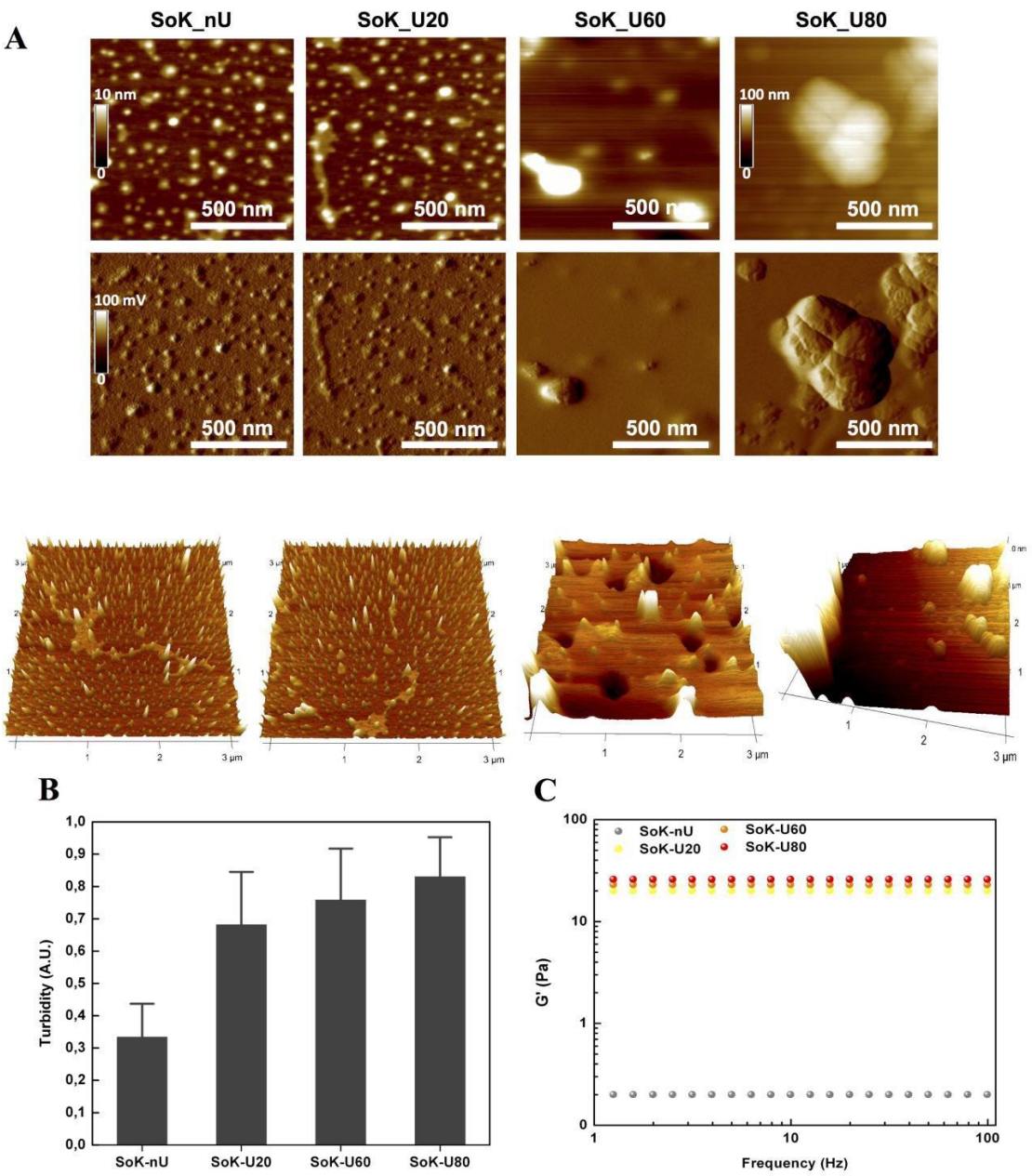

Figure II-4 Morphological property. A) Morphological organization of extracted proteins. B) Turbidity of okara proteins measured at 405 nm. C) Frequency-depended oscillatory rheology (1-100 Hz) of extracted proteins at fixed strain 0.1%. SoK_nU (control, untreated), Sok_U80 (ultrasonicated at 80°C), Sok_U60 (ultrasonicated at 60°C), and Sok_U20 (ultrasonicated at 20°C)

II-3.8 Protein solubility, water binding capacity (WBC), and viscosity of extracted proteins

The ultrasonication process affected also the protein solubility, which represents a good index of protein functionality (Arzeni, Martinez, Zema, Arias, Perez, & Pilosof, 2012).

This feature reflects protein denaturation and aggregation, which modulate many important functional properties, such as emulsification, solubility, gelation and viscosity (Arzeni et al., 2012). The solubility of control and treated samples by ultrasound is shown in **Figure II-5A**. The protein solubility of SoK_U20 is 6.5- fold more (38.2 ± 1.3 mg protein/g biomass SoK_U20) than the untreated sample (5.9 ± 0.1 mg protein/g biomass). In addition, the temperature during the ultrasound process proportionally increases the protein solubility that for SoK_U60 (59.6 ± 1.2 mg protein/g biomass) and SoK_U80 (86.1±1.1 mg protein/g biomass) were greater by 1.5 and 2.3 folds, respectively, than that of SoK_U20 (**Figure II-5A**). This evidence is supported by the fact the during ultrasonication the cavitation bubbles induce the unfolding of proteins causing an increased exposure of hydrophilic amino acid residues towards water thus contributing to the formation of soluble protein aggregates (Jiang et al., 2014). In addition, the increase of peptides within the samples may also contribute to the improvement of solubility.

An important property of proteins is the ability to interact with water, which influences their propensity to form gels, to dissolve, to swell, and to act as stabilizer in emulsions (Kinsella, 1982). The measurement of their WBC is a conventional way to describe the interaction of proteins with water. Therefore, in order to evaluate the effect on WBC, dedicated experiments were carried out (**Figure II-5B**). The WBC of the proteins obtained with the classical extraction method (SoK_nU) was 7.2 ± 0.01 g H_2O/g protein (**Figure II-5B**), in line with a previous study, which compared the WBC of soybean, pea, and lupin isolated proteins, reporting that the specific WBC of soybean proteins is 9.2 g H_2O/g protein respectively (Peters, Vergeldt, Boom, & van der Goot, 2017). Moreover, the ultrasonication at 20 °C (SoK_U20) did not produce a significant effect on the WBC (7.0 ± 0.01 g H_2O/g protein). On the contrary, a significant variation of WBC was observed after ultrasound extraction at 60 and 80 °C: the WBC's of SoK_U60 and SoK_U80 were 18±0.5% and 31.4±0.8% higher than SoK_U20, respectively (**Figure II-5B**).

In light of these observations, rheology was employed to evaluate the viscous properties: all samples displayed a non-Newtonian shear-thinning behavior with a decrease of

viscosity that was concomitant with the shear-rate increase (**Figure II-5C**). Even if the SoK_U60 showed an increased viscosity (0.032 Pa.s) in respect to the standard SoK_nU (0.017 Pa.s), SoK_U20 (0.016 Pa.s), and SoK_U80 (0.016 Pa.s), all samples had negligible differences at higher shear rate values (700–1000 s^{-1}). The non-Newtonian shear-thinning behavior of all samples was also confirmed by assessing the shear stress (σ) trend alongside shear-rate increments (**Figure II-5D**).

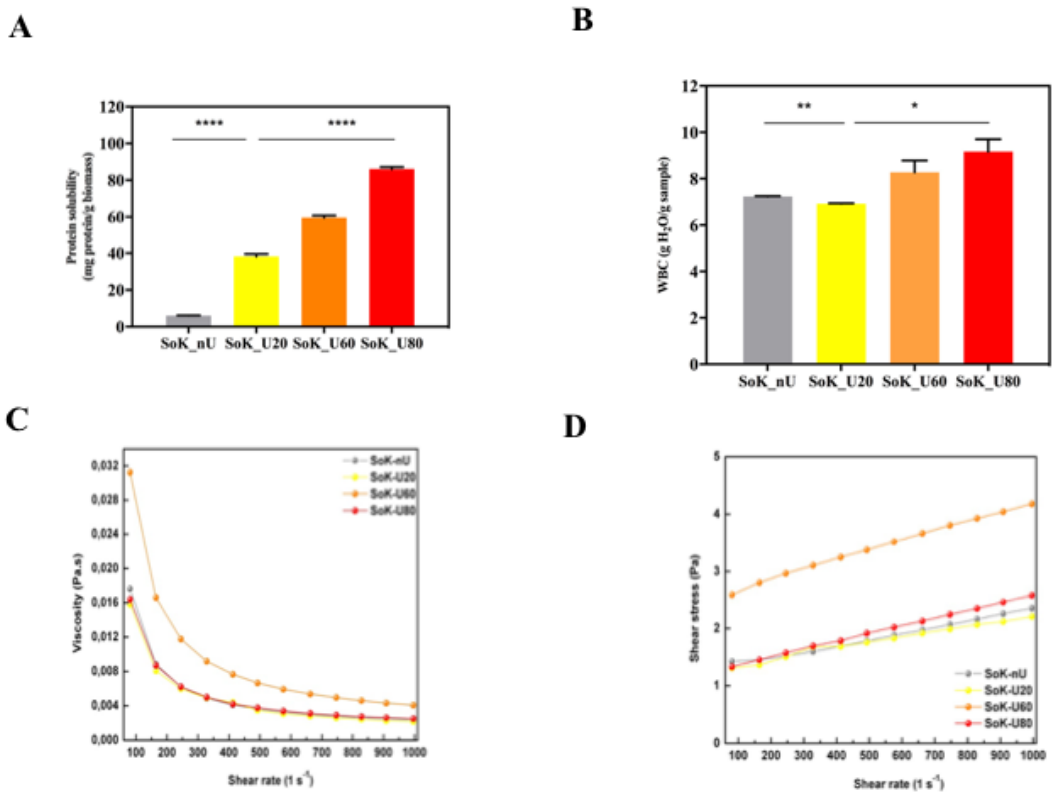

Figure II-5 Solubility and rheological properties. A) Protein solubility. B) Water binding capacity (WBC). C) Viscosity measurements at increasing shear rate. D) Shear stress (σ) measurements at increasing shear rate of extracted proteins confirmed the non-Newtonian shear-thinning behavior of untreated and sonicated proteins. SoK_nU (control, untreated), Sok_U80 (ultrasonicated at 80 °C), Sok_U60 (ultrasonicated at 60 °C), and Sok_U20 (ultrasonicated at 20 °C). Statistical analysis was performed by one-way ANOVA (*) $p<0.5$, (**) $p<0.0$, and (****) $p<0.0001$. The data are represented as the means ± s.d. of three independent experiments.

II-3.9 In vitro antioxidant activity assayed by DPPH

The DPPH radical scavenging assay is one of the most commonly used single electron transfer (SET) based antioxidant procedure. Each sample was tested at the concentration of 0.1 mg/mL. A comparison of the result of the untreated sample with that of the sample treated with ultrasound at room temperature shows that this treatment increases the ability of the sample to scavenge the DPPH radical: in fact, Sok_U20 diminished the DPPH radicals by 90 ± 5.6% compared to SoK_nU ($p < 0.0001$) (**Figure II-6A**). In addition, further improvements of the antioxidant capacity are induced by the thermal treatments, since SoK_U60 and SoK_U80 reduced the DPPH radical by 56.3 ± 0.6% and 72.2 ± 0.3%, respectively ($p < 0.0001$, **Figure II-6B**). The increased antioxidant capacity may be due to the exposure of hidden amino acid residues and side chains with antioxidant capacities (which are usually hidden within the three-dimensional structure of protein molecules). However, it is also important to underline that the peptidomic analysis had already shown that a higher temperature during the ultrasound treatment has the consequence of a relevant increment of the presence of short peptides that may have additional roles in the detected antioxidant activity. Moreover, previous studies carried out on different food matrices (soybean included) have demonstrated that an improved antioxidant ability might be attributed to the formation of short-chain peptides induced by the ultrasound treatment (Tian et al., 2020).

II-3.10 Phytic acid reduction by ultrasound treatment

Since literature indicates that ultrasounds may be successfully applied to reduce the anti-nutritional factor phytic acid (Sivakumar, Swaminathan, & Rao, 2004), it was decided to investigate also this aspect. By normalizing the content of phytic acid in respect to the protein content of each sample, our finding shows that the ultrasonication coupled to temperatures simultaneously reduced the phytic acid proteins interactions compared to the raw sample as reported in **Figure II-6C**. In details, a reduction of phytic acid content by 37.0±1.0% was observed in SoK_U20 (0.5 ± 0.01 mg/g of

protein) versus SoK_nU (0.9 ± 0.06 mg/g of protein) ($p<0.05$, **Figure II-6C**). This may be explained considering that the acoustic effect of cavitation leads to a disruption of phytic acid, mainly localized in bran layer of soybean okara, by increasing the area and extraction rate of phytic acid into the solvent. Furthermore, the increase of temperature leads to an additional significant reduction of the phytic acid content compared to the ultrasound extraction performed at 20 °C. In fact, in SoK_U60 (0.36 ± 0.03 mg/g of protein) and SoK_U80 (0.30 ± 0.05 mg/g of protein) the phytic acid content decreased by 28±3% and 40±5%, respectively, versus Sok_U20 (0.5 ± 0.01 mg/g of protein) ($p<0.0001$, **Figure II-6C**).

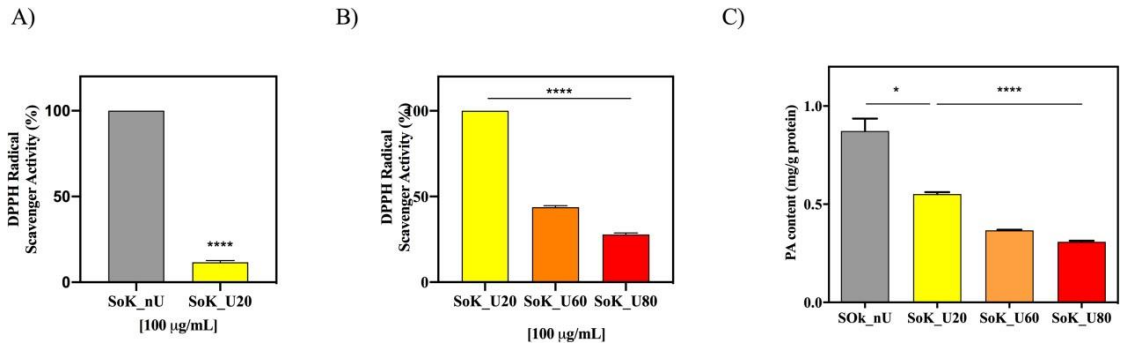

Figure II-6 A) and B) Antioxidant evaluation of SoK_nU, SoK_U20, SoK_U60, and SoK_U80 by DPPH assay; C) PA content determination. SoK_nU (untreated), Sok_U80 (ultrosonicated at 80°C), Sok_U60 (ultrosonicated at 60°C), and Sok_U20 (ultrosonicated at 20°C). Statistical analysis was performed by one-way ANOVA (****) $p < 0.0001$. The data are represented as the means ± s.d. of three independent experiments.

II-4. Conclusion

The effect of ultrasound on the separation and extraction has been extensively studied: it is widely accepted that this process intensifies the extraction of valuable components from soybeans, leading to an overall improvement of protein yield. In this context, our investigation confirms that the ultrasound assisted extraction coupled to a gradient of temperature is also a useful strategy to improve the recovery of proteins from soy okara by-products. From an economical and environmental point of view, these findings contribute to fostering the soy okara protein extracted by ultrasonication processing as

valuable and high-quality products for new applications, thus providing a sustainable way to solve the environmental criticism related to the huge quantities of okara produced annually.

An overall consideration of our results permits to conclude that the ultrasound procedure coupled to a temperature gradient modifies in a significant way the protein secondary and tertiary structures. In fact, a local reduction of α-helices structures and an improvement of beta-sheets and random coil conformations were observed depending on the applied temperature. In addition, a reduction of the free thiol groups and a different distribution of Trp were also detected within the protein samples. The AFM analysis demonstrated a significant morphological transition from well-defined single round structures to highly aggregated ones after the ultrasonication at the higher temperature, suggesting that these aggregates possessed more hydrophilic surfaces and more hydrophobic cores than the untreated sample. This feature was confirmed by measuring the water contact angle, whose results clearly indicated that untreated samples were more hydrophobic than the treated ones, a fact further confirmed by the slower ability of the untreated sample to absorb water drop than ultrasound extracted proteins. All these results were in agreement with the enhancement of the protein yields induced by the ultrasound treatments at different temperatures.

The improvement of protein yields may have a twofold explanation: a) the cavitation phenomenon induced by ultrasound process enhances the disruption of intact cells leading to an increased extracellular release; b) the improvement of protein solubility has the consequence of an increase of the recovery. Notably, in this ultrasound extraction the improvements of protein solubility and water binding capacity appear to depend on the temperature in a similar way. On the contrary, rheological experiments do not support any variation of protein viscosity.

Finally, from a functional point of view, the improvement of peptides generation and the different amino acid exposition within the protein after the ultrasound process led to an increase of the antioxidant properties of the samples and to a reduction of their PA content.

SUPPORTING INFORMATION

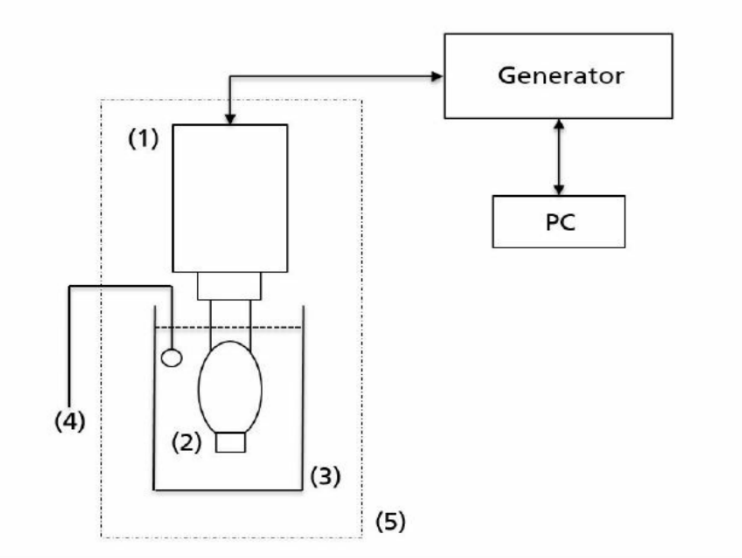

(1) Transducer; (2) Sonotrode; (3) Beaker; (4) Temperature sensor; (5) Sound insulation

Figure II-S1. Experimental setup of ultrasound-assisted extraction.

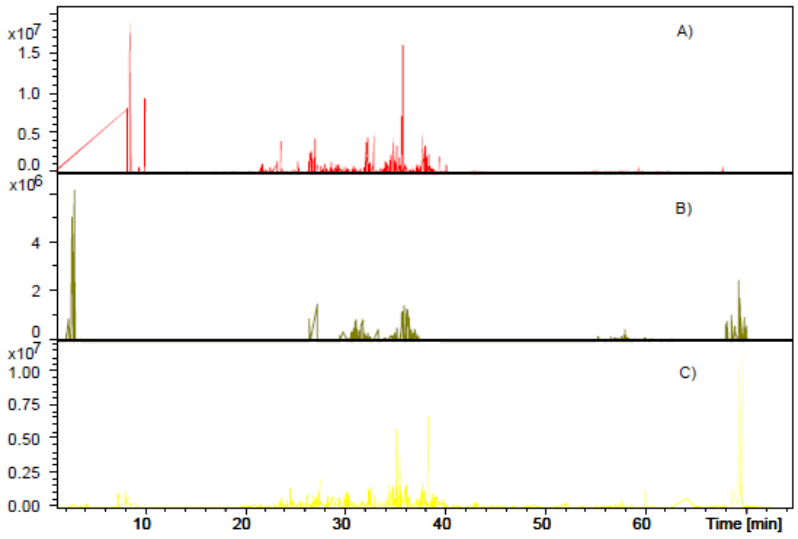

Figure II-S2. Total ion current (TIC) chromatograms of A) Sok_U80; B) Sok_U60 and C) Sok_U20, respectively.

Table II-S1. Protein identified in SoK_nU, SoK_U80, SoK_U60, SoK_U20 after tryptic digestion

Sok_U80	Distinct Peptides (#)	Distinct summed MS/MS Search Score	% AA Coverage	Total Protein Spectral Intensity	Protein MW (Da)	Protein pI	Database Accession #	Protein Name		
	4	60.52	8.3	7.93E+08	72764.3	5.32	Q948X9	Beta-conglycinin alpha-subunit		
	Score	Spectrum Intensity	N-term	Start AA	Sequences		C-term	m/z (Da)	MH^+ (Da)	Peptide pI
	11.41	5.21E+07	Hydrogen	358	(R)NILEASYDTKFEEINK(V)		Free Acid	638.97	1913.94	4.41
	11.05	8.94E+07	Hydrogen	389	(R)LQESVIVEISKEQIR(A)		Free Acid	591.28	1770.99	4.79
	13.91	5.18E+07	Hydrogen	389	(R)LQESVIVEISK(E)		Free Acid	623.08	1244.71	4.53
	15.79	2.09E+07	Hydrogen	337	(R)FESFFLSSTEAQQSYLQGFSR(N)		Free Acid	820.49	2459.15	4.53
Sok_U80	3	41.28	4.3	3.69E+08	74614.2	5.47	P11827	Beta-conglycinin, alpha' chain		
	Score	Spectrum Intensity	N-term	Start AA	Sequences		C-term	m/z (Da)	MH^+ (Da)	Peptide pI
	11.41	5.21E+07	Hydrogen	375	(K)NILEASYDTKFEEINK(V)		Free Acid	638.97	1913.94	4.41
	13.91	5.18E+07	Hydrogen	406	(R)LQESVIVEISK(K)		Free Acid	623.08	1244.71	4.53
	11.72	4.26E+07	Hydrogen	406	(R)LQESVIVEISKK(Q)		Free Acid	458.4	1372.80	6.14
Sok_U80	6	91.05	17	2.38E+08	50533	5.88	I1NGF4	Beta-conglycinin beta subunit		
	Score	Spectrum Intensity	N-term	Start AA	Sequences		C-term	m/z (Da)	MH+ (Da)	Peptide pI
	12.93	1.02E+08	Hydrogen	256	(K)FFEITPEKNPQLR(D)		Free Acid	540.44	1618.85	6.14
	14.49	1.21E+07	Hydrogen	195	(R)VLFGEEEEQRQQEGVIVELSK(E)		Free Acid	816.19	2446.24	4.2
	15.75	2.50E+07	Hydrogen	231	(R)KTISSEDEPFNLR(S)		Free Acid	512.69	1535.77	4.68
	18.95	1.63E+07	Hydrogen	232	(K)TISSEDEPFNLR(S)		Free Acid	704.44	1407.67	4.14
	15.42	3.68E+07	Hydrogen	387	(R)QVQELAFPGSAQDVER(L)		Free Acid	887.48	1773.87	4.14

	13.51	1.57E+07	Hydrogen	26	(K)VREDENNPFYLR(S)		Free Acid	517.87	1551.75	4.68
Sok_U80	**2**	**30.64**	**5.4**	**5.72E+07**	**56343.8**	**5.89**	**A0A0R0KKD6**		**Glycinin G1**	
	Score	**Spectrum Intensity**	**N-term**	**Start AA**	**Sequences**		**C-term**	**m/z (Da)**	**MH+ (Da)**	**Peptide pI**
	13.92	4.64E+07	Hydrogen	181	(R)RFYLAGNQEQEFLK(Y)		Free Acid	581.86	1742.88	6.14
	16.72	1.08E+07	Hydrogen	411	(R)VLIVPQNFVVAAR(S)		Free Acid	713.56	1425.85	9.72
Sok_U80	**2**	**28.21**	**8.4**	**5.64E+07**	**54970.2**	**5.46**	**P04405**		**Glycinin G2**	
	Score	**Spectrum Intensity**	**N-term**	**Start AA**	**Sequences**		**C-term**	**m/z (Da)**	**MH+ (Da)**	**Peptide pI**
	13.92	4.64E+07	Hydrogen	178	(R)RFYLAGNQEQEFLK(Y)		Free Acid	581.86	1742.88	6.14
	14.29	1.01E+07	Hydrogen	42	(R)IESEGGFIETWNPNNKPFQCAGVALSR(C)		Free Acid	1007.94	3022.43	4.79
Sok_U60	**7**	**87.73**	**14.4**	**3.12E+08**	**72535.9**	**5.51**	**Q7XXT2**		**Prepro beta-conglycinin alpha prime subunit**	
	Score	**Spectrum Intensity**	**N-term**	**Start AA**	**Sequences**		**C-term**	**m/z (Da)**	**MH+ (Da)**	**Peptide pI**
	8.46	9.34E+06	Hydrogen	438	(K)LFEITPEKNPQLR(D)		Free Acid	793.41	1584.87	6.14
	18.41	3.57E+07	Hydrogen	303	(R)VPAGTTYYVVNPDNDENLR(M)		Free Acid	713.28	2137.02	4.03
	11.02	1.33E+07	Hydrogen	372	(K)VLFGREEGQQQGEER(L)		Free Acid	588.13	1761.85	4.49
	11.69	1.47E+07	Hydrogen	560	(K)DNVISQIPSQVQELAFPGSAK(D)		Free Acid	743.56	2228.15	4.37
	10.41	3.60E+07	Hydrogen	387	(R)LQESVIVEISKK(Q)		Free Acid	458.35	1372.80	6.14
	12.7	2.70E+07	Hydrogen	387	(R)LQESVIVEISK(K)		Free Acid	622.95	1244.71	4.53
	8.39	6.38E+07	Hydrogen	356	(K)NILEASYDTK(F)		Free Acid	577.34	1153.57	4.37
Sok_U60	**5**	**67**	**9.1**	**5.18E+08**	**72764.3**	**5.32**	**Q948X9**		**Beta-conglycinin alpha-subunit**	
	Score	**Spectrum Intensity**	**N-term**	**Start AA**	**Sequences**		**C-term**	**m/z (Da)**	**MH+**	**Peptide pI**

									(Da)	
	11.55	1.15E+08	Hydrogen	440	(K)FFEITPEKNPQLR(D)		Free Acid	540.61	1618.85	6.14
	19.24	3.86E+07	Hydrogen	305	(R)VPSGTTYYVVNPDNNENLR(L)		Free Acid	718.29	2152.03	4.37
	14.22	4.33E+07	Hydrogen	389	(R)LQESVIVEISKEQIR(A)		Free Acid	591.22	1770.99	4.79
	12.7	2.70E+07	Hydrogen	389	(R)LQESVIVEISK(E)		Free Acid	622.95	1244.71	4.53
	8.39	6.38E+07	Hydrogen	358	(R)NILEASYDTK(F)		Free Acid	577.34	1153.57	4.37
Sok_U60	**5**	**52.13**	**8.7**	**1.92E+08**	**74614.2**	**5.47**	**P11827**	**Beta-conglycinin, alpha-chain**		
	Score	**Spectrum Intensity**	**N-term**	**Start AA**	**Sequences**		**C-term**	**m/z (Da)**	**MH+ (Da)**	**Peptide pI**
	9.61	5.16E+07	Hydrogen	322	(R)MIAGTTFYVVNPDNDENLR(M)		Free Acid	723.93	2169.02	4.03
	11.02	1.33E+07	Hydrogen	391	(K)VLFGREEGQQQGEER(L)		Free Acid	588.13	1761.85	4.49
	10.41	3.60E+07	Hydrogen	406	(R)LQESVIVEISKK(Q)		Free Acid	458.35	1372.80	6.14
	12.7	2.70E+07	Hydrogen	406	(R)LQESVIVEISK(K)		Free Acid	622.95	1244.71	4.53
	8.39	6.38E+07	Hydrogen	375	(K)NILEASYDTK(F)		Free Acid	577.34	1153.57	4.37
Sok_U60	**2**	**25.24**	**6.3**	**3.53E+07**	**55318.5**	**5.3**	**A0A0R0KK84**	**Glycinin G2**		
	Score	**Spectrum Intensity**	**N-term**	**Start AA**	**Sequences**		**C-term**	**m/z Measured (Da)**	**MH+ Measured (Da)**	**Peptide pI**
	13.56	5.93E+06	Hydrogen	242	(R)NLQGENEEEDSGAIVTVK(G)		Free Acid	966.79	1931.91	3.91
	11.68	1.99E+07	Hydrogen	182	(R)FYLAGNQEQEFLK(Y)		Free Acid	794.08	1586.78	4.53
Sok_U20	**1**	**15.45**	**2**	**8.11E+07**	**72764.3**	**5.32**	**Q948X9**	**Beta-conglycinin alpha-subunit**		
	Score	**Spectrum Intensity**	**N-term**	**Start AA**	**Sequences**		**C-term**	**m/z (Da)**	**MH+ (Da)**	**Peptide pI**
	12.14	2.69E+07	Hydrogen	440	(K)FFEITPEKNPQLR(D)		Free Acid	540.55	1618.85	6.14

Sok_U20	**1**	**14.79**	**2**	**6.71E+07**	**72535.9**	**5.51**	**Q7XXT2**	**Prepro beta-conglycinin alpha prime subunit**		
	Score	**Spectrum Intensity**	**N-term**	**Start AA**	**Sequences**		**C-term**	**m/z (Da)**	**MH+ (Da)**	**Peptide pI**
	13.45	2.27E+07	Hydrogen	438	(K)LFEITPEKNPQLR(D)		Free Acid	529.26	1584.87	6.14
Sok_U20	**1**	**12.82**	**2.6**	**7.62E+07**	**64397.6**	**5.21**	**P02858**	**Glycinin G4**		
	Score	**Spectrum Intensity**	**N-term**	**Start AA**	**Sequences**		**C-term**	**m/z (Da)**	**MH+ (Da)**	**Peptide pI**
	12.82	7.62E+07	Hydrogen	260	(K)QIVTVEGGLSVISPK(W)		Free Acid	764.22	1526.87	6

Table II-S2. Peptide sequences identified in Sok_U80, Sok_U60, Sok_U20, respectively after ultrasound treatment

Sok_U80

Spectrum Intensity	N-term	Start AA	Sequence	m/z (Da)	MH+ (Da)	Peptide pI
2.54E+08	Hydrogen	13	(K)LGEGGFGPVYKGTLSDQQE(V)	661.07	1981.951	4.43
2.03E+08	Hydrogen	303	(S)LKILASNCQ(S)	989.05	989.545	8.22
2.01E+08	Hydrogen	3010	(K)NLPPNHSLI(N)	1005.6	1004.553	6.74
1.54E+08	Hydrogen	1700	(K)PFDPERMI(A)	1004.78	1004.488	4.37
1.43E+08	Hydrogen	410	(E)VAAGRLEDK(S)	959.67	958.532	6.04
1.39E+08	Hydrogen	14	(N)KVIKYYF(I)	959.67	960.556	9.53
1.37E+08	Hydrogen	846	(E)KAPGDSAARD(S)	987.41	987.486	6.14
1.32E+08	Hydrogen	17	(E)DGDGKVSPSE(L)	991.25	990.438	4.32
1.19E+08	Hydrogen	98	(S)SLLASHVTM(A)	959.01	958.503	6.46
1.10E+08	Hydrogen	496	(D)FVSHGTYY(T)	973.09	973.442	6.74
1.05E+08	Hydrogen	60	(N)ATSSRQFY(N)	959.08	959.459	8.79
1.03E+08	Hydrogen	2496	(A)KPAASIL(E)	700.06	699.441	8.75
9.85E+07	Hydrogen	590	(S)SDQRKLDM(S)	991.86	992.484	5.68
7.96E+07	Hydrogen	173	(E)SGLKLELSDIPVENLVPEPLRGSSSAEE(F)	989.58	2965.537	4.31
7.52E+07	Hydrogen	36	(T)TPNLPGT(P)	699.73	699.368	5.18
6.96E+07	Hydrogen	675	(D)VSSDGNEMR(Q)	994.78	994.426	4.37
6.71E+07	Hydrogen	117	(T)QVDKPRFV(S)	989.31	988.558	8.75
6.65E+07	Hydrogen	213	(S)LGAMPVSSFS(G)	995.65	995.487	5.52
6.36E+07	Hydrogen	230	(G)FSGDAFKSH(H)	994.82	995.459	6.74
6.20E+07	Hydrogen	585	(R)GFVCPSRGAT(S)	994.77	994.478	8.25

6.02E+07	Hydrogen	148	(R)SFHSFPSSV(P)	994.82	994.463	6.46
5.95E+07	Hydrogen	4	(R)AEQIGGGKAVTTVLAIGTANPPNFILQED(Y)	975.34	2924.537	4.38
5.34E+07	Hydrogen	505	(S)VPVPGTPYK(S)	957.36	957.541	8.56
5.01E+07	Hydrogen	177	(A)YFSALKDN(D)	956.72	957.468	5.83
4.93E+07	Hydrogen	216	(I)RTAIADSIME(P)	1105.87	1106.552	4.75
4.89E+07	Hydrogen	84	(Q)PTRDFLLDE(L)	1106.08	1105.553	4.32
4.70E+07	Hydrogen	2	(M)APKPITGPVP(D)	975.48	976.583	8.8
4.51E+07	Hydrogen	497	(A)VLERTGITAF(D)	1105.86	1106.621	5.97
4.21E+07	Hydrogen	134	(T)ISPELGAKY(R)	976.36	977.531	6
4.11E+07	Hydrogen	273	(G)ITLPTHFF(L)	974.37	975.53	6.74
4.08E+07	Hydrogen	514	(N)VVRDSSGKK(I)	975.18	975.559	9.99
3.96E+07	Hydrogen	441	(Q)SRKGGSCYFGGTSYVVTQEPSEYSINP(F)	972	2913.336	5.86
3.92E+07	Hydrogen	152	(F)YFPGSGAIF(T)	957.69	958.467	5.52
3.73E+07	Hydrogen	1952	(S)YLVHNQCV(E)	974.43	975.472	6.73
3.51E+07	Hydrogen	131	(L)VVGGHGGNE(L)	826.12	825.385	5.47
3.14E+07	Hydrogen	381	(L)SNSAITGYF(P)	958.55	959.447	5.24
3.03E+07	Hydrogen	344	(Y)KTNRLTDK(S)	976.56	975.559	9.99

Sok_U60 **Spectrum Intensity**	**N-term**	**Start AA**	**Sequence**	**m/z (Da)**	**MH+ (Da)**	**Peptide pI**
2.14E+08	Hydrogen	534	(V)GPSIEHQFIPSFIGRSPL(H)	661.12	1982.05	6.75
2.08E+08	Hydrogen	48	(P)APVASPTSSPPASSPNAATATP(P)	660.44	1978.972	5.57
9.39E+07	Hydrogen	168	(S)FDGCGSCVKIPQASSEGPEA(R)	661.02	1981.864	4.14
8.67E+07	Hydrogen	64	(F)VDEPNQFSAGIRFNSKSIP(Y)	702.38	2106.062	6.04
8.47E+07	Hydrogen	295	(G)SGLGAYGRGGGAYGTY(G)	502.95	1506.698	8.22

8.09E+07	Hydrogen	384	(D)DGMLSFTSLPAANIKSGSGGA(G)	661.1	1980.97	5.84
7.91E+07	Hydrogen	695	(F)GGPAESNAANYGVDGNAAESDH(G)	701.54	2102.865	3.92
6.07E+07	Hydrogen	946	(A)RKAGIEQCLPASNECSVPP(K)	666.77	1998.974	6.13
5.95E+07	Hydrogen	70	(Y)ASASALPAFLTSQG(D)	660.73	1320.68	5.57
5.37E+07	Hydrogen	179	(R)GIGPQKSYISNLLK(D)	506.83	1517.869	9.7
5.36E+07	Hydrogen	460	(S)HLLSDLPPNDQDVDVCH(P)	639.59	1916.881	4.13
4.98E+07	Hydrogen	63	(L)GLASVGKPYCPLDVV(V)	506.63	1517.804	5.83
4.78E+07	Hydrogen	68	(I)IPASKAASDVSRSDFLPYL(S)	679.93	2037.066	5.96
4.68E+07	Hydrogen	1471	(R)LQKVHGPSAI(S)	350.48	1049.611	8.76
4.56E+07	Hydrogen	78	(G)FGAQVKEFKPCDDRYI(D)	639.62	1915.938	6.11
4.52E+07	Hydrogen	17	(L)RHHAHVSPSPSLAACLILK(H)	679.77	2037.118	9.51
4.36E+07	Hydrogen	588	(E)SLSLHTESGSSSV(E)	431.12	1290.618	5.22
4.36E+07	Hydrogen	242	(S)HELMEALQVISSDKQLFL(R)	700.73	2101.1	4.65
4.29E+07	Hydrogen	342	(S)AGIASDVAASALVGASNVFGTI(V)	664.2	1991.045	3.8
3.82E+07	Hydrogen	188	(G)ESLPVTRNPGQQ(V)	662.9	1325.681	6.1
3.53E+07	Hydrogen	337	(K)RSGSSSIDPEDVEIPASTF(S)	665.29	1993.936	3.91
3.49E+07	Hydrogen	107	(G)GGVGNGGGAGLGGGVGGGSGRGGGGGF(G)	663.97	1988.929	9.75
3.38E+07	Hydrogen	298	(L)KREPYASKRCG(C)	432.38	1294.669	9.79
3.38E+07	Hydrogen	326	(V)PTPARGVPSPDGIVGP(E)	506.18	1516.812	6.27
3.34E+07	Hydrogen	146	(L)QGLSMPGCNLSGPLDPSLAR(L)	671.9	2012.99	5.83
3.33E+07	Hydrogen	43	(G)SSRQRRIDAEI(R)	665.72	1330.719	9.23
3.24E+07	Hydrogen	31	(R)KLPNPDTGESREPSSLER(K)	671.58	2012.005	4.87
3.17E+07	Hydrogen	44	(L)VDSGNNNYLPTTARADSPP(Y)	663.94	1988.931	4.21
3.15E+07	Hydrogen	78	(I)KTLKTERRSNSPIDRNE(G)	681.94	2044.09	9.98
3.04E+07	Hydrogen	610	(C)LVGIKGDPEVNR(N)	433.16	1296.728	6.07

Sok_U20

Spectrum Intensity	N-term	Start AA	Sequence	m/z (Da)	MH+ (Da)	Peptide pI
1.25E+08	Hydrogen	755	(K)AKLLPGT(P)	699.27	699.441	8.8
1.10E+08	Hydrogen	108	(P)VTPKPGT(L)	699.63	699.404	8.72
1.06E+08	Hydrogen	172	(V)PVHATH(V)	660.98	661.342	7.33
9.86E+07	Hydrogen	728	(H)INDGSDLPR(E)	987.4	986.491	4.21
9.73E+07	Hydrogen	278	(M)MKNLSAPTK(F)	989.3	989.545	10
8.11E+07	Hydrogen	81	(P)FSPHPPPLD(D)	1005.58	1006.5	5.33
8.08E+07	Hydrogen	210	(S)RKSASDPSTG(Y)	1005.8	1005.497	8.75
7.90E+07	Hydrogen	245	(E)KDPGASATLQ(K)	987.23	987.511	5.84
7.88E+07	Hydrogen	179	(N)PIEKLVKY(G)	989.39	989.604	8.9
7.71E+07	Hydrogen	154	(Q)KPTPPFCVT(F)	989.43	989.513	8.22
7.44E+07	Hydrogen	260	(P)PRGDGVV(N)	699.55	699.379	6.27
7.36E+07	Hydrogen	109	(D)YKLNGSPKV(M)	1004.9	1005.573	9.7
6.87E+07	Hydrogen	478	(V)VSRTSDGGVK(T)	1005.67	1005.533	8.72
6.21E+07	Hydrogen	104	(S)FVERDPPD(C)	974.04	974.458	4.27
6.11E+07	Hydrogen	176	(P)LVLSADVKK(V)	973.4	972.609	8.59
4.94E+07	Hydrogen	61	(Y)FSSIYEQT(F)	974.59	974.447	4
4.89E+07	Hydrogen	291	(V)TTHEGHFY(W)	991.34	991.427	5.92
4.76E+07	Hydrogen	183	(L)AGGAYSAASMNPARSFGPALVT(G)	699.64	2096.023	8.79
4.66E+07	Hydrogen	569	(T)NPPPEKDY(D)	959.57	959.447	4.37
4.55E+07	Hydrogen	573	(V)VPISGLN(Y)	699.72	699.404	5.49
4.25E+07	Hydrogen	187	(M)EANPGSLAMC(T)	991.5	992.418	4
4.10E+07	Hydrogen	154	(V)DRSISCYD(Q)	959.25	958.394	4.54

3.67E+07	Hydrogen	211	(I)VIDPRNPY(Y)	973.45	973.511	5.8
3.43E+07	Hydrogen	496	(D)FVSHGTYY(T)	973.14	973.442	6.74
3.37E+07	Hydrogen	225	(I)KNCAPDPTK(P)	973.16	973.478	8.2
3.05E+07	Hydrogen	103	(Y)EARQSAPSIARSNTGDHSENS(Q)	738.62	2214.014	5.45

Video 1, 2,3, and 4: wettability of SoK_nU, SoK_U20, SoK_U60, and SoK_U80, respectively

Click here to access/download **Video** SoK_nU.mov

Click here to access/download **Video** SoK_U20.mov

Click here to access/download **Video** SoK_U60.mov

Click here to access/download **Video** SoK_U80.mov

References

Aiello, G., Fasoli, E., Boschin, G., Lammi, C., Zanoni, C., Citterio, A., & Arnoldi, A. (2016). Proteomic characterization of hempseed (Cannabis sativa L.). Journal of Proteomics, 147, 187-196.

Aiello, G., Lammi, C., Boschin, G., Zanoni, C., & Arnoldi, A. (2017). Exploration of Potentially Bioactive Peptides Generated from the Enzymatic Hydrolysis of Hempseed Proteins. Journal of Agricultural and Food Chemistry, 65(47), 10174-10184.

Arzeni, C., Martinez, K., Zema, P., Arias, A., Perez, O. E., & Pilosof, A. M. R. (2012). Comparative study of high intensity ultrasound effects on food proteins functionality. Journal of Food Engineering, 108(3), 463-472.

Burstein, E. A., Vedenkina, N. S., & Ivkova, M. N. (1973). Fluorescence and the location of tryptophan residues in protein molecules. Photochemistry and Photobiology, 18(4), 263-279.

Chemat, F., Rombaut, N., Sicaire, A. G., Meullemiestre, A., Fabiano-Tixier, A. S., & Abert-Vian, M. (2017). Ultrasound assisted extraction of food and natural products. Mechanisms, techniques, combinations, protocols and applications. A review. Ultrasonics Sonochemistry, 34, 540-560.

Chemat, F., Zill e, H., & Khan, M. K. (2011). Applications of ultrasound in food technology: Processing, preservation and extraction. Ultrasonics Sonochemistry, 18(4), 813-835.

Colletti, A., Attrovio, A., Boffa, L., Mantegna, S., & Cravotto, G. (2020). Valorisation of By-Products from Soybean (Glycine max (L.) Merr.) Processing. Molecules, 25(9).

Esclapez, M. D., Garcia-Perez, J. V., Mulet, A., & Carcel, J. A. (2011). Ultrasound-Assisted Extraction of Natural Products. Food Engineering Reviews, 3(2), 108-120.

Gao, Y., Shang, C., Maroof, M. A. S., Biyashev, R. M., Grabau, E. A., Kwanyuen, P., Buss, G. R. (2007). A modified colorimetric method for phytic acid analysis in soybean. Crop Science, 47(5), 1797-1803.

Gulseren, I., Guzey, D., Bruce, B. D., & Weiss, J. (2007). Structural and functional changes in ultrasonicated bovine serum albumin solutions. Ultrasonics Sonochemistry, 14(2), 173-183.

Higuera-Barraza, O. A., Torres-Arreola, W., Ezquerra-Brauer, J. M., Cinco-Moroyoqui, F. J.,

Figueroa, J. C. R., & Marquez-Rios, E. (2017). Effect of pulsed ultrasound on the Physicochemical characteristics and emulsifying properties of squid (Dosidicus gigas) mantle proteins. Ultrasonics Sonochemistry, 38, 829-834.

Hu, H., Li-Chan, E. C. Y., Wan, L., Tian, M., & Pan, S. Y. (2013). The effect of high intensity ultrasonic pre-treatment on the properties of soybean protein isolate gel induced by calcium sulfate. Food Hydrocolloids, 32(2), 303-311.

Jacotet-Navarro, M., Rombaut, N., Deslis, S., Fabiano-Tixier, A. S., Pierre, F. X., Bily, A., & Chemat, F. (2016). Towards a "dry" bio-refinery without solvents or added water using microwaves and ultrasound for total valorization of fruit and vegetable by-products. Green Chemistry, 18(10), 3106-3115.

Jambrak, A. R., Lelas, V., Mason, T. J., Kresic, G., & Badanjak, M. (2009). Physical properties of ultrasound treated soy proteins. Journal of Food Engineering, 93(4), 386-393.

Jiang, L. Z., Wang, J., Li, Y., Wang, Z. J., Liang, J., Wang, R., Zhang, M. (2014). Effects of ultrasound on the structure and physical properties of black bean protein isolates. Food Research International, 62, 595-601.

Kinsella, J. E. (1982). Protein-structure and functional-properties - emulsification and flavor binding effects. Acs Symposium Series, 206, 301-326.

Lammi, C., Arnoldi, A., & Aiello, G. (2019). Soybean Peptides Exert Multifunctional Bioactivity Modulating 3-Hydroxy-3-Methylglutaryl-CoA Reductase and Dipeptidyl Peptidase-IV Targets in Vitro. Journal of Agricultural and Food Chemistry, 67(17), 4824-4830.

Lammi, C., Bellumori, M., Cecchi, L., Bartolomei, M., Bollati, C., Clodoveo, M. L., Nadia, M. (2020). Extra Virgin Olive Oil Phenol Extracts Exert Hypocholesterolemic Effects through the Modulation of the LDLR Pathway: In Vitro and Cellular Mechanism of Action Elucidation. (Vol. 12 (6), p. 1723): Nutrients.

Li, B., Qiao, M. Y., & Lu, F. (2012). Composition, Nutrition, and Utilization of Okara (Soybean Residue). Food Reviews International, 28(3), 231-252.

20. Li, H. Z., Pordesimo, L., & Weiss, J. (2004). High intensity ultrasound-assisted extraction of oil from soybeans. Food Research International, 37(7), 731-738.

Malomo, S. A., He, R., & Aluko, R. E. (2014). Structural and functional properties of hemp seed protein products. J Food Sci, 79(8), C1512-1521.

Messina, M., & Messina, V. (2010). The Role of Soy in Vegetarian Diets. Nutrients, 2(8), 855-888.

Nowak, E., Combes, G., Stitt, E. H., & Pacek, A. W. (2013). A comparison of contact angle measurement techniques applied to highly porous catalyst supports. Powder Technology, 233, 52-64.

Peters, J., Vergeldt, F. J., Boom, R. M., & van der Goot, A. J. (2017). Water-binding capacity of protein-rich particles and their pellets. Food Hydrocolloids, 65, 144-156.

Preece, K. E., Hooshyar, N., Krijgsman, A., Fryer, P. J., & Zuidam, N. J. (2017). Intensified soy protein extraction by ultrasound. Chemical Engineering and Processing-Process Intensification, 113, 94-101.

Raussens, V., Ruysschaert, J. M., & Goormaghtigh, E. (2003). Protein concentration is not an absolute prerequisite for the determination of secondary structure from circular dichroism spectra: a new scaling method. Analytical Biochemestry, 319(1), 114-121.

Rizzo, G., & Baroni, L. (2018). Soy, Soy Foods and Their Role in Vegetarian Diets. Nutrients, 10(1).

Rosenthal, A., Pyle, D. L., & Niranjan, K. (1998). Simultaneous aqueous extraction of oil and protein from soybean: Mechanisms for process design. Food and Bioproducts Processing, 76(C4), 224-230.

Shirsath, S. R., Sonawane, S. H., & Gogate, P. R. (2012). Intensification of extraction of natural products using ultrasonic irradiations A review of current status. Chemical Engineering and Processing-Process Intensification, 53, 10-23.

Sicaire, A. G., Vian, M. A., Fine, F., Carre, P., Tostain, S., & Chemat, F. (2016). Ultrasound induced green solvent extraction of oil from oleaginous seeds. Ultrasonics Sonochemistry, 31, 319-329.

Sivakumar, V., Swaminathan, G., & Rao, P. G. (2004). Use of ultrasound in soaking for improved efficiency. Journal of the Society of Leather Technologists and Chemists, 88(6), 249-251.

Sun, Y. J., Chen, J. H., Zhang, S. W., Li, H. J., Lu, J., Liu, L., Lv, J. P. (2014). Effect of power ultrasound pre-treatment on the physical and functional properties of reconstituted milk protein concentrate. Journal of Food Engineering, 124, 11-18.

Tian, R., Feng, J., Huang, G., Tian, B., Zhang, Y., Jiang, L., & Sui, X. (2020). Ultrasound driven conformational and physicochemical changes of soy protein hydrolysates. Ultrasonics Sonochemistry, 68, 105-202.

Vera, A., Valenzuela, M. A., Yazdani-Pedram, M., Tapia, C., & Abugoch, L. (2019). Conformational and physicochemical properties of quinoa proteins affected by different conditions of high-intensity ultrasound treatments. Ultrasonics Sonochemistry, 51, 186-196.

Vishwanathan, K. H., Singh, V., & Subramanian, R. (2011). Wet grinding characteristics of soybean for soymilk extraction. Journal of Food Engineering, 106(1), 28-34.

Xiong, W. F., Wang, Y. T., Zhang, C. L., Wan, J. W., Shah, B. R., Pei, Y. Q., . Li, B. (2016). High intensity ultrasound modified ovalbumin: Structure, interface and gelation properties. Ultrasonics Sonochemistry, 31, 302-309.

Zhu, Z. B., Zhu, W. D., Yi, J. H., Liu, N., Cao, Y. G., Lu, J. L., McClements, D. J. (2018). Effects of sonication on the physicochemical and functional properties of walnut protein isolate. Food Research International, 106, 853-861.

Zou, Y., Xu, P., Wu, H., Zhang, M., Sun, Z., Sun, C., Xu, W. (2018). Effects of different ultrasound power on physicochemical property and functional performance of chicken actomyosin. International Journal Biological Macromolecules, 113, 640-647.

Zou, Y., Yang, H., Li, P. P., Zhang, M. H., Zhang, X. X., Xu, W. M., & Wang, D. Y. (2019). Effect of different time of ultrasound treatment on physicochemical, thermal, and antioxidant properties of chicken plasma protein. Poultry Science, 98(4), 1925-1933.

SCIENTIFIC PUBLICATIONS & COMMUNICATIONS

Published Article

Aiello G., **Li Y.,** Boschin G., Bollati C., Arnoldi A., Lammi C. Chemical and biological characterization of spirulina protein hydrolysates: Focus on ACE and DPP-IV activities modulation. *Journal of Functional Foods* **2019**, *63*, 103592.

Li Y., Lammi C., Boschin G., Arnoldi A., Aiello G. Recent Advances in Microalgae Peptides: Cardiovascular Health Benefits and Analysis. *Journal of agricultural and food chemistry* **2019**, *67*, 11825-11838.

Li Y., Aiello G., Bollati C., Bartolomei M., Arnoldi A., Lammi C. Phycobiliproteins from Arthrospira Platensis (Spirulina): A New Source of Peptides with Dipeptidyl Peptidase-IV Inhibitory Activity. *Nutrients* **2020**, *12*.

Aiello G., **Li Y**., Boschin G., Stanziale M., Lammi C., Arnoldi A., Analysis of Narrow-Leaf Lupin Proteins in Lupin-Enriched Pasta by Untargeted and Targeted Mass Spectrometry. *Foods* **2020**, 9(8).

Aiello G., Pugliese R., Rueller L., Bollati C., Bartolomei M., **Li Y**., Robert J., Arnoldi A., Lammi C. Assessment of the Physicochemical and Conformational Changes of Ultrasound-Driven Proteins extracted from Soybean Okara Byproduct. *Foods* **2021**, 10(3).

Submitted Manuscript

Li Y.; Aiello G., Locatelli, P., Boschin, G., Arnoldi, A., Grazioso, G., Lammi, C., Investigation of *Chlorella pyrenoidosa* protein as a source of novel angiotensin I-converting enzyme (ACE) and dipeptidyl peptidase-IV (DPP-IV) inhibitory peptides. *Nutrients* **2021**.

Abstract in Conference Proceedings

Li Y., Aiello G, Arnoldia A. Identification of potential bioactive peptides released from Spirulina protein digestion by LC-MS/MS and in silico peptides analysis. Italian Proteomics Association XIII Annual conference. Como, 5-7th September 2018.

Li Y., Aiello G., Lammi C., Arnoldia A. Prediction of dipeptidyl peptidase IV inhibitory peptides from Chlorella pyrenoidosa based on peptidomics and bioinformatic approaches. Summer school -*Valorization of by-products from agri-food supply chains for the development of functional ingredients, foods and nutraceuticals*. Verona, 24-26th June 2019.

Li Y., Aiello G., Lammi C., Boschin G., Arnoldia A. Angiotensin-Converitng-Enzyme and Dipeptidyl Peptidase IV Inhibitory Peptides from *Spirulina Platensis*: Chemical and Biological Characterization. Milan, 23-24th September 2019.

Awards

"Young Researcher Poster Prize" in the congress at Italian Proteomics Association XIII Annual conference.